Permafrost and Frozen Sub-Seabottom Materials in the Southern Beaufort Sea

J.A.M. HUNTER, A.S. JUDGE, H.A. MacAULAY,
R.L. GOOD, R.M. GAGNE and R.A. BURNS

Technical Report No. 22

Beaufort Sea Project

THE OCCURRENCE OF PERMAFROST AND FROZEN SUB-SEABOTTOM MATERIALS IN THE SOUTHERN BEAUFORT SEA

J.A.M. Hunter*, A.S. Judge**, H.A. MacAulay*,
R.L. Good*, R.M. Gagne*, and R.A. Burns*

*Geological Survey of Canada and
**Earth Physics Branch
Department of Energy, Mines and Resources

Beaufort Sea Technical Report #22

Beaufort Sea Project
Dept. of the Environment
512 Federal Building
1230 Government St.
Victoria, B.C. V8W 1Y4

April, 1976

TABLE OF CONTENTS

TABLE OF CONTENTS, CONTINUED

TABLE OF CONTENTS, CONTINUED

TABLE OF CONTENTS, CONTINUED

1. SUMMARY

1.1 Summary Statement

Permafrost conditions exist beneath most of the Beaufort Sea shelf area. As a result of large changes in the surface thermal régime in the recent geological past, non-equilibrium conditions are probably found in most areas; hence permafrost is both aggrading and degrading. Permafrost is generally at much higher temperatures offshore than the equivalent permafrost conditions onshore and as a result is much more susceptible to thawing by a thermal disturbance.

The occurrence of ice-rich sub-seabottom sediments over large areas of the shelf has been interpreted from seismic data. Such sediments are potentially susceptible to hazardous thermal degradation.

Because of low sediment temperatures, natural gas in shallow sediments may be found in the form of clathrate hydrates, which may cause additional technical problems for exploratory drilling. No such shallow occurrences have been documented in offshore drilling done to date; however, these deposits are seismically indistinguishable from ice-bonded sediments.

1.2 Acknowledgements

This work would not have been possible without the support of G.D. Hobson, director of the Polar Continental Shelf Project, in the capacity of seismologist and who acted as a catalyst in the negotiations with industry participants and gave helpful advice throughout the field and interpretational components of the work. As well, we would like to thank the Polar Continental Shelf Project for logistics support over the last four field seasons.

We wish to thank the following companies and individuals for their support and contributions to this work: John Hnatiuk, Jim Alexander, Al Randell and Grant Fawcett of Gulf Oil Canada Ltd.; Ken Gillies of Dome Petroleum Ltd.; Peter Savage and Lionel Cane of Pan Canadian Petroleum Ltd.; Gerry Rempel, Bob Auld, Wesley Hatlelid and John MacDonald of Imperial Oil Ltd.; Doug Brown and John Card of Sun Oil Ltd.; Reed Johnson of Geophysical Services Inc.; Cameron O'Rourke of Canmar Drilling Ltd.; Roger Argument of Shell Canada Ltd.; Aquitaine Co. of Canada Ltd.; Elf Oil Exploration and Production Ltd.; Hunt International Petroleum Co.; Mobil Oil Corp.; and Amoco Ltd. The assistance of the Oil and Gas Division of I.A.N.D., in particular Jim El-Defrawy and Milos Rajicic in the acquisition and preservation of well-sites and Martin Smith in logging assistance, is gratefully acknowledged. The drilling program in Kugmallit Bay would have been impossible without the valuable help of Vic Allen, John Dugal and Ken Dubinsky of EMR. Such extensive collection and analysis of results would have been impossible without the diligent computational efforts of Susan Pullan, Alan Taylor and John Collier of EMR.

2. INTRODUCTION

Seabottom sediments with mean annual temperatures less than 0°C are defined to be permafrost materials whether or not inter-granular ice bonding is present. This study concerns itself with the nature of permafrost in the southern Beaufort Sea shelf, and examines:

a) the areal and vertical distribution of permafrost and ice bonded materials, their relationship with known geological and geomorphological features, and

b) thermal models applicable to this particular sub-seabottom environment based on the thermal history of the shelf and measured thermal parameters.

The existence and nature of sub-seabottom parmafrost must be taken into consideration in advance of exploratory drilling for hydrocarbons; the ambient temperature conditions and the extent of thermal degradation or aggradation of ice-bonded sediments and the response of those sediments to man-induced thermal perturbation must be known for proper design of casing programs and positioning of sub-seabottom structures (Perkins et al., 1974; Perkins and Ruedrich, 1973; Ruedrich and Perkins, 1974; Linell, 1973). Further, the occurrence of gas hydrates in association with permafrost is well known on-shore in the Mackenzie delta area. The possible existence of such materials in association with permafrost areas offshore cannot be overlooked (Hitchon, 1975). In some cases occurrences of both gas hydrates and permafrost have led to unforeseen technical problems in exploratory drilling.

3. RESUMÉ OF THE CURRENT STATE OF KNOWLEDGE

3.1 Direct Evidence of Sub-seabottom Permafrost

The first evidence for the existence of offshore and sub-seabottom permafrost in the Beaufort Sea was obtained from shallow engineering drilling by the Arctic Petroleum Operator's Association reported by MacKay (1972). Fig. 3-1 shows the location of the holes drilled and those containing frozen ground. Ice-bonded frozen material was obtained in four of these holes at depths less than 50 metres below seabottom. In-hole temperature measurements were not made and it is not possible to determine how many of the other holes may have encountered permafrost (sub-zero temperatures). Detailed descriptions of the logs for holes encountering ice are reproduced from A.P.O.A. Report No. 3 by Golden et al. (1970) in Appendix A.

Recently increasing numbers of reports have described frozen sediments recovered from the seabottom. Lewellen (1973; 1974) has reported extensively on frozen sediments in coastal areas along the Alaskan coast of the Beaufort Sea. Molochuskin (1973) has reported on the presence of frozen ground beneath the Laptev Sea of Siberia. His observations confirm the presence of permafrost in water depths to 4 m and to 900 m offshore beneath waters with slightly positive mean annual bottom-water temperatures. In Canadian waters Samson and

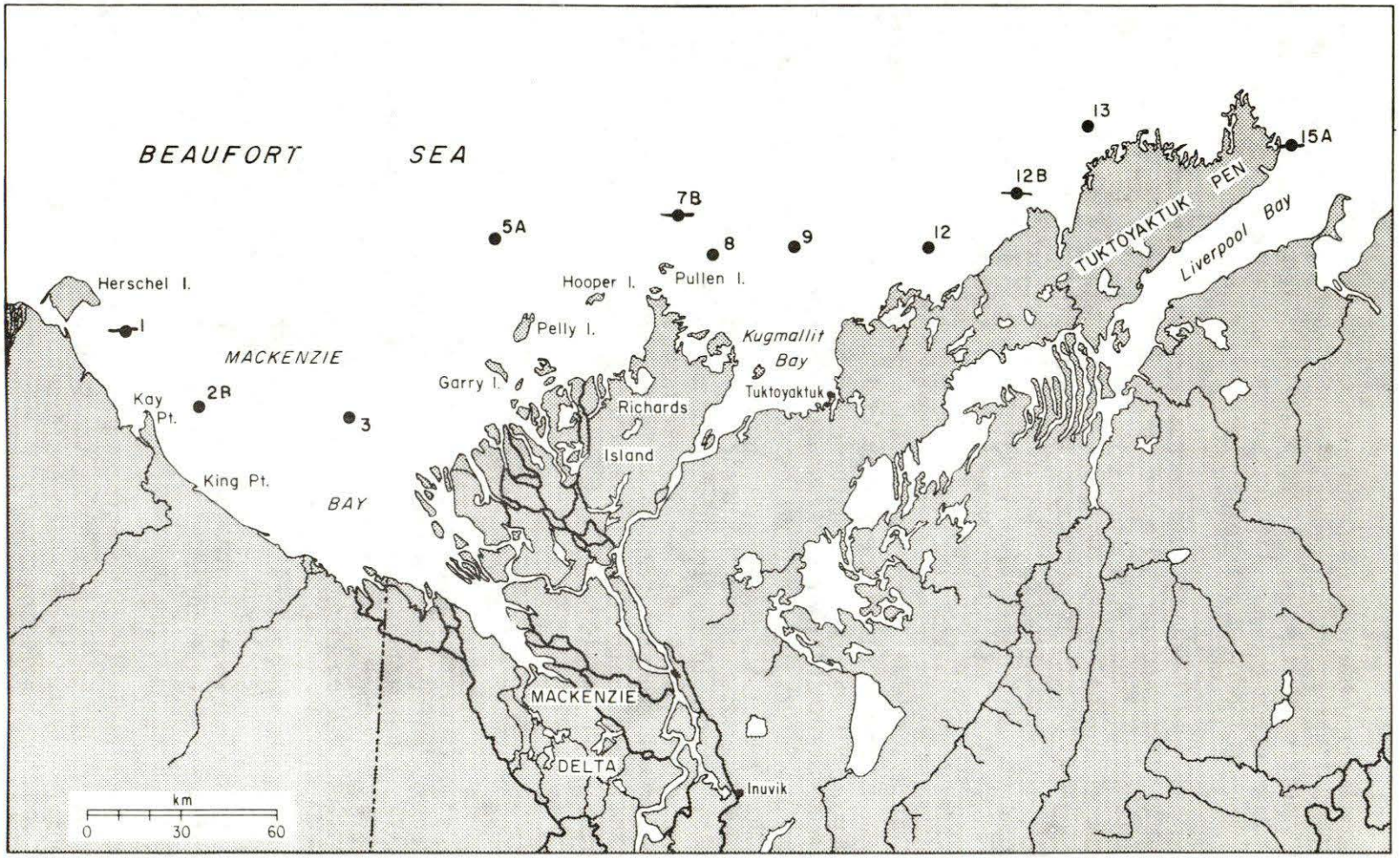

—●— ENGINEERING BORE HOLES PERMAFROST ENCOUNTERED

● ENGINEERING BORE HOLES PERMAFROST NOT ENCOUNTERED

Fig. 3-1 Location of A.P.O.A. shallow drillholes (after Mackay, 1972).

Tordon (1969) encountered frozen ground beneath Deception Bay in northern Quebec.

Seabottom sampling during the Beaufort Sea portion of the Hudson-70 cruise (B. Pelletier, G.S.C., pers. comm.) encountered evidence of frozen materials on the seabottom. Samples taken in the vicinity of a point 30 km north of Cape Bathurst showed evidence of ice lensing in both fine-grained and coarse-grained materials.

Shearer et al. (1971) describe numerous underwater seabottom mounds mapped on the outer portions of the shelf by shallow reflection seismic studies. These have been interpreted as pingoes formed in the bottom of ancient lakes subsequently inundated by rising sea levels. Formation of pingoes would require both seabottom temperatures below 0°C and sediments containing large quantities of low-salinity water (MacKay, 1973). A typical pingo-like seabottom feature is shown in Fig. 3-2. Some of these submarine peaks rise 30 m to within 15 m of the surface.

McDonald et al. (1973) have examined shot-hole data from near-shoreline seismic surveys along the Tuktoyaktuk Peninsula. The top of ice-bonded permafrost was mapped in detail in unconsolidated sediments composed primarily of silty sands. Wherever the sea was frozen to bottom in winter, i.e. in shallow water, ice-bonded permafrost was found within 5 m of the seabottom. However, the occurrence of a small amount of water below the ice cover could be correlated with considerable depths to the top of ice-bonded permafrost. A typical section from McDonald et al.'s work is shown in Fig. 3-3. Permafrost rises to surface beneath offshore spits as abruptly as at the mainland shore. Local unfrozen zones were encountered within the ice-bonded permafrost section.

3.2 Geophysical Evidence for Offshore Permafrost

Geophysical evidence for the existence of permafrost offshore has been given by Hunter (1973) and by Hunter and Hobson (1974). A marine seismic refraction technique, developed for shallow profiling, was employed in some selected areas of the Beaufort shelf. High seismic velocities observed at depth beneath the seabottom were interpreted to indicate the top of ice-bonded permafrost. A typical section is shown in Fig. 3-4 for an area north of Atkinson Pt. The top of the ice-bonded layer was mapped at depths down to 120 m below the sea-surface at water depths out to 40 metres. This work served to demonstrate the wide spread occurrence of sub-seabottom ice-bonded permafrost.

Direct current resistivity soundings made on the seabottom by Scott (1975) in the Kugmallit Bay area of the Beaufort Sea showed evidence of a highly resistive layer which could be interpreted as ice-bonded material at depth below seabottom.

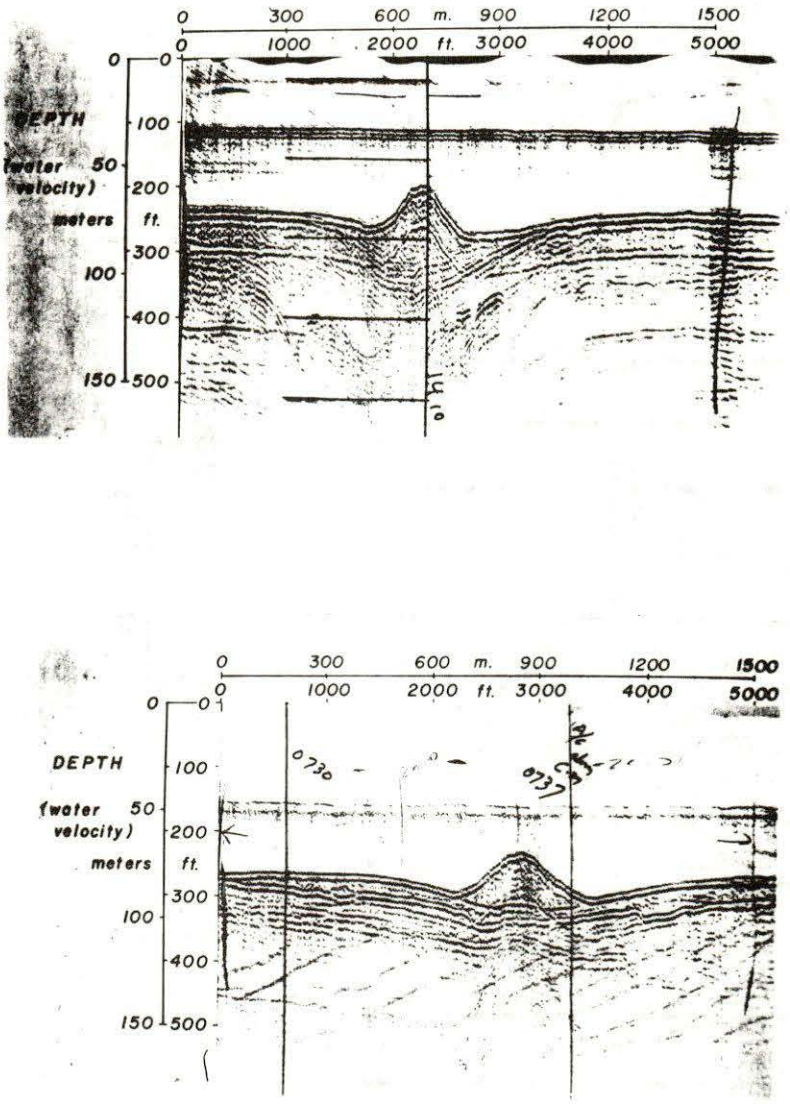

Fig. 3-2 Acoustic reflection profiles over pingo-like features in the southern Beaufort Sea.

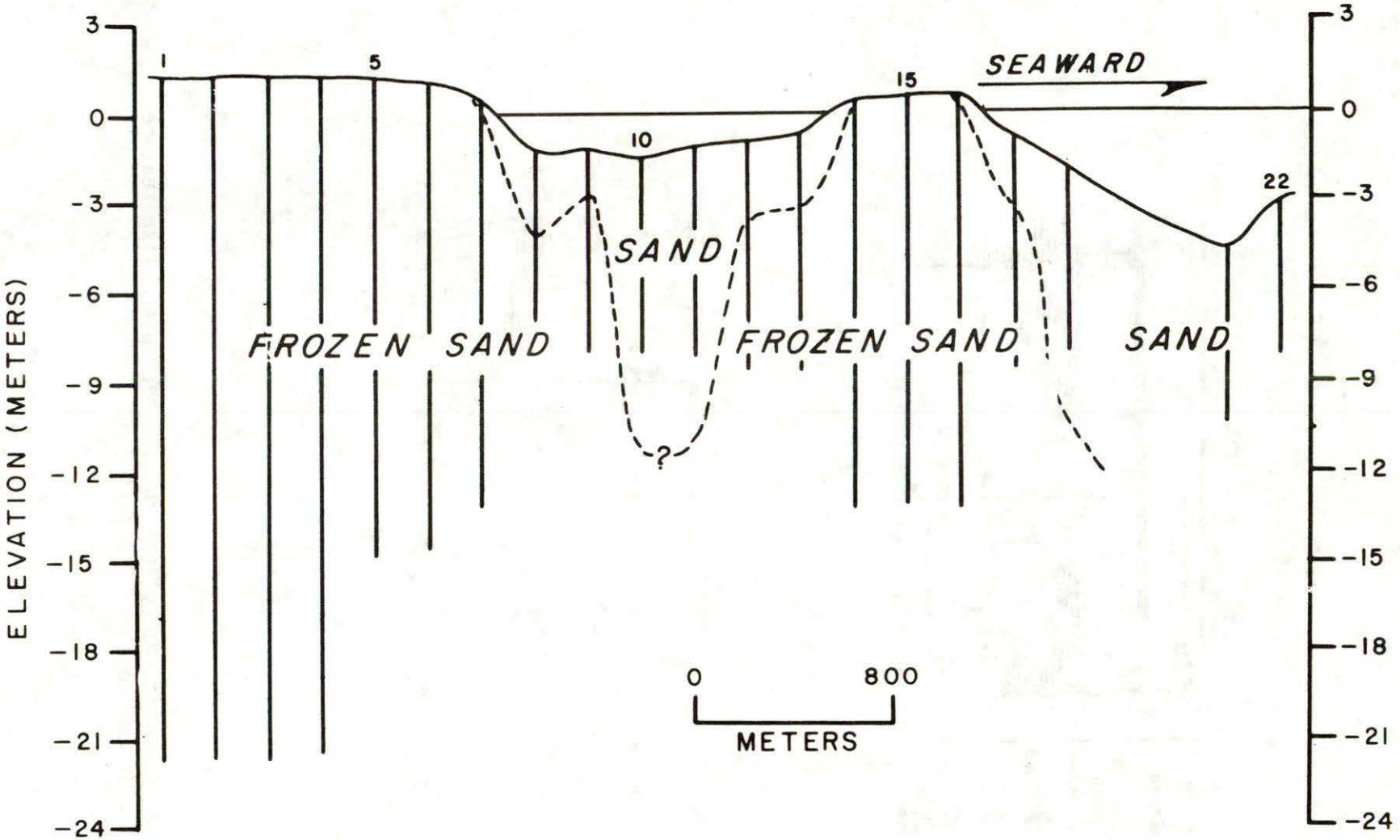

Fig. 3-3 A north-south geological section at the shoreline along the Tuktoyaktuk Peninsula from seismic shot-hole logs (after McDonald et al., 1972).

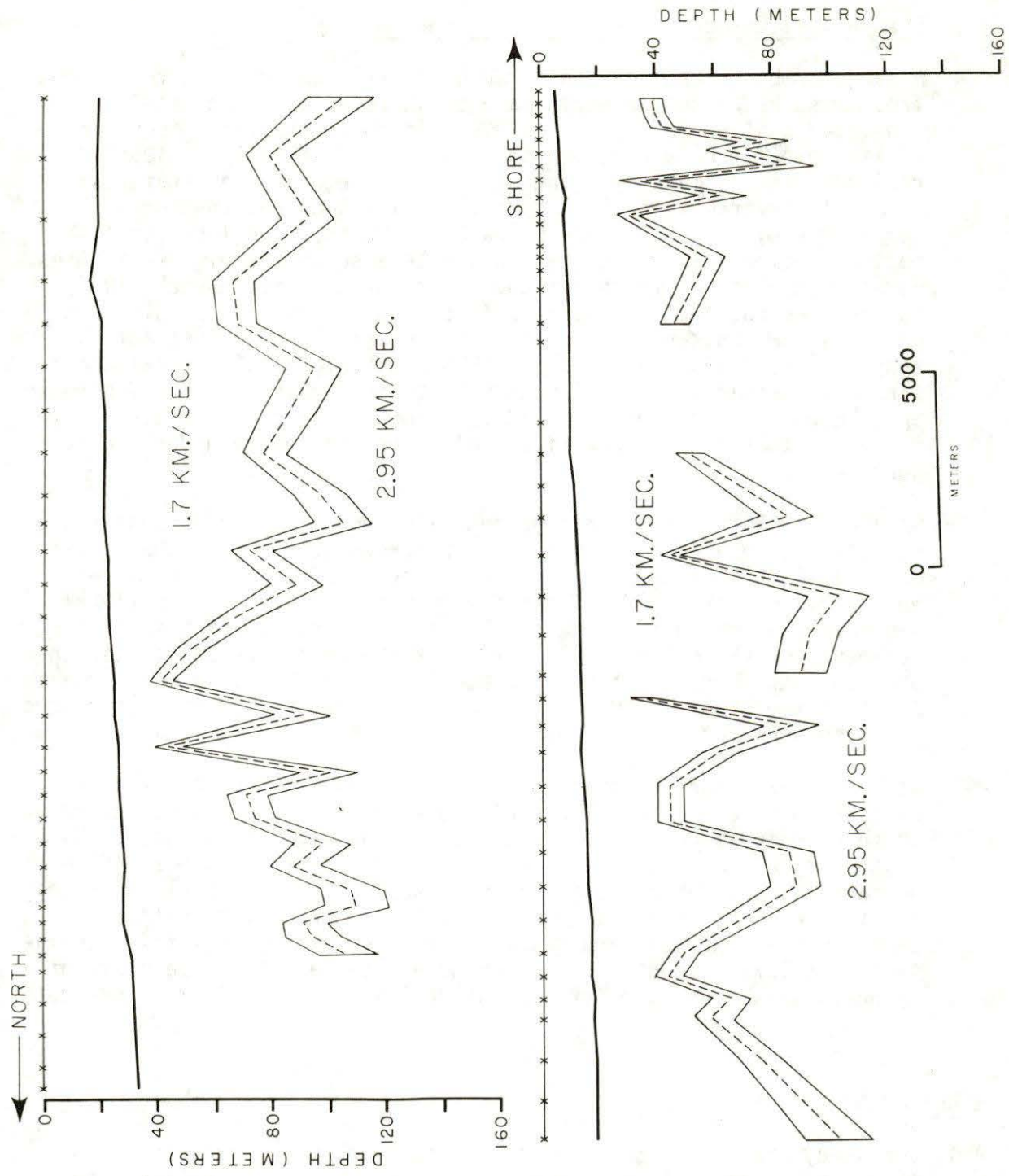

Fig. 3-4 Seismic refraction section north of Atkinson Pt. showing depth to top of ice-bonded permafrost (dashed line) with observational error limits (solid lines).

3.3 Theoretical Evidence for Offshore Permafrost

A large number of authors inferred on theoretical grounds that permafrost must be present beneath many offshore areas; Black (1950) suggested that permafrost up to 300 m in thickness might occur tens of kilometers from a northern shoreline. However, Black (1954) revised this estimate by pointing out that negative temperatures penetrate several kilometers into the polar seas and that ocean temperatures, in places, are below 0°C. He then concluded that the bottom sediments would contain no ice because of the high salinities. Permafrost, but not frozen ground, is present. Lachenbruch (1957) has pointed out that extensive offshore permafrost could only exist within a few thousand metres of northern shorelines unless active shoreline recession was occurring. Werenskiold (1953) likewise confirmed theoretically that frozen ground could exist 100 m offshore in Spitsbergen as had been observed in a local colliery. He also suggested that many narrow fiords might be completely underlain by permafrost.

Baranov (1959) mentions that perennially frozen ground is observed beneath the water in many recently submerged sections of the continental shelf bordering the northern shores of Siberia. Available evidence, however, was sufficiently sparse that Lachenbruch (1968) was only able to conclude that "the mean temperature of bottom sediments on the continental shelves of the Arctic Ocean is less than 0°C, and hence these waters are underlain by a thin layer of permafrost on the order of 30 m thick, or less. Whether or not ice occurs in these sediments is unknown."

MacKay (1972) observed that the sea-level history had resulted in exposure of the Beaufort Sea shelf for long periods of time during which permafrost could have grown to much greater thicknesses. Using an analytical conduction model he calculated that as much as 450 m of permafrost might underlie sections of the shelf. Judge (1974) using a numerical model calculated the probable general distribution of permafrost in the southern Beaufort Sea, suggesting that thick permafrost was largely confined to nearshore areas and the area north of Richards Island and the Tuktoyaktuk Peninsula to the 80 m water-depth contour.

4. STUDY AREA

4.1 The study area under consideration extends from Herschel Island on the west to the Baillie Islands on the east (see Fig. 4-1) and from the shoreline to the 200 m bathymetric contour line at the edge of the Beaufort shelf.

4.2 Relevant Geomorphological Seabottom Features

As seen from Fig. 4-2, a bathymetric chart of the Beaufort shelf, the study area is far from being monotonously flat. The largest feature is the Mackenzie Canyon, thought to be glacial in origin, and

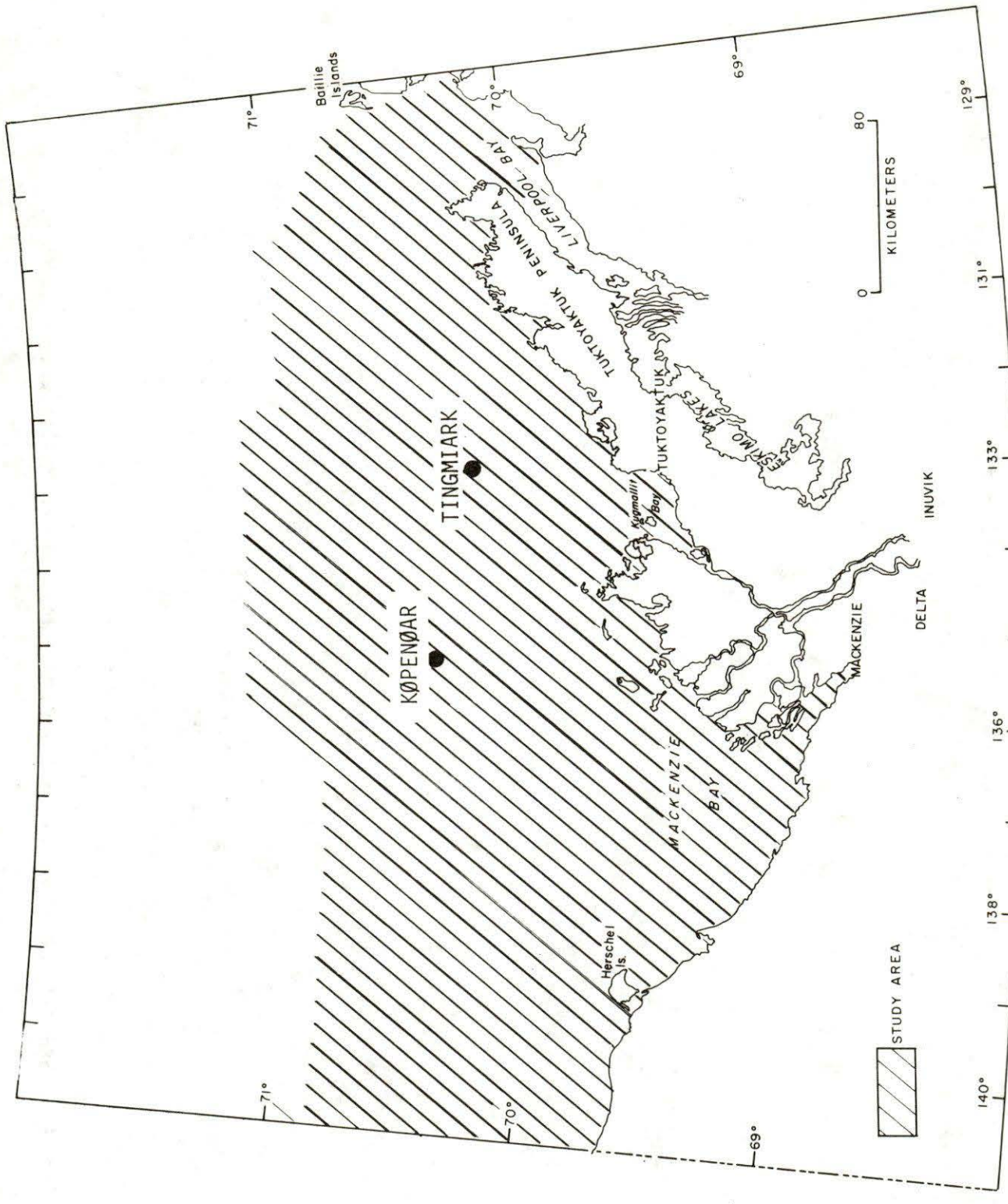

Fig. 4-1 Survey area showing the location of the two proposed drilling sites.

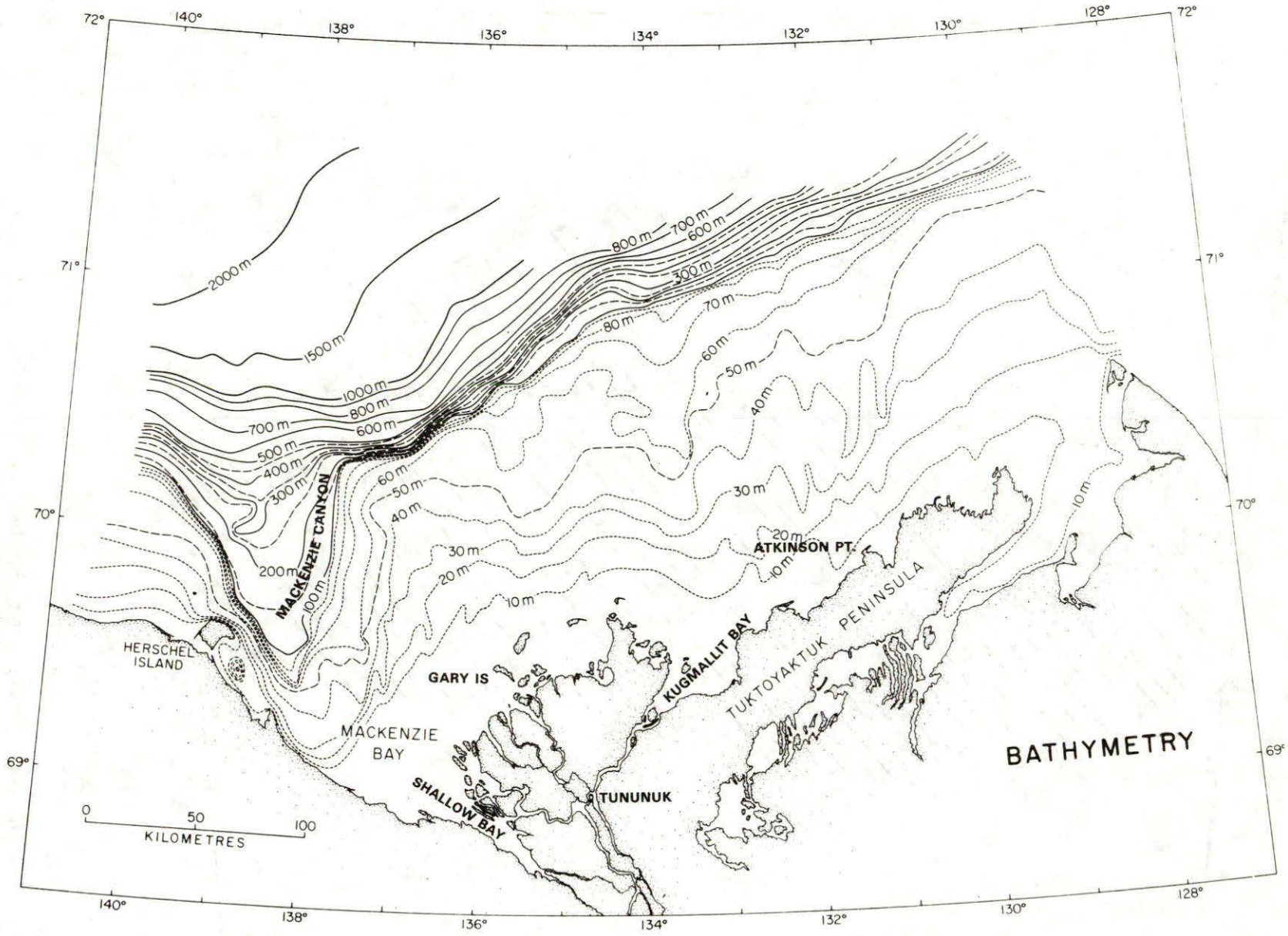

Fig. 4-2 Seabottom bathymetry in the survey area (after Pelletier, pers. comm.).

presently being filled in by Mackenzie River sediments in the Shallow Bay area. The eastern boundary of the Canyon can be traced inshore from Gary Island to Tununuk.

Other N-S trending seabottom troughs exist to the northeast of Gary Island, north of Kugmallit Bay, and north of Atkinson Pt. These are thought to be erosional expressions of old river valleys from some earlier time period of lower sea levels (J. Shearer, pers. comm.).

Further offshore (see Fig. 4-2) large areas containing numerous pingo-like features have been outlined. These features are found in water depths exceeding 20 metres primarily in the central and eastern portions of the study area.

5. METHODS AND SOURCES OF DATA

5.1 Geophysical Studies

The geophysical method most amenable to studies of the offshore permafrost is seismic refraction. The difference between seismic wave properties of frozen and unfrozen material form the basis of our seismic interpretation.

5.1.1 Compilation of laboratory data

Terrestrial field observations in Arctic and Antarctic areas (Barnes, 1966; Bush and Schwarz, 1964; Ferriens and Hobson, 1973; Hunter, 1973; Roethlesberger, 1972; Ogilvy, 1970; McGinnes et al., 1973; Bell, 1966) recorded very high compressional wave velocities in both unconsolidated surficial materials and in consolidated rocks. Several laboratory studies of various types of earth materials have been made Antsyferov et al., 1964; Apikaev, 1964; Nakano et al., 1971; Nakano and Froula, 1973; Muller, 1961; Kaplar, 1966; Kurfurst and King, 1971; Timur, 1968; Frolov, 1961; Nakano and Arnold, 1973; Frolov and Zykov, 1971; Zykov and Baulin, 1973; Dzhurik and Leshchikov, 1973; Gagne and Hunter, 1975; Kurfurst, 1976). The highlights of these studies have been summarized in Appendix B. The following generalizations can be made for unconsolidated materials:

a) The velocity of ice-bonded frozen material is greater than that of the unfrozen state. Changes in magnitude up to five times the unfrozen velocity can occur.

b) The compressional wave velocity in both fine- and coarse-grained materials varies directly as the amount of intergranular ice for values in the range 0-40% by volume ice.

c) The rate of change of compressional velocity with temperature, in the temperature range of natural occurring permafrost, varies directly as the grain size of the

material. Hence, most clays at -2°C exhibit velocities only slightly higher than that of the unfrozen state; whereas sands and gravels containing intergranular fresh water, which are almost completely ice-bonded at -2°C, exhibit high velocities compared to the unfrozen state.

An example of the variation of compressional velocity with temperature for sand and clay containing pore water with no dissolved salts is shown in Fig. 5-1. If either temperature or mean grain size is known, field measurements of compressional velocities can be used to estimate the other parameter. The presence of dissolved salts in interstitial pore water, however, lowers the freezing point such that coarse-grained sands and gravels may contain no interstitial ice at -2°C and seismic velocities may be identical to those above 0°C (e.g. 35°/$_{oo}$ sea-water, ice appears at -2.1°C).

In field situations where no data is available on sediment temperature, grain size, or pore water salinity, seismic compressional wave velocities may serve only as a qualitative estimate of ice content. The velocities of ice-bonded sands and gravels with no observed excess ice (in the range of 30% by volume ice), are in general much higher than the compressional velocities of massive ice lenses (Hunter, 1973; Gagne and Hunter, 1975) and it is not possible to distinguish ice lensing on the basis of seismic velocities; a frozen silt with ice content in the order of 20% by volume may exhibit a velocity close to that of fresh water ice.

The occurrence of ice-like substances, known as "gas hydrates", in exploration wells in the Mackenzie delta has been documented by Bily and Dick (1974). Gas hydrates may exist over a broad range of temperatures up to 20°C and at overburden pressures as low as 0.41 MPa (Katz et al., 1959; Deaton and Frost, 1946). In the Mackenzie delta, gas densities do not exceed 0.65. Hydrates formed from such gases are stable at 0.69 MPa (Bily and Dick, 1974). Few seismic velocity measurements have been made of materials containing these substances. Stoll et al. (1971) and Stoll (1974) have obtained laboratory acoustic velocity measurements of sands containing methane hydrate. Velocities obtained range between 2000 and 2700 m/sec for temperatures between +2°C and +8°C and for pressures between 4.8 and 8.3 MPa. From these results, it is suggested that gas hydrate-bonded surficial unconsolidated materials may be seismically indistinguishable from ice-bonded permafrost.

5.1.2 Seismic refraction studies

The existence of ice-bonded permafrost at depth between the seabottom, from the point of view of seismic surveying, lends itself to interpretation by the refraction method. The basic criterion for the successful application of this technique is

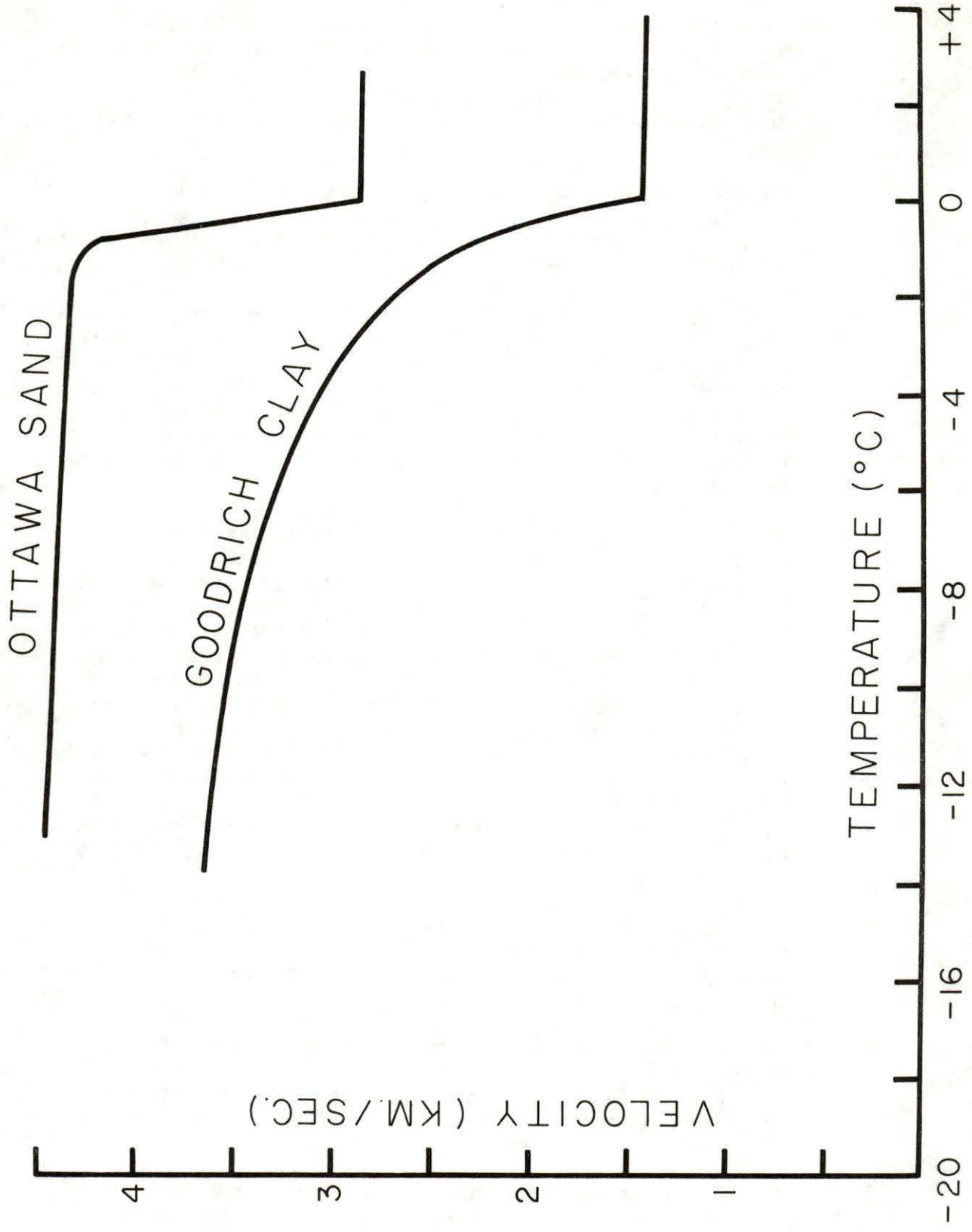

Fig. 5-1 Typical compressional velocity vs temperature for water-saturated sediments (after Nakano et al., 1971).

the continual increase of seismic velocities with depth in the geological section. The velocity model applicable to the Beaufort Sea consists of a low velocity water layer (1420 m/sec) overlying unfrozen bottom sediments (1420-2000 m/sec) which in turn overlies ice-bonded frozen materials (2000-4500 m/sec).

Unfrozen consolidated sedimentary rocks (shale, sandstone) exhibit velocities in the range of frozen ice-bonded unconsolidated materials. However, much of the southern Beaufort Sea shelf area is thought to be underlain by a thick sequence of unconsolidated Tertiary and Quaternary muds, silts and sands (Hofer and Varga, 1972). Generalized velocity sections from analyses of reflection seismic records of the Mackenzie Bay area (see Fig. 5-2) indicate more than 1000 m of sediments with velocities less than 2000 m/sec. Hence for most of the area, no ambiguity in the interpretation of ice-bonded permafrost should occur; a special case is made for the shoreline area of the southern Mackenzie Bay and it will be dealt with in a later section.

The seismic refraction method is illustrated in Fig. 5-3. Seismic rays radiating from a point source pressure pulse (dynamite or air-gun array) are refracted through the water, sediments, and ice-bonded permafrost. Refracted energy from the two lower high velocity layers is continuously radiated upwards into the water column. At large distances from the source, energy from these high velocity layers constitutes the first arrival event at the surface detectors. Analysis of the travel times of first arrival events along the detector array yields velocities of the underlying layers. These, in conjunction with the "break-over" distance (the shot-detector distance denoting the onset of first arrival energy from a lower layer) can be used to compute the depths to these layers using standard refraction computations as outlined by Dobrin (1970).

The Geological Survey of Canada has developed a marine refraction array for use in mapping of shallow high velocity refractors. Details of the method have been given by Hunter and Hobson (1974) and Hunter et al. (1974). The array consists of 24 hydrophones placed in-line at 15 m intervals. A dynamite source is detonated off one end of the array yielding a "single-ended" refraction profile. The accuracy involved in this type of refraction shooting in the case of dipping refractors and the errors involved in detector array curvature are examined in detail in Appendix C.

The GSC refraction array has been operated from a variety of small vessels in various near-shore areas of the Beaufort Sea and the results have been published by Hunter (1973); Hunter and Good (1974); Hunter et al. (1974); Hunter and Hobson (1974); Carson et al. (1975). As well, surveying continued in the 1975 field season from the *M.V. Pressure Ridge* and the

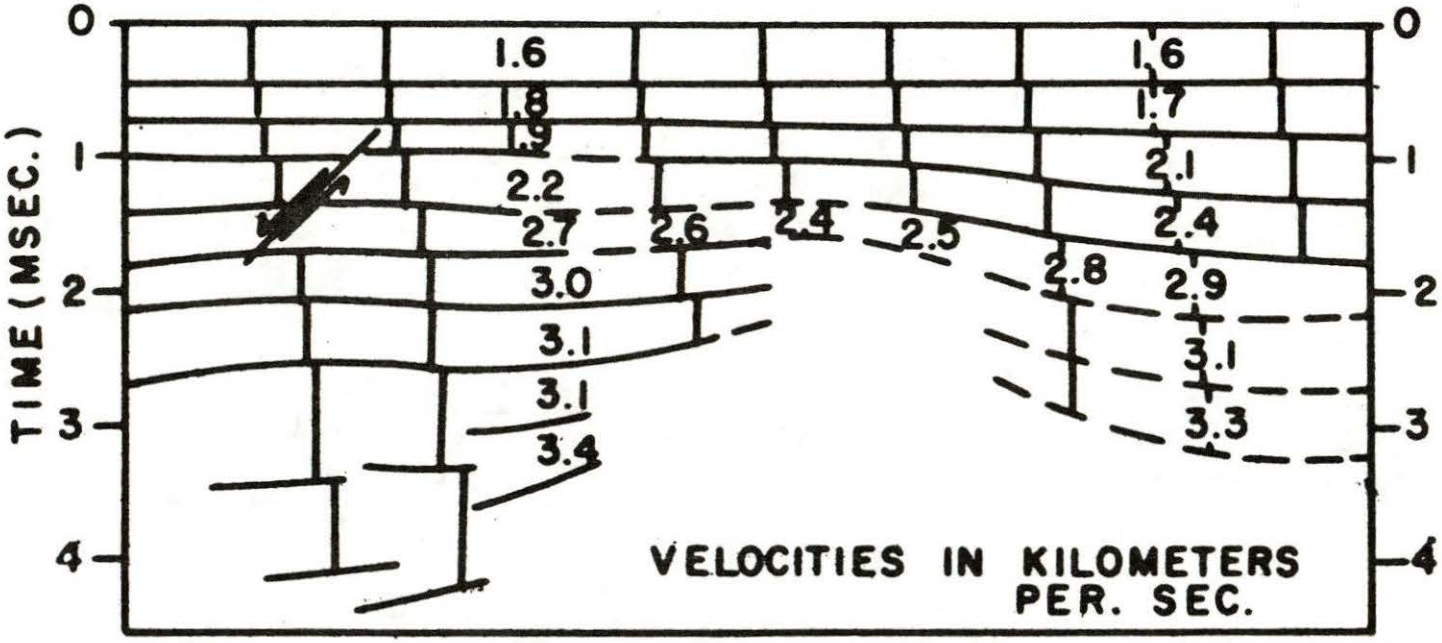

Fig. 5-2 Velocity-depth section for the Mackenzie Bay area (after Hofer and Varga, 1972).

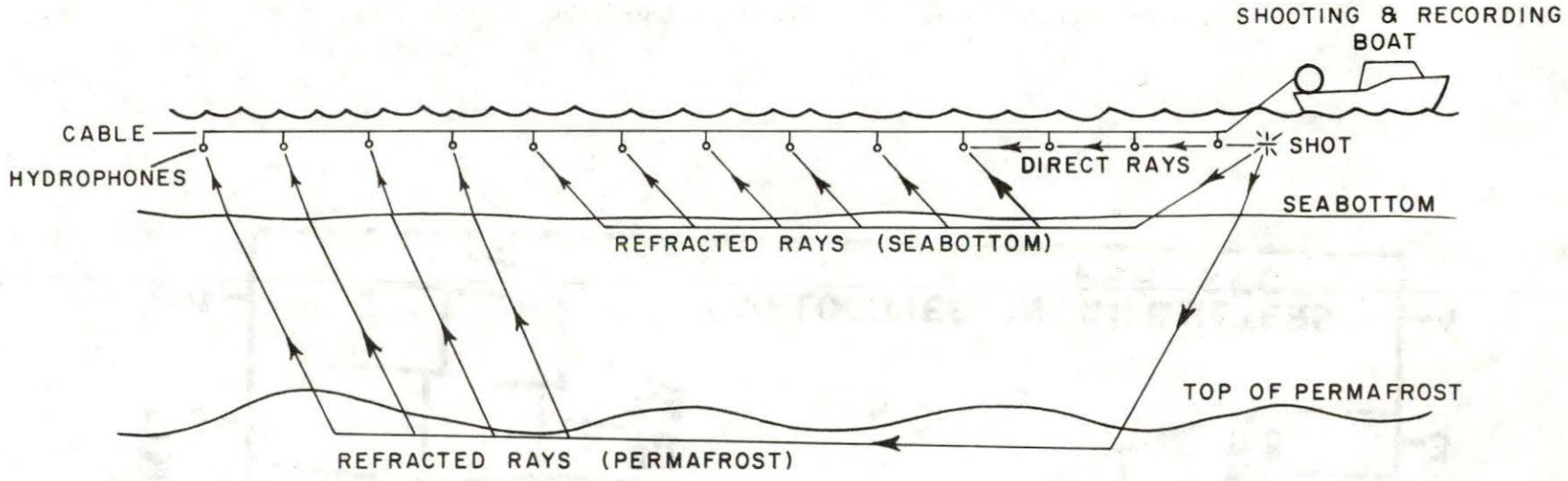

Fig. 5-3 The marine seismic refraction technique.

C.C.G.S. Nahidik. Fig. 5-4 is a compilation map of all GSC refraction lines from 1971 to 1975. Detailed seismic sections for each of the survey lines are given in Appendix D.

The GSC array is limited in depth of penetration by the shot-detector distance. The depth limitation is also in part dependent upon velocity contrasts between refractors; for contrasts found in the Beaufort Sea the approximate limit of penetration is 130 m from sea surface.

Frequency response of seismic signals depends upon the initial spectrum of the source, the distance travelled by the pulse, the attenuation coefficient of the medium and, in the case of thin refracting layers, the layer thickness and velocity contrast. For this array the observed centre frequency of recorded pulses is approximately 100 hertz at the farthest shot-detector distance; hence thin ice-bonded permafrost layers (5-10 m thick) can be detected by the array.

An example of a seismic refraction record shot in the Beaufort Sea is shown in Fig. 5-5. Here, because of shallow water and a small velocity contrast between water and sediments, only two layers are interpreted.

5.1.3 Seabottom refraction profiling

In addition to the sea-surface array outlined above, the GSC has been experimenting with a refraction array which can be deployed on bottom. This array is 180 m long with a 15 m spacing between hydrophones (see Fig. 5-6). Small explosive sources are detonated off each end of the array; positioning of the hydrophones with respect to the source can be done by measuring the water-wave arrival time. The array was successfully deployed through leads in the sea-ice during April 1975 at eight sites in the offshore shelf area, including both the Kopenoar and Tingmiark proposed drill sites (Fig. 4-1).

5.1.4 Compilation of industry seismic data

At the successful conclusion of initial experiments with the GSC refraction array, it was felt that the first arrival refractions on marine reflection records of exploration companies involved in offshore oil and gas exploration should be examined for high velocity near-surface events. Such records are specifically electronically tailored to enhance deep reflected events, and the first arrival events are usually attenuated. On the other hand, the hydrophone arrays used are generally long (2400 m) compared to the GSC array (400 m) and the source used, an air gun array, is of high energy with a low centre frequency (for low attenuation); hence the possibility of deeper penetration.

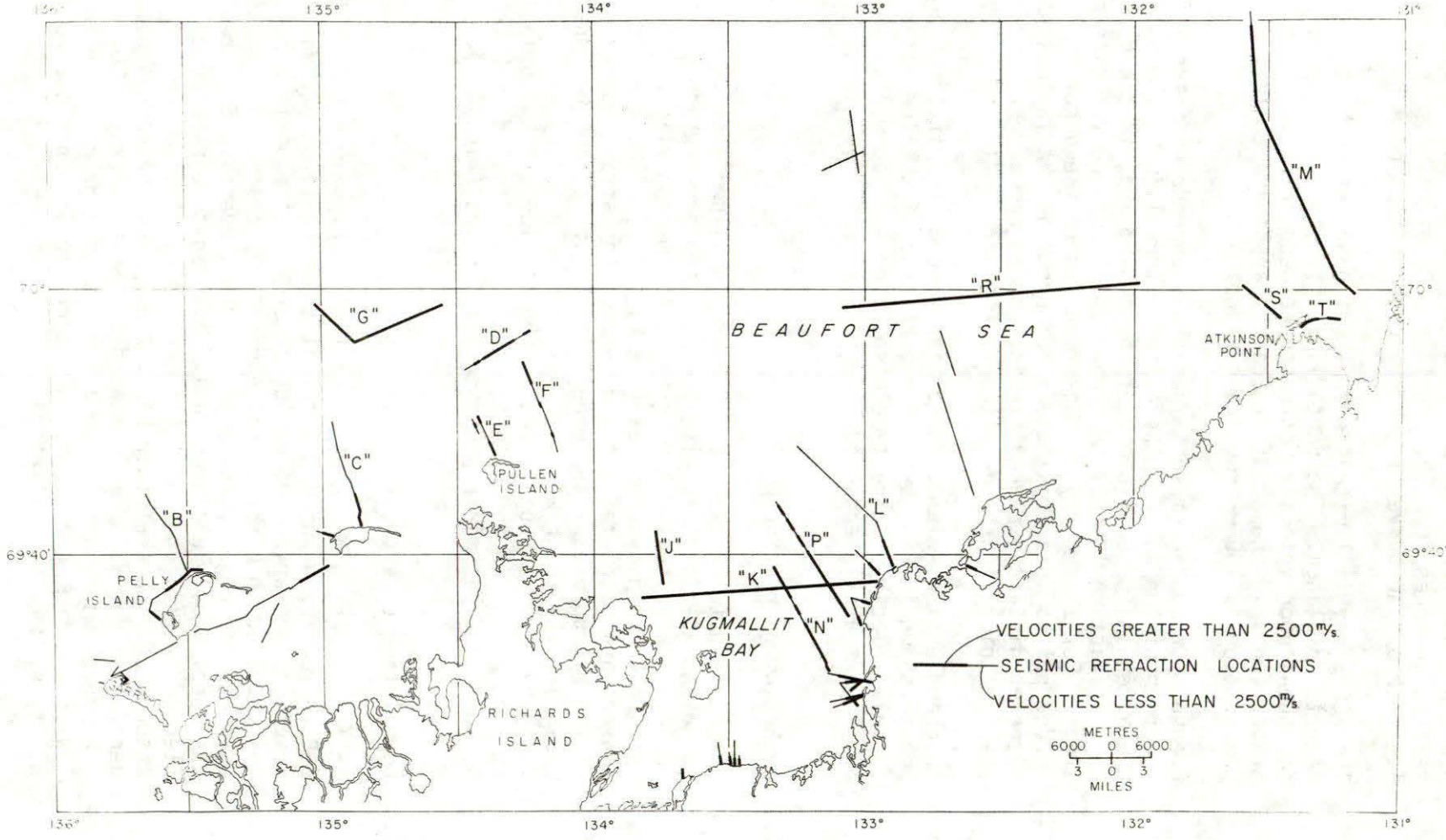

Fig. 5-4 The location of refraction profiles shot with the GSC array during the 1971-1975 field seasons.

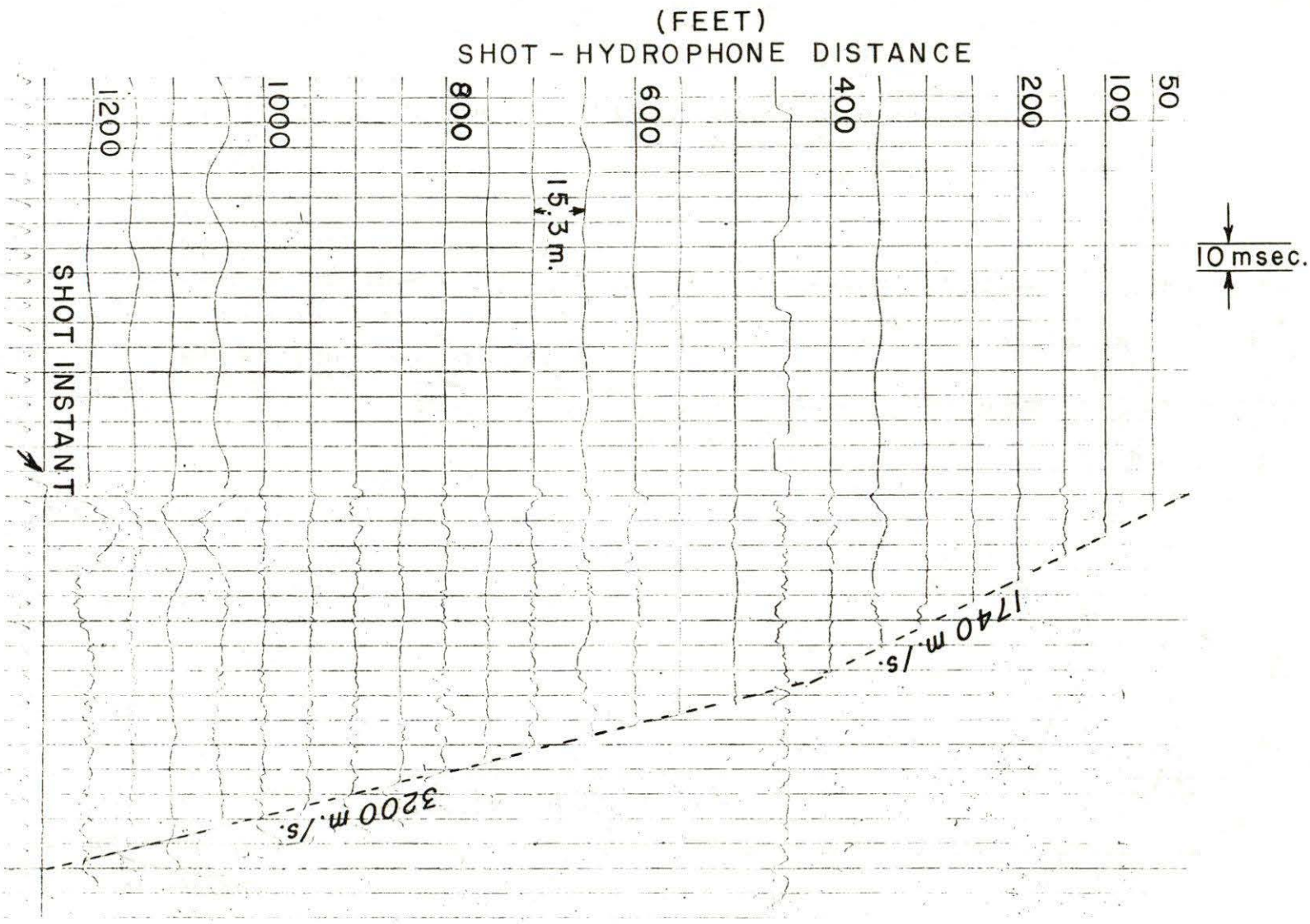

Fig. 5-5 A typical marine refraction record taken with the GSC array.

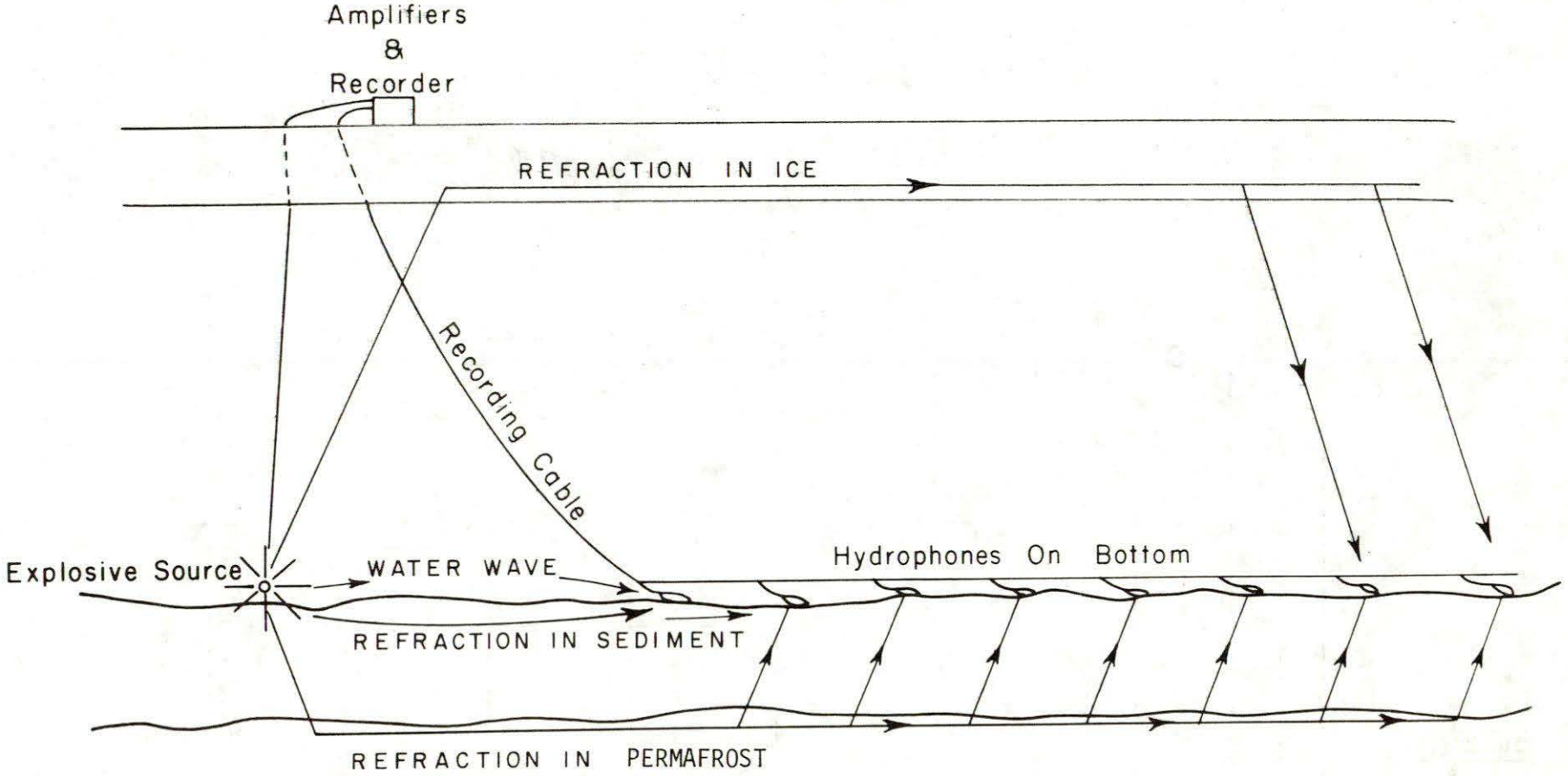

Fig. 5-6 The GSC seabottom refraction array configuration.

A pilot test was arranged with Gulf Oil Canada Ltd. to test the feasibility of the proposal. Approximately 60 line miles of uncorrected monitor records were examined from a survey area approximately 10 miles north of Pullen Island. The results of this test are summarized in Appendix E. Most of the records examined contained some evidence of high velocity refractions. The amplitudes of these refracted events were of poor quality, demonstrating rapid attenuation and the phenomenon of "shingling" (apparent transfer of energy from the first to later cycles of the refracted events as shot-detector distance increases). However, most records could be adequately interpreted and depth determinations to the top of the high velocity layer could be made.

As a result of the successful pilot test, the remainder of the companies involved in offshore exploration were canvassed for their support and contributions. Approximately 40,000 seismic records were obtained from survey lines from the shoreline to the edge of the shelf. The records were replayed for our use without normal move-out corrections, and wherever possible, with true amplitude recovery. Later reflected events were de-emphasized in deference to the first arrival refracted energy. In order to examine all the records in a short time interval, it was decided to dispense with individual trace examination and to develop graphical overlays to obtain approximate velocity estimates. This was done at the expense of fine structure along each refractor; however, the average depth to the refractor horizon was computed using the "intercept time" method of interpretation (Dobrin, 1970). The velocity of the upper sediment layer is not well determined from the industry records since it manifests as a later arrival with a poorly defined onset time. Measured values agreed closely with those observed with the GSC refraction array and an average velocity of 1615 m/sec was used throughout the survey area in depth calculations.

Interpretation quality varied throughout the survey as a result of systematic changes in record quality and the measurement accuracy from different types of record displays. The everage error assigned to depth determination from measurement limitations is ± 20 m. Errors in depth determination resulting from average dip of the refractor over the length of the array has been mentioned previously and is given in Appendix C.

The records examined constitute approximately one-third the total number offered to us by the companies for interpretation. Survey lines were selected for maximum coverage of the shelf in a reconnaissance manner. Hence, line spacings are approximately 6 km or more and record spacing along the lines varies between 0.5 and 1 km. Except for some of the inshore regions all records were obtained as stacked "pops" from air gun arrays. In the near-shore areas, records from conventional seismic arrays placed on landfast ice were used wherever

interferring high frequency seismic events were filtered out sufficiently to observe later events.

Fig. 5-7 shows a typical record suite for the outer shelf area. The detector interval is 100 m; first arrival events plot with a velocity of approximately 3000 m/sec. An earlier cycle of this event may be too low in amplitude to be recorded above the noise level; hence it is possible that depth determinations made from later cycles of the event would give a depth in excess of true depth. The amplitudes of the first arrivals attenuate rapidly with distance and "shingling" is evident on the records. There are no clearly identifiable shallow reflected events in the early portions of the seismograms. The presence of an ice bonded permafrost layer results in poor quality later reflected events. The permafrost layer acts as an energy trap resulting in shallow reverberations and filtering of later events.

Fig. 5-8 shows a record suite typical of those found in the inshore regions where thick ice bonded permafrost is thought to exist. In these areas the depth to the top of ice bonded permafrost can vary between 10 m and 200 m below seabottom. The first arrival energy is clearly traced across each record and attenuation of the signal with shot-detector distance is small. There are several strong reverberations with apparent high velocities which are probably trapped modes in the high velocity layer. Again, clearly discernible shallow reflections are not evident on the records.

Fig. 5-9 is a suite of records from an area where no high velocities were observed. The first arrival break shows strong amplitudes and a slightly increasing velocity with depth. Reflection quality of shallow reflected events is good since there is no masking by high velocity surface layers.

Fig. 5-10 shows a suite of records from the Mackenzie Bay area. Although a high velocity event has been identified, no ice-bonded permafrost has been interpreted. The refracted event is a single pulse, no later reverberation or shingling is evident and the quality of shallow reflected events is good. The depths to the top of this layer range from 400 m to beyond 700 m below sea level. This anomalous high velocity layer is confined to the Mackenzie Bay area; a detailed discussion of one anomalous zone will be given in a later section (6.2).

5.2 Drilling Data

5.2.1 Onshore drilling

Several exploration wells have been drilled in the shoreline area and in the shallow waters offshore from artificial drilling-islands. The drill logs of most of these holes still

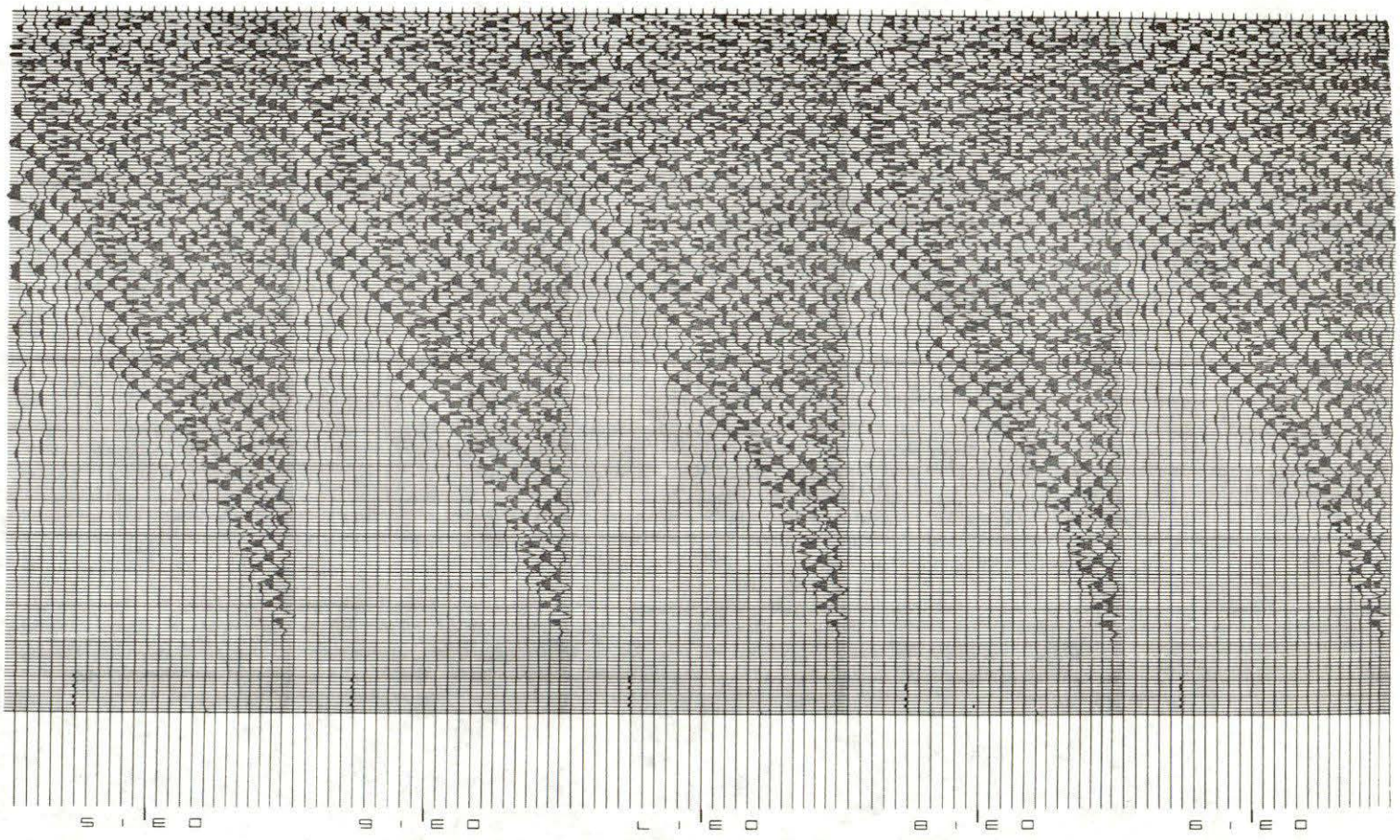

Fig. 5-7 Industry seismic records showing refraction arrivals from thin ice-bonded permafrost.

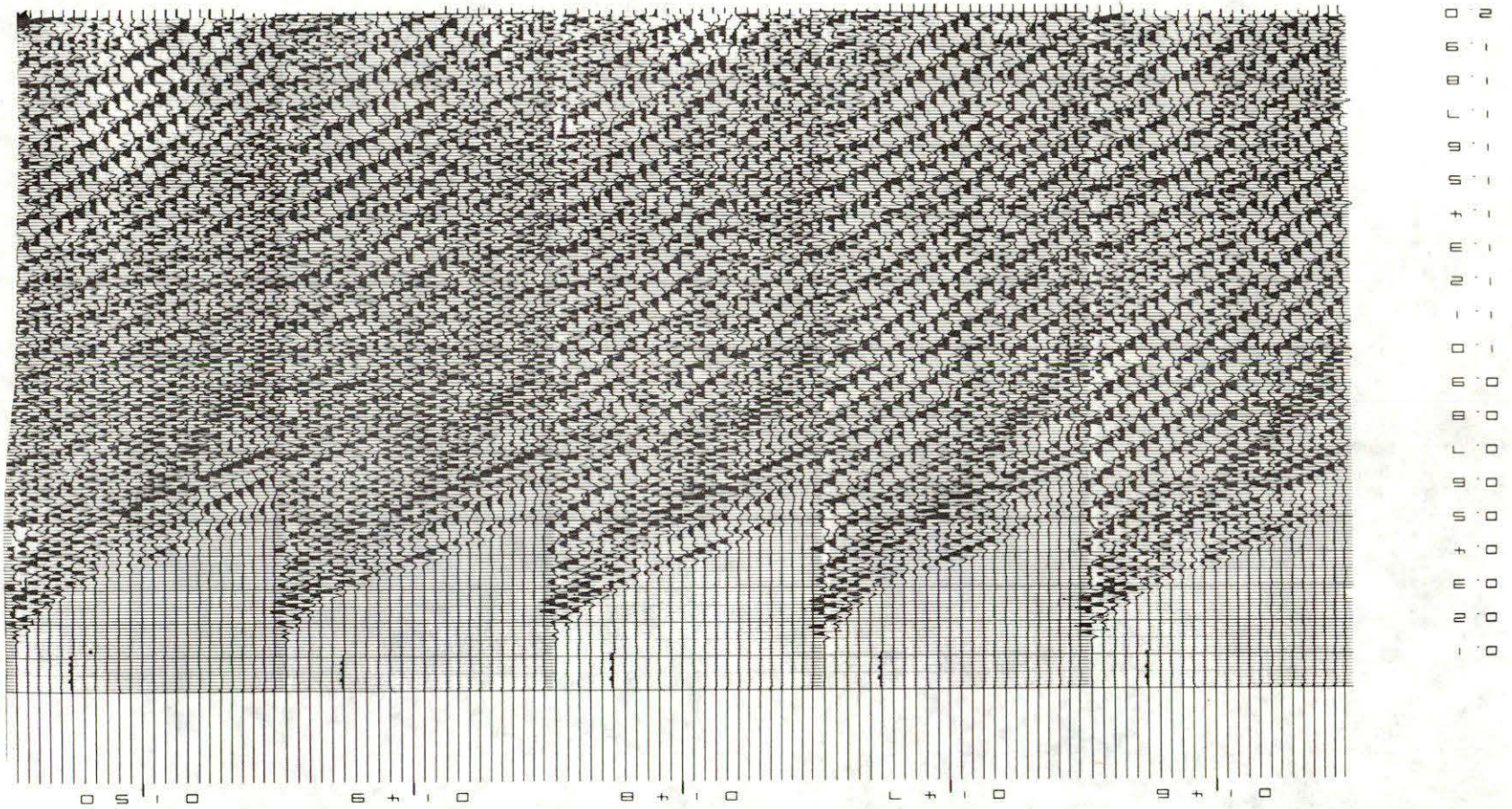

Fig. 5-8 Industry seismic records showing refraction arrivals from thick ice-bonded permafrost.

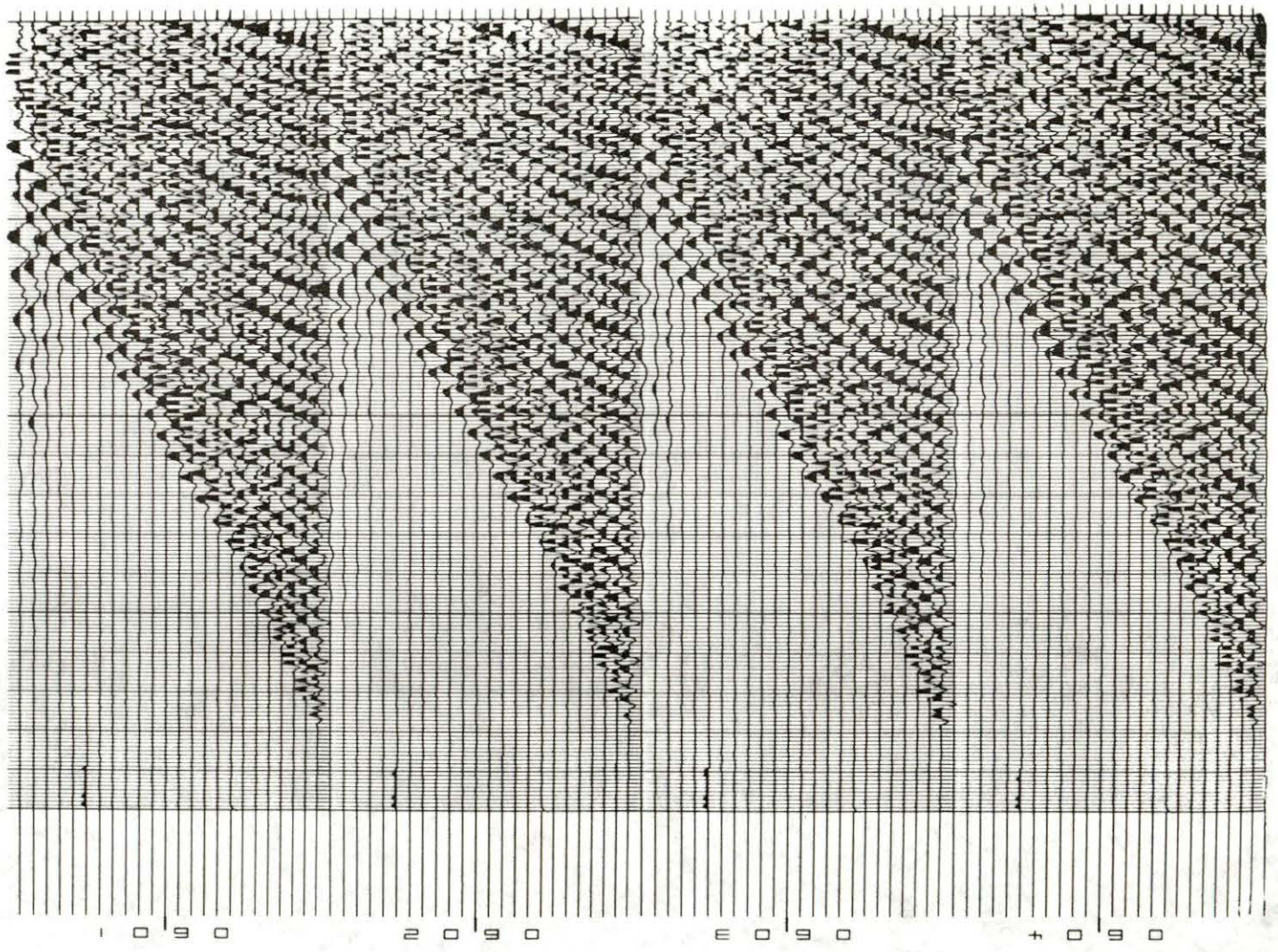

Fig. 5-9 Industry seismic records from Mackenzie Bay showing no high velocity refraction events.

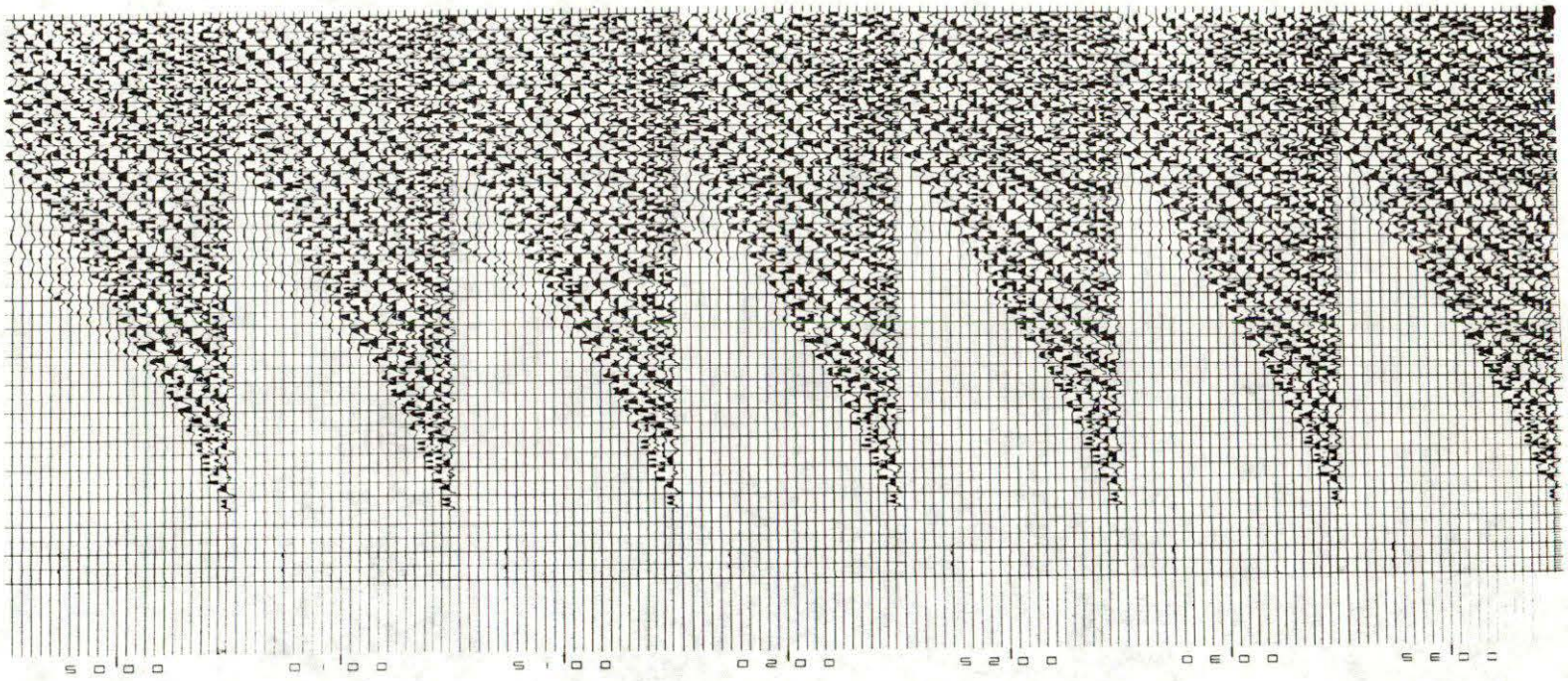

Fig. 5-10 Industry seismic records from Mackenzie Bay showing anomalous high velocity refractors not considered to be ice-bonded permafrost.

remain confidential information at the date of this writing. However, two of these wells with non-confidential status are of interest; these are Imperial Nuktak P-50 (Hooper Island) and Imperial Immerk B-48 (situated between Hooper and Pelly Islands, Fig. 3-1). The generalized geology and "crystal cable" up-hole velocity logs for the upper sections of the holes are shown in Fig. 5-11. From the log of the Hooper Island well it is apparent that the section is frozen and ice-bonded with relatively high seismic velocities from surface to a depth of 685 m. The Immerk well, on the other hand, contains ice-bonded material from only 150 m to 380 m below surface. No temperatures are available for the upper section and it is not possible to determine whether the upper section is below 0°C.

Although only one of the 9 wells drilled from offshore artificial islands is presently beyond the confidential period, sub-surface temperatures have been determined at three of the island sites to date and these results are in the public domain. Sun Oil Company Ltd. installed shallow thermistor strings at Unark L-24 (Richards Island near-shore) and Pelly B-35 (Pelly Island near-shore), the results of which were reported by Brown and Barrie (1976); and Imperial Oil Ltd. installed a deep cable at Adgo P-25 (near Gary Island) which has been read by EMR (Taylor and Judge, 1976). Extensive sub-surface temperature measurements have also been made at 25 wells in the onshore Mackenzie delta which, in view of the counterminous surface history of the on- and offshore, provide valuable background data. Profiles for those in which equilibrium or near-equilibrium temperatures have been achieved, or can be predicted are shown in Appendix D. The permafrost distribution determined from these results is shown in Fig. 5-12.

Accurate determinations of permafrost occurrence at the shoreline is important to the understanding of the offshore régime. As further well information becomes available to the public, it may be possible to correlate permafrost characteristics from hole to hole and with offshore occurrences.

5.2.2 A.P.O.A. drilling

The Arctic Petroleum Operator's Association shallow drilling program on the Beaufort Sea shelf has been mentioned in section 3.1. In addition to mapping the occurrence of ice-bonded permafrost, the program yielded information on the near-surface stratigraphy. Fig. 5-13 is a generalized section composed from all the drill logs as taken from A.P.O.A. report #13. West of Richards Island the thickness of the surface silty clay layer increases rapidly, representing an ancient in-filled proto-Mackenzie delta. Superimposed on this is the Mackenzie Canyon which in turn receives most of the sediment discharge from the modern Mackenzie River.

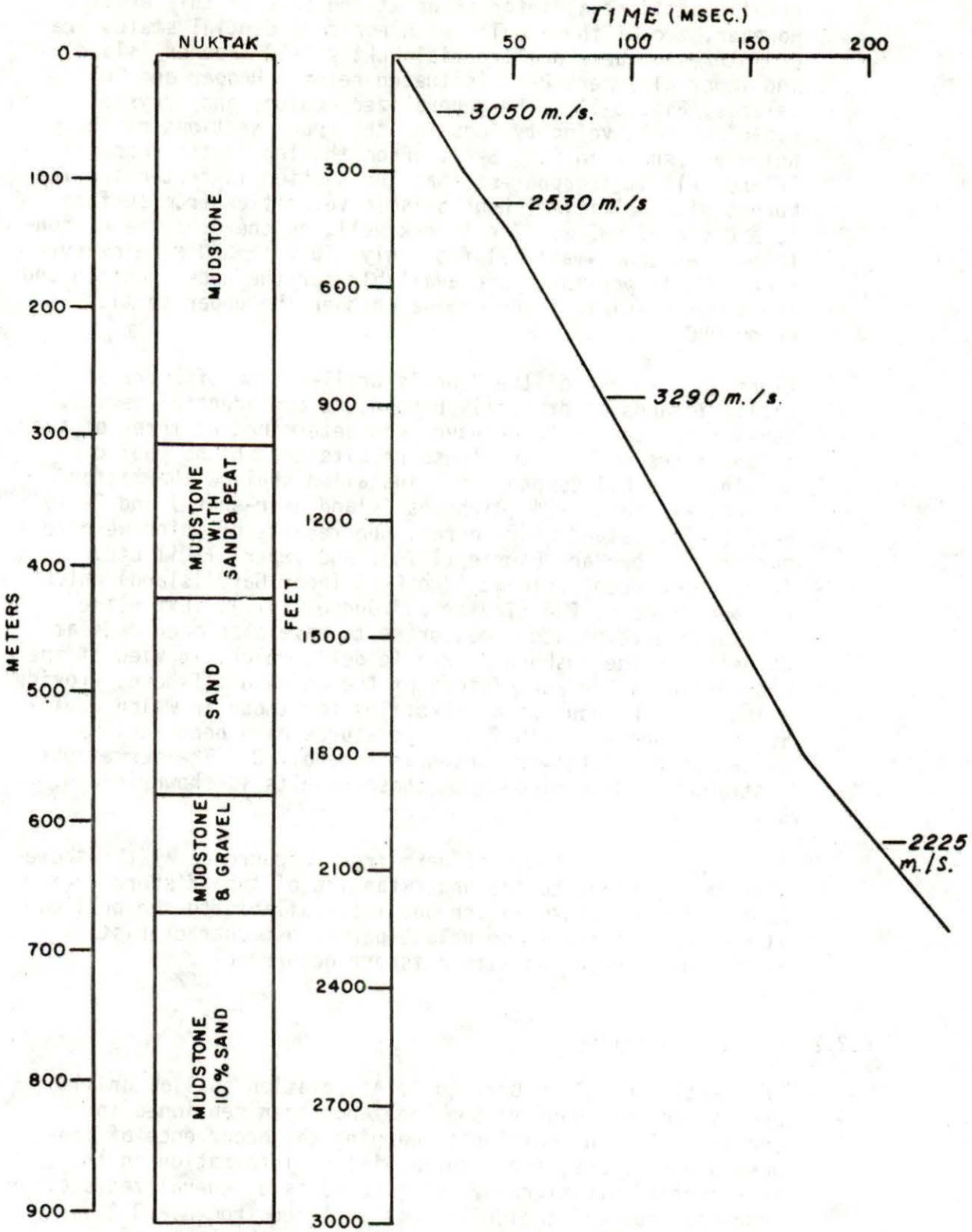

Fig. 5-11(a) Generalized geology and crystal cable velocity log from I.O.E. Hooper Naktak C-22.

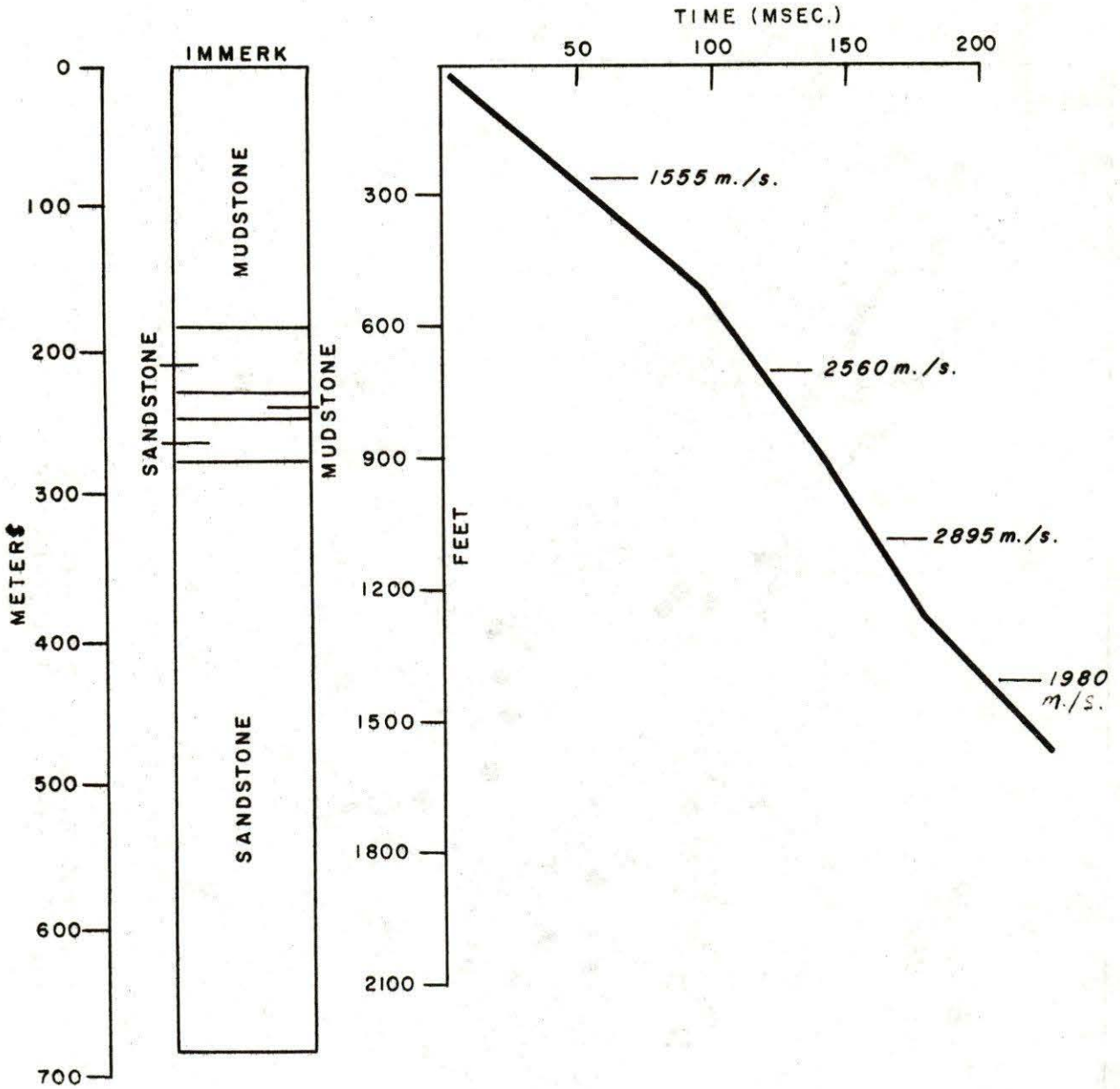

Fig. 5-11(b) Generalized geology and crystal cable velocity log from I.O.E. Immerk B-48.

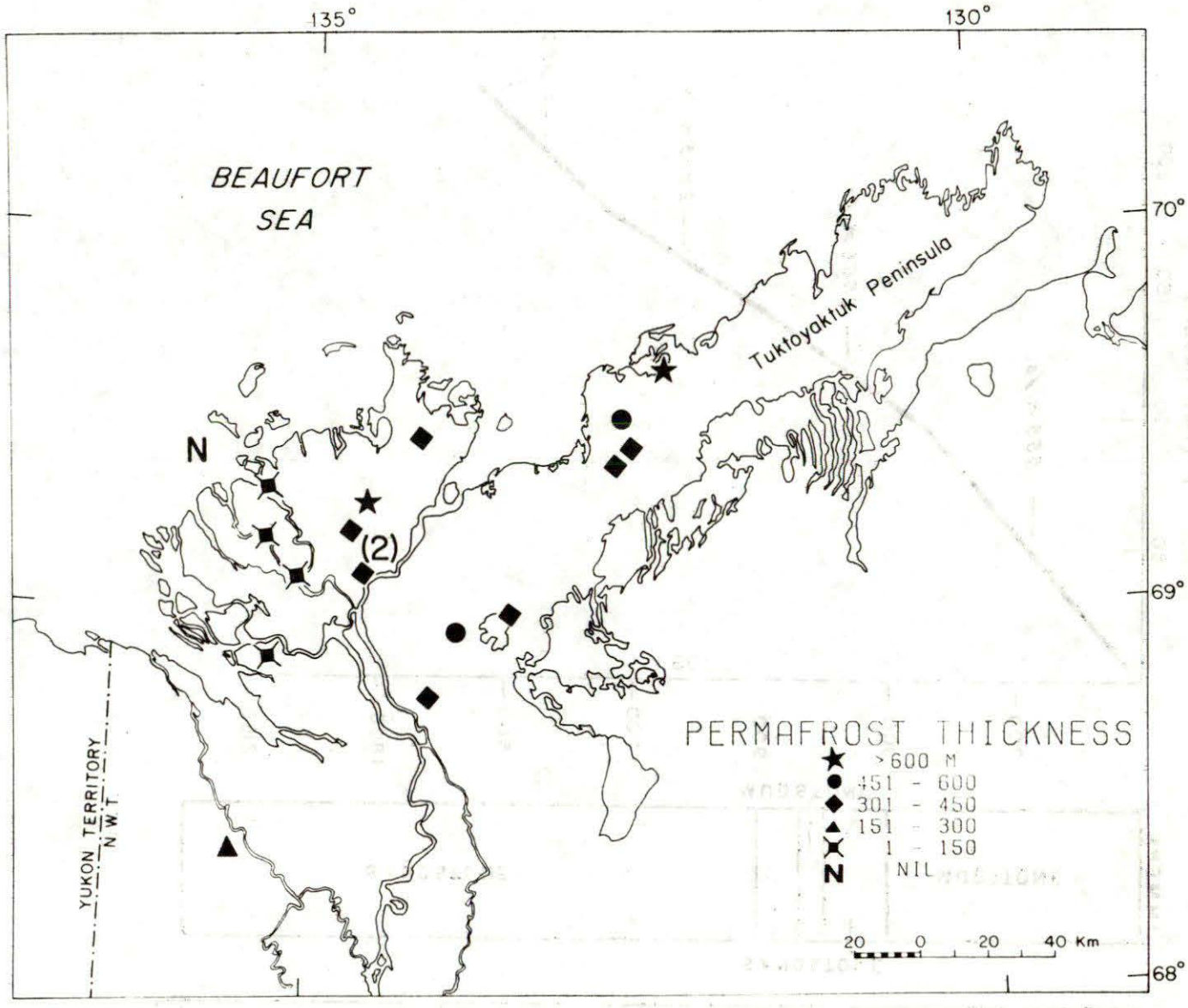

Fig. 5-12 Permafrost thickness determinations in the Mackenzie delta-Beaufort Sea region. (Depths given in metres.)

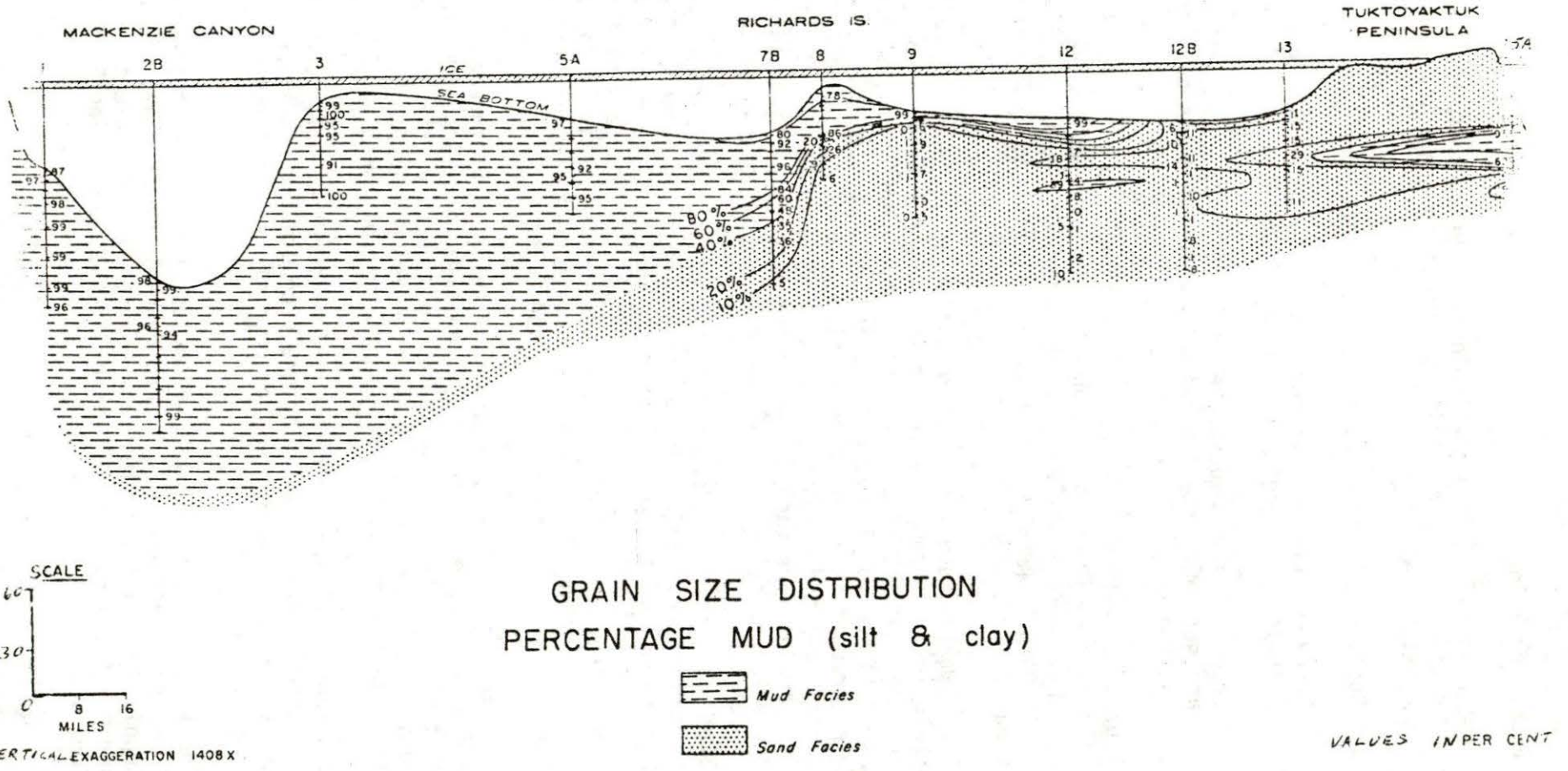

Fig. 5-13 East-west geological section showing grain size of (unconsolidated) sea floor materials in the near-shore area of the Beaufort Sea (from A.P.O.A. project report #4, M.M. Lerand, 1971).

5.2.3 G.S.C. drilling

In the spring of 1974 the Geological Survey of Canada supported an offshore drilling program in Kugmallit Bay near Tuktoyaktuk, NWT to

a) Confirm the nature of the seismic refractor

b) Recover frozen and unfrozen cores to determine their lithology and engineering properties

c) Determine the temperature profiles beneath the seabottom and determine the thermal properties of the seabottom materials.

Four holes were drilled at the locations shown in Fig. 5-14 with a portable and skid-mounted Helli-Drill on contract from Big Indian Drilling Co. Ltd. On-site logging, sampling and drill hole temperature readings were performed by EMR personnel.

Core samples were taken with modified split barrel (spoon) and Shelby carbide samplers to prevent sample contamination by the drilling mud. Unfrozen samples were placed in plastic bags and retained for laboratory examination. Frozen core samples were wrapped in aluminum foil, plastic-bagged, and placed in styrofoam-lined boxes to prevent thawing while in transit. The samples were then tested in the laboratory for grain size, thermal conductivity, moisture content and pore-water salinity.

Downhole temperature observations were made as frequently as the coring program and the state of the hole allowed. The equipment used for the measurements was similar to the "portable mode" described by Judge (1973). The accuracy of the sensor used was ± 0.01°C and accuracy in determining sensor depth ± 0.05 m. Mud temperatures were monitored in drill-holes 1 and 2 using similar equipment and a sensor accuracy of ± 0.1°C.

Loss of circulation and cave-in while drilling through sands and gravels were the two major and time consuming problems that plagued the drilling operations. Future drilling through similar type deposits might be improved considerably if a drill unit using hollow drillstems were employed.

The four drillholes in Kugmallit Bay penetrated varying thicknesses of clays and silts before encountering sands and gravels. The stratigraphy for each of the drill-holes is shown in Fig. 5-15.

The fine-grained sediments in the upper sections of the boreholes represent the more recent deposits in the bay. They are supplied primarily by the East Channel of the Mackenzie River and partially by coastal erosion of the surrounding Pleistocene deposits.

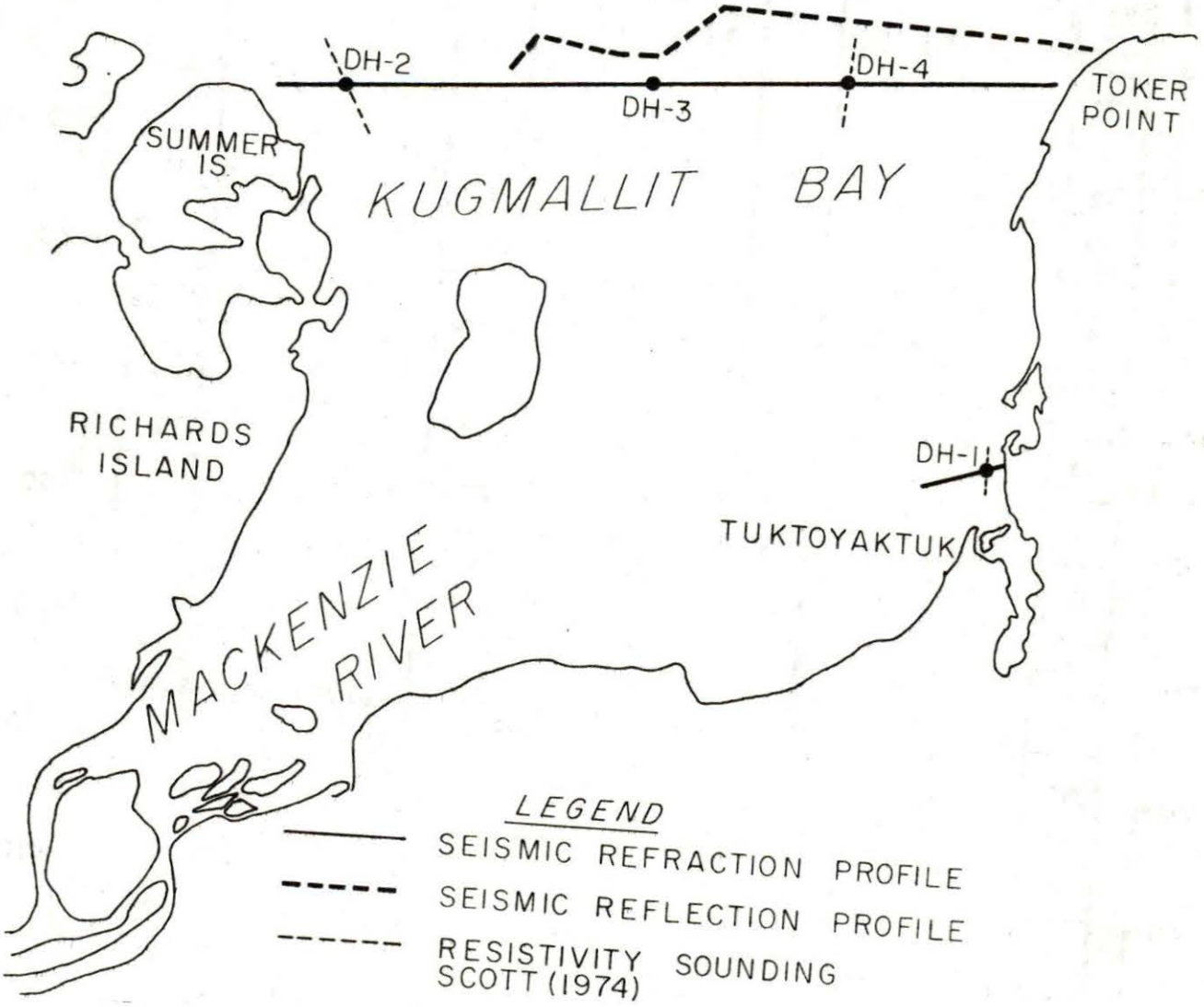

Fig. 5-14 Location of GSC drillholes in Kugmallit Bay showing positions of geophysical profiles.

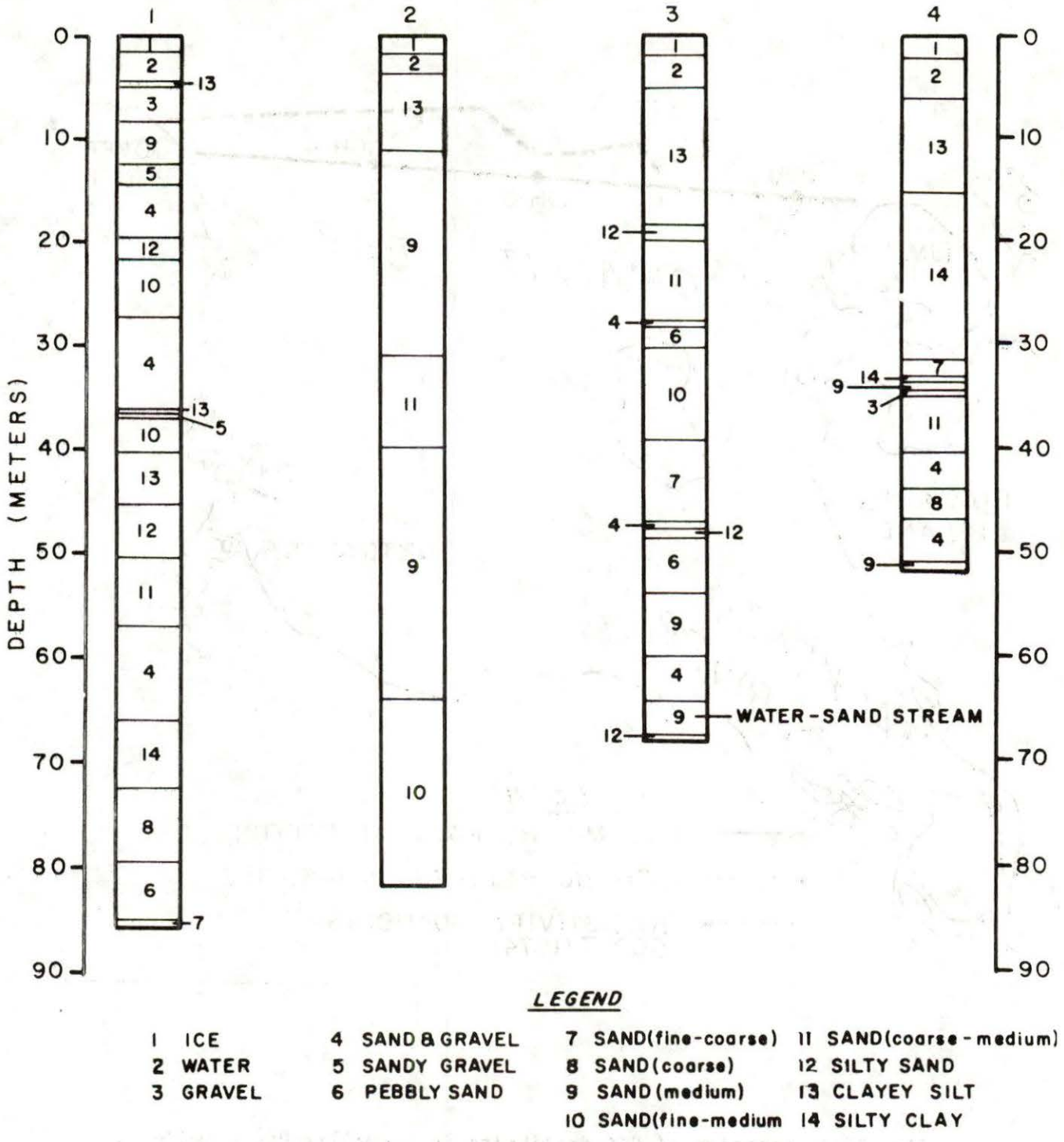

Fig. 5-15 Lithological description of GSC Kugmallit Bay drillholes.

Immediately under the silts and clays are Pleistocene glacio-fluvial and deltaic deposits of sands and gravels (Mackay, 1963). Their exact age is questionable, but it is probable that they belong to pre-classical Wisconsin or classical Wisconsin time (Rampton, 1972).

In the third drill hole, an interesting geological feature was observed when a saltwater-sand stream was encountered below the permafrost table. Samples from the 3.5 m deep channel gave temperature readings between +.8°C and +1.8°C. Deeper sampling and temperature recordings were impossible as mud circulation was lost in the free-flowing saltwater-sand stream.

Small pieces of wood and shell fragments were also found in many of the different sediments. However, insufficient quantity and poor quality made dating impractical.

In-hole temperature and mud temperature measurements indicated that permafrost was present in holes #1, 2 and 3 at respective depths of 37-40 m, 70 m and 61 m. Permafrost was not detected in hole #4, although temperature:depth characteristics suggest its presence below 70 m. Although core recovery was poor at greater depths, changes in drilling speed could be used as an indicator of frozen ground. The permafrost table indicated by this method was generally 3 m deeper than that given by temperature measurements. Frozen core samples were recovered in drill holes #1 and 2.

Thermal conductivity, moisture contents, pore water salinities and sand-silt-clay ratios were obtained for 34 samples taken from the four holes. The physical properties are summarized in Appendix G.

5.2.4 Shallow drilling at a proposed offshore well site

Engineering drilling at one of the two proposed Canmar offshore well sites was completed during the 1975 season. A hole was drilled at the Tingmiark site 50 miles north of Tuktoyaktuk in a water depth of 30 m to a depth of 60 m below bottom (C. O'Rourke, Canmar Ltd., pers. comm.). The hole encountered medium sand to a depth of 43 m below bottom and silty clay from that point to the bottom of the hole (see Fig. 5-16). Ice bonded permafrost was encountered from 34 m to 43 m below bottom. The sediment temperature at the bottom of the hole was -1.6°C, indicating a total permafrost thickness considerably in excess of that depth, although no further ice-bonding was encountered.

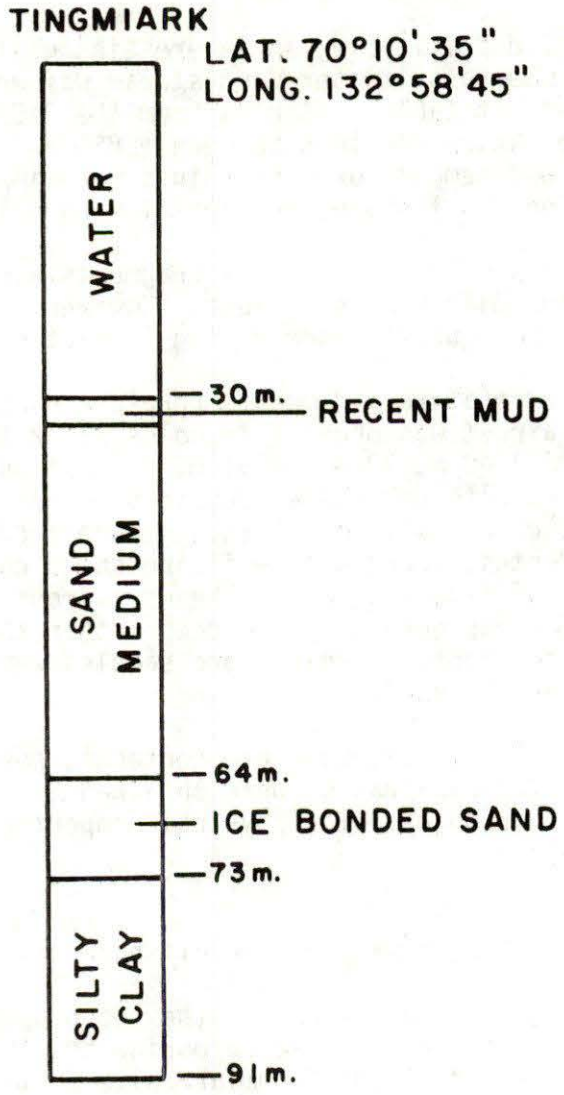

Fig. 5-16 Generalized geological log from the Tingmiark drill site (C. O'Rourke, Canmar Ltd., pers. comm.).

5.3 Thermal Data

5.3.1 Offshore thermal régime

The presence of offshore permafrost can only be determined by other than temperature measurements if the sediments are frozen. Hence, much of the observational evidence is really that for frozen ground rather than for permafrost. It is also possible that a thin veneer of seasonal ice may form close to the surface under several northern offshore situations, especially in shallow nearshore areas. Such conditions could result from sedimentation in warm fresh water during summer months being replaced by cold saline water during winter months.

The problem of both the thickness and distribution of the permafrost is essentially a thermal one. The subsurface thermal régime is usually controlled by heat conduction, although this is often modified locally by mass transfer processes, such as rapid sedimentation, erosion, or sub-surface fluid migration. An extreme example of the latter is the 1,500 m of permafrost reported by Balobaev et al. (1973) in central Siberia. All calculations made in this report assume heat conduction only. Current evidence for non-conductive processes is discussed in section 6.5.

The thermal régime is controlled by past and present surface temperatures, the solid to fluid interface temperature, the terrestrial heat flow generated within the earth, the thermal properties of the earth materials present, and the phase characteristics of the pore fluid present. In equilibrium, the sub-surface thermal régime is governed by the present mean annual surface temperature, the terrestrial heat flow, and the thermal conductivity of the earth materials. If this surface temperature is below 0°C, permafrost is present and the thermal conductivity may be different within and below the permafrost. This difference is more marked in high-porosity materials in which some, or all, of the pore water within the permafrost is frozen. Ice has a thermal conductivity four times that of water. For a sandstone lithology of porosity 25%, the equilibrium temperature gradient difference between frozen and unfrozen material may be for example 20°C km^{-1} to 30°C km^{-1}. In the equilibrium state the contrast in seabottom and land-surface mean temperatures causes distortion of the isotherms near a cold northern shoreline, thus setting up a lateral component of heat flow. This results in a thickening of the seabottom permafrost in the vicinity of the shore, and vice versa on land.

If the surface temperature changes for some reason, the sub-surface temperatures will move to a new equilibrium at a rate dependent on the thermal diffusivity of the medium. In porous rocks in northern Canada, this may involve a depth change of the water-ice phase boundary and, consequently, the release or absorption of latent heat, resulting in a zone of

apparent low diffusivity, because of the apparent high heat capacity while the phase change occurs. If, during this non-equilibrium state, the frozen layer is growing in thickness, the measured heat flow will be greater within the frozen layer than below it. The converse is true as the frozen layer degrades. In both of these cases a sharp change in heat flow occurs at the frozen-to-unfrozen boundary. If no frozen ground is present, variations in heat flow with depth will be smoothly varying.

Whether pore water is frozen at 0°C depends on three major factors: (1) the molecular concentration of dissolved salts in the pore water; (2) the depth of burial of the sediments, or more strictly the pore pressure; and (3) surface tension effects. In a coarse-grained sand the first two are more important, but the freezing characteristics of fine silts and clays are quite complex and not entirely understood (Anderson and Morgenstern, 1973). Interstitial or pore water salinities of between 10 and 20% will lower the freezing point of the water to between -0.5°C and -1.1°C in coarse sand. The effect of pressure is to depress the freezing point by an average of 0.13°C per 100 m of burial (Ahlmann, 1948). Williams (1964) has observed that fine sediments, such as the Leda clay, freeze over a range of temperatures between 0°C and -5°C, and still retain as much as 5 to 10 percent of their moisture unfrozen at -20°C.

Surface temperatures have varied by considerable amounts in the past few hundreds of thousands of years. The effect of fairly recent variations of climate alone on underground temperatures is well substantiated (Beck and Judge, 1969; Cermak, 1971; Judge, 1975; Mackay, 1975). However, much of the presently exposed northern land surface of Canada, for the past few hundreds of thousands of years, has been covered intermittently by Pleistocene ice sheets or the Arctic Ocean. Also, many currently submerged areas have been either exposed land or covered by ice sheets. During periods of ice cover over the land, surface temperatures probably increased beneath the ice sheets and decreased in front of them, resulting in respective thinning and thickening of the permafrost. During periods of submergence of the exposed land, surface temperatures probably increased and caused degradation of permafrost.

It is useful to compare the Arctic Channels with the Beaufort Sea because they each reflect a specific thermal history. The Arctic Channels are more akin to Beaufort Sea waters of greater than 100 m depth. Bottom water temperatures in M'Clure Strait and Viscount Melville Sound are generally below 0°C to depths of 250 to 280 m. Below this range, the temperatures are from 0° to 0.4°C to depths of 500 m.

The deeper water, the polar Atlantic, is generally of higher salinity than the overlying Arctic cold and intermediate

waters. Water temperature and salinity profiles are useful in identifying possible areas of equilibrium permafrost. At depths between 20 and 250 m, water temperatures are generally below 0°C throughout the year. In depths of less than 20 m, water temperatures during the short summer may rise above 0°C because of large inflows of fresh water. Bottom water temperatures and heat flow measured by Law et al. (1965), by Paterson and Law (1966) and by the author indicate that the maximum permafrost thickness offshore (away from the shoreline) may range from 25 to 75 m in water depths to 250 m, depending on whether the bottom sediments are frozen. If only a thin veneer of sediments overlies bedrock, then permafrost thickness might be as much as 125 m.

Gradiometer casts with penetrations of 3 m have not encountered frozen material, even in water less than 100 m deep. The surface history of much of the Arctic Islands during the Pleistocene is one of land depression, and hence submergence, alternated with cover by ice sheets. Consequently, remnant offshore permafrost due to the non-equilibrium state is likely to be a localized phenomenon in a few isolated areas rather than a widespread condition. Thus, in general, only relatively thin, shallow permafrost is expected in offshore areas. Similar arguments regarding permafrost thickness are applicable in the eastern Beaufort Sea at water depths exceeding 100 m which, therefore, were not emergent during the Pleistocene.

The effect of nearby northern shorelines, with much lower mean annual surface temperatures than the neighbouring seabottom, leads to local thickening of the equilibrium offshore permafrost. Measurements made in offshore drill-holes near Little Cornwallis Island have indicated as much as 150 m of seabottom permafrost 200 m offshore below 12 m of water. This is compared to 500 m of permafrost onshore. Water bottom temperatures average -1.5°C, as compared with mean land surface temperatures between -13° and -15°C.

Unlike the Arctic Islands, the eastern Beaufort Sea was not depressed by ice sheets (Andrews, 1973) and much of it remained unglaciated, at least during the Wisconsin. Changes as great as 100 m in the eustatic sea-level resulted in periods of emergence and submergence of the present seabottom. During emergence, the northern parts of Tuktoyaktuk Peninsula, Richards Island (Mackenzie Delta), and most of the offshore region probably remained unglaciated (Mackay et al., 1972), and hence subjected to low surface temperatures. Fig. 5-17 shows the emergence history of the Beaufort Shelf.

To the west of the Mackenzie delta as far as Herschel Island, the surface environmental history was different. A lobe of the Laurentide ice sheet covered this area and hence, because of probable basal temperatures of the ice sheet similar to seabottom temperatures, remnant permafrost due to past sea-

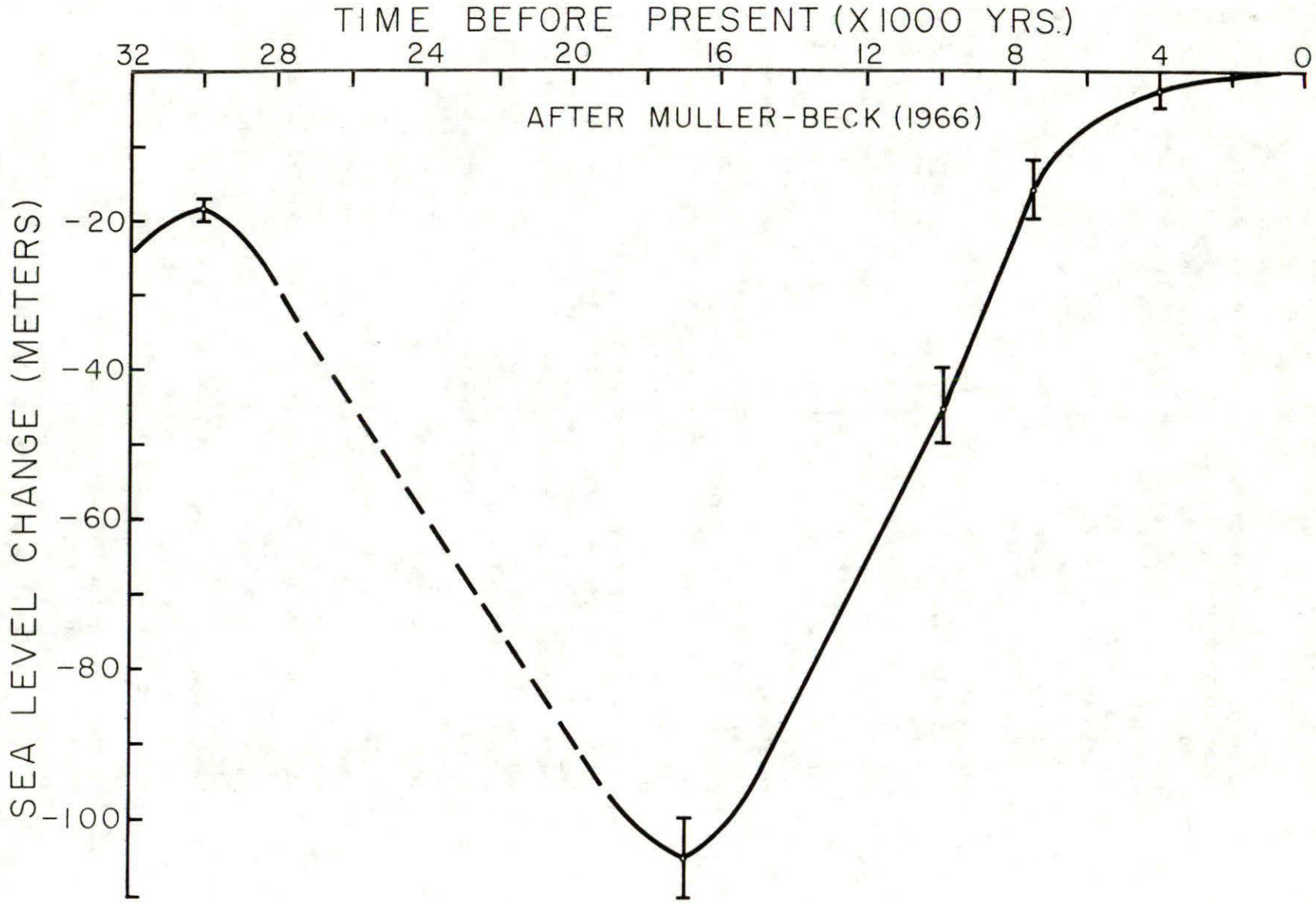

Fig. 5-17 Sea level history of the Beaufort Sea shelf (after Mackay, 1972).

level changes may not exist. If any remnant permafrost is present, it is probably a result of rapid shoreline recession.

5.3.2 Bottom water and sediment temperature data

Seabottom temperature and salinity data for the southern Beaufort Sea were collected from the Marine Environment Data Service, Fisheries and Marine Branch, Department of Environment, and from unpublished surveys carried out by GSC and Earth Physics Branch, EMR. A compilation and discussion of data is given in Appendix H. Figs. 5-18 and 5-19 show the bottom temperature and salinity conditions on the Beaufort Sea shelf for both winter and summer conditions. Although the data is somewhat scanty, the mean annual seabottom 0° isotherm should be somewhere between the shoreline and 20 m water depth. The winter and summer 0° isotherms follow the edge of the Beaufort Sea shelf; hence, most of the shelf area experiences permafrost temperatures. The central portion of the map area, north of Kugmallit Bay and the Mackenzie delta are subjected to temperatures below -1.5°C. The winter and summer seabottom salinities are closely related to the bottom temperatures. In summer, warm Mackenzie River water can be found on bottom along the shallow coastal areas of the Tuktoyaktuk Peninsula. Although much of the river discharge is towards the west into Mackenzie Bay, cold saline water is found at seabottom in the deeper portions of the Mackenzie Canyon.

Essentially beyond the influence of the Mackenzie outflow the water masses present in the southern Beaufort Sea are those identified by Coachman (1963) and O'Rourke (1974) as:

Arctic water: 0 to 200 m, low salinity, cold (-1.5°C)

Atlantic water: 200 to 900 m, high salinity, warm (>0°C)

Bottom water: >900 m, high salinity, cool (-0.3°C).

The detailed results of Herlinveaux (1973) for a profile across the continental shelf north of Tuktoyaktuk suggest a depth of 250 m for the transition from Arctic to Atlantic water. Sub-zero bottom-water temperatures and hence sub-bottom permafrost is essentially confined to the shelf.

The geothermal gradients observed onshore are useful in determining input parameters for offshore models. Fig. 5-20 shows temperature gradients observed in two delta wells (Taylor and Judge, 1974), Reindeer D-27 and Unipkat I-22. The Reindeer well is in thick permafrost in old pre-Wisconsin sediments and is typical of most of the wells on the Tuktoyaktuk Peninsula and the highland portion of Richards Island. The Unipkat well was drilled through recent Mackenzie delta silts; here permafrost has only begun to form in response to negative mean annual surface temperatures as the deltaic island emerged above sea-level. Profiles for 19 instrumented

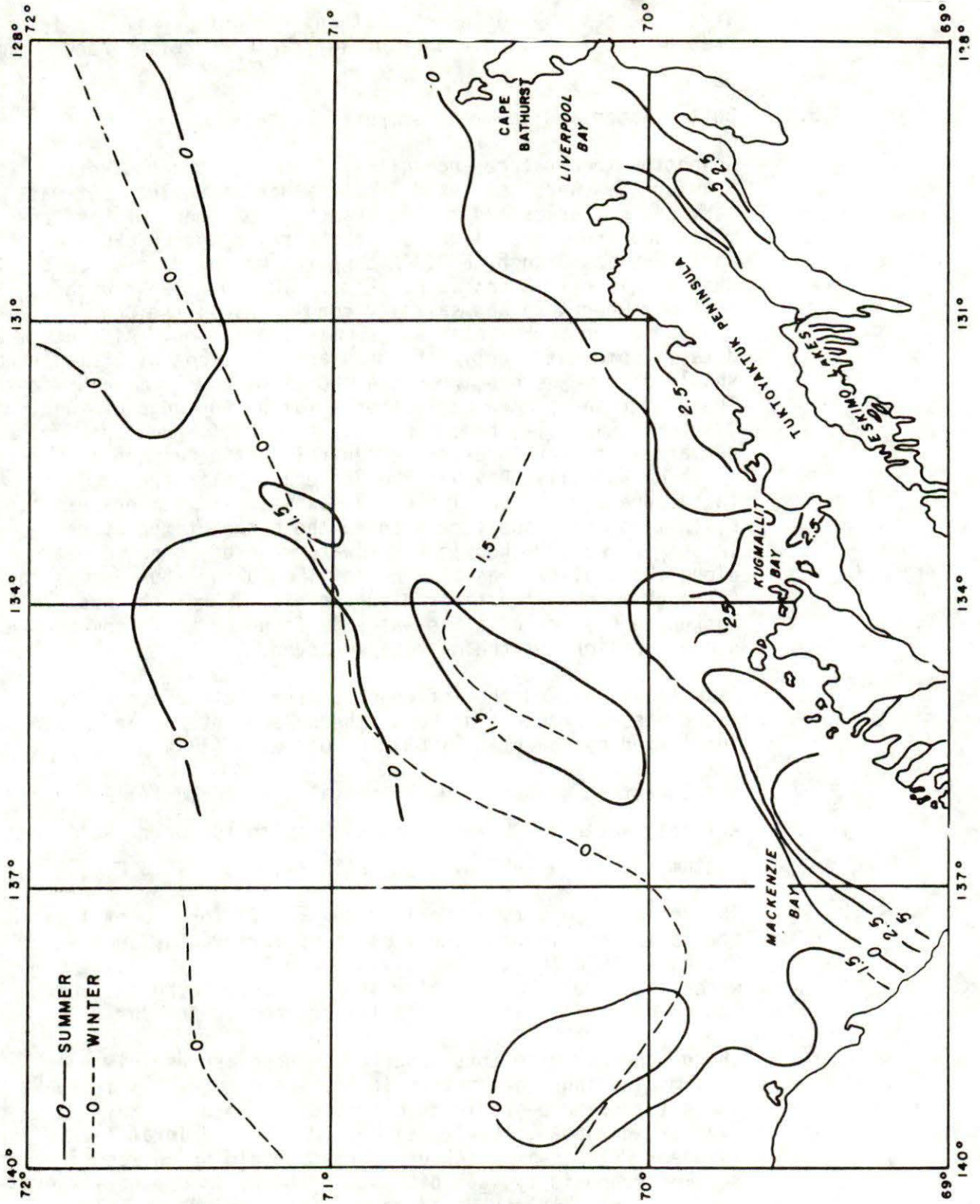

Fig. 5-18 Summer and winter bottom water temperatures in the southern Beaufort Sea. (Temperature contours in °C.)

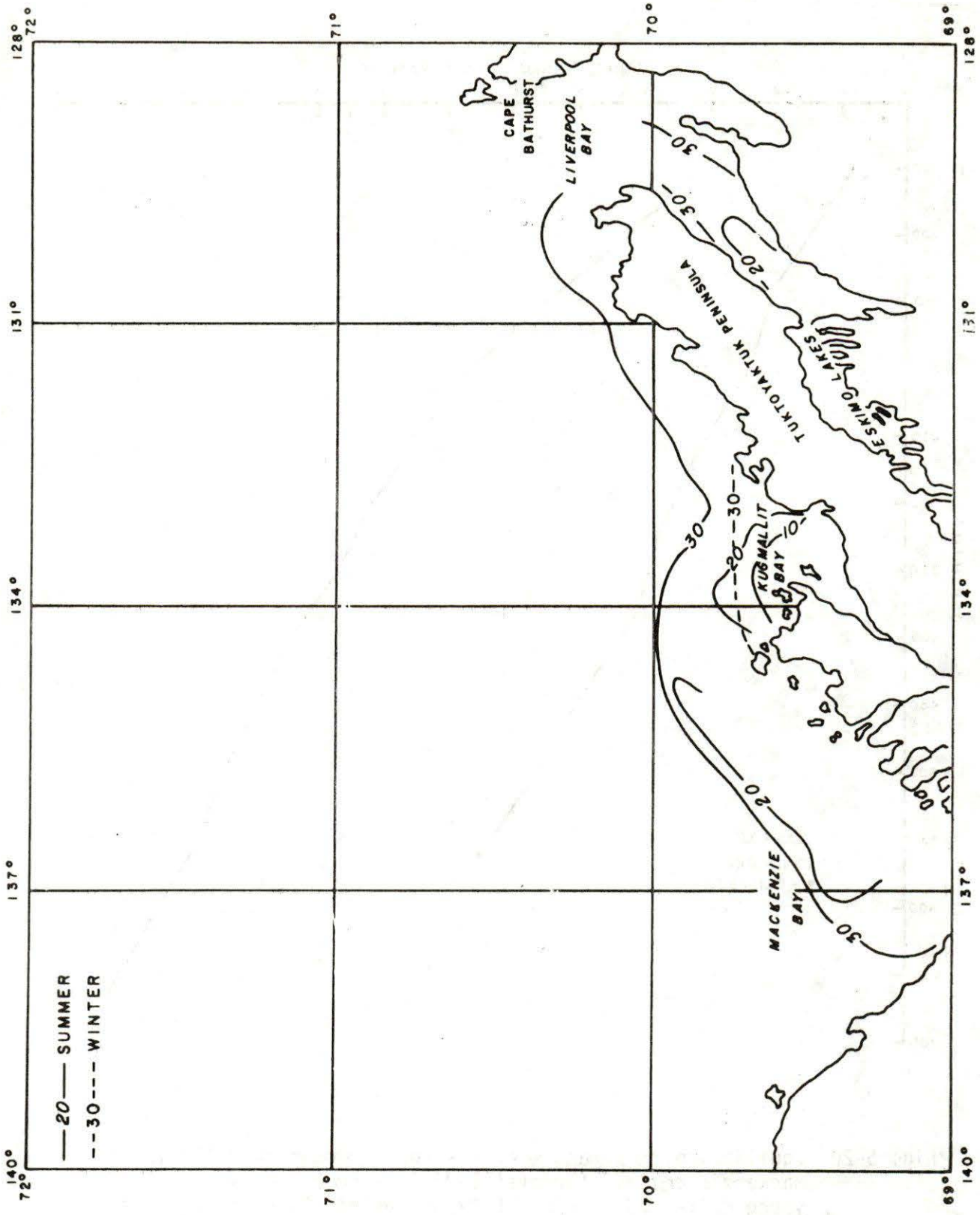

Fig. 5-19 Summer and winter bottom water salinities in the southern Beaufort Sea. (Salinity contours in parts per thousand.)

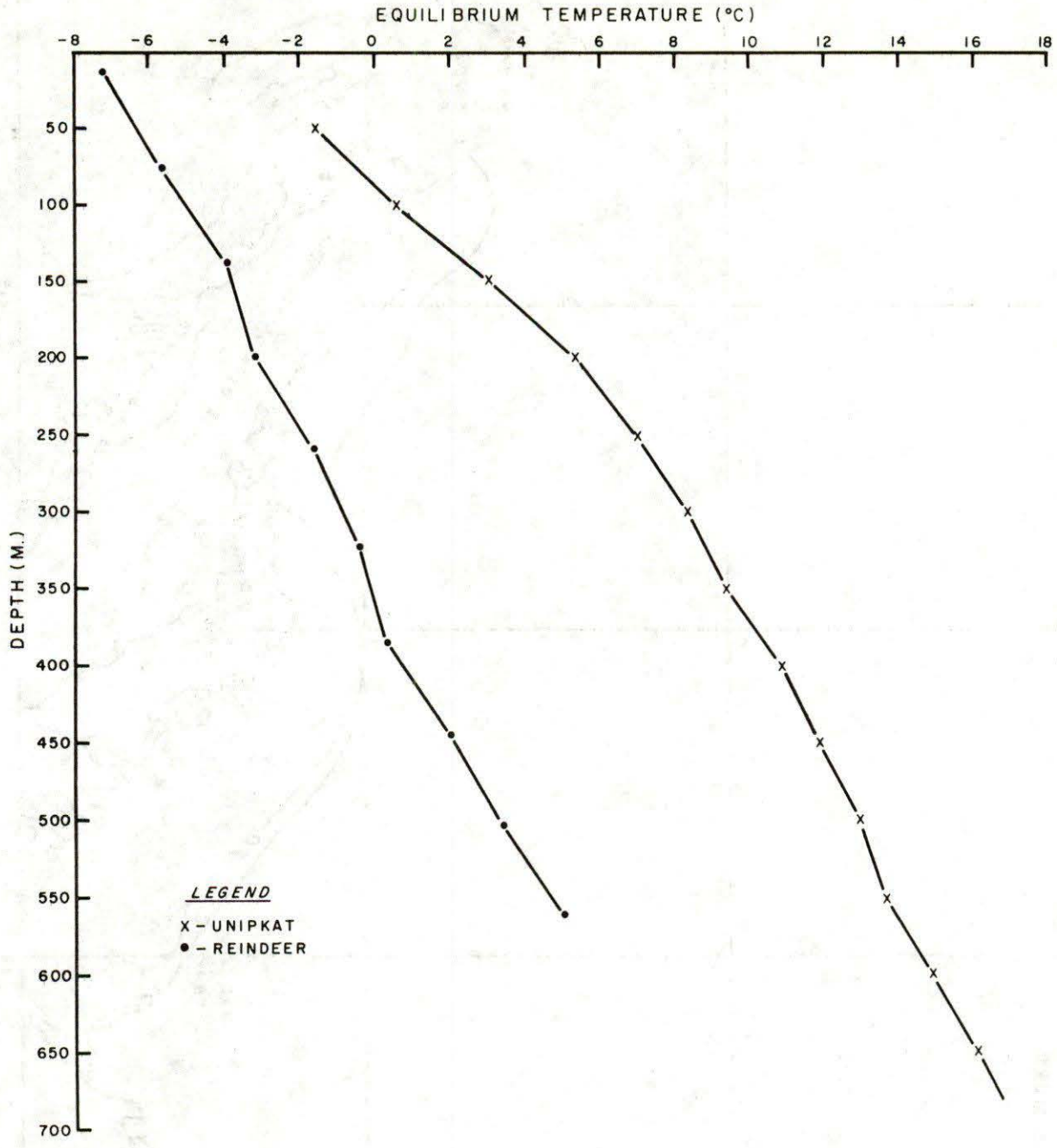

Fig. 5-20 Equilibrium temperature curves for two onshore wells in the Mackenzie delta. (Unipkat I-22 is representative of the young delta and Reindeer D-27 of the highlands of the old delta.)

wells in the Mackenzie delta are shown in Appendix D. These profiles are taken from the northern geothermal data collection (Taylor and Judge, 1974; 1975; 1976). The onshore distribution of permafrost derived from these papers is shown in Fig. 5-12.

Temperature data of sub-seabottom areas from the 1970 A.P.O.A. drilling program are given in Appendix A. Sample temperatures as low as -2.2°C were recorded.

Brown and Barrie (1976) have reported on the design and construction of two artificial islands (Pelly and Unark) in the shallow waters of the Beaufort Sea. Shallow sub-seabottom temperatures measured were 2 to 4°C at 4 m below seabottom at the Pelly location and -3°C at a depth of 7 m below seabottom at Unark.

Imperial Oil Ltd. installed a multithermistor cable in Adgo P-25 at the completion of the well on the artificial site south of Gary Island. The cable was read on three occasions prior to its destruction this winter and the results are reported by Taylor and Judge (1976). Extrapolating the results to equilibrium indicates the absence of permafrost temperatures. The mean surface intercept temperature is +2.5°C and the mean gradient 17°C km^{-1}.

Downhole variation of temperature measured in each of the four GSC boreholes mentioned in section 5.2.2 is given in Fig. 5-21. Immediately below the water to mud interface measured mud temperatures were 0 ± 0.5°C reflecting the low water temperatures in early spring. Temperatures increased with depth to maxima of 1.4°C to 2.5°C at depths ranging from 3 to 26 m. In boreholes #1 and #2 the maxima occur at 3 and 9 m respectively and rise systematically to those depths and decrease systematically below, whereas borehole #4 shows evidence of a periodicity in the temperatures to a deeper maximum. A similar periodicity to that in #4 could exist in #3 with a secondary maximum occurring at 14 m. Below these shallow maxima, observed temperatures decrease systematically although there are substantial gaps where downhole temperatures were not measured due to the condition of the hole. The shallowest permafrost temperatures were measured at depths of 56 m, 84 m and 63.5 m below the surface respectively in the first three boreholes. No sub-zero temperatures were encountered in borehole #4. Closer estimates of the depth to the top of permafrost were possible by interpolation and, in the case of #1 and #2, by observation of the temperatures of the circulated drilling fluid. In #1, for example, the output temperature of the fluid fell by 1.5°C between depths of 46 and 61 m and remained constant at greater depths. The depth at which output temperatures started to fall is interpreted to be the depth at which frozen sediments were first encountered. Interpolation between observed downhole temperatures places the top of permafrost at 43 m. The combined use of bottom-

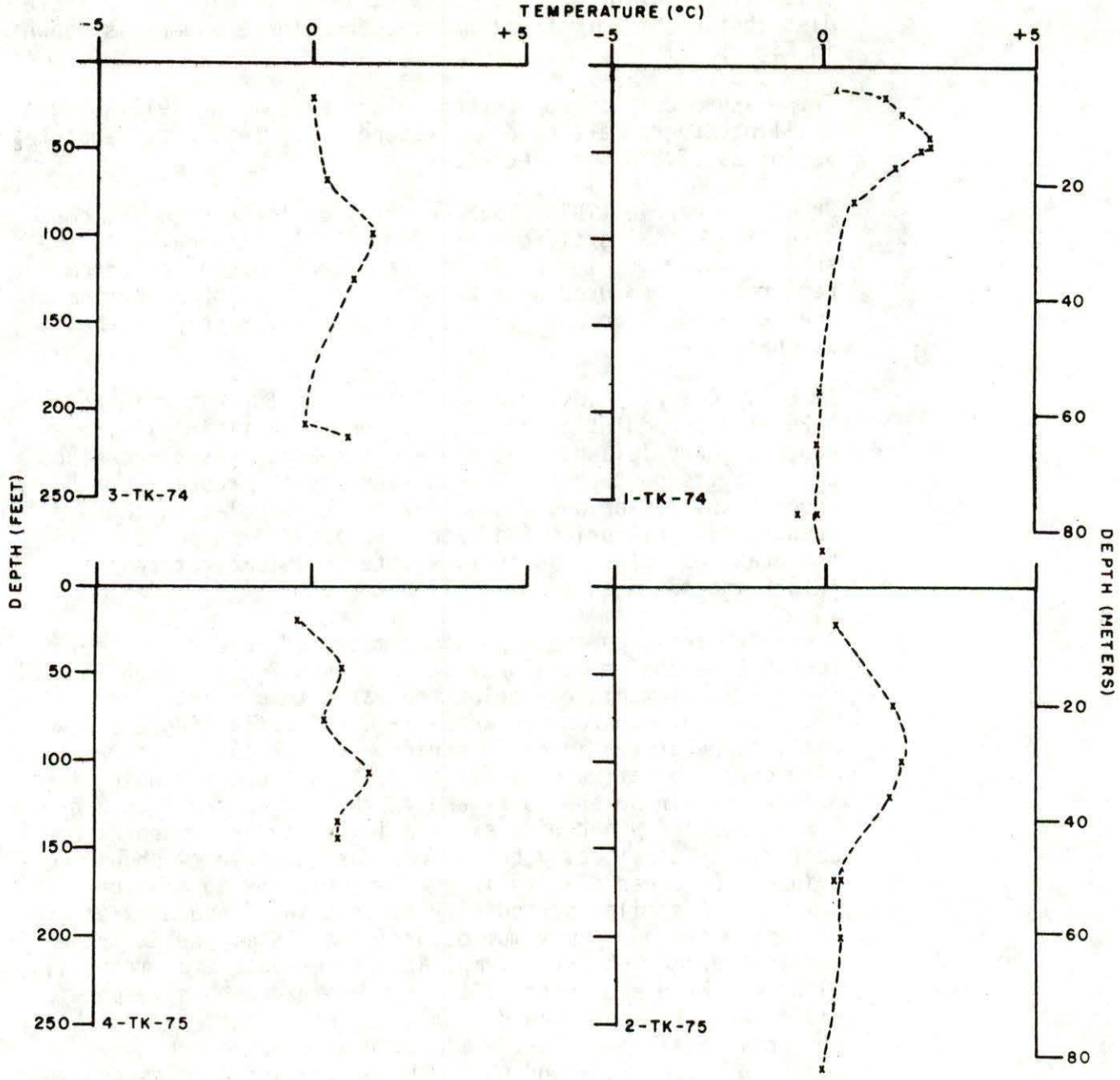

Fig. 5-21 Sub-surface temperatures measured in the Kugmallit Bay drillholes.

hole temperatures, core temperatures and fluid circulation temperatures indicates depths to the top of permafrost of 46 ± 2 m, 67 ± 3 m and 61 ± 2 m in the three holes in which permafrost was encountered. Extrapolation of temperatures in #4 indicates that permafrost could not be present at depths of less than 73 m. Depths to the top of the frozen section of the permafrost as determined by drilling speed were 54 m, 68 ± 2 m and 64 ± 1 m respectively.

5.3.3 Thermal properties of sediments

A relatively large number of measurements of the thermal parameters of unfrozen soils are reported in the literature - to name a few, Kersten (1949), DeVries (1952), DeVries and Peck (1958), Penner (1962; 1963). Because of the partially water-saturated nature of soils, the extent to which many of these results represent conduction alone has been questioned (Philip and DeVries, 1957; DeVries and Peck, 1958; Woodside and Cliffe, 1959; Yen, 1966). Many equations, both theoretically and empirically determined, exist to estimate the thermal properties of unfrozen soils, given information on composition, effective porosity and moisture content (e.g. DeVries, 1962; Woodside and Mesmer, 1959; Hutt and Berg, 1966).

Fewer measurements of the thermal properties of frozen soils have been reported, the most extensive collection still being Kersten (1949). Other measurements have been reported by Higashi (1953), Lachenbruch (1957), Martynov (1963), Wolfe and Thieme (1964), Penner (1970). In the past several years, extensive measurements on Mackenzie Valley soils have appeared (Judge, 1973; Isaacs, 1974; Shusarchuk and Watson, 1975; Penner et al., 1975). Many of the samples discussed are essentially artificially prepared. In very few cases are samples taken through repeated sessions of freezing and thawing or recovered in the frozen state and maintained that way. As in unfrozen soils, questions arise on the true nature of heat transfer in partially frozen, partially saturated soils. Considerable moisture movement to a freezing front is possible (Hoekstra, 1966; McRoberts and Nixon, 1975).

At the present insufficient experimental observations exist to relate lithology with thermal conductivity with any degree of confidence. Judge (1973) has shown that a simple relationship based on Woodside and Mesmer (1959) seems successfully to relate thermal conductivity and temperature.

Failing simple predictive techniques, thermal conductivity as well as moisture content and pore-water salinity were measured on each of the recovered samples of core and cuttings from the Kugmallit Bay experiment.

Thermal conductivities were measured on the divided-bar using perspex cells to contain the samples. Obtained values for 34

samples are shown in Appendix G. The most apparent feature is the distinct difference between the sands and gravels as one group, and the silts and clays as another. Average thermal conductivities for the 27 samples of silts and clays were 2.61 ± 0.29 $Wm^{-1}K^{-1}$ and for the seven samples of silts and clays 1.47 ± 0.10 $Wm^{-1}K^{-1}$. Corresponding volumetric moisture contents were 31 ± 6% and 50 ± 2% in the unfrozen material. The frozen sand cores had substantially higher moisture contents of 44% and 70%. Thus, excess ice was certainly present in the second core and probably in the first, although cubic packing of sand grains could result in interstitial porosities of up to 48%.

Salinity of the interstitial waters in the sediments was measured for 29 of the recovered samples, 24 of which were core samples. The method used was to add distilled water to the sample until a sufficient volume of water could be extracted to enable the use of a Yellow Springs salinometer.

Results, corrected to the original moisture content of the samples, are summarized in Appendix G. No sea-water salinities were measured during the drilling period but Kelly (1967) quotes values of up to 29°/$_{oo}$ under the ice of Kugmallit Bay so there could be some contamination of samples by the sea-water used in mud circulation resulting in higher values for the interstitial water than in-situ values. Mean values were lowest in the two boreholes, #1 and #2, closest to the shorelines and highest in #3 in which the sand stream was encountered. Grouping the results by lithology shows the lower salinities of the pore fluids of the sands and gravels compared with the silts and clays.

Further determinations of thermal conductivity were made on core samples recovered during the *C.C.G.S. Nahidik* cruise in the summer of 1975. The cores recovered (up to 2 m in length), consisting entirely of recent silts and clays, were divided into 15 cm sections and the conductivity samples drawn from each of these short sections. Measurements were made on a total of 94 samples yielding an average thermal conductivity of 1.11 ± 0.10 $Wm^{-1}K^{-1}$ and an average moisture content of 68 ± 6%. The mean values of thermal conductivity are considerably higher than the values determined by Ratcliffe (1960) for deep ocean sediments which, at moisture contents of 50 and 68%, are 0.84 and 0.73 $Wm^{-1}K^{-1}$ respectively. Although complete grain-size analyses are not yet available, the higher conductivity probably reflects higher silt contents in shelf sediments.

The ice content of frozen offshore sediments is a crucial factor in assessing the performance of offshore structures. Probably with the exception of areas in which permafrost aggradation is occurring (such as in the vicinity of the suspected seabottom pingoes) the ice contents are lower than onshore. Presumably the excessive near-surface ice in such

onshore features as ice-wedges undergo serious thermal or chemical erosion during the initial period of coastal recession and submergence. Lewellen's (1973; 1974) observations in the Barrow region, where average values of ice in the subsurface materials range from 36 to 49% as compared with 65 to 82% onshore, appear to confirm this. Excess ice in offshore sediments has also been reported by Mackay (1972), Molochuskin (1973), McDonald et al. (1973) and Judge et al. (1976). Considerably more information relating to ice content of offshore sediments in the southern Beaufort Sea exists in unpublished industrial reports.

5.3.4 Thermal models

Failing the availability of extensive deep offshore subsurface temperature information, thermal simulation models must be used to assess the thermal character of the permafrost. To calculate the maximum thickness of permafrost which may have developed and how much may still remain today, information is necessary on the surface temperature history at different water depths, the terrestrial heat flow, the thermal properties of the rocks encountered, rock porosities and the temperatures at which the pore water will freeze. For the calculations, sub-surface thermal properties were derived from onshore wells such as Reindeer D-27 and from the Kugmallit Bay measurements; that similar lithologies occur both onshore and offshore has been verified by Hofer and Varga (1972). Times of emergence and submergence have been taken from Mackay (1972), and the surface temperatures used are -2°C during submergence and -9°C during emergence. The emergence temperature of -9°C is similar to surface temperatures in northern Richards Island today. This may be warmer than surface temperatures in front of a continental ice sheet. A bottom water temperature of -2°C may be too low, since measured bottom water temperatures seem to range from -1.5° to -1.8°C in deep water, and may be 0°C or above in water <20 m deep.

As a consequence of the A.P.O.A. drilling, Mackay (1972), through the application of the Neuman analytical solution for heat conduction in the presence of a phase boundary, suggested that permafrost may underlie much of the Beaufort Shelf area. He calculated that, as a result of past lowering of the sea-level and ensuing low mean annual surface temperatures, relic permafrost with a thickness up to 450 m may exist in the southern Beaufort Sea. Sharbatyn (1973) has suggested an analytical form of solution based on the Stefan equation for heat conduction in the presence of a phase boundary and Sharbatyn and Shumskiy (1974) have modelled the development of permafrost in the Western Siberian lowland using the solutions.

A one-dimensional finite difference heat conduction model has been used with the above input data to estimate the approximate thickness of remnant permafrost which might exist in the area north and east of the Mackenzie delta (the area that underwent long periods of emergency during the Wisconsin ice are). Similar simulations have been used to determine the rate at which the subsurface thermal régime in this area will change as a terrestrial surface is incorporated into the offshore by recession of the coastline.

As mentioned in section 5.3.2, the western delta exhibits very different thermal characteristics reflecting the very different thermal history. Using appropriate thermal input data for this area, simulations were used to place limits on permafrost occurrence and thickness and thus to explain anomalous seismic velocities in Mackenzie Bay (section 6.2). In Mackenzie Bay and Shallow Bay, deltaic islands are emerging from the waters, creating a new land surface beneath which permafrost is aggrading anew.

The true picture in each of these areas is, of course, far more complex than these simple simulations allow. If the present Tuktoyaktuk Peninsula can be used as an example, much of the present offshore area may have been covered with lakes during emergence. Permafrost will begin to aggrade in such areas as they are submerged beneath low temperature waters. Other complexities arise because of the true nature of shoreline recession, from the effects of rapid sedimentation, shifting river channels, complex shoreline geometries, etc. At present, knowledge of even the times of emergence and submergence and of ice-sheet boundaries remains somewhat speculative. Although it is believed that heat conduction is the predominant mechanism of heat transfer, the observations at site #3 of the Kugmallit Bay drilling suggest that coupled heat and mass transfer may play a predominant role at least locally. The evidence is discussed in greater detail in section 6.5.

6. RESULTS

6.1 Distribution of Ice-Bonded Sediments

The interpretation of high velocity refracted events on industry records is shown in Fig. 6-1. From this distribution of data, the shelf area has been divided into three zones, continuous, discontinuous, and non-ice-bonded (see Fig. 6-2). There are several outstanding features:

(1) No ice-bonded permafrost occurs in the offshore region (at water depths >20 m) west of a N-S line through Pelly Island. A sharp boundary is found on both industry and GSC refraction records.

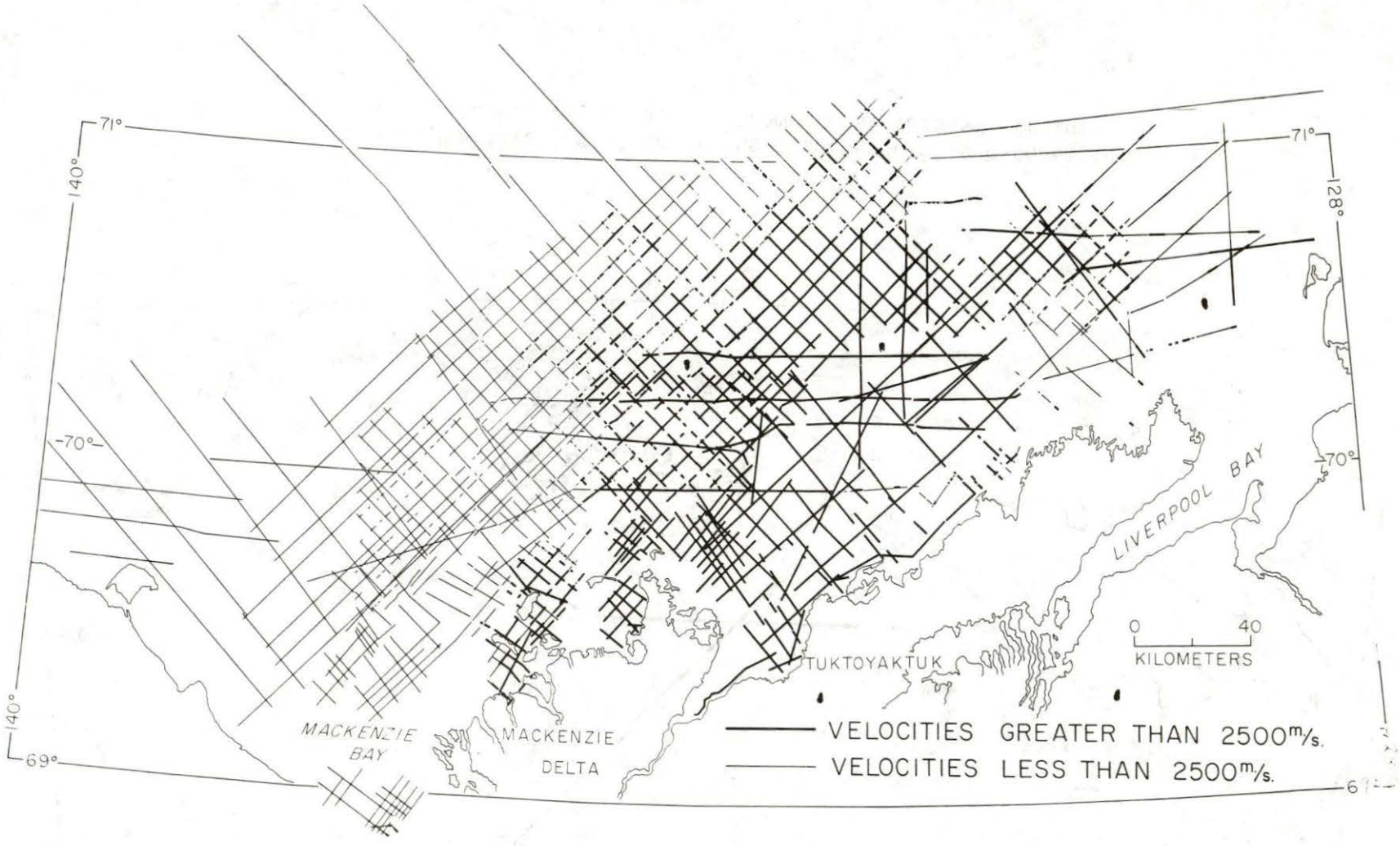

Fig. 6-1 Location of industry data analysed for high velocity refraction events.

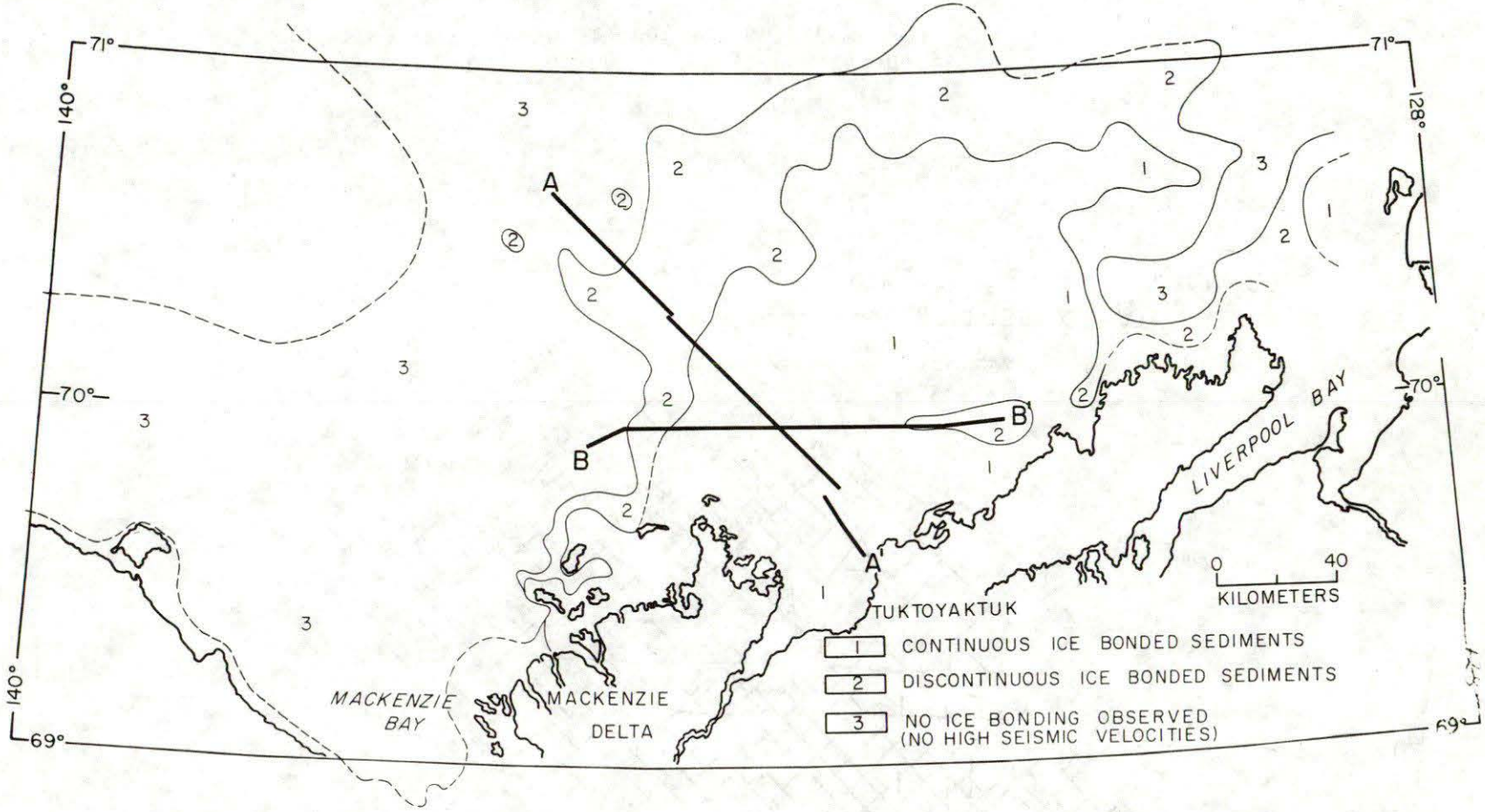

Fig. 6-2 An interpretation of the occurrence of sub-seabottom ice-bonded permafrost from industry seismic records.

(2) No ice-bonded permafrost is found in the inshore zone north of Cape Dalhousie, in water depths between 20 and 30 metres.

(3) The continuous zone is surrounded by a discontinuous or "patchy" permafrost zone. In this zone, seismic records indicate only a thin high velocity layer.

(4) There are no corrections between interpreted boundaries and such major seabottom features as the Mackenzie Canyon and seabottom depressions north of Kugmallit Bay and Atkinson Point.

(5) With few exceptions, submarine pingo swarms are associated with the discontinuous ice-bonded permafrost zone.

(6) In offshore regions, seabottom topography is much more rugged in zones of ice-bonded permafrost than in areas where none is indicated.

A good comparison of these zones can be made north of Cape Dalhousie and along the N-S line north of Pelly Island.

(7) No evidence of ice-bonded permafrost has been found in water depths in excess of 90 metres.

Fig. 6-3 shows two sections across the shelf, in the ice-bonded permafrost region as indicated in Fig. 6-2. Section A-A' extends from the shoreline to the shelf edge. In the near-shore area, the top of ice-bonded permafrost is quite rugged with slopes of 10° and more. Further offshore, the top drops to a depth of 150 m on this section. This can be correlated with the interpreted "ancient" Mackenzie River channel shown by seabottom topography to be seaward of this line. Further offshore, the top of ice-bonded permafrost is much closer to surface (10 m below seabottom in one location) and becomes discontinuous. It is not known whether the sudden descent of the top to depths beyond 200 m in isolated locations is real or whether the refracted energy is so rapidly attenuated on the seismic record that a later high velocity event is taken to be the first arrival in error. Observed velocities of ice-bonded permafrost are in excess of 3000 m/sec, indicating ice-rich coarse-grained materials. In the "non-permafrost" zone at the seaward end of section A-A' velocity stratification has been observed which correlates well with velocities given by Hofer and Varga (1972).

Section B-B' in Fig. 6-3 runs E-W from the "non-permafrost" zone to the Atkinson Point area. The top of ice-bonded permafrost in the middle portion of the section is depressed to a depth of 150 m; this again correlates well with the position of the "ancient" Mackenzie River channel. On the eastern side of the section, the industry data did not detect continuous high velocities but only sporadic indications at depths between 150 and 250 m. Data from the GSC refraction shooting aboard the *C.C.G.S. Nahidik* indicated the presence of thin near-surface refractor with a velocity slightly less than that observed from industry data. The attenuation rate of this event was so large that, with the industry detector array, most of the

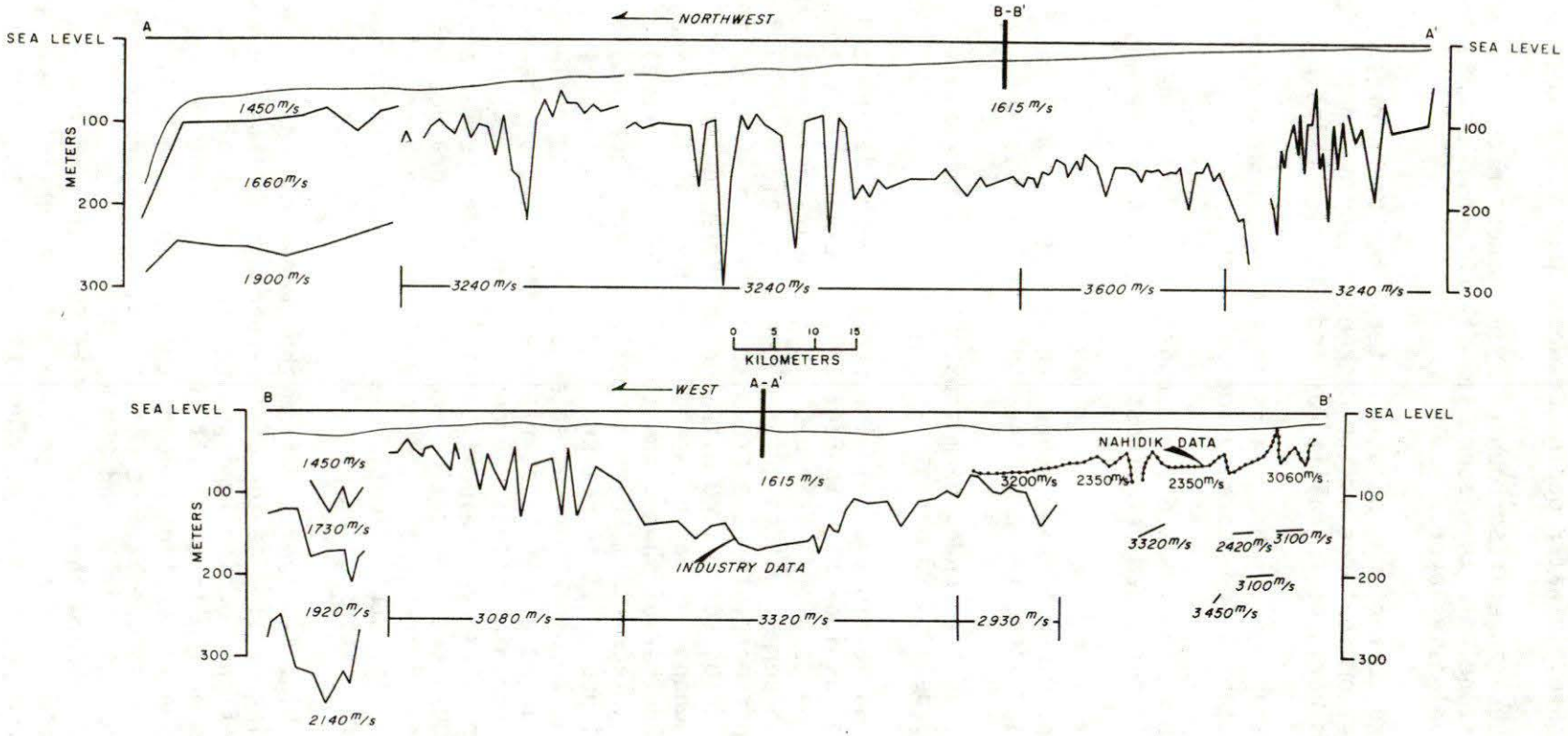

Fig. 6-3 Interpreted sections from industry seismic records showing the occurrence of high velocity (ice-bonded) sediments. Locations of sections are shown in Fig. 6-2.

refractor energy would have been dissipated before reaching the first hydrophone.

The boundary between ice-bonded and non-ice-bonded material on the west side of section B-B' is abrupt. The nature of this boundary was confirmed from the GSC *Nahidik* data; the boundary was crossed in two places and results similar to the industry interpretation were found. West of the boundary, typical velocity stratification of non-ice-bonded materials is found.

6.2 Anomalous Shallow Seismic Velocities in Mackenzie Bay

A detailed study was made of 250 km of industry seismic records northeast of Shingle Point in the "Mackenzie Canyon" area (see Fig. 6-4).

A high velocity refractor with an average velocity of 3000 m/sec was observed over most of the area. Near the northeast offshore ends of the survey lines the refractor velocity decreases to 1800 m/sec. An average velocity of 1520 m/sec was used for the combined water-unfrozen sediment layer to calculate depths to the high velocity refractor. A contoured map of depths to the refractor is shown in Fig. 6-5; the average depth is about 200 m but decreases to about 100 m near the shoreline. From a generalized velocity-depth function for Mackenzie Bay given by Hofer and Varga (1972), the high velocity refractor observed at these shallow depths is anomalous.

To seaward of the study area, Shearer (1972) has mapped the base of the buried Mackenzie scour channel from high resolution seismic reflection profiling. The depths obtained for the base of the channel are in the same range as the depths computed to the high velocity refractor in the study area.

Several records obtained near the shore indicate two high velocity events: the shallowest is derived from a refractor near the water-bottom interface followed by a deeper second event delayed in time by about 200 milliseconds. An example is shown in Fig. 6-6; the first event (A) attenuates rapidly and is interpreted to indicate a thin frozen layer; the second event (B) has a persistently high amplitude across the record, which merges into a wide angle reflection on traces close to the shot. The second event is that which is mapped throughout the survey area.

Included in Fig. 6-5 is an interpreted section beginning at the shoreline formed by recent deltaic sediments; the high velocity refractor apparently correlates with the bottom of the scour channel offshore but departs from it in the inshore region. Where the present shoreline coincides with the edge of the scour channel, the top of the high velocity layer generally conforms to the base of the scour channel. If the sediment type forming the bottom of the scour canyon is uniform and is below 0°C, then the seaward decrease of refractor velocity may result from increasing temperatures in frozen ice-bonded material.

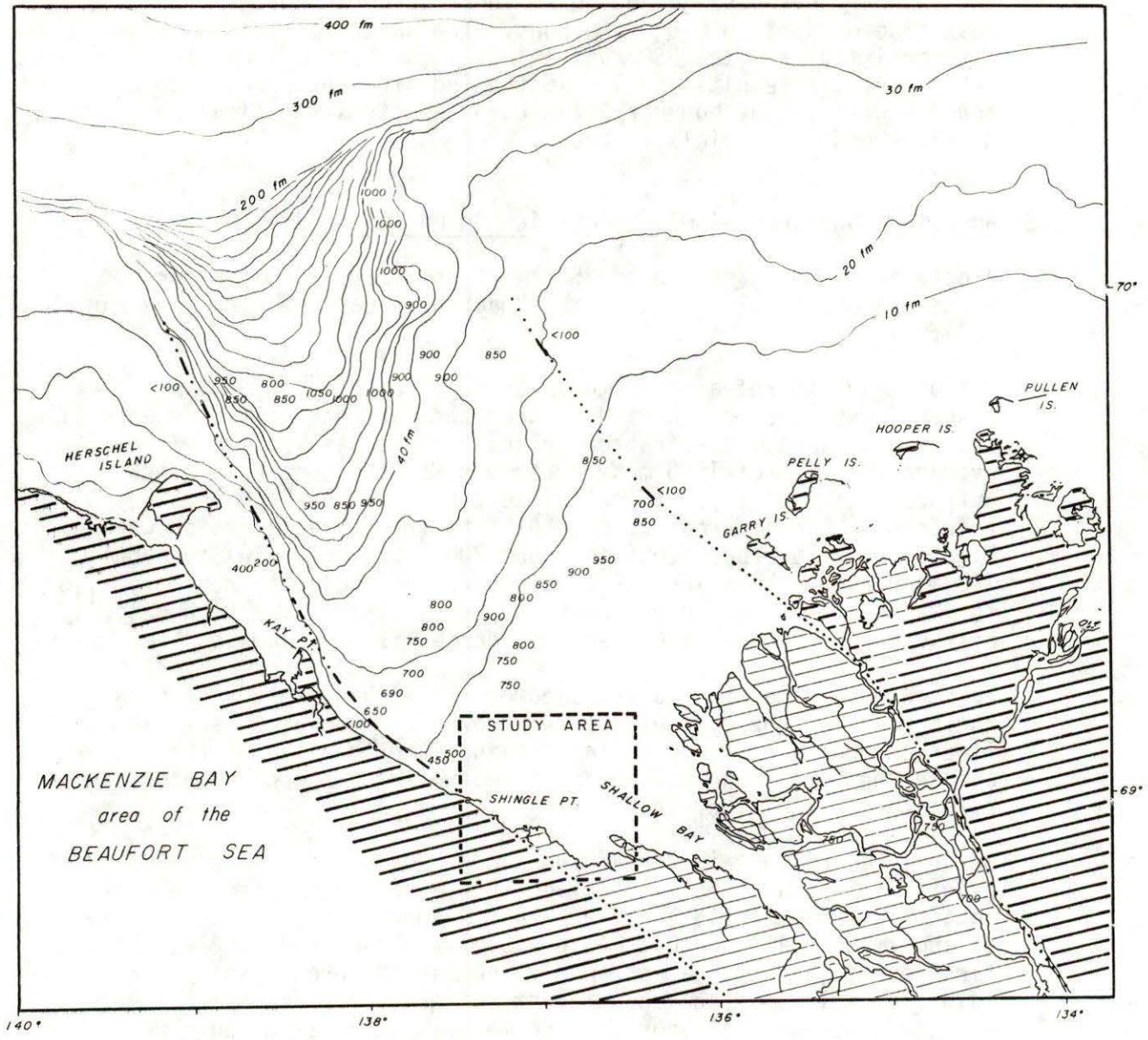

Fig. 6-4 Location of the survey area in Mackenzie Bay. Offshore bathymetric contours show the extent and magnitude of the Mackenzie Canyon. Dotted line denotes the interpreted edges of the buried ice scour channel, after Shearer, 1972. Small figures are the depths in feet to the base of the scour channel and those outside of the channel represent thickness of sediment deposited in post-scour times. Light hachured lines delineate distribution of modern Mackenzie delta sedimentation: dark hachured, areas of older Quaternary sediment.

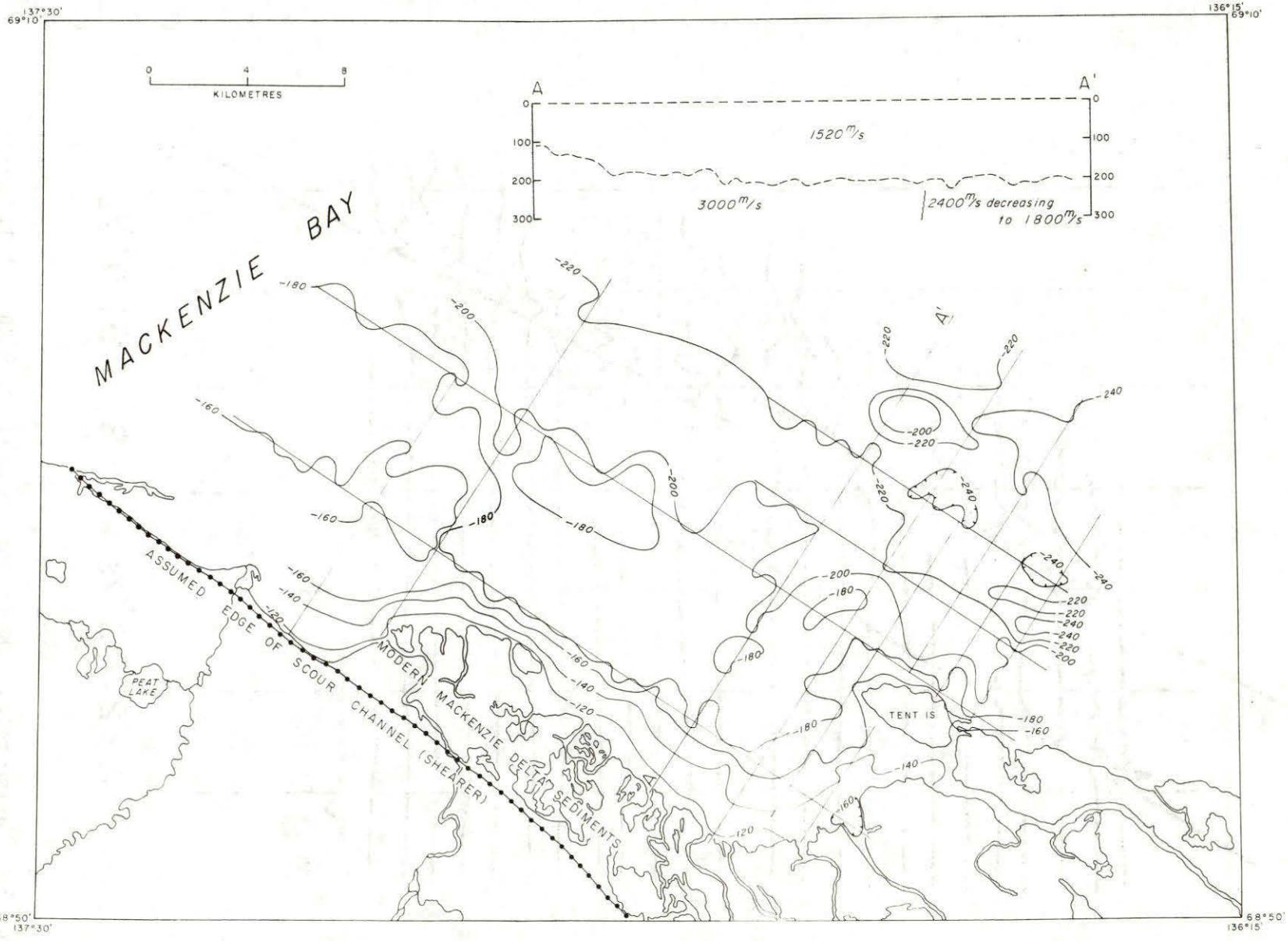

Fig. 6-5 Depths to high velocity refraction below sea level. Contours are in metres.

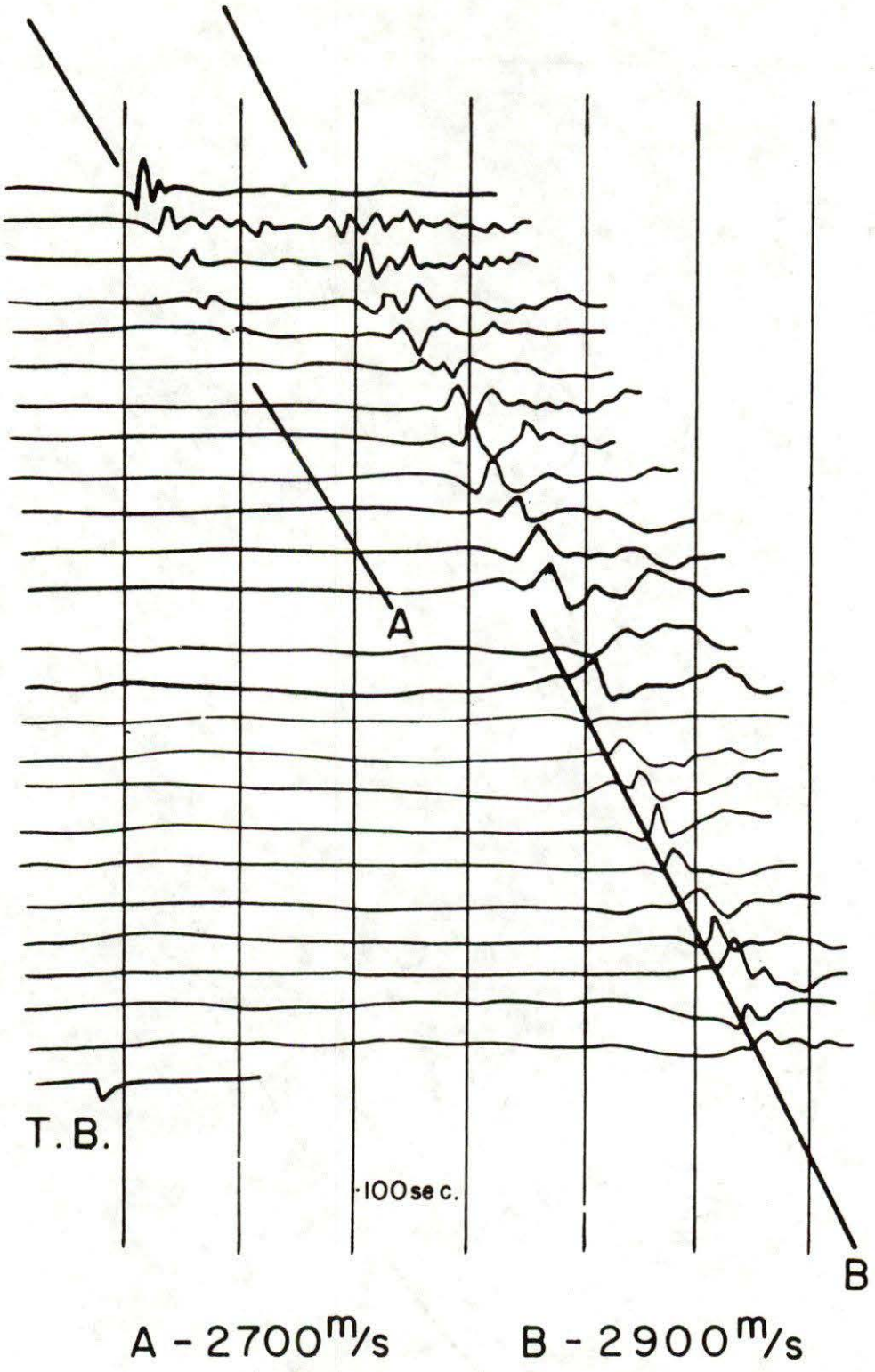

Fig. 6-6 Marine refraction records showing two high velocity events indicating a thin high-speed surface layer.

Pursuant to a permafrost interpretation in the vicinity of the shoreline, the top of the frozen section would rise and the total thickness of it would probably increase due to the proximity of a cold northern shoreline of mean surface temperature -10°C compared with seabottom temperatures close to 0°C. However, the wedge-shape of the frozen ground persists to too great a distance offshore for an explanation based solely on the effect of the shoreline. A simple explanation of this elongation offshore could be found in a rapidly receding shoreline. At present the shoreline in the area is aggrading as is shallow permafrost evidenced by a thin near-surface high velocity layer. Permafrost in the area is apparently very complex in nature. Aggradation is occurring at the present shoreline both from the surface and from an older shoreline producing a thin permafrost layer in the near-surface and a wedge-shaped section at depth extending out under the sea to a distance of several kilometers from the present coast. Hence, permafrost underlying the seabed remote from the shoreline would be relict in nature and degrading at present since present seabottom temperatures are too high to support deep permafrost in thermal equilibrium. Even if present seabottom temperatures in Shallow Bay were below 0°C, the terrestrial heat flux could only support a current permafrost thickness of 100 m. That same flux is sufficient to have also melted a maximum of 200 m of relict permafrost in the past 10,000 years.

Thus, it is difficult to explain the high velocity refractor by the presence of the permafrost unless conditions were suitable in the past for thicknesses in excess of 300 m to have accumulated on the south side of Shallow Bay. As discussed by Judge (1974), the Mackenzie Canyon area of which it formed part underwent a very different history to that of the offshore north of Richards Island. For much of the Wisconsin it was covered by an ice sheet (Mackay et al., 1972) and thus exposed to less severe surface temperatures than the unglaciated parts of the Beaufort Sea. Consequently, permafrost at the end of the Wisconsin period was, for example, probably thinner than that on Richards Island today. At the time of recession of the ice sheet 14,000 to 16,000 years B.P., sea level was as much as 70 m below present sea-level. Therefore, the rate of inundation of the area by the sea depends on the rate of accumulation of post-glacial sediments. Assuming an ice-base temperature during the Wisconsin of -2°C and an exposed land surface to have existed between glacial recession and the time of stabilization of sea-level 5000 years B.P. as much as 200 m of permafrost could have aggraded. Decreasing the Wisconsin ice-base temperature increases this thickness by approximately 35 m per 1°C decrease. For the top of the frozen section to now be at a depth of 200 m either very high rates of degradation or very rapid burial is necessary. Neither explanation seems likely.

In the central and northern parts of the Mackenzie Canyon area, seismic velocities indicate unfrozen sands at the base of the scour channel. These results are confirmed by subsurface temperature measurements made in the onshore portions of Shallow Bay (Taylor and Judge, 1974). At each of these sites, permafrost is relatively thin (60 to 150 m) and commences at the surface consistent with young

sediments in which permafrost is aggrading. Positive temperature gradients of 22 to 45°C/km indicate no relict permafrost at depth. These observations place severe limits on the total amount of permafrost which could have accumulated in the Mackenzie Bay area.

It is perhaps worth re-iterating that permafrost and hydrofrost (gas hydrates) may possess similar seismic velocities in coarse-grained materials. Once again, however, the limited sub-surface temperature measurements in the onshore portions of Shallow Bay would tend to rule out the presence of gas hydrates under equilibrium geothermal conditions unless they are of high specific gravity (>0.6). Under highly non-equilibrium conditions, thick, shallow gas reservoirs might remain at present in the hydrate form almost anywhere in Shallow and Mackenzie Bays. A more reasonable history for the area such as that suggested in the permafrost interpretation could result in gas hydrate deposits at depths exceeding 100 m in areas that formed the margins of the Wisconsin ice lobe (the edges of the canyon?).

Alternatively, the high refractor velocity may result from an older geological formation which has been structurally uplifted.

In summary, no definite interpretation of the seismic refractor can be made. It may be ice-bonded permafrost, although from what is known of the surface history of the area it is difficult to explain its presence remote from the shoreline. It may be hydrofrost under suitable conditions which could pertain to certain parts of Mackenzie Bay or, yet a third alternative, it could represent an older uplifted formation. A final solution must await the acquisition of deep sub-surface temperature profiles in the area.

6.3 A Comparison of Seismic and Drilling Results, Kugmallit Bay

The results of shallow refraction shooting with the GSC array near Base Summit in Kugmallit Bay are compared with the drilling results from GSC drill hole #1 in Fig. 6-7. Close to shore, the top of a high velocity layer is detected at a depth of 20 m, but becomes apparently discontinuous (beyond the range of the shallow refraction array), and disappears to seaward. The depth to the top of ice-bonded permafrost given by the seismic refraction results are reasonably close to that given by temperature measurements in the drill-hole.

Fig. 6-8 shows a refraction section across Kugmallit Bay shot with the GSC array along with an interpretation of air gun shallow reflection data (J. Shearer, GSC, pers. comm.) for a line approximately one mile north of the refraction line, from Toker Pt. to the middle of the bay. The data indicates that the interpreted upper boundary of ice-bonded permafrost is considerably shallower towards either shore. In the centre portions of the bay, the interface drops to a depth of 90 m and becomes discontinuous in some areas. The discontinuities in permafrost are seen on both reflection and refraction records and suggests that the top of ice-bonded permafrost is either

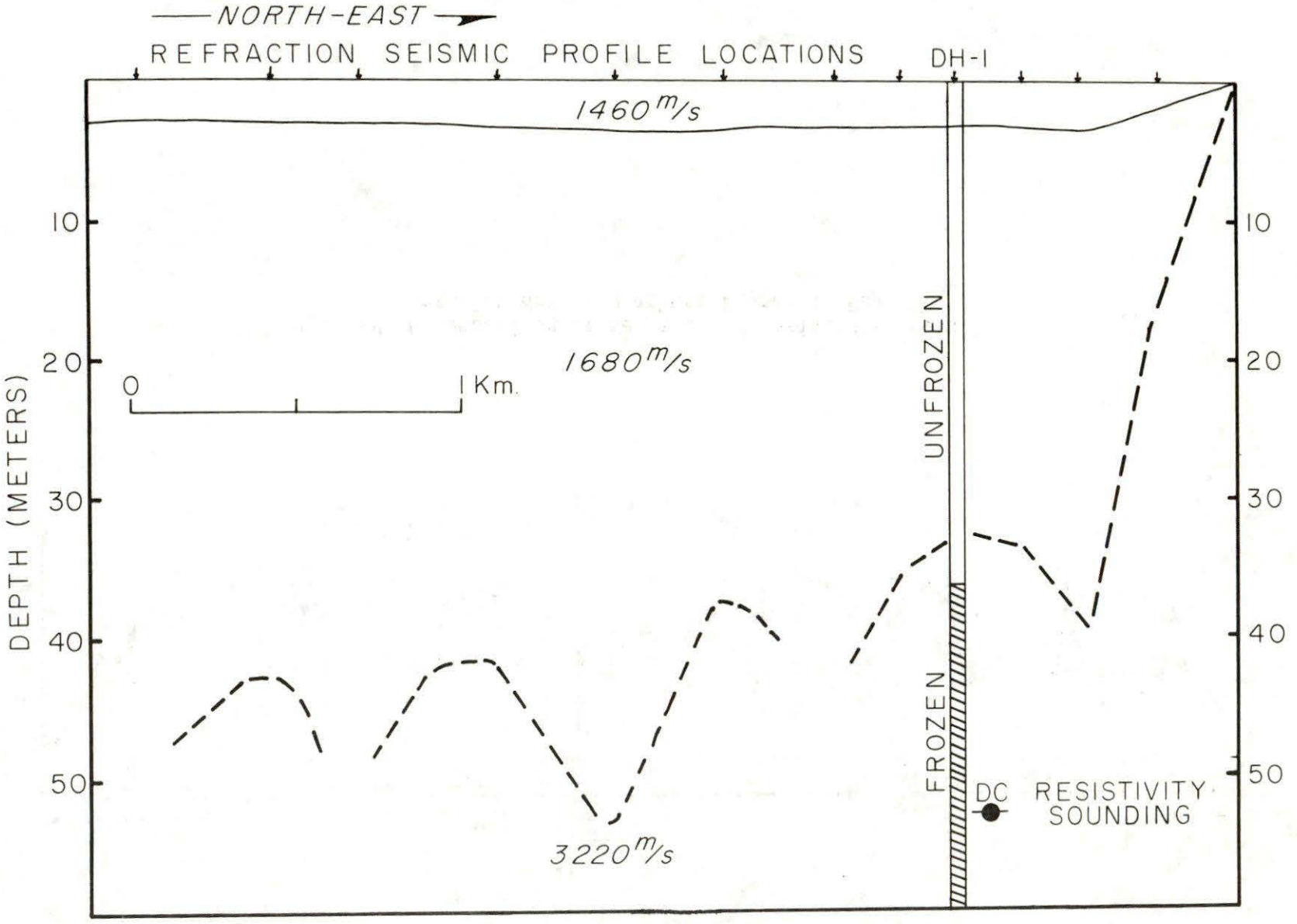

Fig. 6-7 A comparison seismic refraction, DC resistivity and drilling results for the top of ice-bonded permafrost at GSC DH #1 in Kugmallit Bay.

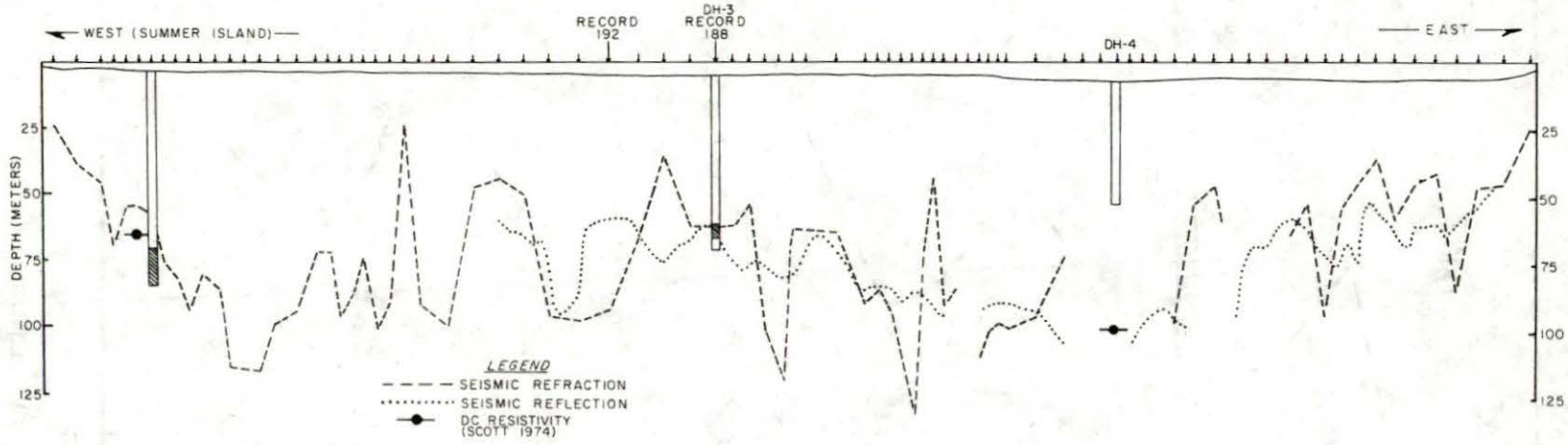

Fig. 6-8 A comparison of seismic and resistivity results with GSC drilling across Kugmallit Bay.

quite deep (>100 m deep) or absent. Alternatively, since clay at temperatures of -1° to -2°C is usually indistinguishable seismically from the unfrozen state, the areas lacking high velocities could be interpreted as thick clay deposits in the frozen state. The average velocity of permafrost interpreted over the section is 3290 m/sec, suggesting that the material is frozen coarse-grained silts or sands. A good correlation exists in general between the top of ice-bonded permafrost as determined by the seismic work and the top of permafrost as given by temperature measurements. DH #2 was placed in an area where seismic data suggests that the top of ice-bonded permafrost is rising sharply, hence a navigation error of a 100 m and possible computation error of 10% resulting from the dipping interface would more than account for the difference in interpreted depths to the top of permafrost.

Seismic evidence for the existence of the thin permafrost lens at DH #3 can be found from a close examination of the seismic records. Fig. 6-9 shows the measured "first-break" amplitudes for the permafrost refractor for record #188 shot over DH #3 and for record #192 shot approximately 2400 m away in an area which is interpreted as thick permafrost. Studies on the thin layer problem by Riznichenko and Shamina (1957), Rosenbaum (1965), Donato (1965), and Poley and Nooteboom (1965) and others suggest that the refracted wave along a thin high-speed layer is characterized by a low amplitude and a high attenuation rate compared to that of a refractor in a thick layer. If proper assumptions are made for mathematical constants, approximate formulae given by Rosenbaum and Donato can be employed to determine the layer thickness. With no information on which to base these assumptions, however, it is still possible to qualitatively assess the relative thickness of the permafrost layer from examination of "first-break" amplitude-distance curves since the attenuation rate increases with decreasing layer thickness.

Marine DC resistivity soundings made by Scott (1975) and in the Kugmallit Bay area indicated that a highly resistive layer lies at depth below the seabottom. Depths determined to the top of this layer are given on Fig. 6-7 and Fig. 6-8. The depth to permafrost given by the soundings is in general somewhat deeper than that given by the seismic and drilling. This is probably in part a result of non-planar layering encountered in the large area over which the resistivity sounding is made. It is interesting to note that permafrost is interpreted to be present at considerable depth below DH #4. No indication of permafrost was found on the seismic reflection or refraction records although the interpreted depth is at the limit of the range of both seismic systems employed.

6.4 Seismic Results at Proposed Well Sites

Seismic refraction work was conducted at the two proposed Canmar well sites in the through-ice seabottom mode (Scott and Hunter, 1976) and with the GSC array from the *C.C.G.S. Nahidik*. As well, a detailed record interpretation of the nearest industry records to each site was carried out.

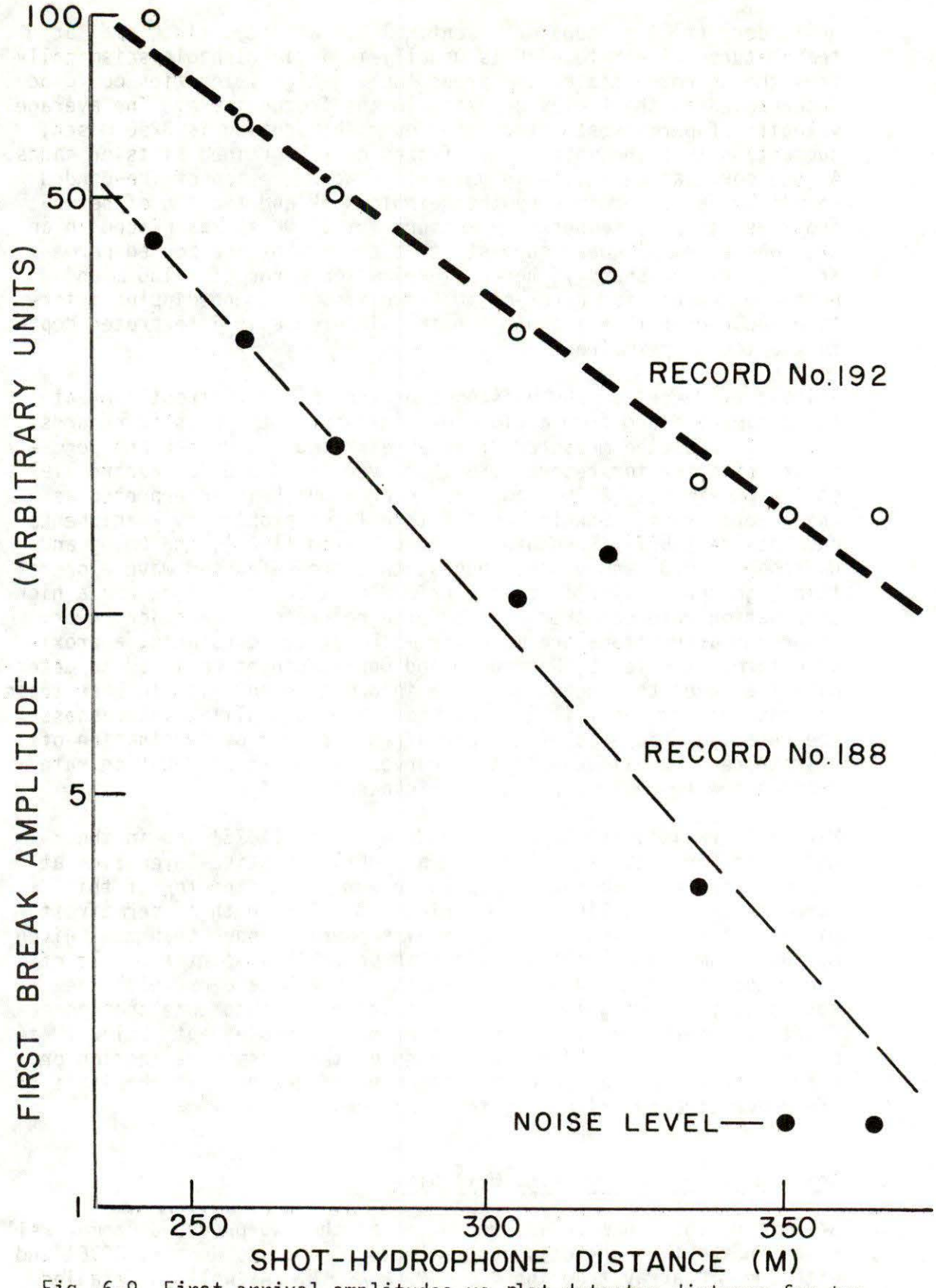

Fig. 6-9 First arrival amplitudes vs plot-detector distance for two refraction records in Kugmallit Bay showing attenuation from thick (#192) and thin (#188) ice-bonded permafrost layers.

At Tingmiark (Fig. 6-10), both the seabottom and *Nahidik* data indicated a thin high speed layer close to bottom (approximately 30 m depth) which correlates well with the top of ice-bonded permafrost determined from drilling. The event demonstrates rapid attenuation and shingling; a later event with higher amplitudes was computed at a depth of 65 m below bottom from the seabottom array data (after taking into account the transit time through a 10 m thick high velocity layer). This correlates well with the industry data interpretation (54 m below bottom).

At Kopenoar, the results based on marine seismic refraction techniques incorporating high resolution reflection mapping is shown in Fig. 6-11. The seabottom array (Fig. 6-12) indicated a high velocity material on bottom which could be interpreted as either unfrozen coarse-grained material or frozen clay with low ice content. From high frequency sub-bottom profiling done from the *Nahidik*, approximately 3 m of signal penetration was achieved, indicating a surface clay layer. The GSC array data obtained from the *C.C.G.S. Nahidik* detected only the water layer (1430 m/sec) and the ice-bonded layer (3960 m/sec). The high velocity bottom layer appears as a "hidden" layer; its position is plotted with the *Nahidik* data. If the "hidden" layer is not taken into account in the computations, an error of 5 m in the depth of the ice-bonded layer would result. Again with the industry data, when the seabottom velocity is included in the interpretation, the depth to the top of the ice-bonded layer correlates closely with those obtained by the other two arrays.

6.5 Thermal Models of Offshore Conditions

In spite of the uncertainties in the input data, Fig. 6-13 taken from Judge (1974) illustrates the general permafrost thickness to be expected in the seabottom beneath different water depths (namely 20 m, 40 m and 60 m) and how that thickness changed with time in response to the time dependent surface temperature history. The effect of latent heat in retarding the establishment of thermal equilibrium is pronounced as is illustrated by comparison with the calculations of Lachenbruch (1957). As an illustration of how dependent the present distribution is on the pre-Wisconsin Pleistocene history, the present thickness below 20 m of water is shown for both an emergent and a submerged land surface prior to the Wisconsin glacial period. Thickness predicted by the two models is 500 and 250 m respectively. Of particular interest and directly amenable to measurement in drill holes are the differences in heat flow which result. In this example, in which permafrost is degrading at present and in which the equilibrium heat flow below the base of the frozen layer is 63 mWm^{-2}, the heat flow exhibited within the permafrost ranges from 25 in 20 m of water to 50 in 80 m of water.

On a more local scale, Fig. 6-14 illustrates the change in subsurface temperature after a typical emergent land area, with a lithology of unconsolidated sands and gravels, a fresh-water ice content of 25% by volume and initial temperature conditions similar to the Tuktoyaktuk area today, is inundated by the sea with a mean

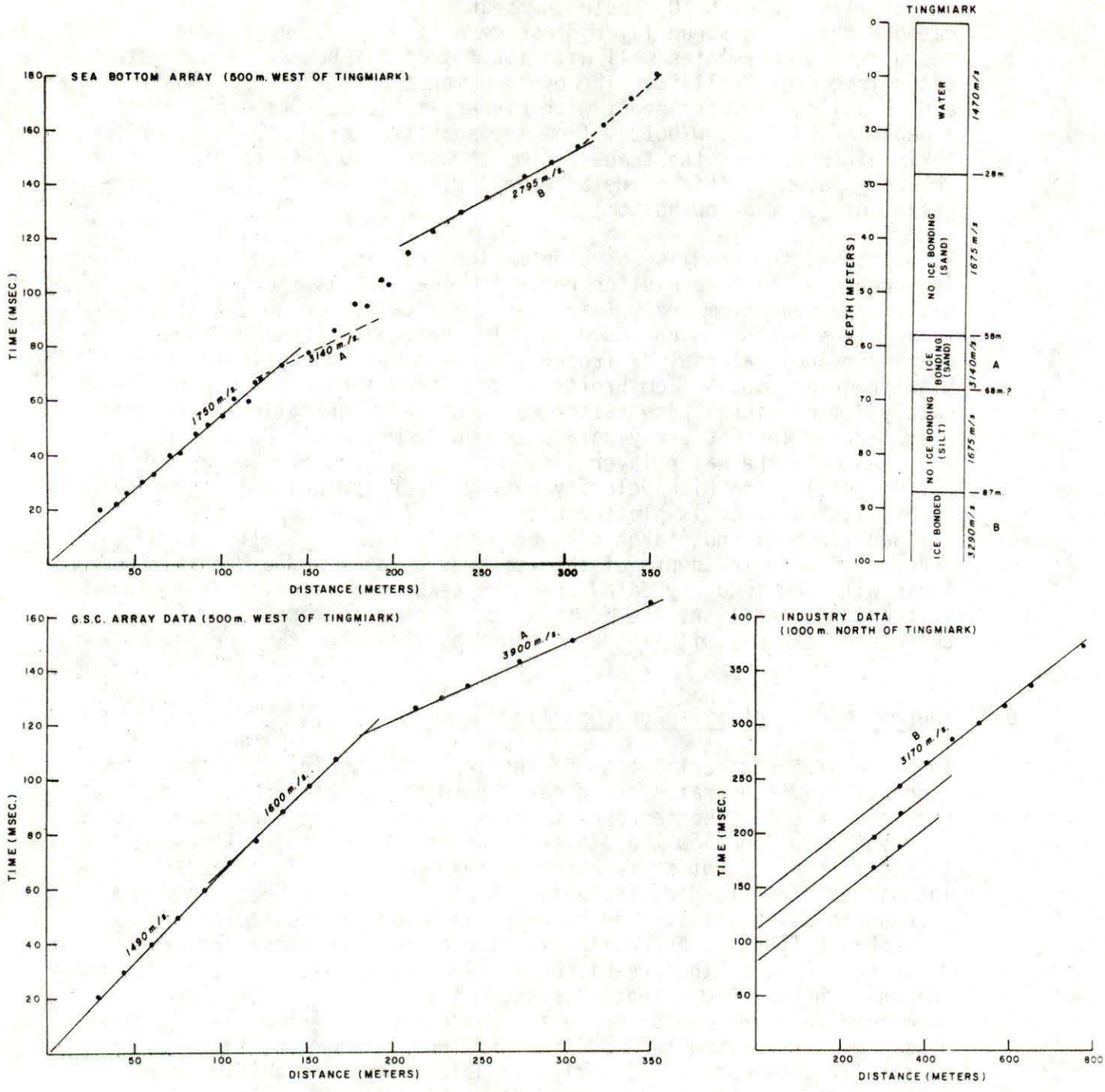

Fig. 6-10 A compilation of refraction seismic data at the proposed Tingmiark drill site.

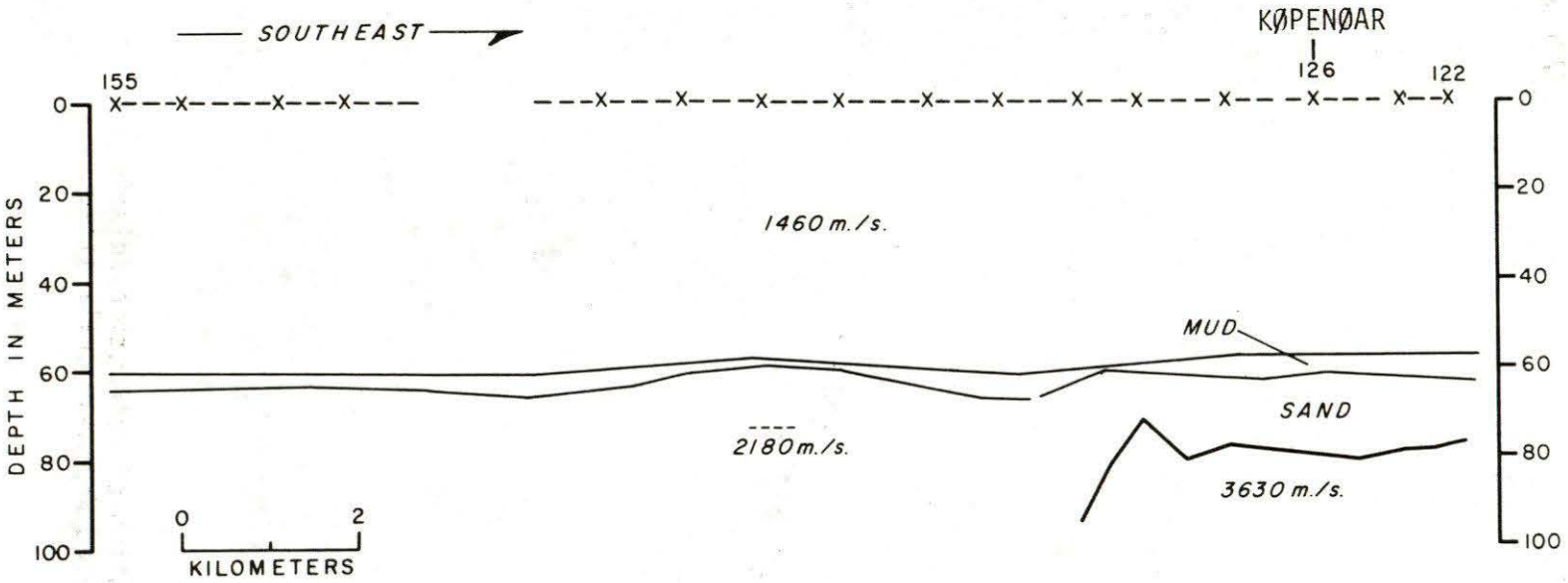

Fig. 6-11 An interpreted section over the Kopenoar proposed drilling site from surface marine refraction and acoustic profiling.

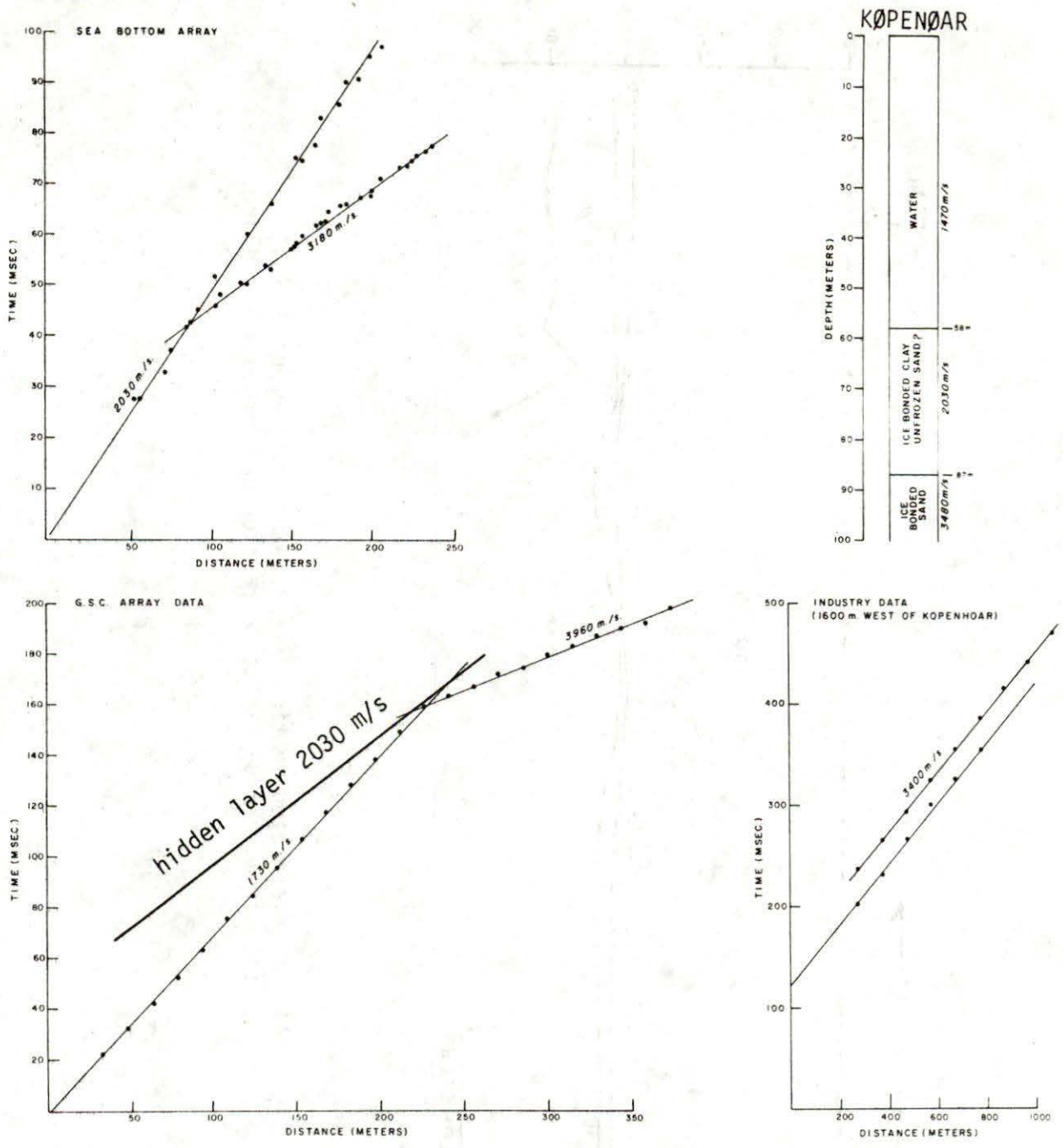

Fig. 6-12 A compilation of refraction seismic data at the proposed Kopenoar drill site.

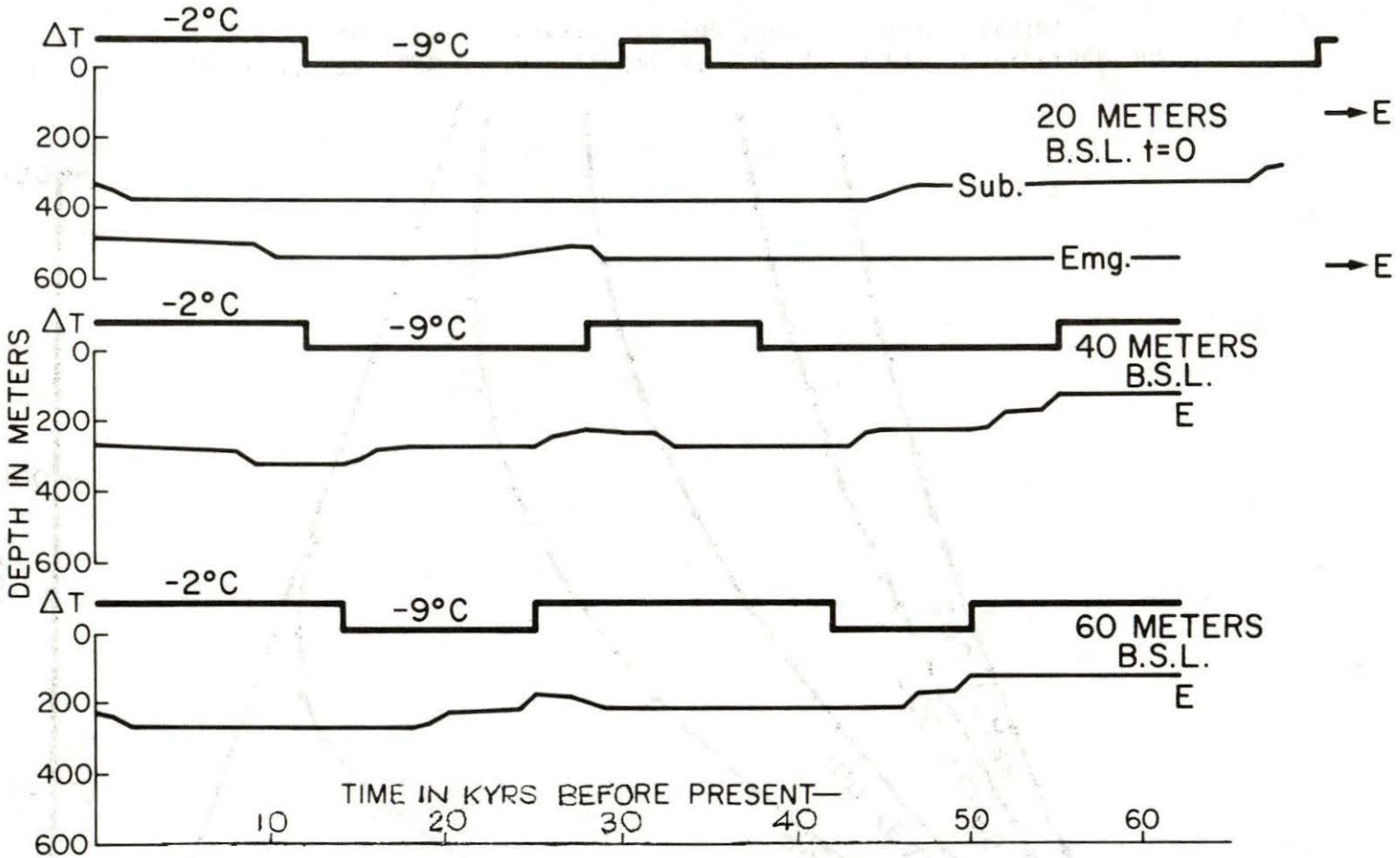

Fig. 6-13 Remanent permafrost thickness of sediments in the Beaufort Sea. Times of emergence and submergence are shown together with the depth of the 0°C isotherm, and the depth of the equilibrium position of the isotherm denoted by E. (B.S.L. means below sea level; Emg. means surface emerged more than 85,000 years ago; sub. means surface submerged more than 115,000 years ago.)

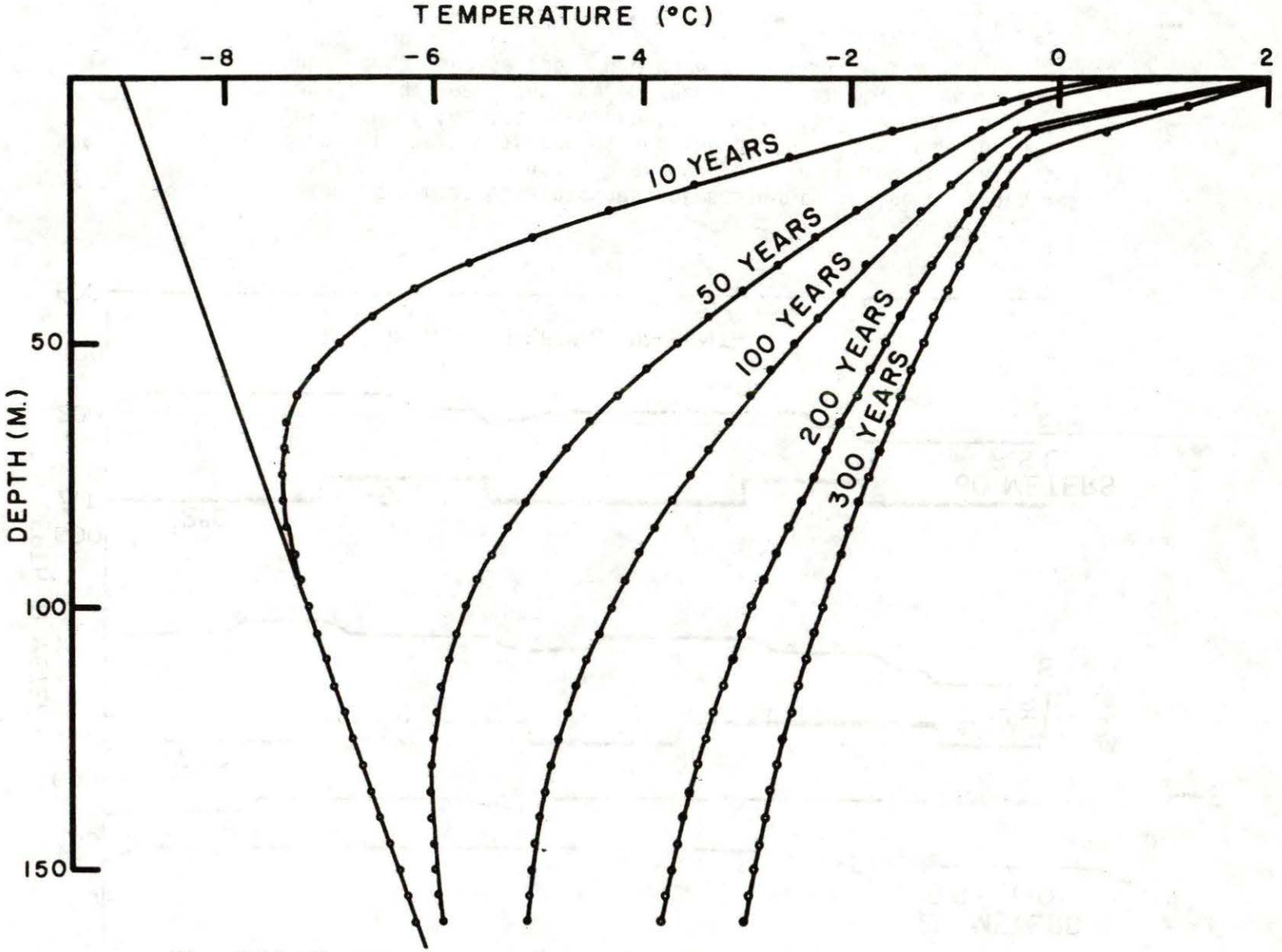

Fig. 6-14 The temperature régime of the near-shore sub-surface during shoreline recession on the Tuktoyaktuk Peninsula.

annual bottom water temperature of +2°C. The time taken to achieve a new equilibrium state is, of course, many tens of thousands of years. The figure, however, represents only the first 300 years, which in the Tuktoyaktuk townsite area with an average recession of 1 m yr^{-1} represents the first 300 m offshore. At the end of the 300 year period, sub-surface temperature gradients remain negative and the melting of frozen ground from the surface has only penetrated a depth of 12 m.

In the shallow waters of the Beaufort Sea, seabottom temperatures are primarily positive, whereas in deeper waters they are negative. As the sea-level rose after Wisconsin glaciation, the land surface was gradually submerged, initially in the warm nearshore waters and then in waters with negative temperatures. As a consequence, permafrost initially degraded at the seabottom but later reformed. Fig. 6-15 illustrates this process. Initially, the land surface at -10°C is submerged in waters at +2.5°C and permafrost degraded to a depth of 70 m in 4000 years, but at 5000 years the seabottom temperature fell to -1.5°C, causing permafrost to reform so that a further 4000 years later it had reformed to a depth of 60 m. Penecontemperaneously, the original thick section of the offshore permafrost was degrading and had for much of the time existed at marginally negative temperatures.

As mentioned in Judge (1975) and in section 6.6, the western delta exhibits very different thermal characteristics reflecting the very different thermal history. Using appropriate thermal input data for this area, simulations were used to place limits on permafrost occurrence and thickness and thus to explain anomalous seismic velocities in Mackenzie Bay (section 6.2). In Mackenzie Bay and Shallow Bay, deltaic islands are emerging from the waters, creating a new land surface beneath which permafrost is aggrading anew.

Fig. 6-16 illustrates the regrowth of permafrost as a new land surface aggrades in the western delta area. Initially, the surface temperature is -2.5°C but falls to -1.5°C as the land surface emerges. At the end of 1000 years, permafrost has grown to a thickness of 40 m and after 10,000 years to a depth of 52 m on the way to a final equilibrium value of 65 m.

The true picture in each of these areas is, of course, far more complex than these simple simulations allow. If the present Tuktoyaktuk Peninsula can be used as an example, much of the present offshore area may have been covered with lakes during emergence. In such areas when submerged beneath below-zero waters, permafrost will begin to aggrade. Other complexities arise in the true nature of shoreline recession, and from the effects of rapid sedimentation, shifting river channels, complex shoreline geometries, etc. At present, knowledge of even the times of emergence and submergence and of ice-sheet boundaries remains somewhat speculative.

Not considered above and perhaps of some importance are the roles played by the processes of heat transfer in the sub-surface environment. There is some limited evidence that mass transfer processes may play a role in determining the sub-surface temperatures in some

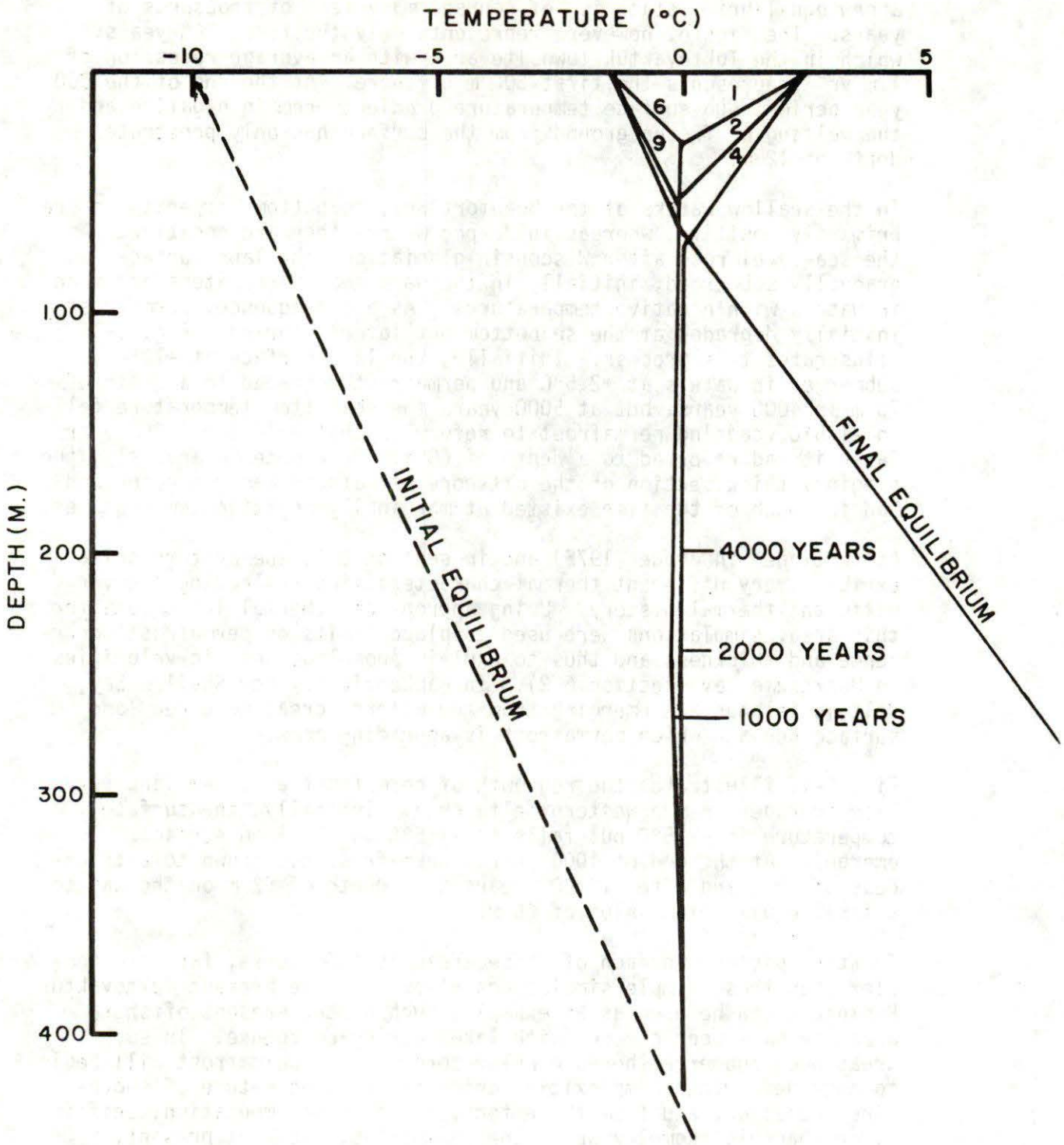

Fig. 6-15 Permafrost degradation and aggradation during shoreline recession on the Tuktoyaktuk Peninsula.

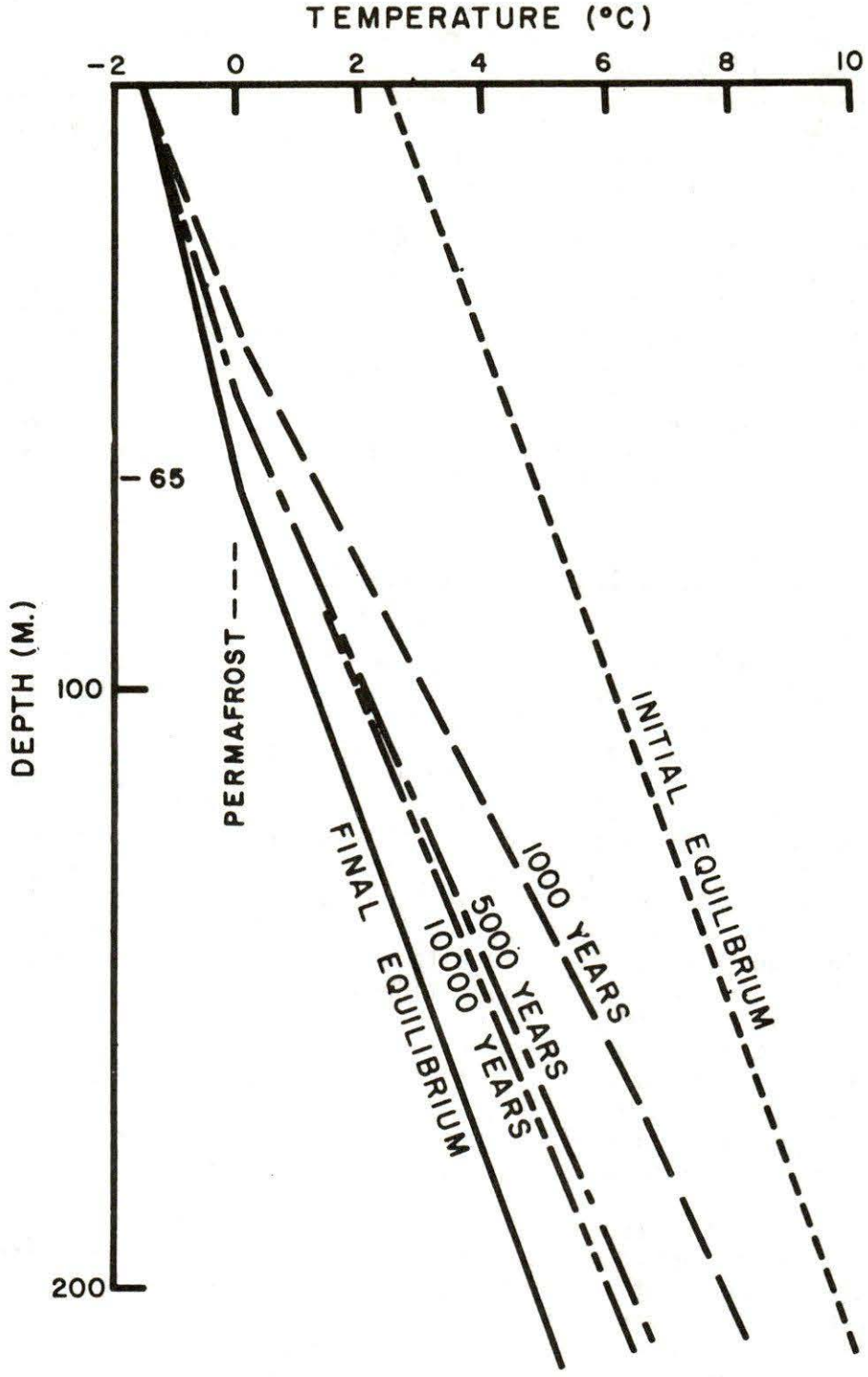

Fig. 6-16 Permafrost aggradation at an emerging shoreline.

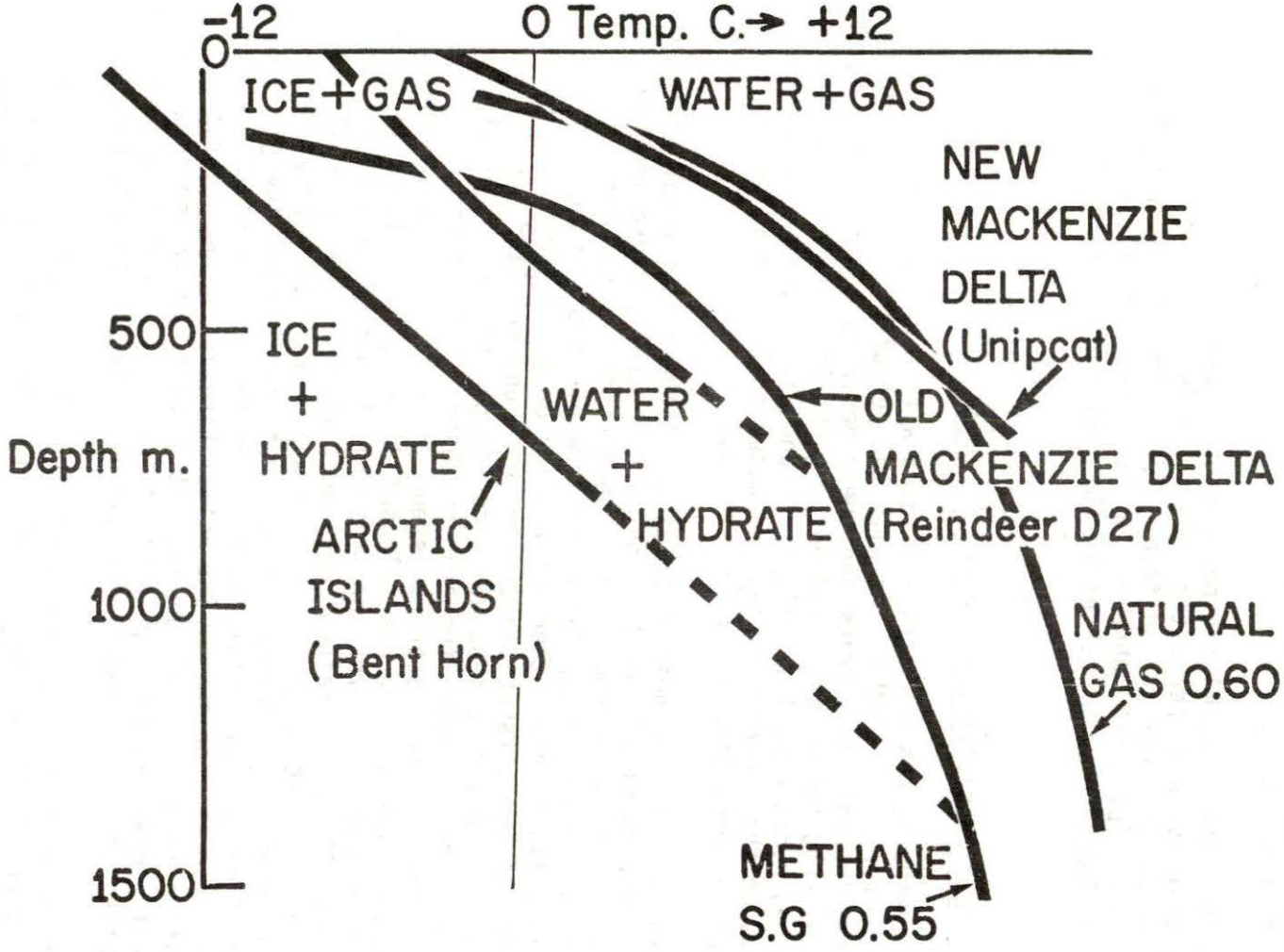

Fig. 6-17 Gas hydrate potential in the Mackenzie Delta-Beaufort Sea area (phase curves after Katz (1972); sub-surface temperature curves after Taylor and Judge (1975)).

be somewhat speculative at this stage. However, if essentially isothermal conditions exist through a permafrost column of 500 m, then the potential hydrate zone will likely extend to a depth of at least 1000 m. The presence of a hydrate below the permafrost also further retards the return to thermal equilibrium and essentially isolates the ice-bonded sections of the permafrost from degradation.

7. DISCUSSION OF RESULTS

7.1 Interpretation of Seismic Results

From the meagre correlatable drilling data available, it appears from the seismic interpretation that ice-bonded permafrost is confined to areas of coarse-grained sub-seabottom materials where abundant fresh water has been available to form inter-granular ice. In the offshore regions (where mean annual seabottom temperatures are less than 0°C) ice-bonded permafrost is probably aggrading at the upper surface and degrading at the lower boundary. Inshore, where seabottom temperatures are under the influence of the Mackenzie River discharge, ice-bonded permafrost is degrading from both the upper and lower surfaces. Rugged topography on the upper boundary in the inshore regions bears witness to the differential degradational rates resulting from river channel development at lower sea levels.

Although in the western portion of the survey area there is no indication of ice-bonding from the seismic records, bottom temperature data in the offshore portions suggest that permafrost conditions exist; hence we suggest that most of the upper 100 metres of sub-seabottom material is fine-grained silts and clays. This interpretation correlates well with the A.P.O.A. drilling results in the inshore area given in Fig. 5-13, indicating a thickening of fine-grain sediments to the west of Richards Island. Further, we suggest that thick fine-grained materials probably can be found below seabottom north of Cape Dalhousie in the area where our seismic interpretation indicates no ice-bonding present.

Most cores taken in coarse-grained ice-bonded materials in the thermokarst area on shore (Rampton and Mackay, 1971) indicate excess ice present. Indeed, seabottom topography, not unlike onshore thermokarst areas, is found in areas of interpreted ice-bonded permafrost. However, it is not unreasonable to expect excess ice conditions to exist offshore in similar materials. We suggest that our interpretation of ice-bonded sub-seabottom permafrost may be taken as a guide to areas where potentially hazardous conditions exist.

As well, since gas hydrates in sediments are seismically indistinguishable from ice-bonded permafrost, an interpretation of high seismic velocities may also serve as a guide to the potential occurrence of such shallow deposits.

7.2 Drilling in Frozen Sediments: Onshore Wells

Ice-bonded permafrost, as northern onshore wells have shown, produces additional problems in drilling a well. Two gas wells in the Arctic islands suffered blowouts as a result of poor casing procedures. Many early discovery wells were left for possible development. Most of them suffered casing collapse within a few months of suspension and within several hundred feet of the surface.

Careful casing procedures have been developed for the onshore environment, consisting of a 60 ft refrigerated conductor pipe, a 500 ft permafrost string and a surface casing to a depth in excess of the maximum depth of occurrence of permafrost. This upper section is generally drilled quickly with a cool mud. To the authors' knowledge, no blowouts attributable solely to permafrost conditions have occurred since these procedures were implemented.

7.3 Drilling Through Gas Hydrates

As onshore wells have shown, gas hydrate presence can pose problems in northern drilling. Several severe gas 'kicks' in the delta are known to have resulted from gas hydrate composition during drilling. Several fires on seismic rigs may have been associated with hydrates or their decomposition.

Careful casing and drilling design, detailed mud and gas logging programs, plus special personnel training programs, have been developed for the onshore environment. The objective is to drill with a cool, heavy mud to minimize both pressure and temperature disturbance to the hydrate until the section is adequately cased and cemented off. A rigorous training program ensures that drill crews know what procedures to adopt if and when gas kicks occur.

8. CONCLUSIONS

1) Sub-seabottom permafrost exists over much of the Beaufort Sea shelf.

2) Ice-bonded permafrost is confined to the eastern half of the survey area.

3) Excess ice has been observed in shallow offshore drill holes.

4) Seabottom morphological features can be associated with ice-bonded permafrost.

5) Permafrost thickness varies from 600 m at the shoreline to thicknesses of 100 m in the offshore.

6) The upper boundary of ice-bonded permafrost can occur at depths between seabottom and 200 m below.

7) Because of non-equilibrium thermal conditions, permafrost is aggrading downwards from the sea floor in the offshore, and is degrading in the inshore regions.

8) Gas hydrates probably exist at shallow depths below seabottom in association with permafrost, and are seismically indistinguishable from ice-bonded permafrost.

9) Temperatures of sub-seabottom permafrost are much warmer than that occurring on land and ice-bonded sediments are much more susceptible to thermal degradation than their onshore equivalents.

9. THE IMPLICATIONS OF PERMAFROST OCCURRENCE FOR OFFSHORE OPERATIONS

9.1 General Implications

Offshore permafrost can considerably influence the design of facilities to be used in northern waters. Frozen soil in thermal equilibrium provides an excellent foundation. If ice-rich, however, it will, on thawing, tend to subside differentially with reduced bearing strength. Offshore the potential consequences of an engineering failure are greater than onshore in terms of loss of human life, environmental damage and rectification costs. It is, therefore, imperative that the presence and properties of permafrost and/or gas hydrates be fully considered in the design of bottom or sub-bottom founded structures. The first offshore structures proposed will probably be associated with the discovery, production and transportation of hydrocarbons; those most influenced by the presence of permafrost are pipelines, wellbores, pile-founded platforms and gravity structures resting directly on the sea-floor.

Pipelines are potentially subject to damage by differential movement of a thaw-bulb, which might extend to 30 m from the pipe, or by differential freezing and frost-heave around a chilled pipeline. Wellbores are subject to permafrost damage as discussed previously, i.e. primarily by freeze-back, subsidence and loss of control of high pressure fluids. Gravity structures may be subjected to differential stresses due to freezing and thawing. These structures may be concrete drilling and production platforms, such as those used in the North Sea, Arctic harbour structures and silos containing well-head equipment. These processes may be particularly important at the production stage. Dredging operations might be far more difficult in the presence of permafrost because dredging equipment is usually not designed to handle ice-bonded materials. Once the near-surface material is removed, the deeper material is subject to new thermal conditions and may be subject to additional heave or settlement. Permafrost knowledge will, therefore, be of extreme importance in designing coastal facilities. A misinterpretation of deep structures by exploration seismic reflection records could result from a discontinuous lateral distribution of high velocity ice-bonded permafrost. Such errors in interpretation can result in the drilling of costly dry holes.

Although this report is concerned with the safety of wildcat drilling, it is apparent from the above that permafrost conditions are of prime importance to all aspects of offshore northern resource development.

9.2 Implications for Offshore Drilling

The proposed offshore drilling using drillships in the Beaufort Sea combines many of the hazards of permafrost and offshore drilling, none of which are insurmountable.

Some of the major concerns which pertain to sub-surface conditions are:

a) an adequate casing seal to drill safely through permafrost,

b) a drilling program designed to minimize the thermal disturbance of permafrost and gas hydrates,

c) an adequate casing seal to control hydrate decomposition and other high pressure fluids from greater depths,

d) adequate assurance of the structural stability and integrity of the silo,

e) protection against casing collapse should the well be suspended over a season.

For the present, the concerns are for the safety of wildcat drilling, but the eventual objective is not only to find, but to produce hydrocarbons. At that stage, permafrost and hydrate conditions will be even more important since hot fluids in the wellbore are unavoidable. Thus, it is very important to maximize the derived downhole information at the initial stage of wildcat drilling, should it be approved.

Because of the great variability of shallow sub-surface offshore conditions, extensive survey programs may be necessary at each wildcat location prior to the actual drilling of the well. Without such local information, it may be difficult to assure a safe drilling program.

REFERENCES

AHLMANN, H.W. 1948. Glaciological research on the North Atlantic coasts. Royal Geographical Society, Research Serial No. 1, 83 pp.

ANDERSON, D.M. and N.R. MORGENSTERN. 1973. Physics, chemistry, and mechanics of frozen ground: A review. *In*: Permafrost, North American Contributions, Second International Conference Proceedings, NAS/NRC: 257-288.

ANDREWS, J.T. 1973. The Wisconsin Laurentide ice sheet: dispersal centers, problems of rates of retreat, and climatic implications. Arctic and Alpine Res. 5: 185-199.

ANTSYFEROV, M.S., N.G. ANTSYFEROVA, and YA.YA. KAGAN. 1965. A study of the propagation velocities and absorption of elastic waves in frozen sand. Izv. Akad. Nauk. S.S.S.R. Ser. Geofiz. 1: 85-89.

APIKAEV, F.F. 1965. Temperature field effect on the distribution of seismic velocities in the permafrost zone. *In*: Akademiaa Nauk. S.S.S.R. Sibirskoe otd-ie. Inst. merzlotovedeniia. Teplovve protsessy v merzlykh (in Russian).

BALOBAEV, V.T., V.N. DEVYATKIN, and I.M. KUTASOV. 1973. Contemporary geothermal conditions of the existence and development of perennially frozen rocks. *In*: Proceedings of 2nd International Permafrost Conference, Moscow, 1: 11-19.

BARANOV, I.1a. 1959. Geographical distribution of seasonally frozen ground and permafrost. *In*: Principles of Geocryology, Part I, General Geocryology, NRC-TT 1121, 85 pp.

BARNES, D.R. 1966. A review of geophysical methods for delineating permafrost. *In*: Permafrost: Proceedings of an International Conference, National Academy of Sciences, Washington, D.C.: 349-355.

BECK, A.E. and A.S. JUDGE. 1969. Analysis of heat flow data - detailed observations in a single borehole. Geophys. J. 18: 145-158.

BELL, R.A.I. 1966. A seismic reconnaissance in the McMurdo Sound region, Antarctica. J. Glaciol. 6(44): 209-221.

BILY, C. and J.W.L. DICK. 1974. Naturally occurring gas hydrates in the Mackenzie Delta, N.W.T. Bull. Can. Petrol. Geol. 22: 340-352.

BLACK, R.F. 1950. Permafrost. *In*: Applied Sedimentation, P.D. Trask (ed): 247-275.

BLACK, R.F. 1954. Permafrost - A review. Geol. Soc. Amer. Bull. 65: 839-855.

BROWN, A.D. and K.W. BARRIE. 1976. Artificial island construction in the shallow Beaufort Sea. *In*: Proceedings of 3rd International Conference of Port and Ocean Engineering Under Arctic Conditions. Fairbanks (in press).

BUSH, B.O. and S.D. SCHWARZ. 1964. Seismic refraction and electrical resistivity measurements over frozen ground. *In*: Canadian Regional Permafrost Conference Proceedings, National Research Council of Canada, Ottawa, Tech. Memo. No. 66: 32-37.

CARSON, J.M., J.A. HUNTER, and C.P. LEWIS. 1975. Marine seismic refraction profiling, Kay Pt., Yukon Territory. Geol. Surv. Can. Paper 75-1B: 9-12.

CERMAK, V. 1971. Underground temperature and inferred climatic temperature of the past Millenium, Palaeogeography. Palaeoclimatol. and Palaeoecol. 10(1): 1-19.

COACHMAN, L.K. 1963. Water masses of the Arctic. *In*: Proceedings of the Arctic Basin Symposium, A.I.N.A.: 143-167.

DENTON, W.M. and E.M. FROST. 1946. Gas hydrates and their relation to the operation of natural gas pipelines. U.S. Bureau Mines, Monograph No. 8, 101 pp.

DeVRIES, D.A. 1952. The thermal conductivity of soil. Mededelingen van der Landbouwhogeschool te Wageningen, 52: 1-73.

DeVRIES, D.A. and A.J. PECK. 1958. On the cylindrical probe method of measuring thermal conductivity with special reference to soils. I. Extension of theory and discussion of probe characteristics; II. Analysis of moisture effects. Austral. J. Phys. 11: 411-423.

DOBRIN, M.B. 1970. Geophysical prospecting for oil. McGraw-Hill, New York: 69-104.

DONATO, R.J. 1965. Measurements on the arrival refracted from a thin high-speed layer. Geophysical Prospecting, 13: 387-404.

DZHURIK, B.I. and P.H. LESHCHIKOV. 1973. Experimental investigations of the seismic properties of frozen soils. *In*: Proceedings 2nd International Conference on Permafrost, Yakutsk, USSR, 6: 64-68.

FERRIENS, O.J. and G.D. HOBSON. 1973. Mapping and predicting permafrost in North America. A review 1963-1973. *In*: Proceedings 2nd International Conference on Permafrost, Yakutsk, USSR, Nat. Acad. Sci.: 479-498.

FROLOV, A.D. 1961. The propagation of ultrasonic waves in sandy-clayey rocks. Izvestiya Geophysical Series: 732-736.

FROLOV, A.D. and Y.D. ZYKOV. 1971. Peculiarities of the propagation of elastic waves in frozen rocks (Part 1), Izv. Ucheb. Zaved., Geol. Razvedka, No. 10: 89-97.

GAGNE, R.M. and J.A. HUNTER. 1975. Hammer seismic studies of surficial materials, Banks Island, Ellesmere Island and Boothia Peninsula, N.W.T. Geol. Surv. Can. Paper 75-1B: 13-18.

GOLD, L.W. and A.H. LACHENBRUCH. 1973. Thermal conditions in permafrost - A review of North American literature. *In*: Permafrost, North American Contributions, Second International Conference Proceedings, NAS/NRC: 3-26.

GOLDEN, BRAWNER, and ASSOCIATES. 1970. Bottom sampling program, southern Beaufort Sea. Arctic Petroleum Operators Association Report No. 3.

GOOD, R.L. and J.A. HUNTER. 1974. Marine seismic refraction survey, Pokiak Lake, Tuktoyaktuk, District of Mackenzie. *In*: Geol. Surv. Can. Paper 74-1, Part B: 68.

HERLINVEAUX, R.H. 1973. Some cross-sections of Beaufort Sea data. Marine Sciences, Pacific Region, D.O.E. (unpublished report).

HIGUSHI, A. 1953. On the thermal conductivity of soil with special reference to that of frozen soil. Trans. Amer. Geophys. Union, 34: 737-748.

HITCHON, B. 1975. Occurrence of natural gas hydrates in sedimentary basins. *In*: Natural Gases in Marine Sediments, I.R. Kaplan (ed). Plenum Press, New York: 195-225.

HOEKSTRA, P. 1966. Moisture movement in soils under temperature gradients with cold-side temperature below freezing. Water Resources Res. 2: 241-250.

HOFER, H. and W. VARGA. 1972. Seismogeologic experience in the Beaufort Sea. Geophys. 37: 605-619.

HUNTER, J.A. 1973. Shallow marine refraction surveying in the Mackenzie Delta and Beaufort Sea. Geol. Surv. Can. Paper 73-1B: 59-66.

HUNTER, J.A. and G.D. HOBSON. 1974. Seismic refraction method of detecting sub-seabottom permafrost. *In*: The Coast and Shelf of the Beaufort Sea, J.C. Reed and J.E. Sater (eds), A.I.N.A.: 401-416.

HUNTER, J.A., R.L. GOOD, and G.D. HOBSON. 1974. Mapping the occurrence of sub-seabottom permafrost in the Beaufort Sea by shallow refraction techniques. *In*: Geol. Surv. Can. Paper 74-1B: 91.

HUTT, J.R. and J.W. BERG. 1968. Thermal and electrical conductivities of ocean sediments and sandstone rocks. Geophys. 33: 489-500.

ISAACS, R.M. 1974. Geotechnical studies of permafrost in the Fort Good Hope - Norman Wells region, N.W.T. Envir. Soc. Prog. Northern Pipelines Report No. 74-16, D.I.N.A., 212 pp.

JUDGE, A.S. 1973. Thermal régime of the Mackenzie Valley. Envir. Soc. Prog. Northern Pipelines Report No. 73-38, D.I.N.A., 177 pp.

JUDGE, A.S. 1974. The occurrence of offshore permafrost in northern Canada. *In*: Proceedings of the Symposium on Beaufort Sea Coastal and Shelf Research, A.I.N.A., San Francisco: 427-437.

JUDGE, A.S. 1975. Geothermal studies in the Mackenzie Valley by the Earth Physics Branch. Geothermal Series #2, Earth Physics Br., EMR, 13 pp.

JUDGE, A.S., J.A. HUNTER, and J. DUGAL. 1976. The occurrence of permafrost beneath the seabottom of Kugmallit Bay, Beaufort Sea (in preparation).

KAPLAR, C.W. 1966. Laboratory determination of the dynamic moduli of frozen soils and of ice. *In*: Permafrost, Proceedings of an International Conference, National Academy of Sciences, Washington, D.C.: 293-305.

KATZ, D.L., D. CORNELL, R. KOBAYASHI, E.H. POELTMAN, J.A. VARY, J.R. GLENBAAS, and C.F. WEINANG. 1959. Handbook of Natural Gas Engineering. McGraw-Hill, New York.

KELLY, W.J.B. 1967. Tuktoyaktuk Harbour - A data report. Marine Sciences Branch, Report #7, D.E.M.R., 30 pp.

KERSTEN, J. 1949. Thermal properties of soils. Univ. of Minn. Eng. Bull. #28, 227 pp.

KURFURST, P.J. and M.S. KING. 1972. Static and dynamic elastic properties of two sandstones at permafrost temperatures. J. Pet. Tech., April: 495-504.

KURFURST, P.J. 1976. Ultrasonic wave measurements on frozen soils at permafrost temperatures. Can. J. Earth Sci. (in press).

LACHENBRUCH, A.H. 1957. A probe for the measurement of thermal conductivity of frozen soils in place. Trans. Amer. Geophys. Union, 38: 691-697 and Discussion: 730-732, same volume.

LACHENBRUCH, A.H. 1957. Thermal effects of the ocean on permafrost. Geol. Soc. America Bull. No. 68: 1515-1529.

LACHENBRUCH, A.H. and M.C. BREWER. 1959. Dissipation of the temperature effect of drilling a well in Arctic Alaska. U.S. Geol. Surv. Bull. No. 1083-C: 73-109.

LACHENBRUCH, A.H. 1968. Permafrost. *In*: Encyclopedia of Geomorphology, R.W. Fairbridge (ed). 3: 833-839.

LAW, L.K., W.S.B. PATERSON, and K. WHITHAM. 1965. Heat flow determinations in the Canadian Arctic Archipelag. Can. J. Earth Sci. 2: 59-71.

LEWELLEN, R.I. 1973. The occurrence and characteristics of nearshore permafrost, northern Alaska. *In*: Permafrost, North American Contributions, Second International Conference Proceedings, NAS/NRC: 131-136.

LEWELLEN, R.I. 1974. Offshore permafrost, Beaufort Sea, Alaska. *In*: Proceedings of the Symposium on Beaufort Sea Coastal and Shelf Research, A.I.N.A., San Francisco: 417-426.

LINELL, K.A. 1973. Risk of uncontrolled flow from wells through permafrost. *In*: Proceedings 2nd International Conference on Permafrost, Yakutsk, USSR, Nat. Acad. Sci.: 462-468.

McDONALD, B.C., R.E. EDWARDS, and V.N. RAMPTON. 1973. Position of frost table in the near-shore zone, Tuktoyaktuk Peninsula. Geol. Surv. Can. Paper 73-1B: 165-168.

McGINNES, L.D., K. NAKAO, and C.C. CLARK. 1973. Geophysical identification of frozen and unfrozen ground, Antarctica. *In*: Proceedings 2nd International Conference on Permafrost, Yakutsk, USSR, Nat. Acad. Sci.

MacKAY, J.R. 1972. Offshore permafrost and ground ice, southern Beaufort Sea. Can. J. Earth Sci. 9: 1550-1561.

MacKAY, J.R. 1973. The growth of pingoes, western Arctic coast, Canada. Can. J. Earth Sci. 10(6): 979.

MacKAY, J.R. 1975. The closing of ice wedge cracks in permafrost, Gary Island, N.W.T. Can. J. Earth Sci. 12(9): 1668-1692.

MacKAY, J.R. and V. RAMPTON. 1971. Massive ice and icy sediments throughout the Tuktoyaktuk Peninsula, Richards Island and nearby area district Mackenzie. Geol. Surv. Can. Paper 71-21, 16 pp.

MacKAY, J.R., V.N. RAMPTON, and J.G. FYLES. 1972. Relict Pleistocene permafrost, western Arctic, Canada. Science, 176: 1321-1323.

McROBERTS, E.D. and J.F. NIXON. 1975. Some geotechnical observations on the role of surcharge pressure in soil freezing. *In*: Proceedings Conference on Soil-Water Problems in Cold Regions, J.N. Luthen (ed). Amer. Geophys. Union: 42-57.

MARTYNOV, G.A. 1963. Heat and moisture transfer in freezing and thawing soils. *In*: Principles of Geocryology, Part I, General Geocryology, NRC-TT 1065, 56 pp.

MOLOCHUSKIN, E.N. 1973. The effect of thermal abrasion on the temperature of permafrost rocks in the coastal zone of the Laptev Sea. *In*: Proceedings 2nd International Permafrost Conference, Moscow. 2: 52-58.

MÜLLER, G. 1961. Geschwindigkeitsbestimmungen elastischer wellen in gefrorenen gesteinen und die anwendung auf untersuchungen des frostmantels an gefreirshachten. Geophys. Prospec. 9(2): 276-295.

NAKANO, Y. and R. ARNOLD. 1973. Acoustic properties of frozen Ottawa sands. Water Resources Res. 9(1): 178-184.

NAKANO, Y. and N.H. FROULA. 1973. Sound and shock transmission in frozen soils. *In*: Proceedings 2nd International Conference on Permafrost, Yakutsk, USSR, Nat. Acad. Sci.: 359-368.

NAKANO, Y., M. SMITH, R. MARTIN, H. STEVENS, and K. KNUTH. 1971. Determination of the acoustic properties of frozen soils. U.S. Army CRREL Research Rept. Cold Regions Research and Engineering Laboratory, Hanover, New Hampshire, 72 pp.

OBERMAN, N.G. and B.B. KANUNOV. 1973. Determination of the thickness of the belt of frozen rocks on the Arctic coast. *In*: Proceedings 2nd International Conference on Permafrost, Moscow. 1: 130-137.

OGILVY, A.A. 1970. Geophysical prospecting for groundwater in the Soviet Union. *In*: Mining and Groundwater Geophysics, 1967, L.W. Morley (ed). Geol. Surv. Can. Econ. Geol. Rept. No. 26.

O'ROURKE, J.C. 1974. Inventory of physical oceanography of the eastern Beaufort Sea. *In*: Proceedings of the Symposium on Beaufort Sea Coastal and Shelf Research, A.I.N.A., San Francisco: 65-84.

PATERSON, W.S.B. and L.K. LAW. 1966. Additional heat flow determinations in the area of Mould Bay, Arctic Canada. Can. J. Earth Sci. 3: 237-246.

PENNER, E. 1962. Thermal conductivity of saturated Leda clay. Geotechnique, 12: 168-175.

PENNER, E. 1963. Anisotropic thermal conduction in clay sediments. *In*: International Clay Conference Proceedings, Stockholm, 1: 365-376.

PENNER, E. 1970. Thermal conductivity of frozen soils. Can. J. Earth Sci. 7: 982-987.

PENNER, E. G.H. JOHNSTON, and L.E. GOODRICH. 1975. Thermal conductivity laboratory studies of some Mackenzie Highway soils. Can. Geotech. J. 12: 271-288.

PERKINS, T.K., J.A. ROCHON, and C.R. KNOWLES. 1974. Studies of pressures generated upon refreezing of thawed permafrost around a wellbore. J. Petroleum Tech., Oct.: 1159-1166.

PERKINS, T.K. and R.A. RUEDRICH. 1973. The mechanical behaviour of synthetic permafrost. Soc. Petroleum Engineers J., August: 211-220.

PHILIP, J.R. and D.A. DeVRIES. 1957. Moisture movement in porous materials under temperature gradients. Trans. Amer. Geophys. Union, 38: 222-232.

POLEY, J.Ph. and J.J. NOOTEBOOM. 1961. Seismic refraction and screening by thin high-velocity layers. Geophys. Prospec. 14: 194-203.

RAMPTON, V.N. 1972. Surficial deposits of the Mackenzie delta (107C), Stanton (107D), Cape Dalhousie (107E), and Malloch Hill (97F) map-sheets. *In*: Mackenzie Delta Area Monograph, D.E. Kerfoot (ed). St. Catharine's, Ont., Brock Univ.: 15-27.

RATCLIFFE, E.G. 1960. Thermal conductivities of ocean sediments. J. Geophys. Res. 65: 1535-1541.

RIZNICHENKO, Y.V. and O.G. SHAMINA. 1957. Elastic waves in a laminated solid medium, as investigated on two-dimensional models. Geophys. Ser. Translation, 7: 17-37.

ROETHLESBERGER, H. 1972. Seismic exploration in cold regions. Report to U.S. Army Corps of Engineers, Cold Regions Research and Engineering Laboratory, Hanover, New Hampshire.

ROSENBAUM, J.H. 1965. Refraction arrivals through thin high-velocity layers. Geophysics, 3: 204-212.

RUEDRICH, R.A. and T.K. PERKINS. 1974. A study of the factors influencing the mechanical properties of deep permafrost. J. Petroleum Tech., Oct.: 1167-1177.

SAMSON, L. and F. TORDON. 1969. Experience with engineering site investigations in northern Quebec and northern Baffin Island. *In*: Proceedings 3rd Canadian Conference on Permafrost, NRC Technical Memo. No. 96: 21-38.

SCOTT, W.J. 1975. Preliminary experiments in marine resistivity near Tuktoyaktuk, District of Mackenzie. Geol. Surv. Can. Paper 75-1A: 141.

SCOTT, W.J. and J.A. HUNTER. 1976. Applications of geophysical techniques in permafrost regions. Can. J. Earth Sci. (in press).

SHARBATYN, A.A. 1973. Formula for estimating minimum dates of cryolithozone degradation and development. *In*: Proceedings 2nd International Conference on Permafrost, Yakutsk, USSR, July: 24-25.

SHARBATYN, A.A. and P.A. SHUMSKIY. 1974. Extreme estimations in geothermy and geocryology. C.R.R.E.L. TL 465, 140 pp.

SHEARER, J.M. 1972. Geological structure of the Mackenzie Canyon area of the Beaufort Sea. Geol. Surv. Can. Paper 72-1A: 179-180.

SHEARER, J.M., R.F. MacNAB, B.R. PELLETIER, and T.B. SMITH. 1971. Submarine pingoes in the Beaufort Sea. Science, 175: 816-818.

SHUSARCHUCK, W.A. and G.H. WATSON. 1975. Thermal conductivity of some ice-rich permafrost soils. Can. Geotech. J. 12: 413-424.

STOLL, R.D. 1974. Effects of gas hydrates in sediments. *In*: Natural Gases in Marine Sediments, I.R. Kaplan (ed). Plenum Press, New York: 235-248.

STOLL, R.D., J. EWING, and G.M. BRYAN. 1971. Anomalous wave velocities in sediments containing gas hydrates. J. Geophys. Res. 76: 2090-2094.

TAYLOR, A.E. and A.S. JUDGE. 1974. Canadian geothermal data collection - northern sites 1955-1974. Geothermal Series #1, Earth Physics Br. D.E.M.R., 171 pp.

TAYLOR, A.E. and A.S. JUDGE. 1975. Canadian geothermal data collection - northern sites 1974. Geothermal Series #3, Earth Physics Br., D.E.M.R., 127 pp.

TAYLOR, A.E. and A.S. JUDGE. 1976. Canadian geothermal data collection - northern sites 1975. Geothermal Series (in preparation), Earth Physics Br., D.E.M.R.

TIMUR, A. 1968. Velocity of compressional waves in porous media at permafrost temperatures. Geophysics, 33(4): 584-595.

VAN EVERDINGEN, R.O. 1974. Groundwater in permafrost regions of Canada. *In*: Proceedings of the Workshop Seminar on Permafrost Hydrology, CNC IHD: 83-94.

WERENSKIOLD, W. 1953. The extent of frozen ground under the sea bottom and glacier beds. J. Glaciol. 2: 197-200.

WILLIAMS, P.J. 1964. Experimental determination of apparent specific heat of frozen soils. Geotechnique, 14: 133-142.

WOLFE, L.H. and J.O. THIEME. 1964. Physical and thermal properties of frozen soil and ice. J. Soc. Petrol. Eng. 4: 67-72.

WOODSIDE, W. and J.B. CLIFFE. 1959. Heat and moisture transfer in a closed system of two granular materials. Soil Sci. 87: 75-82.

WOODSIDE, W. and J.H. MESMER. 1961. Thermal conductivity of porous materials; I. Unconsolidated sands; II. Consolidated rocks. J. Appl. Phys. 32: 1688-1706.

YEN, Y-C. 1966. Heat conduction in moist porous medium. C.R.R.E.L. Res. Rept. No. 212, 10 pp.

ZYKOV, YU.D. and YU.I. BAULIN. 1973. Potential use of seismic-acoustic techniques in engineering-geologic investigations of construction on permafrost. *In*: Proceedings 2nd International Conference on Permafrost, Yakutsk, USSR, Vol. 6.

APPENDIX A

Permafrost Determinations from the Arctic Petroleum Operators Association Drilling Program

The drill logs shown below are taken from A.P.O.A. Report #3, 1970, and consist of the detailed geological listing and temperature measurements for those holes encountering permafrost. The location of these holes is shown in Fig. 3-1.

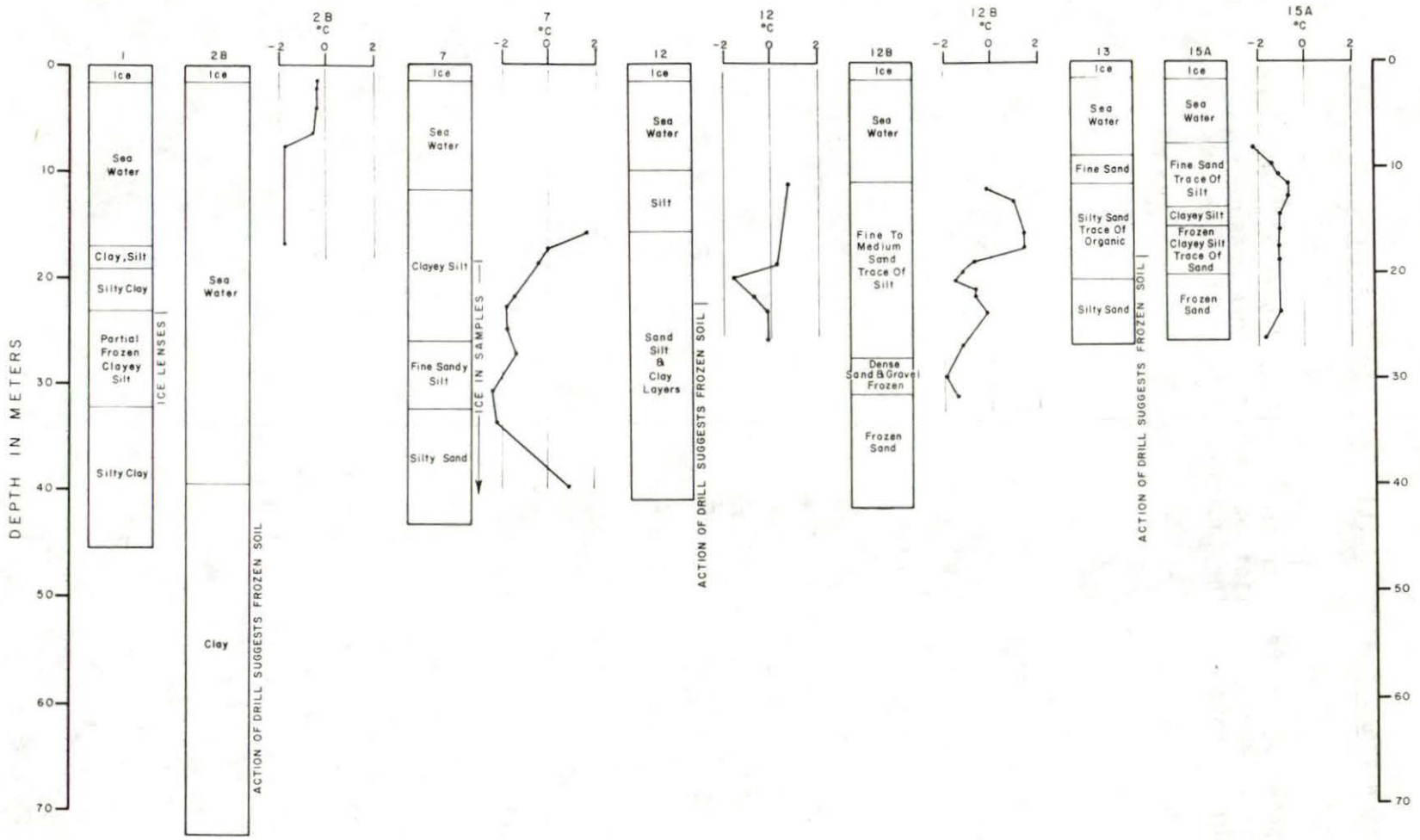

Fig. A-1 A compilation of drilling results from A.P.O.A. report #3 for the holes encountering permafrost. Temperature measurements were obtained from samples.

APPENDIX B

Variation of Seismic Velocities with Temperature

The figures shown herein represent the highlights of the work of the authors denoted. In the case of several measurements made in similar materials or temperature regions, only one typical result is shown. The geological and physical descriptions of the materials studied vary widely in detail and the reader is referred to the particular author for such descriptions. Only gross features (grain size, % porosity, density) are indicated wherever possible.

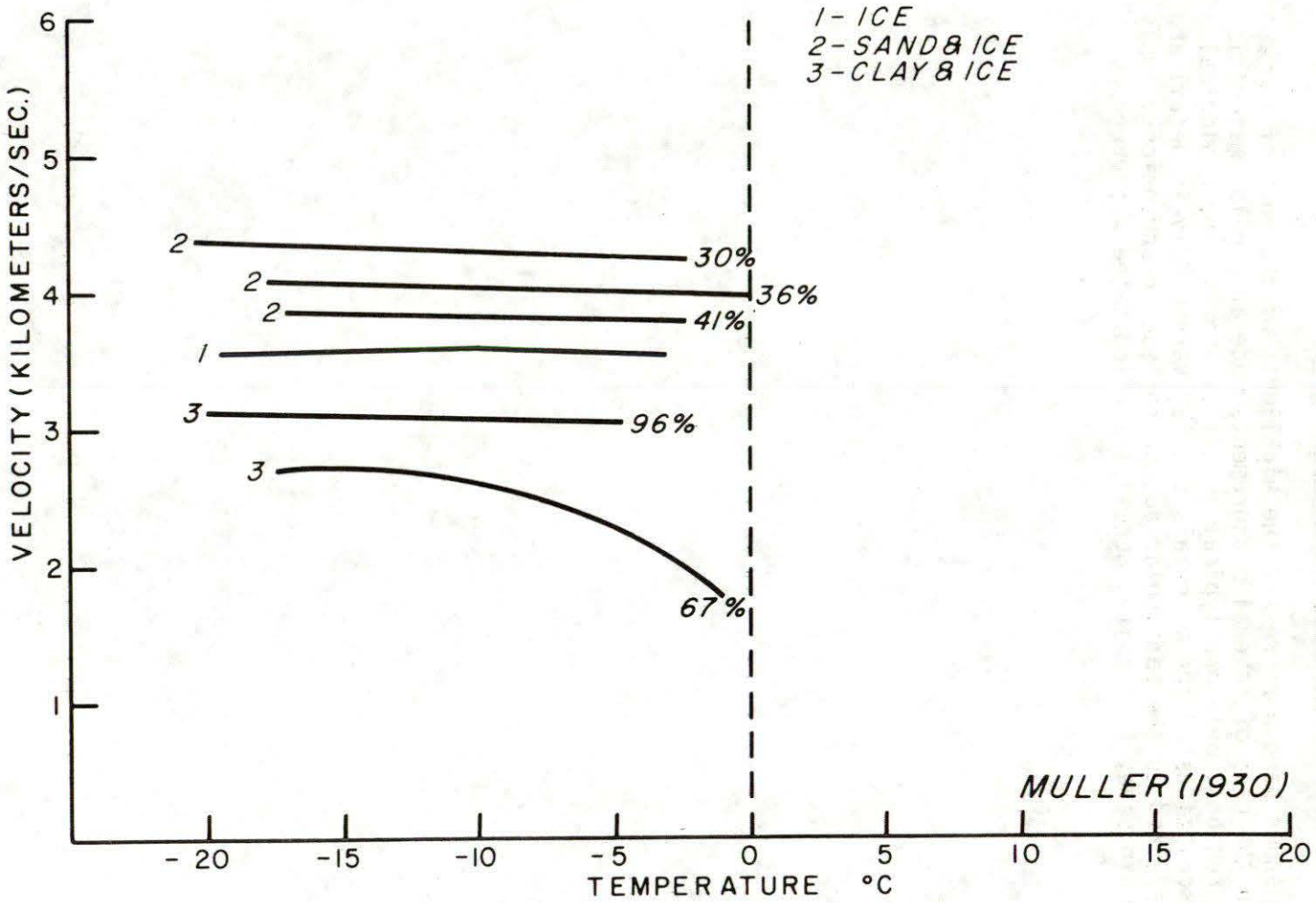
1 - ICE
2 - SAND & ICE
3 - CLAY & ICE
VELOCITY (KILOMETERS/SEC.)
6
5
4
3
2
1
2
30%
2
36%
2
41%
1
3
96%
3
67%
MULLER (1930)
- 20
-15
-10
-5
0
5
10
15
20
TEMPERATURE °C

Fig. B-1

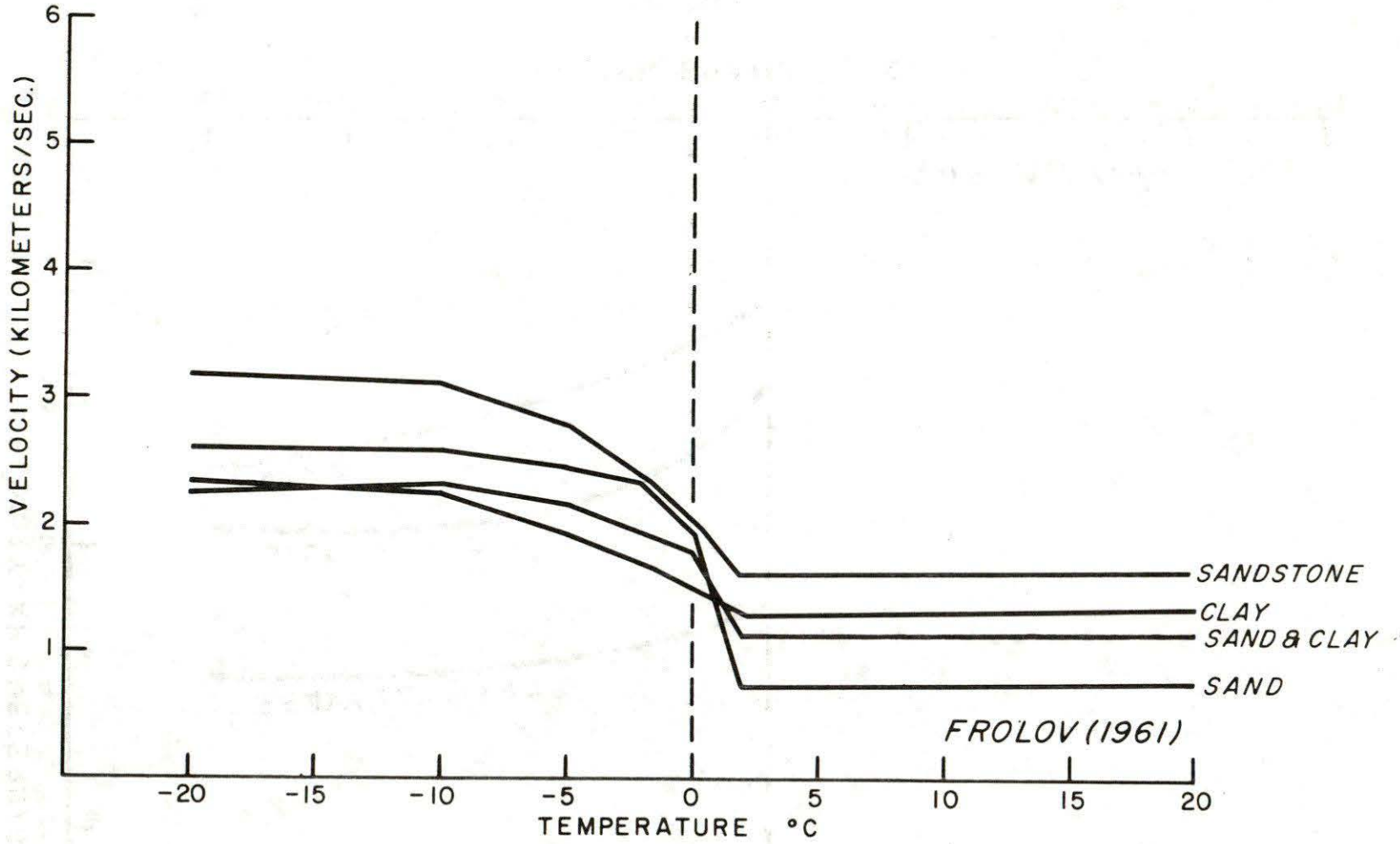
VELOCITY (KILOMETERS/SEC.)
6
5
4
3
2
1
-20
-15
-10
-5
0
5
10
15
20
TEMPERATURE °C
SANDSTONE
CLAY
SAND & CLAY
SAND
FROLOV (1961)

Fig. B-2

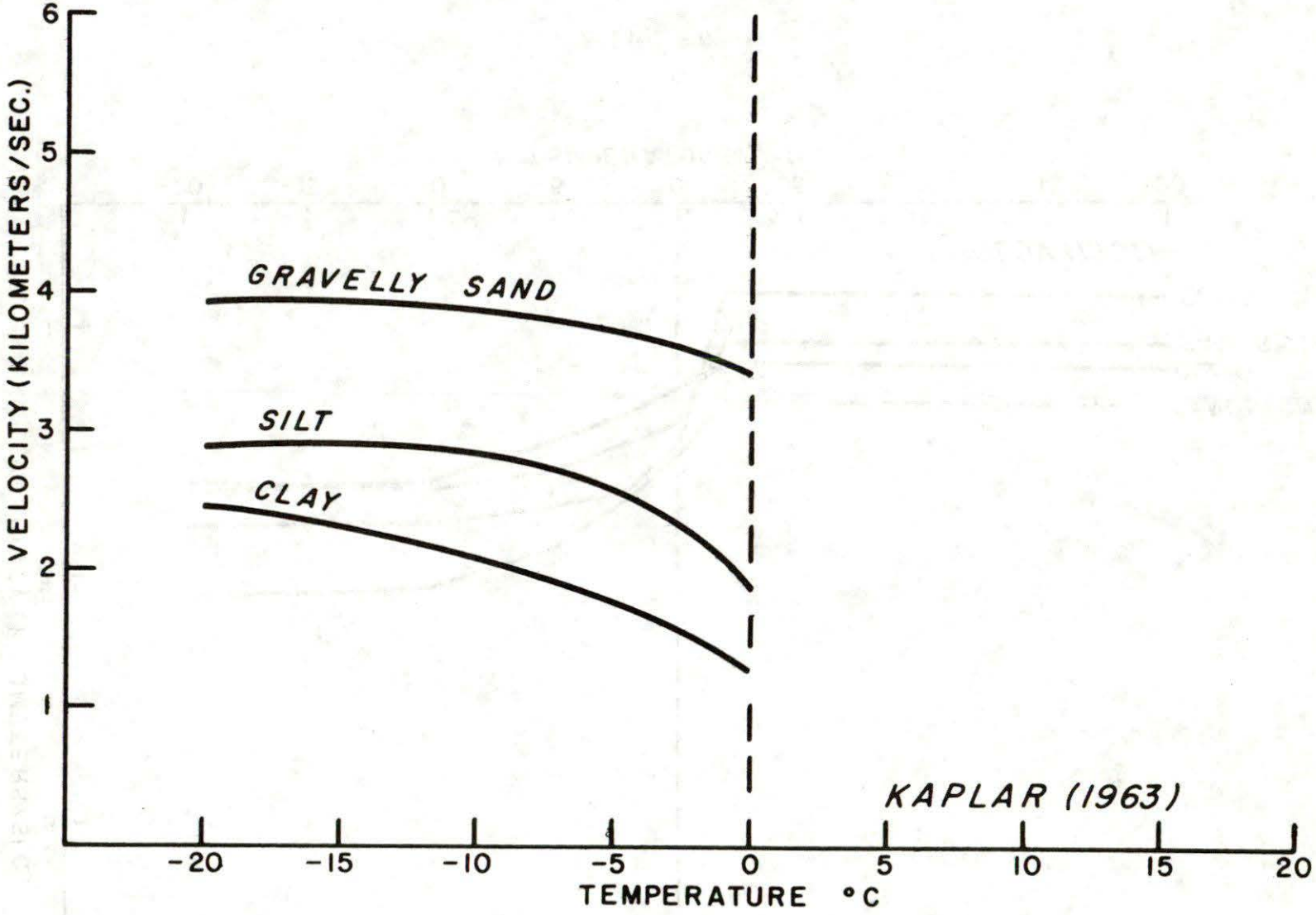
VELOCITY (KILOMETERS/SEC.)
6
5
4
3
2
1
GRAVELLY SAND
SILT
CLAY
KAPLAR (1963)
-20
-15
-10
-5
0
5
10
15
20
TEMPERATURE °C

Fig. B-3

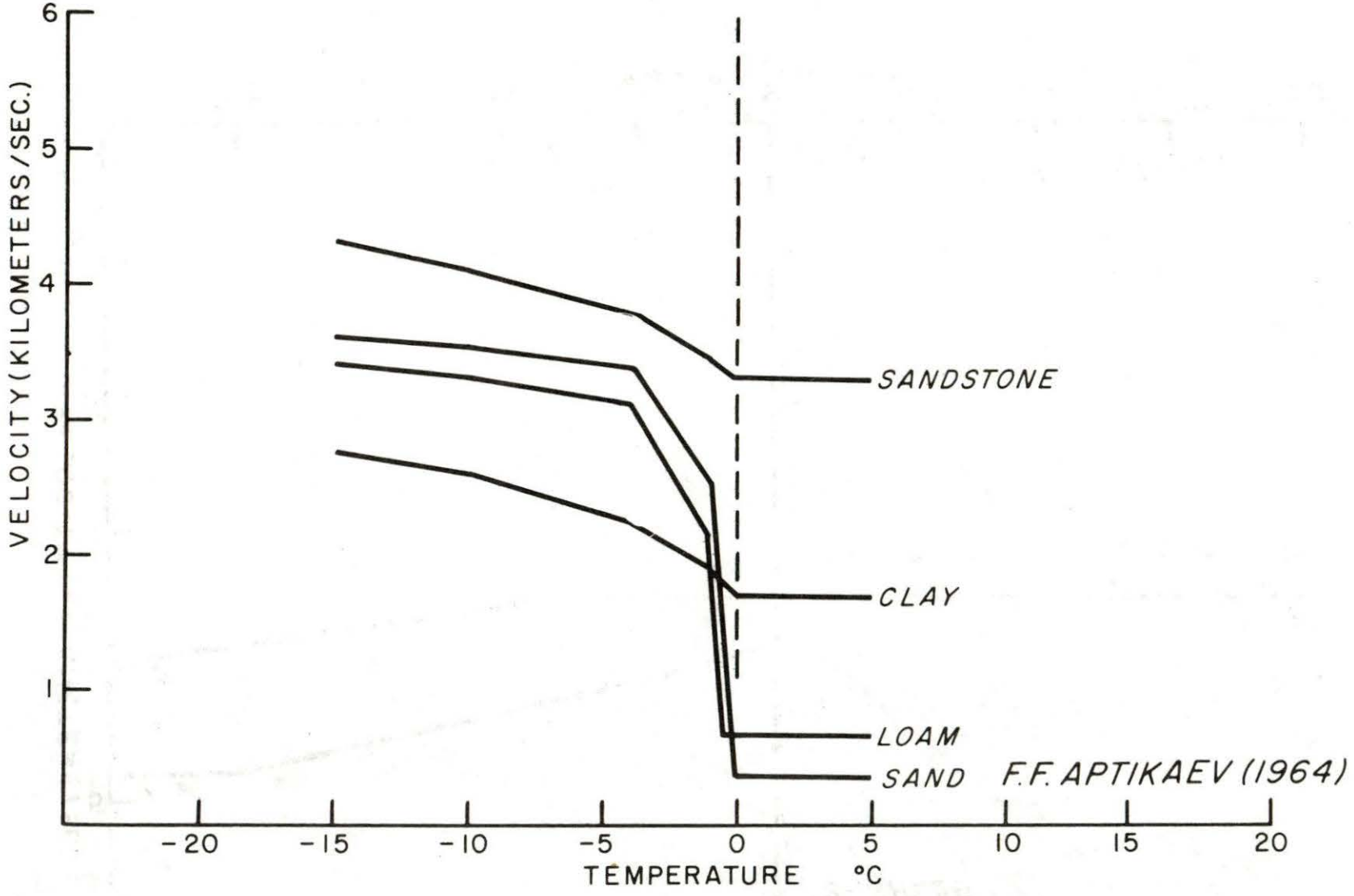
VELOCITY (KILOMETERS/SEC.)
6
5
4
3
2
1
SANDSTONE
CLAY
LOAM
SAND
F.F. APTIKAEV (1964)
-20
-15
-10
-5
0
5
10
15
20
TEMPERATURE °C

Fig. B-4

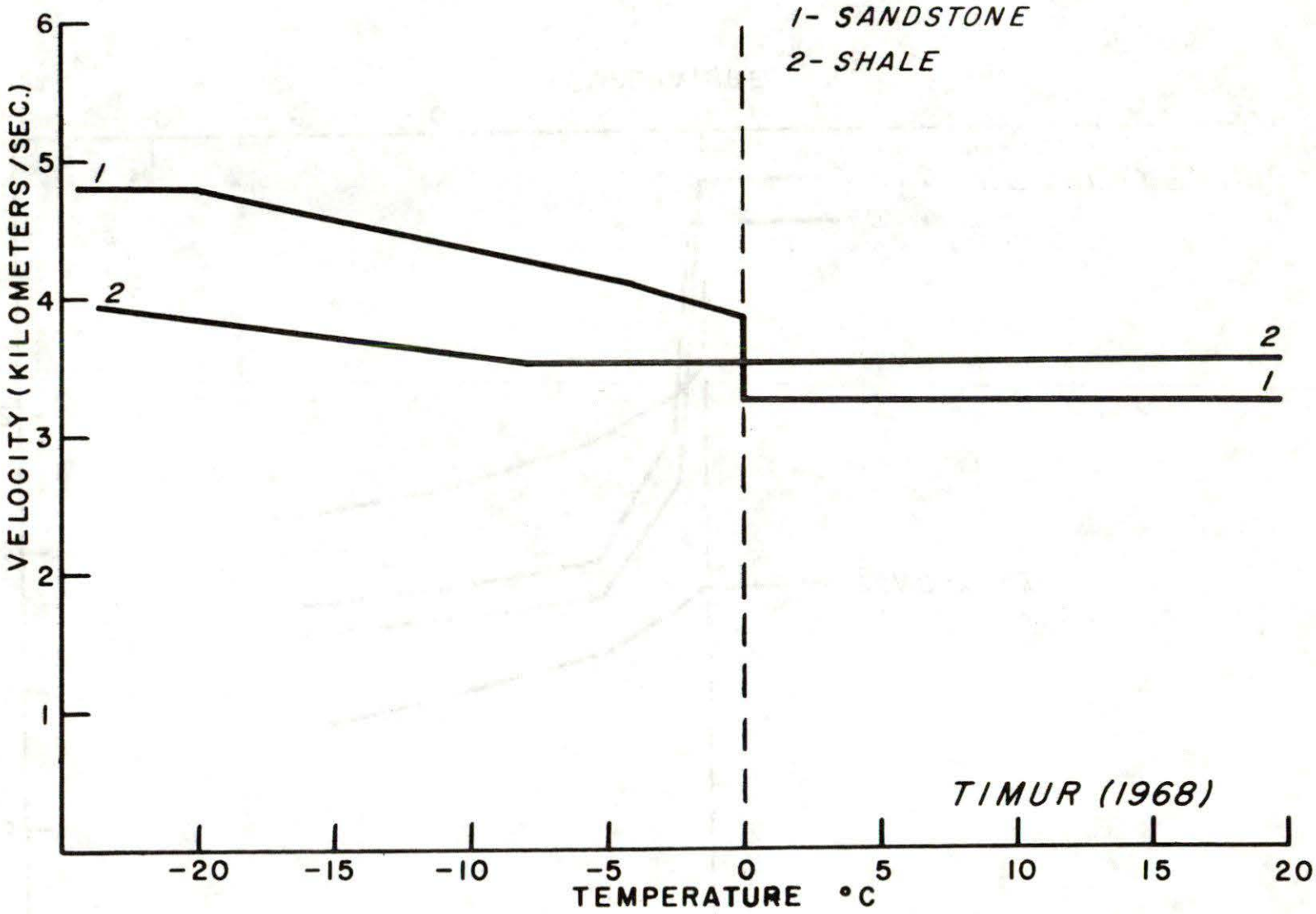
1- SANDSTONE
2- SHALE
VELOCITY (KILOMETERS/SEC.)
6
5
4
3
2
1
1
2
2
1
TIMUR (1968)
-20
-15
-10
-5
0
5
10
15
20
TEMPERATURE °C

Fig. B-5

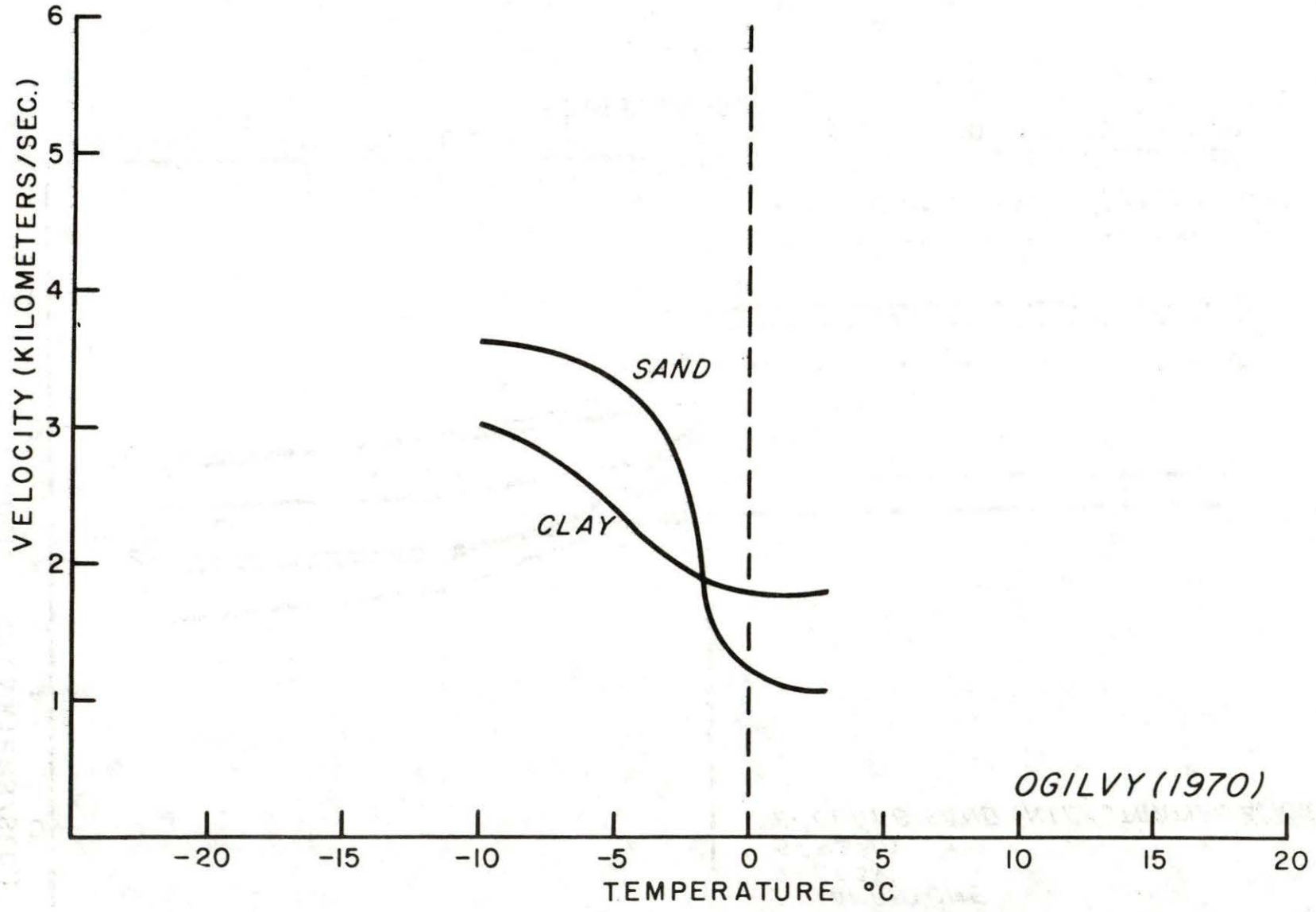
VELOCITY (KILOMETERS/SEC.)
6
5
4
3
2
1
SAND
CLAY
OGILVY (1970)
-20
-15
-10
-5
0
5
10
15
20
TEMPERATURE °C

Fig. B-6

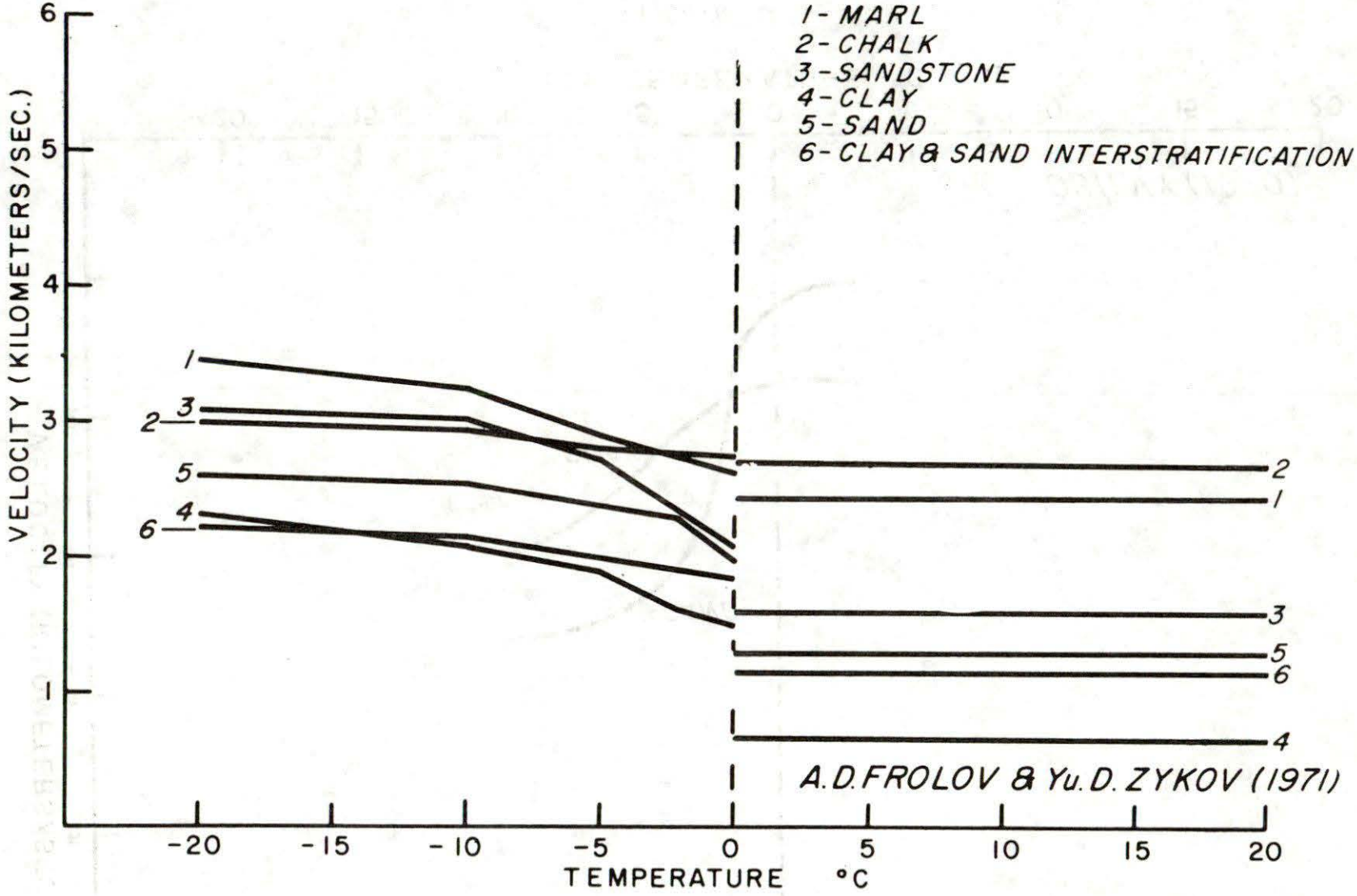
1- MARL
2- CHALK
3- SANDSTONE
4- CLAY
5- SAND
6- CLAY & SAND INTERSTRATIFICATION
VELOCITY (KILOMETERS/SEC.)
TEMPERATURE °C
A.D.FROLOV & Yu.D. ZYKOV (1971)

Fig. B-7

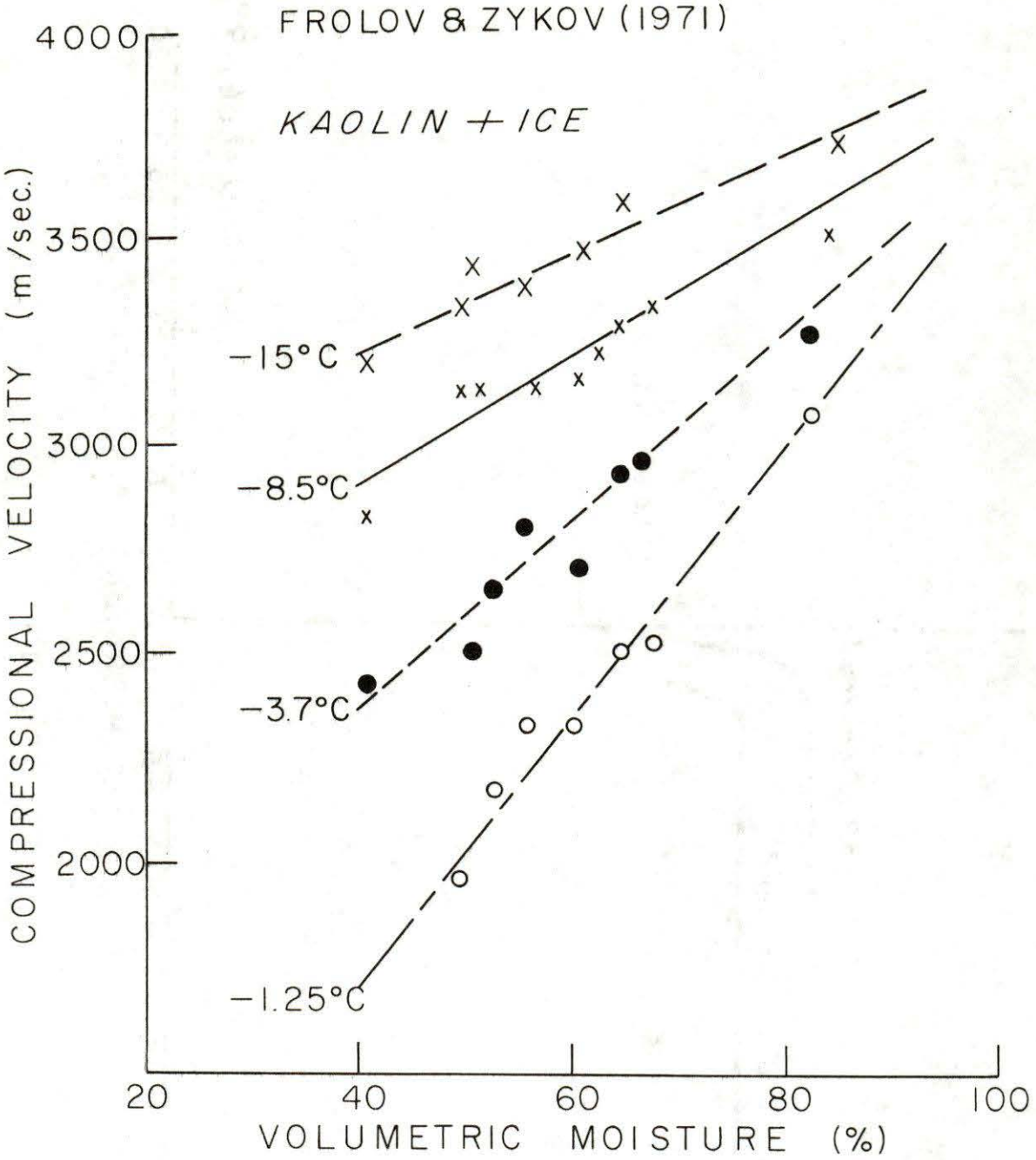
FROLOV & ZYKOV (1971)
KAOLIN + ICE
4000
3500
3000
2500
2000
COMPRESSIONAL VELOCITY (m/sec.)
−15°C
−8.5°C
−3.7°C
−1.25°C
20
40
60
80
100
VOLUMETRIC MOISTURE (%)

Fig. B-8

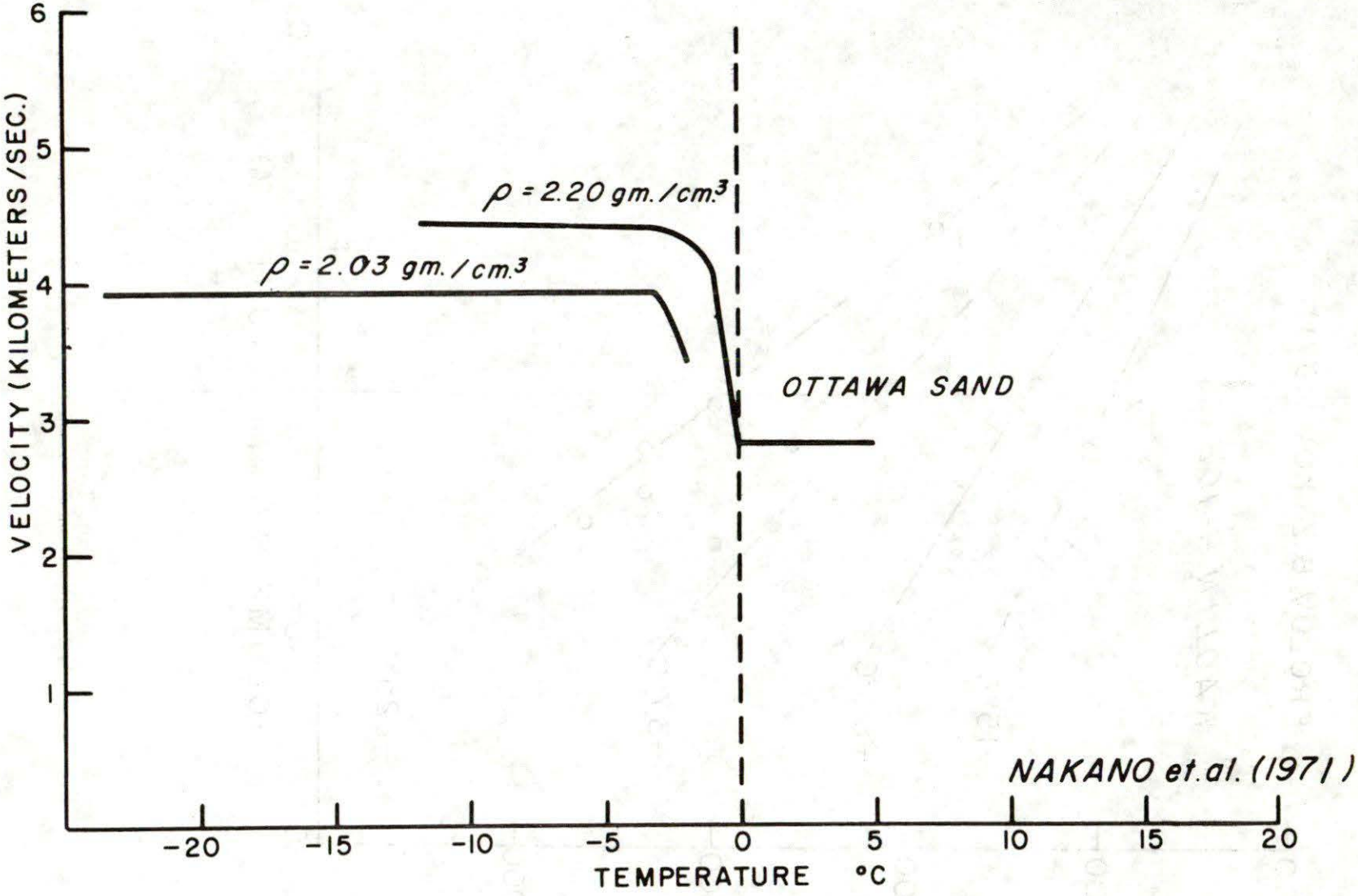
VELOCITY (KILOMETERS/SEC.)
6
5
4
3
2
1
ρ = 2.20 gm./cm.³
ρ = 2.03 gm./cm.³
OTTAWA SAND
NAKANO et.al. (1971)
-20
-15
-10
-5
0
5
10
15
20
TEMPERATURE °C

Fig. B-9

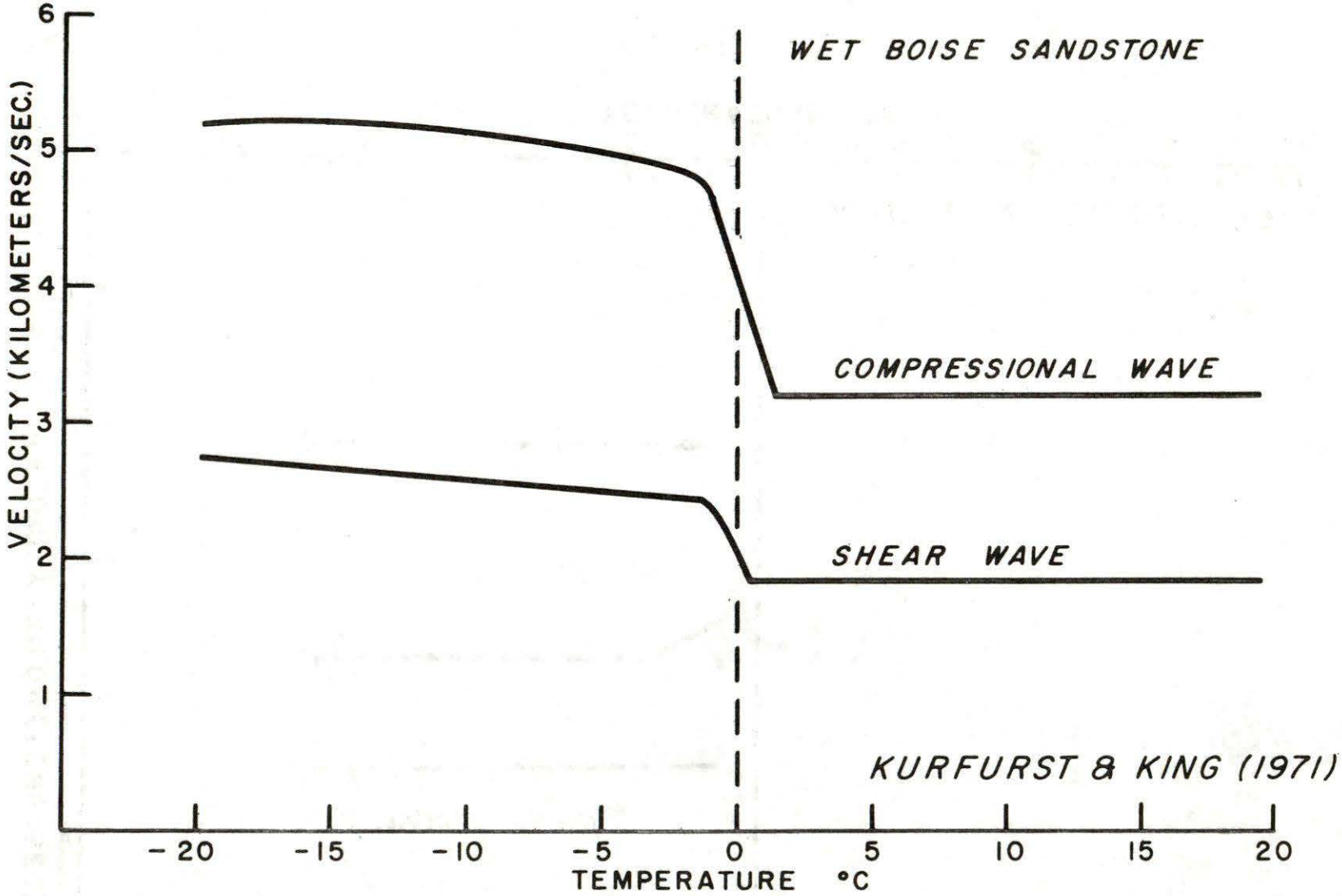
WET BOISE SANDSTONE
COMPRESSIONAL WAVE
SHEAR WAVE
KURFURST & KING (1971)
VELOCITY (KILOMETERS/SEC.)
6
5
4
3
2
1
-20
-15
-10
-5
0
5
10
15
20
TEMPERATURE °C

Fig. B-10

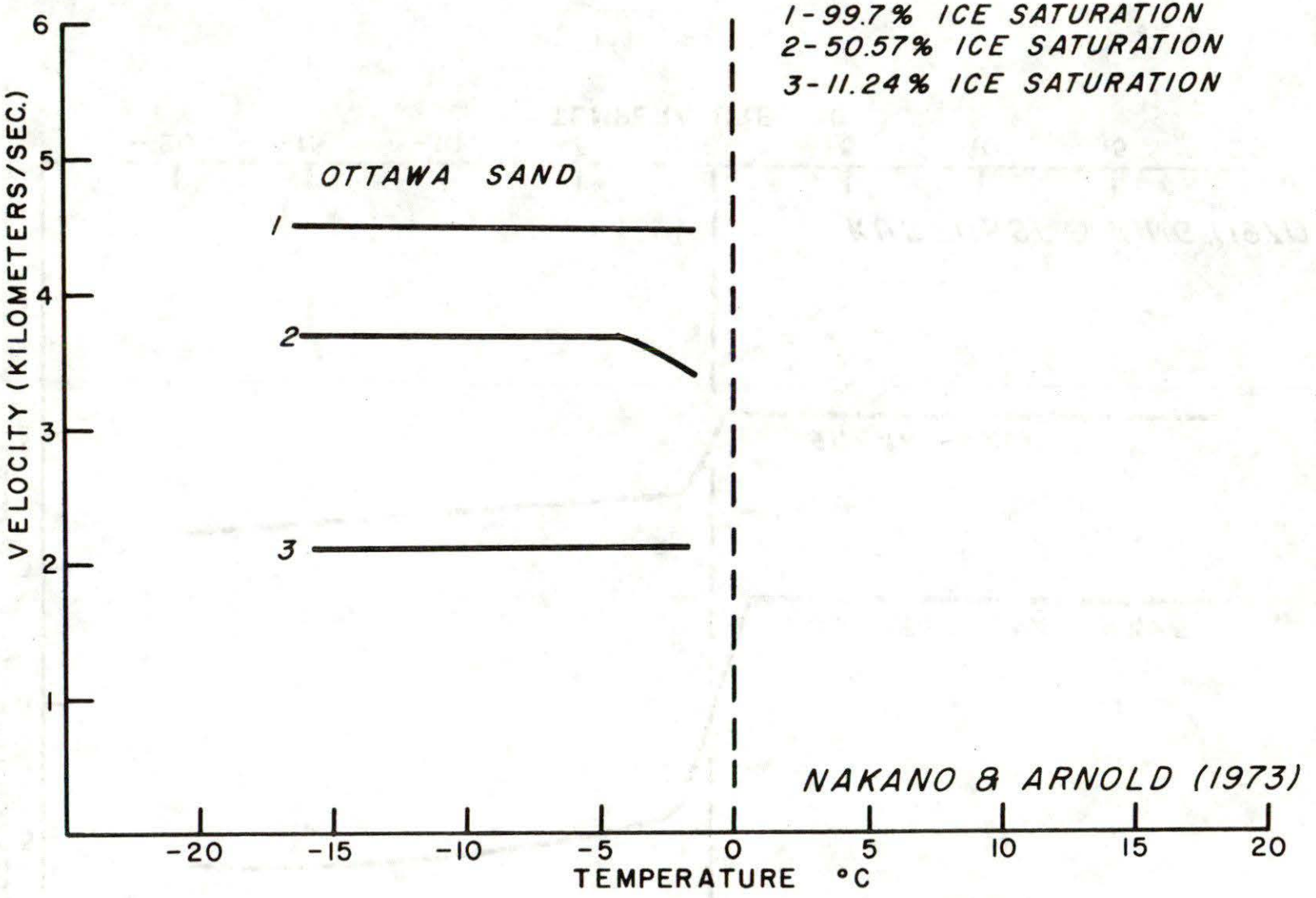
1-99.7% ICE SATURATION
2-50.57% ICE SATURATION
3-11.24% ICE SATURATION
OTTAWA SAND
1
2
3
VELOCITY (KILOMETERS/SEC.)
6
5
4
3
2
1
NAKANO & ARNOLD (1973)
-20
-15
-10
-5
0
5
10
15
20
TEMPERATURE °C

Fig. B-11

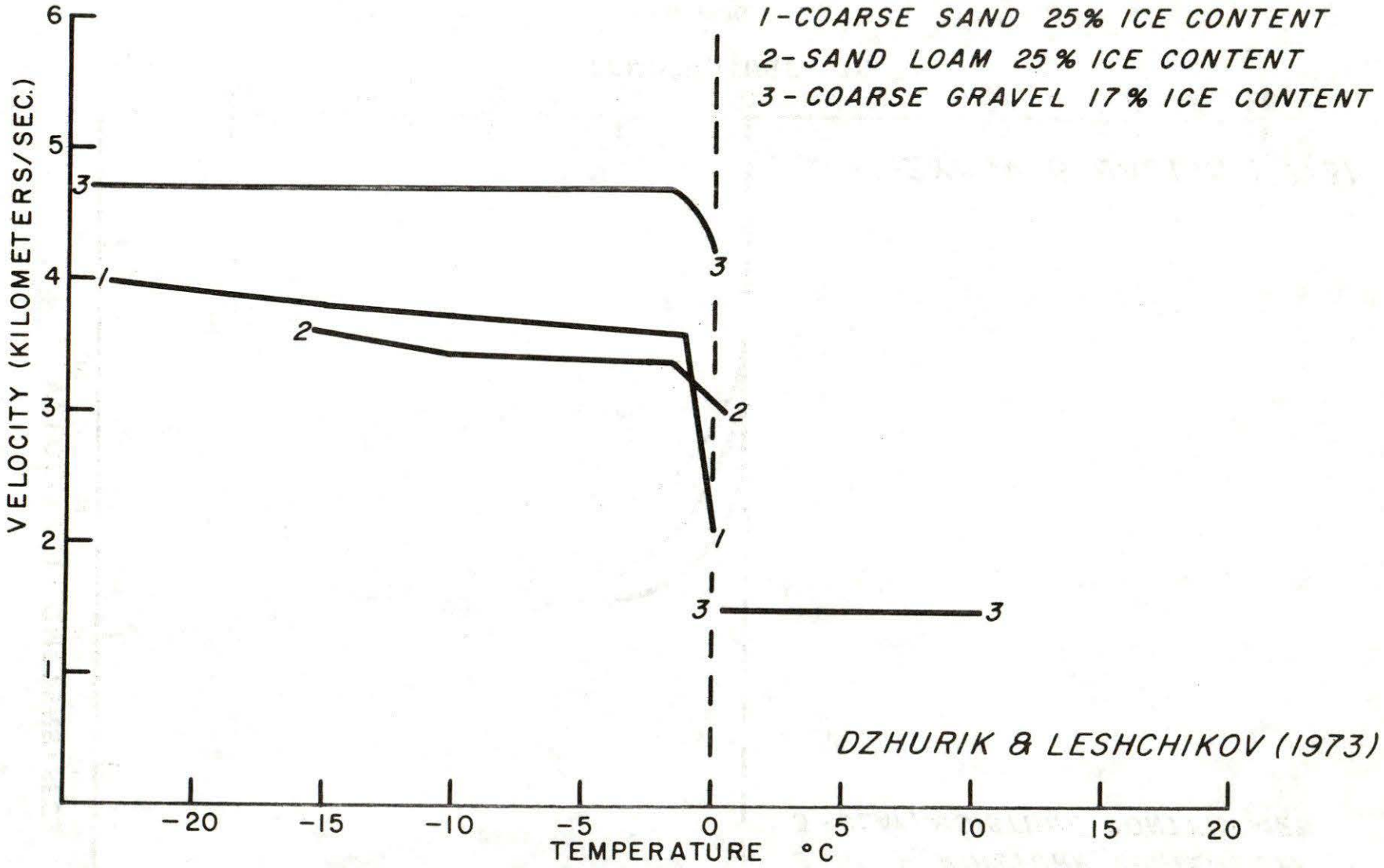
1-COARSE SAND 25% ICE CONTENT
2-SAND LOAM 25% ICE CONTENT
3-COARSE GRAVEL 17% ICE CONTENT
VELOCITY (KILOMETERS/SEC.)
6
5
4
3
2
1
TEMPERATURE °C
-20
-15
-10
-5
0
5
10
15
20
DZHURIK & LESHCHIKOV (1973)

Fig. B-12

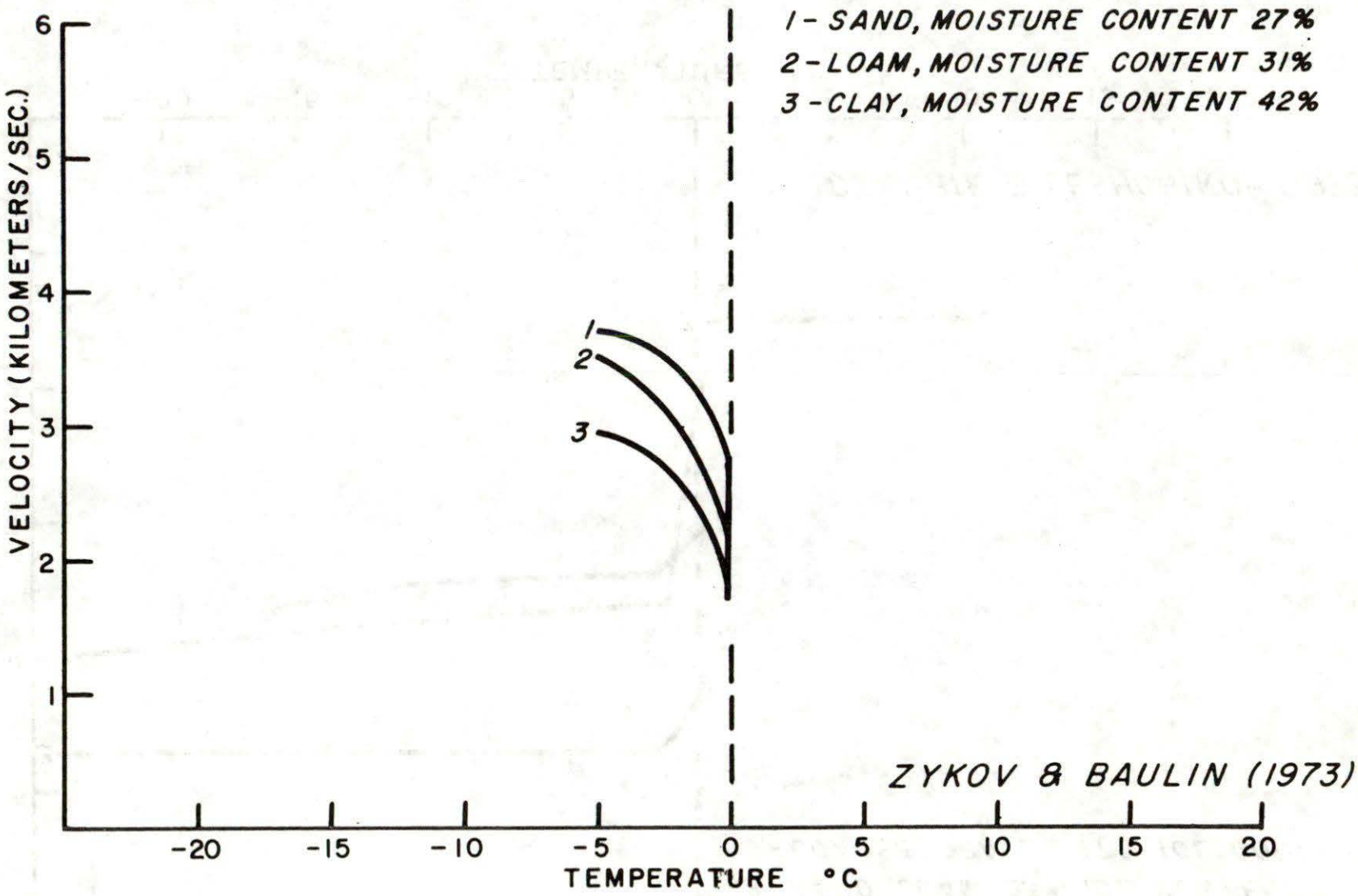
1 - SAND, MOISTURE CONTENT 27%
2 - LOAM, MOISTURE CONTENT 31%
3 - CLAY, MOISTURE CONTENT 42%
VELOCITY (KILOMETERS/SEC.)
6
5
4
3
2
1
1
2
3
ZYKOV & BAULIN (1973)
-20
-15
-10
-5
0
5
10
15
20
TEMPERATURE °C

Fig. B-13

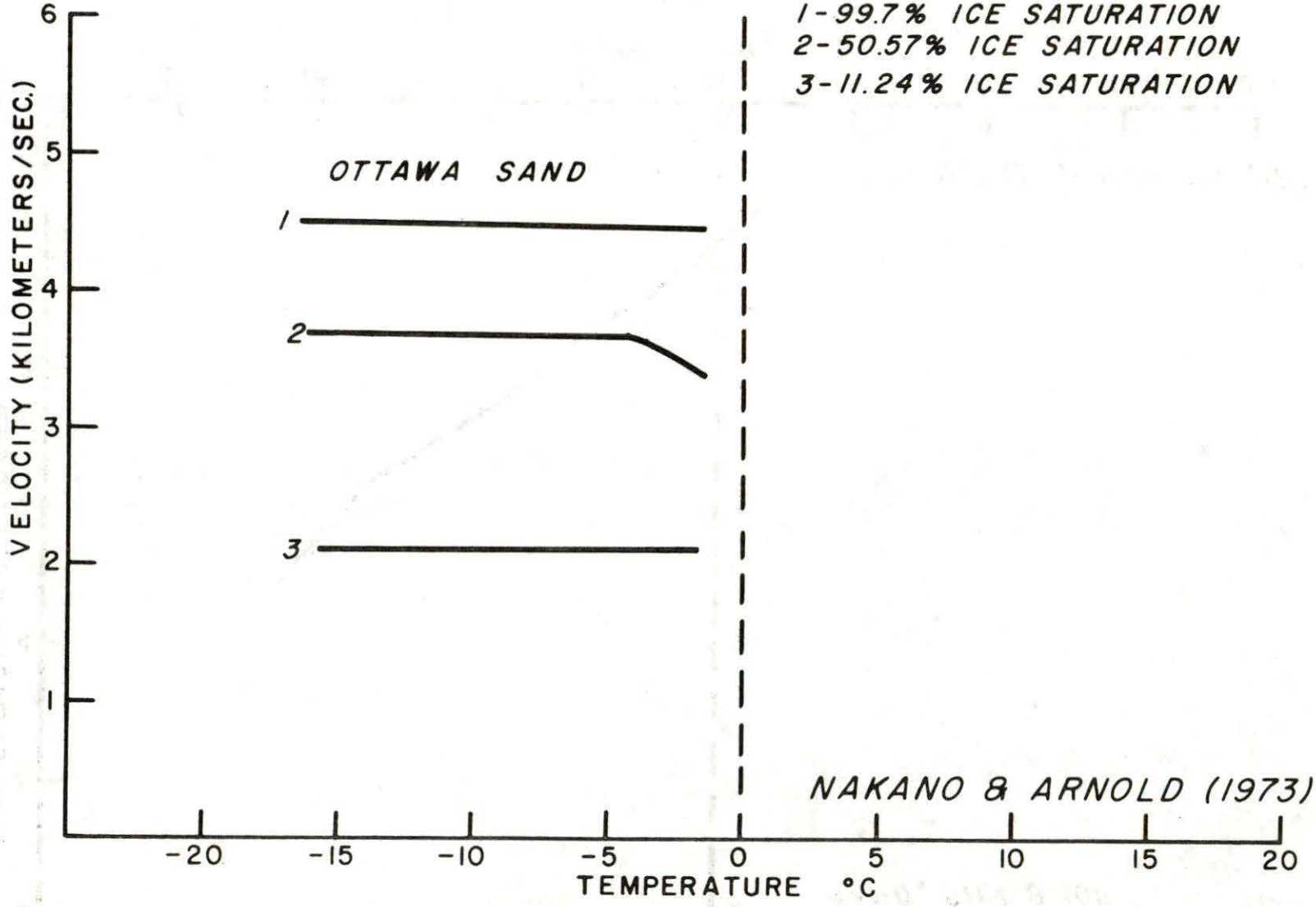
1 - 99.7% ICE SATURATION
2 - 50.57% ICE SATURATION
3 - 11.24% ICE SATURATION
OTTAWA SAND
1
2
3
VELOCITY (KILOMETERS/SEC.)
6
5
4
3
2
1
NAKANO & ARNOLD (1973)
-20
-15
-10
-5
0
5
10
15
20
TEMPERATURE °C

Fig. B-14

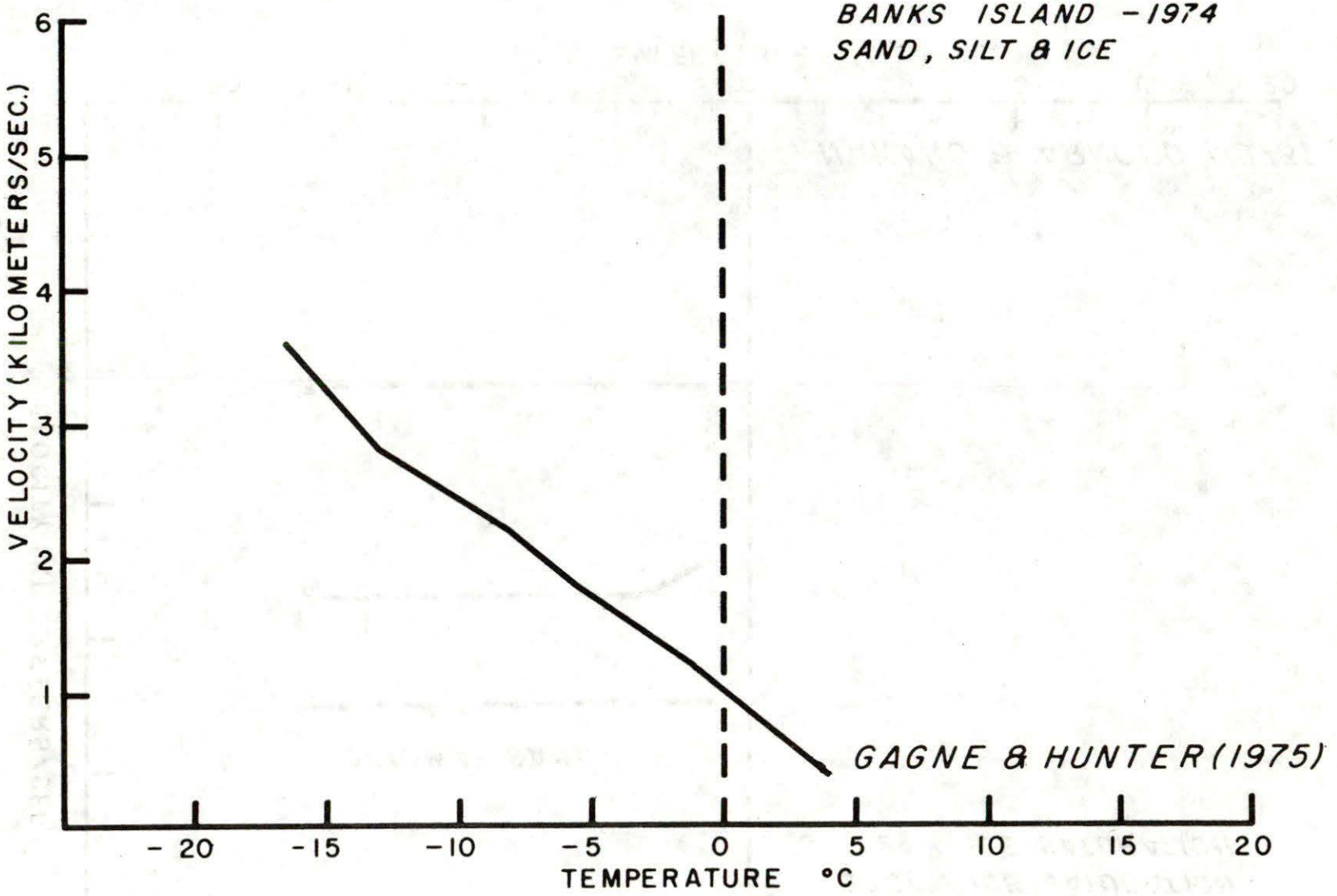
BANKS ISLAND - 1974
SAND, SILT & ICE
VELOCITY (KILOMETERS/SEC.)
6
5
4
3
2
1
- 20
-15
-10
-5
0
5
10
15
20
TEMPERATURE °C
GAGNE & HUNTER (1975)

Fig. B-15

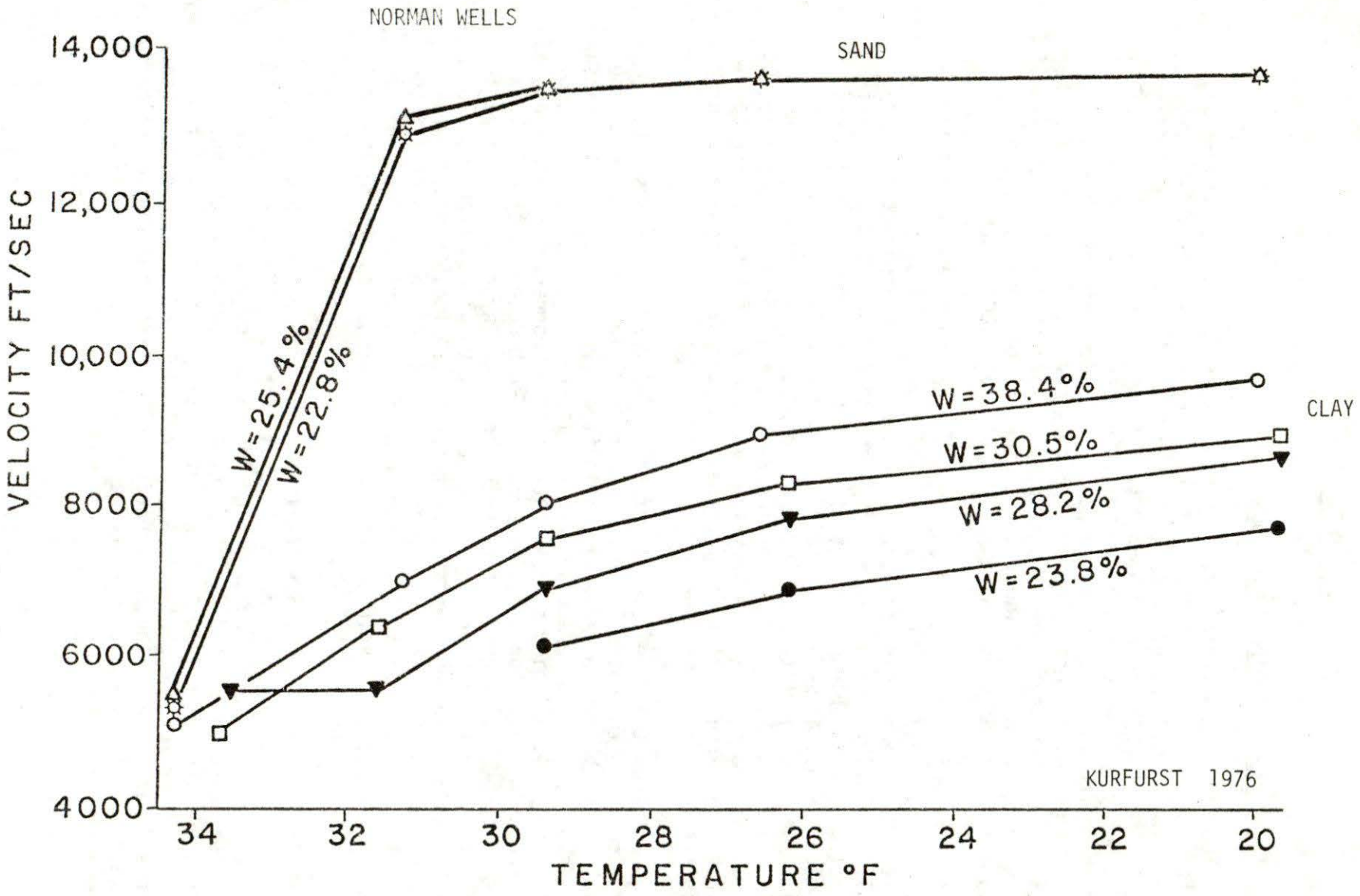

COMPRESSIONAL WAVE VELOCITIES VS TEMPERATURE

Fig. B-16

APPENDIX C

Apparent Velocities of Dipping Refractors

Observed velocities from a refractor at depth in the case of a single-ended profile often show large variations from the true velocity, depending upon the position of the hydrophone array with respect to the slope of the refractor. If the array is located up-dip to the shot point, the change in the apparent velocity of the refractor can be as much as 200% for small slope angles of the refractor. If the array position is down-dip from the shot point, the change in apparent velocity is not as severe. Fig. C-1 shows the cases of a 1,500 m/sec layer overlying a dipping refractor with velocities of 4,000, 3,050, and 2,100 m/sec, which are typical of the Mackenzie delta region. A coarse frozen sand displays a velocity of 4,000 m/sec.

However, if the array is positioned up-dip from the shot, for dips of 10° or less, this velocity may be as high as 7,000 m/sec. In the down-dip case, for slopes up to 10°, there is less than a 25% change in the apparent velocity. For a smaller velocity contrast between V_0 and the refractor, the change in apparent velocity with change in the slope of the interface for up-dip and down-dip cases is not as severe. A velocity of 3,050 m/sec is typical of frozen silt, while a velocity of 2,100 m/sec represents a typical frozen clay. It is assumed that all unfrozen material velocities are represented by 1,500 m/sec. In short, if we are surveying in an area of known frozen coarse-grained materials, an unusually high apparent velocity is an indication of a sloping interface on the refractor.

Since we do not know the true velocity of the refractor, we must use the observed velocity in the calculation of refractor depth. Fig. C-2 shows the error involved in that approximation. The dotted curve is for an actual basal refractor velocity of 2,100 m/sec and a first layer velocity of 1,500 m/sec. Considering the small velocity contrast across this boundary, for slope angles on the refractor of less than 10°, the error in depth determination is less than 10%. As the velocity contrast between the upper layer and the refractor increases, the percentage error in depth determination also decreases. For example, the solid curve represents an unfrozen layer of 1,500 m/sec overlying frozen sands of 4,000 m/sec, and for an interface dip angle of 10° the error in depth determination is 7%. Therefore, for low angles of dip on interfaces, if the observed velocity of the refractor is assumed in the depth calculation, the error is less than 10%.

The observation of unusually high velocities along adjacent traverse lines allows the dip angles on the refractor to be estimated. The three curves of Fig. C-2 are clay, silt and sand in increasing values of velocity. The original values were calculated in feet/sec, which accounts for the unusual numbers on these curves in m/sec. It is interesting to note the differences in percentage error for the small slopes in the values of the velocities near the origin and particularly the small percentage of error for the low-velocity contrast case, up to a considerable degree of slope.

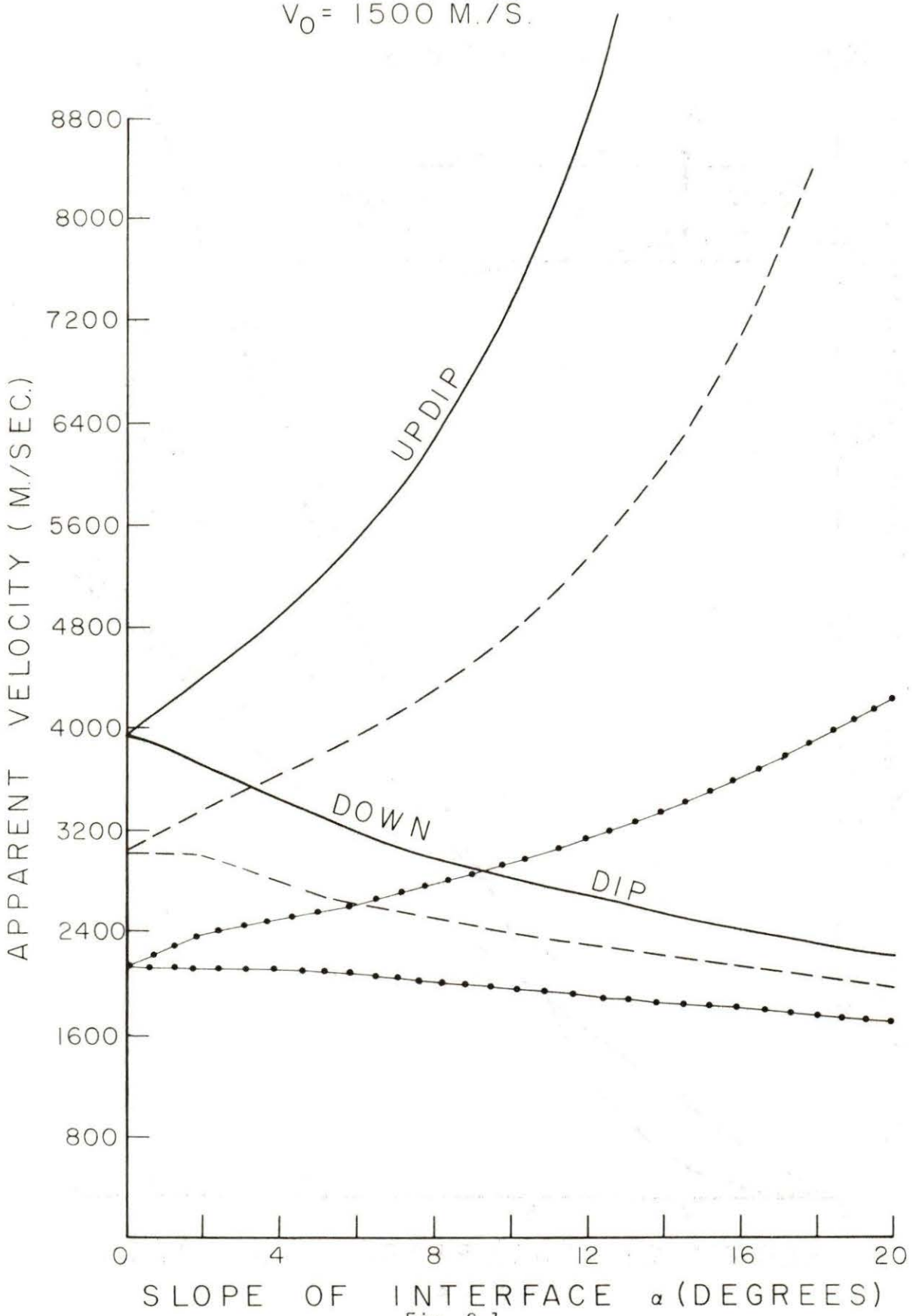
V_0 = 1500 M./S.
APPARENT VELOCITY (M/SEC.)
8800
8000
7200
6400
5600
4800
4000
3200
2400
1600
800
UPDIP
DOWN
DIP
0
4
8
12
16
20
SLOPE OF INTERFACE α (DEGREES)

Fig. C-1

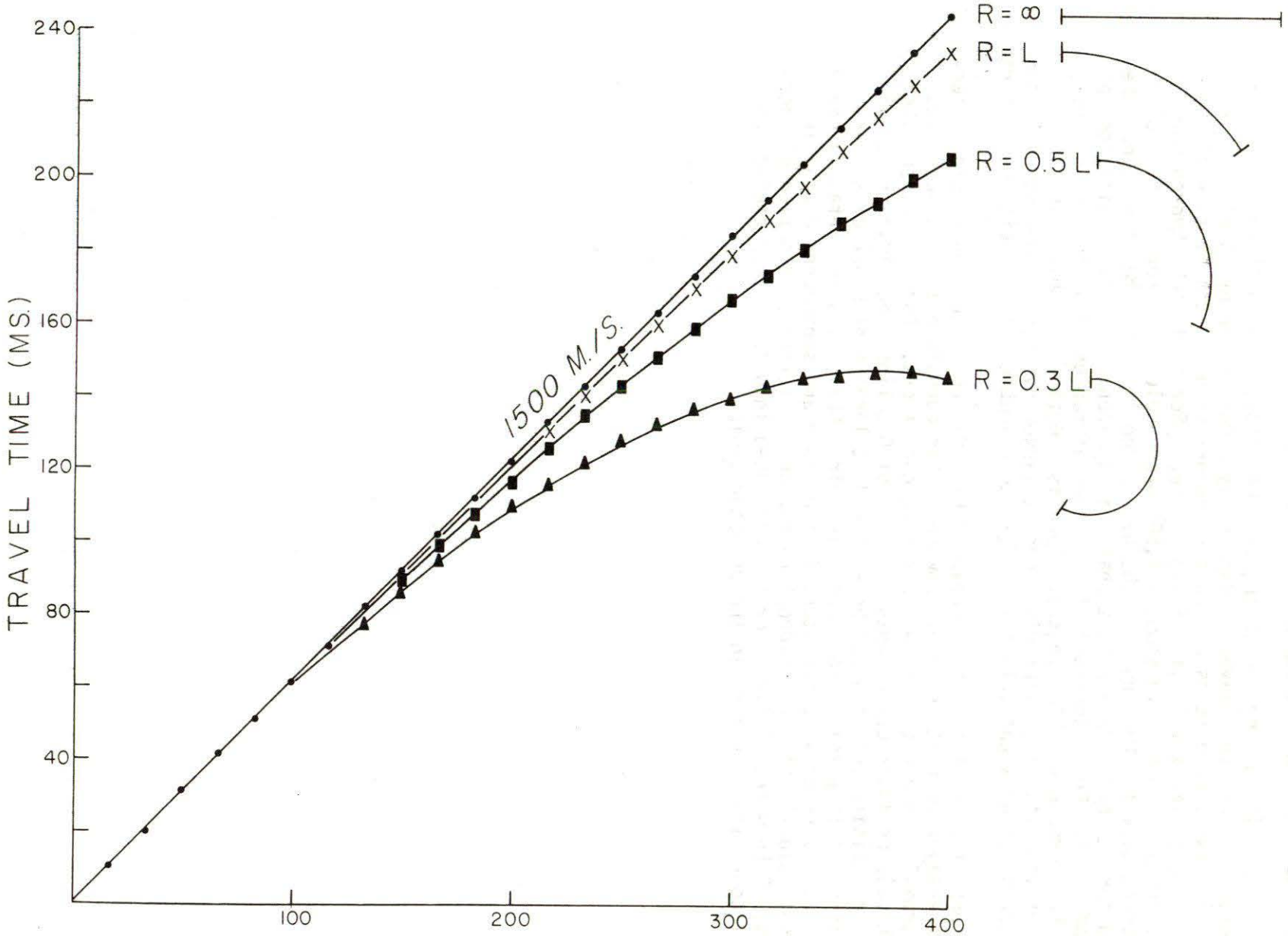
240
200
160
120
80
40
TRAVEL TIME (MS.)
1500 M./S.
R = ∞
R = L
R = 0.5 L
R = 0.3 L
100
200
300
400
HYDROPHONE DISTANCE ON CABLE (METERS)

Fig. C-3

APPENDIX D

Sub-surface Temperature Observation from Deep Wells in the Mackenzie Delta/ Beaufort Sea Area

Sub-surface temperature-depth profiles are shown for 19 deep wells in the region. Measurements have in fact been made at 25 sites but six of the wells have only a single log and are still far from thermal equilibrium. Only one deep set of observations are from an offshore well and it is in the western delta area. Of the results presented here, 14 wells represent the eastern region of the Delta and five the western region.

Temperatures are given in °C and depths in metres for the profiles. Not all individual logs are plotted as this would unnecessarily complicate some of the graphs; however, sufficient logs are plotted to demonstrate their main characteristics. The position coordinates for each well are shown immediately below the well name. Wells are grouped according to Earth Physics Branch file number. Further details on each of these wells and on the observational data may be found in Taylor and Judge (1974; 1975; 1976).

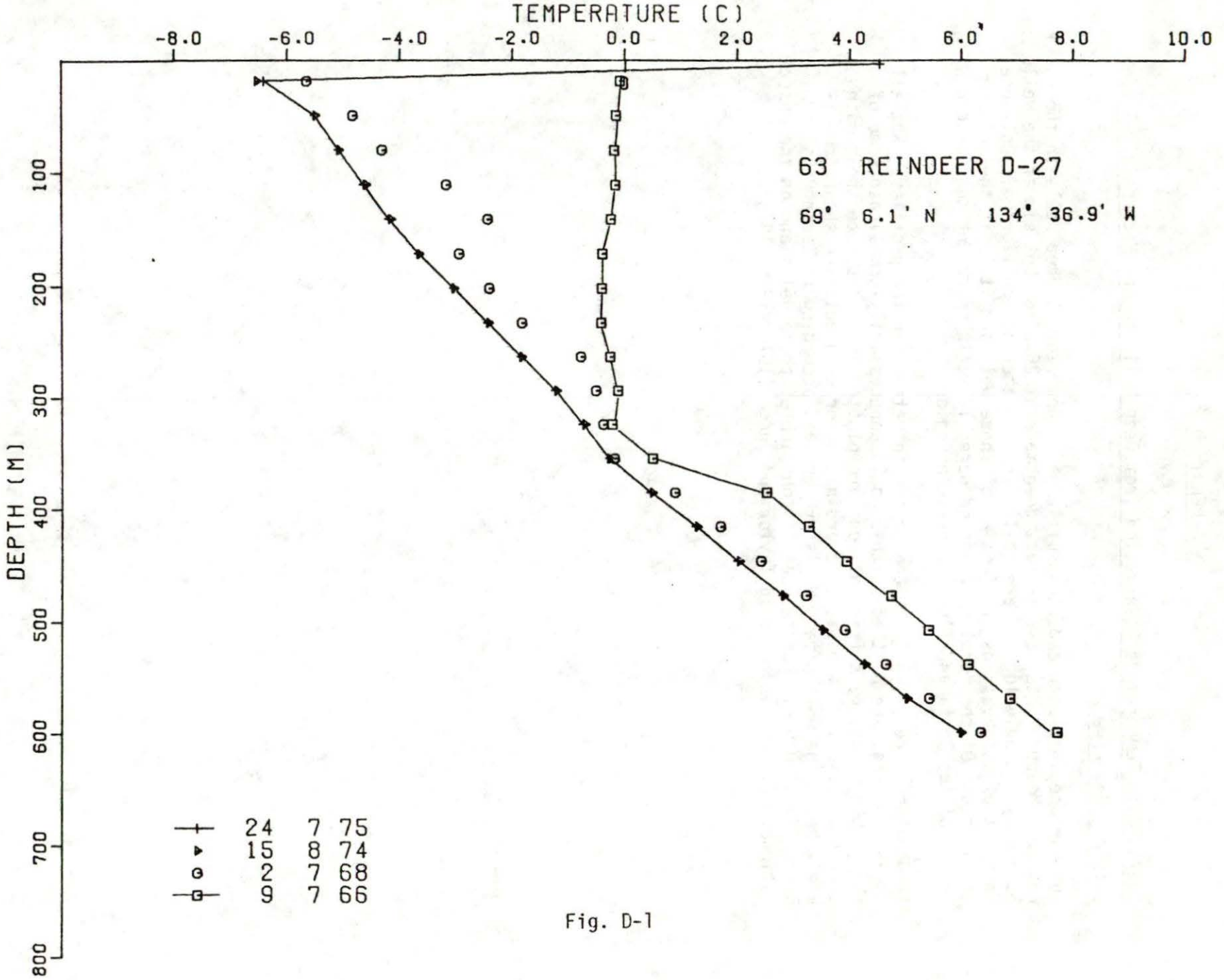
TEMPERATURE (C)
-8.0
-6.0
-4.0
-2.0
0.0
2.0
4.0
6.0
8.0
10.0
DEPTH (M)
100
200
300
400
500
600
700
800
63 REINDEER D-27
69° 6.1' N 134° 36.9' W
24 7 75
15 8 74
2 7 68
9 7 66

Fig. D-1

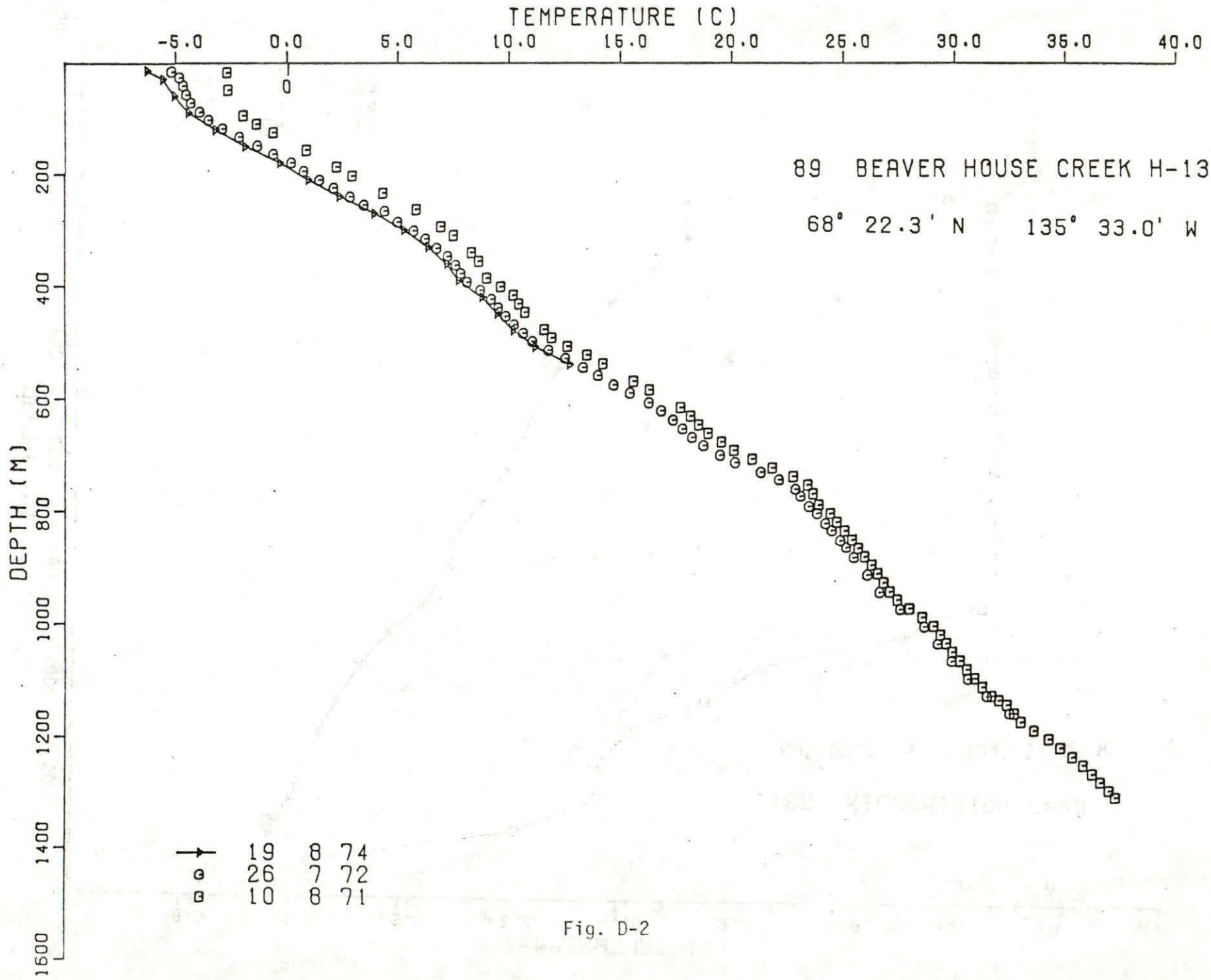
TEMPERATURE (C)
-5.0
0.0
5.0
10.0
15.0
20.0
25.0
30.0
35.0
40.0
0
89 BEAVER HOUSE CREEK H-13
68° 22.3' N 135° 33.0' W
DEPTH (M)
200
400
600
800
1000
1200
1400
1600
19 8 74
26 7 72
10 8 71

Fig. D-2

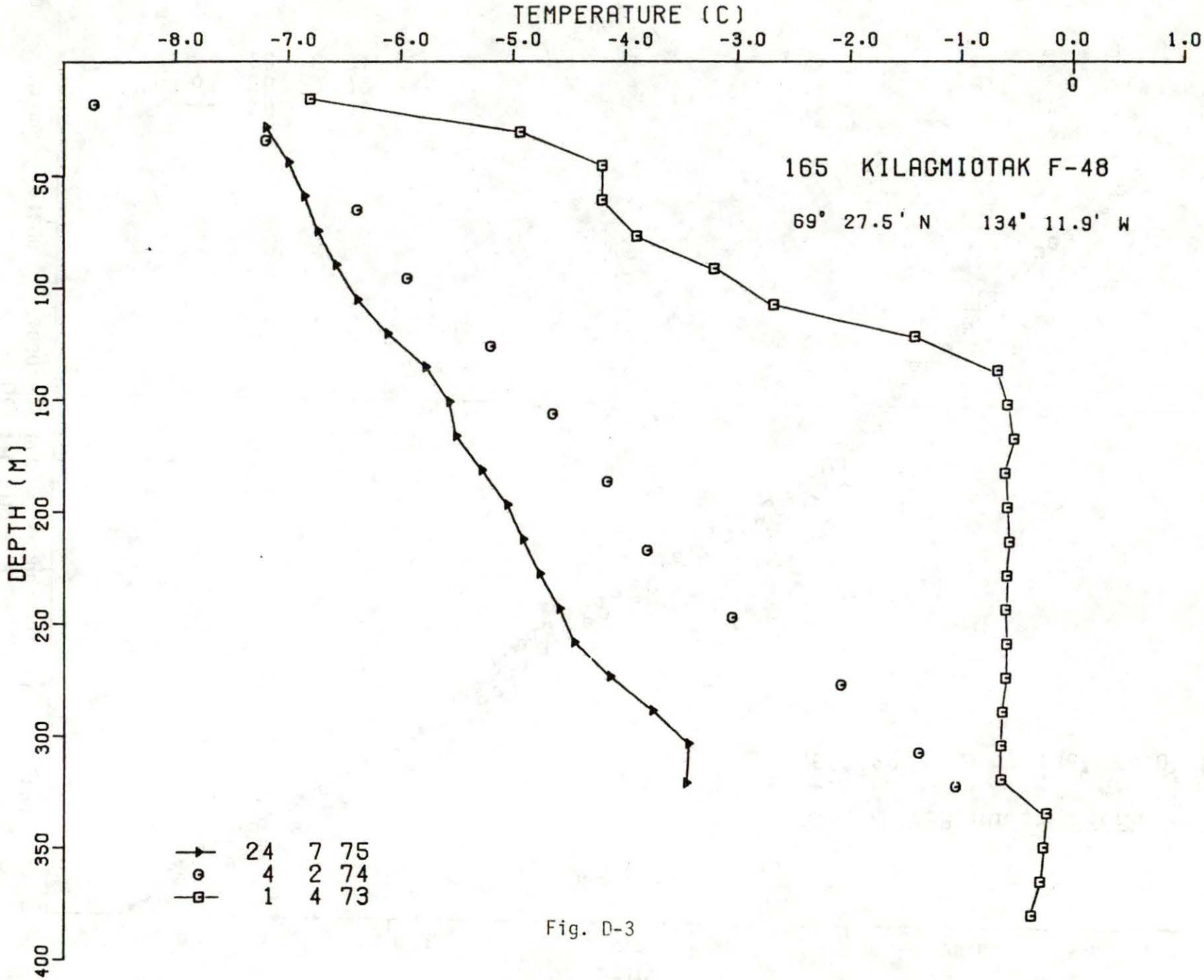
TEMPERATURE (C)
-8.0
-7.0
-6.0
-5.0
-4.0
-3.0
-2.0
-1.0
0.0
1.0
0
165 KILAGMIOTAK F-48
69° 27.5' N 134° 11.9' W
DEPTH (M)
50
100
150
200
250
300
350
400
24 7 75
4 2 74
1 4 73

Fig. D-3

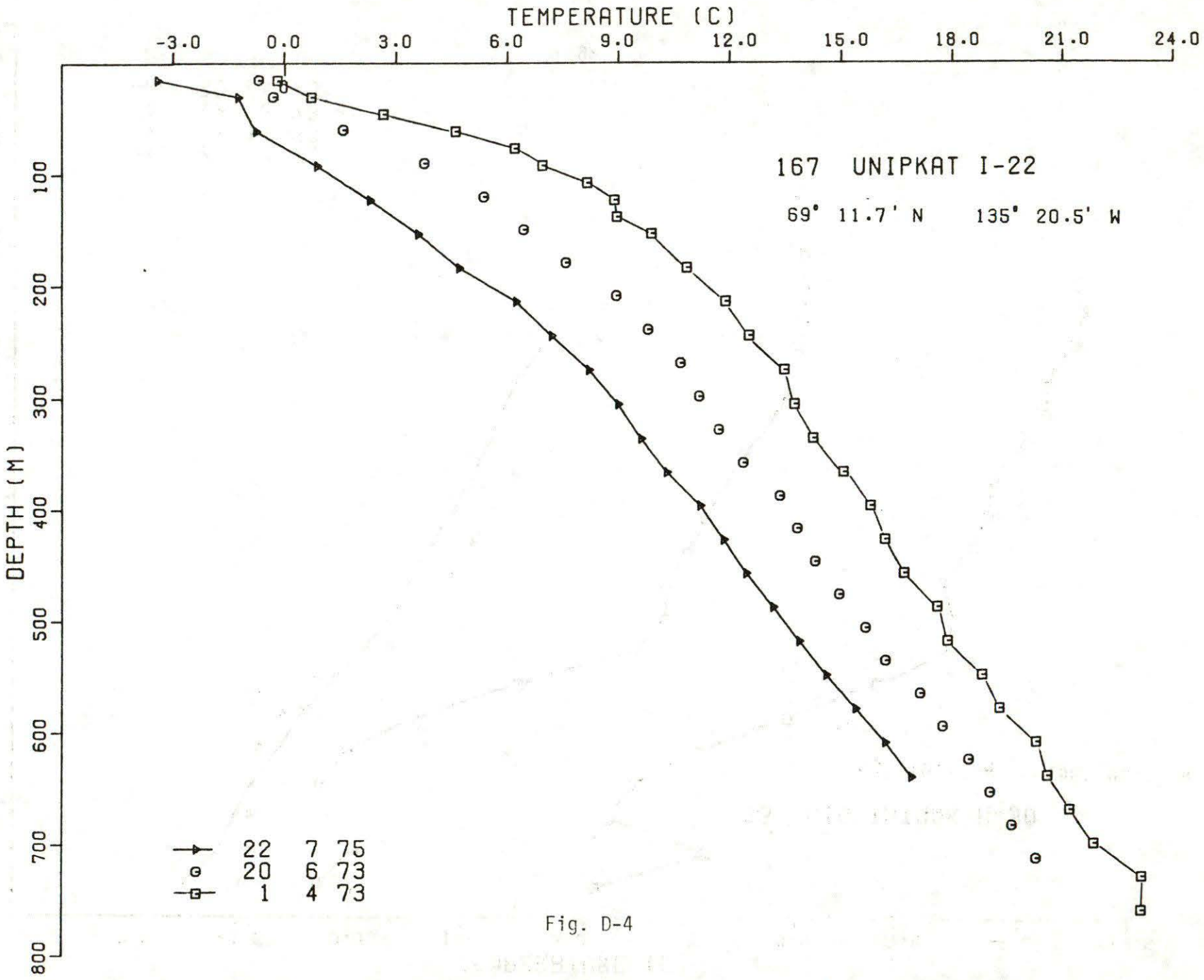
TEMPERATURE (C)
-3.0
0.0
3.0
6.0
9.0
12.0
15.0
18.0
21.0
24.0
DEPTH (M)
100
200
300
400
500
600
700
800
167 UNIPKAT I-22
69° 11.7' N 135° 20.5' W
22 7 75
20 6 73
1 4 73

Fig. D-4

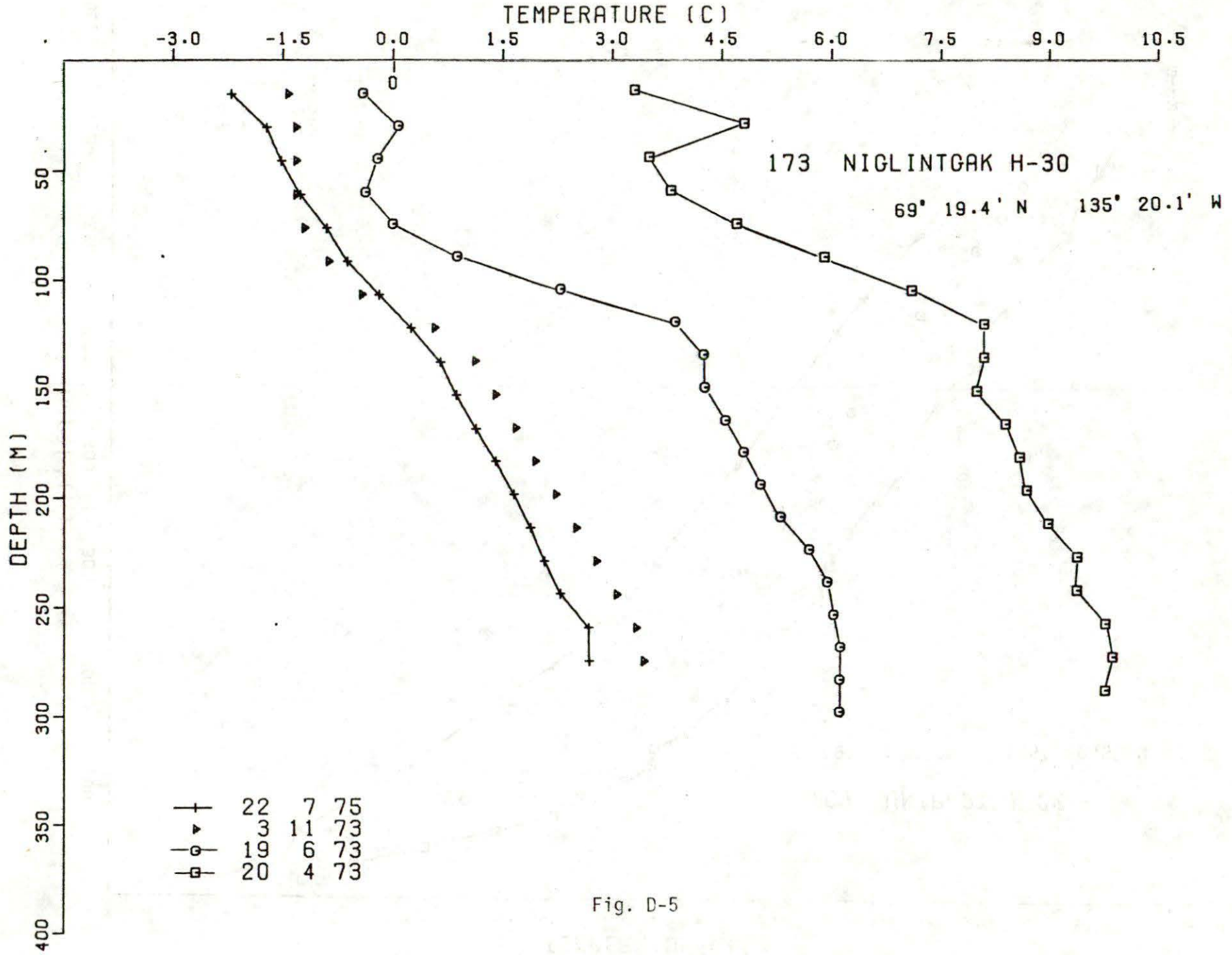
TEMPERATURE (C)
-3.0
-1.5
0.0
1.5
3.0
4.5
6.0
7.5
9.0
10.5
0
DEPTH (M)
50
100
150
200
250
300
350
400
173 NIGLINTGAK H-30
69° 19.4' N 135° 20.1' W
22 7 75
3 11 73
19 6 73
20 4 73

Fig. D-5

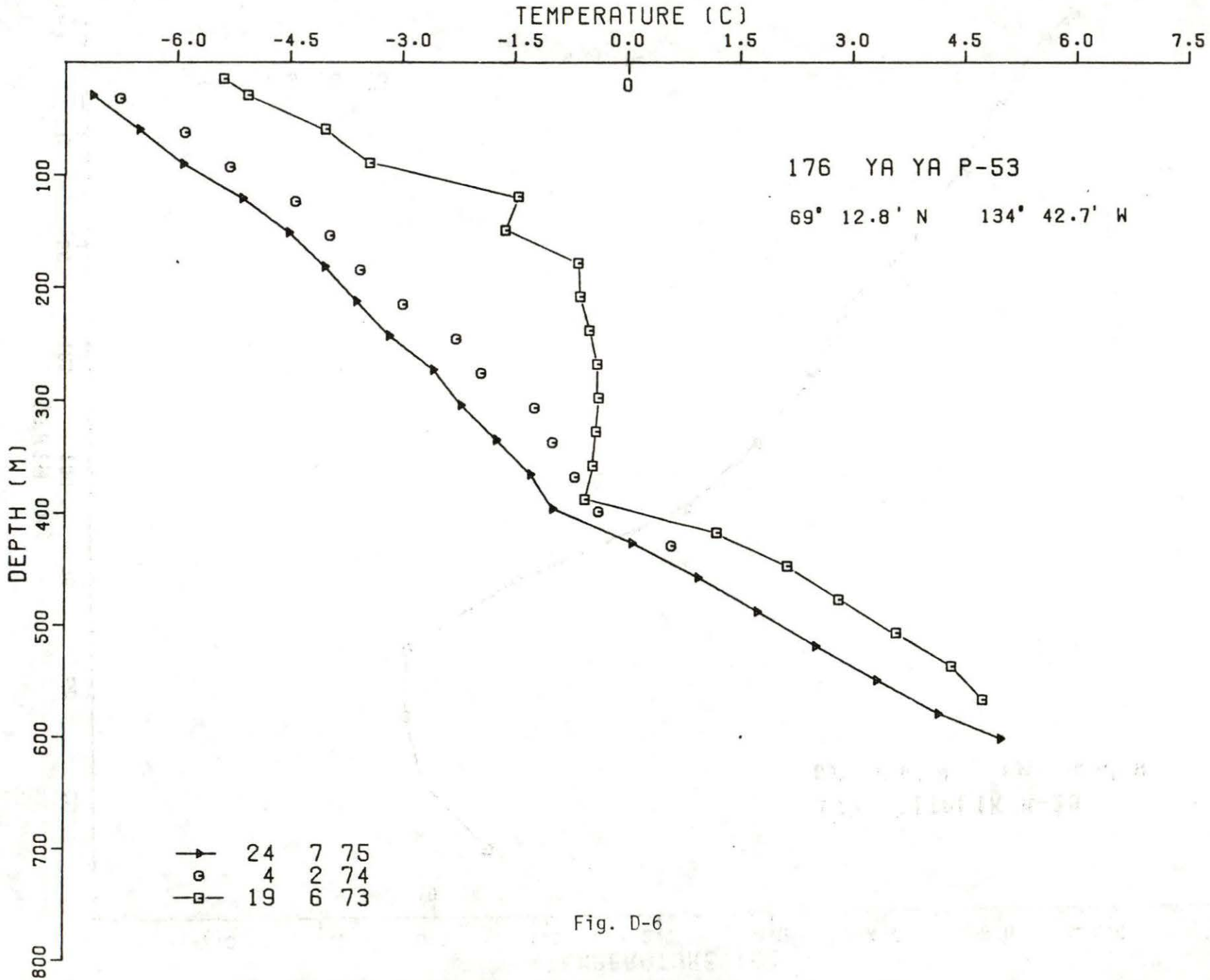
TEMPERATURE (C)
-6.0
-4.5
-3.0
-1.5
0.0
1.5
3.0
4.5
6.0
7.5
0
DEPTH (M)
100
200
300
400
500
600
700
800
176 YA YA P-53
69° 12.8' N 134° 42.7' W
24 7 75
4 2 74
19 6 73

Fig. D-6

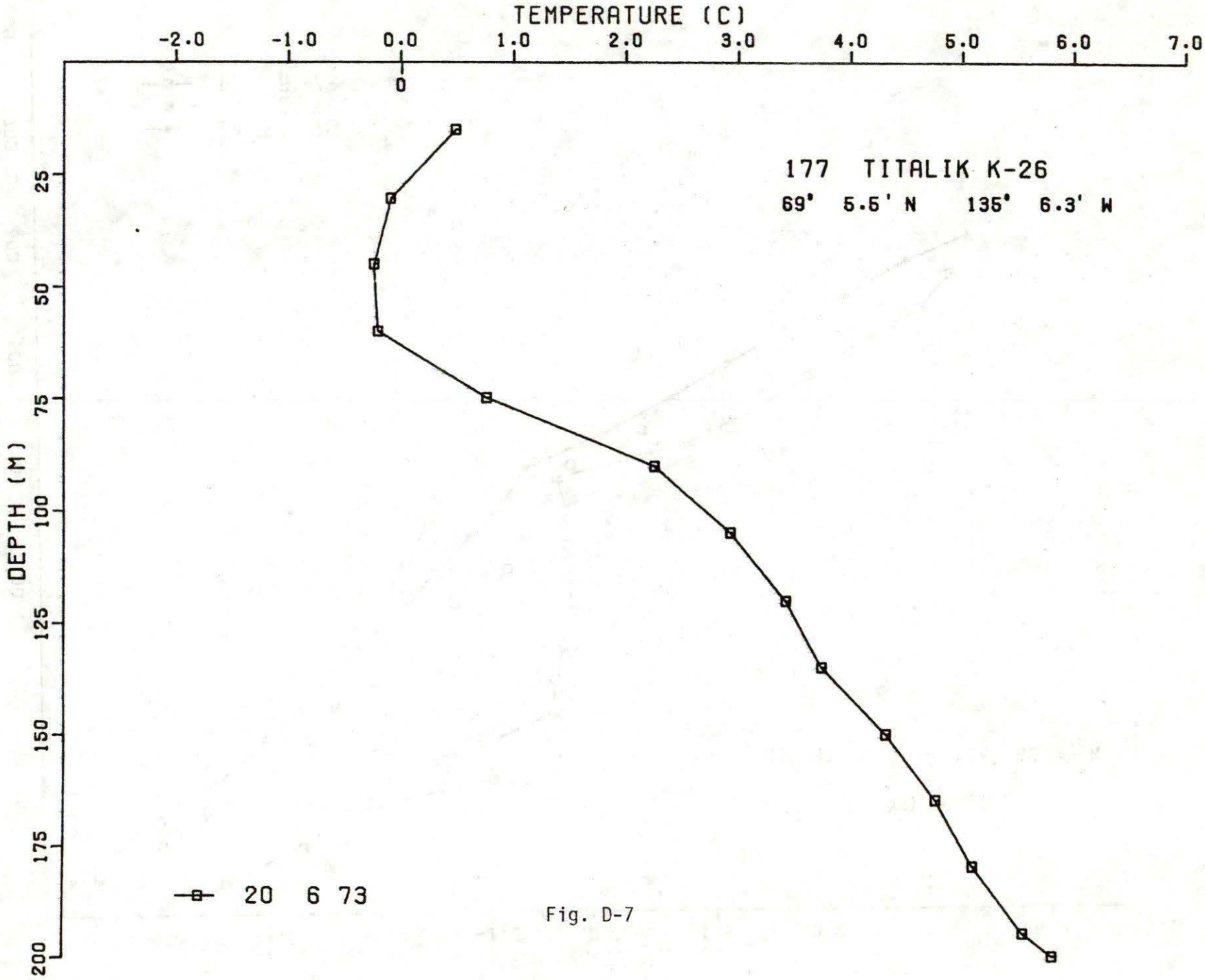
TEMPERATURE (C)
-2.0
-1.0
0.0
1.0
2.0
3.0
4.0
5.0
6.0
7.0
0
177 TITALIK K-26
69° 5.5' N 135° 6.3' W
DEPTH (M)
25
50
75
100
125
150
175
200
20 6 73

Fig. D-7

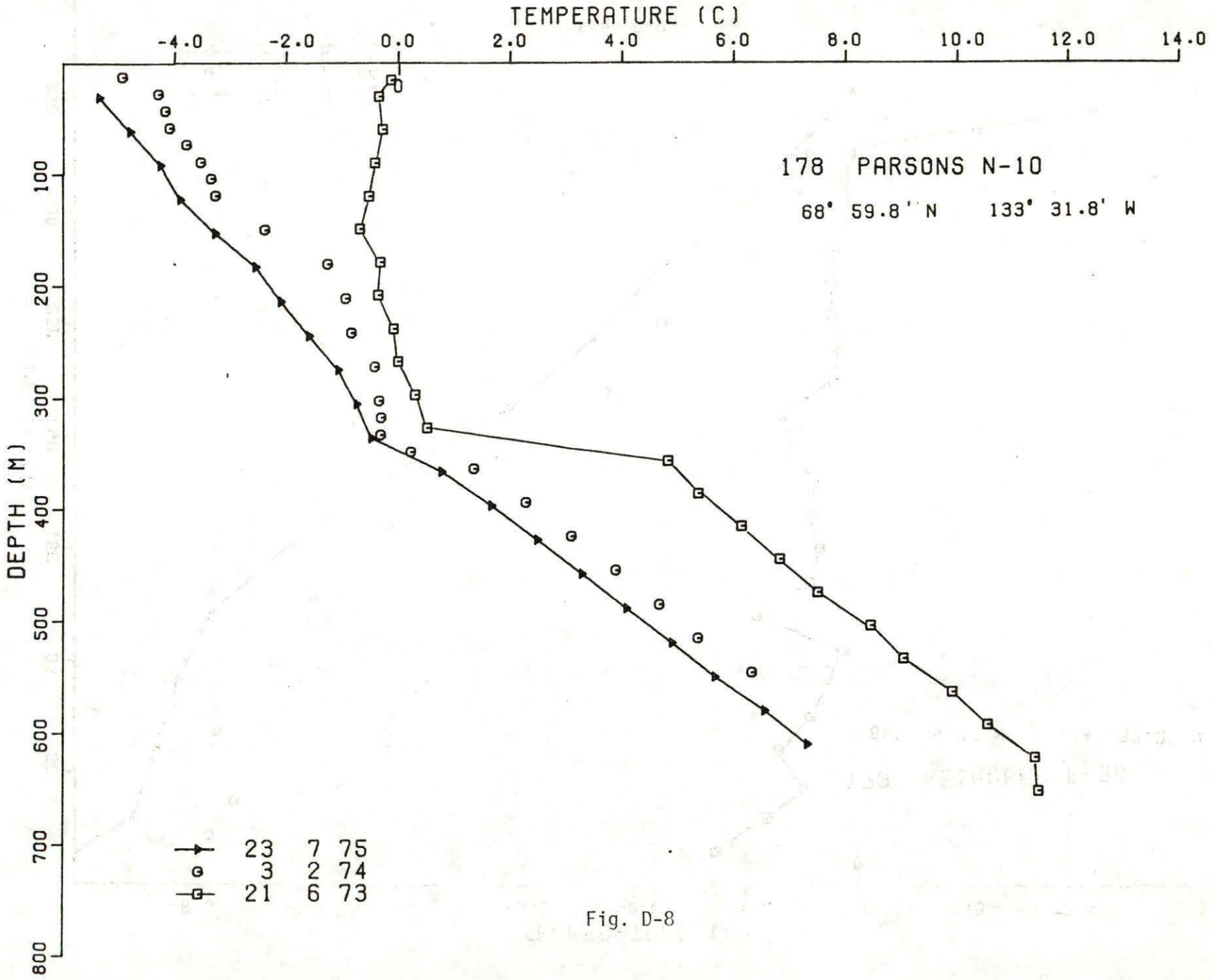
TEMPERATURE (C)
-4.0
-2.0
0.0
2.0
4.0
6.0
8.0
10.0
12.0
14.0
DEPTH (M)
100
200
300
400
500
600
700
800
178 PARSONS N-10
68° 59.8' N 133° 31.8' W
23 7 75
3 2 74
21 6 73

Fig. D-8

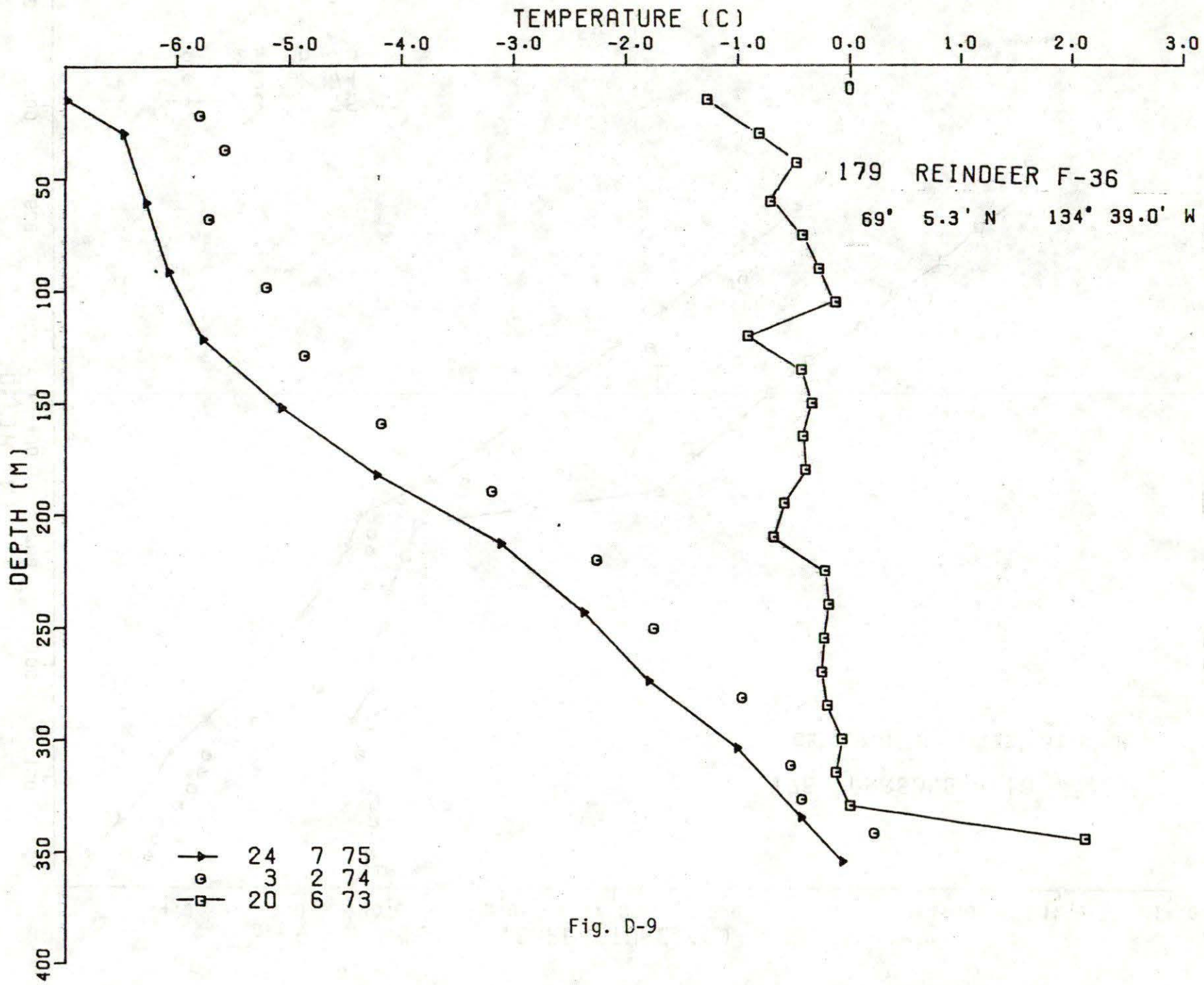
TEMPERATURE (C)
-6.0
-5.0
-4.0
-3.0
-2.0
-1.0
0.0
1.0
2.0
3.0
0
DEPTH (M)
50
100
150
200
250
300
350
400
179 REINDEER F-36
69° 5.3' N 134° 39.0' W
24 7 75
3 2 74
20 6 73

Fig. D-9

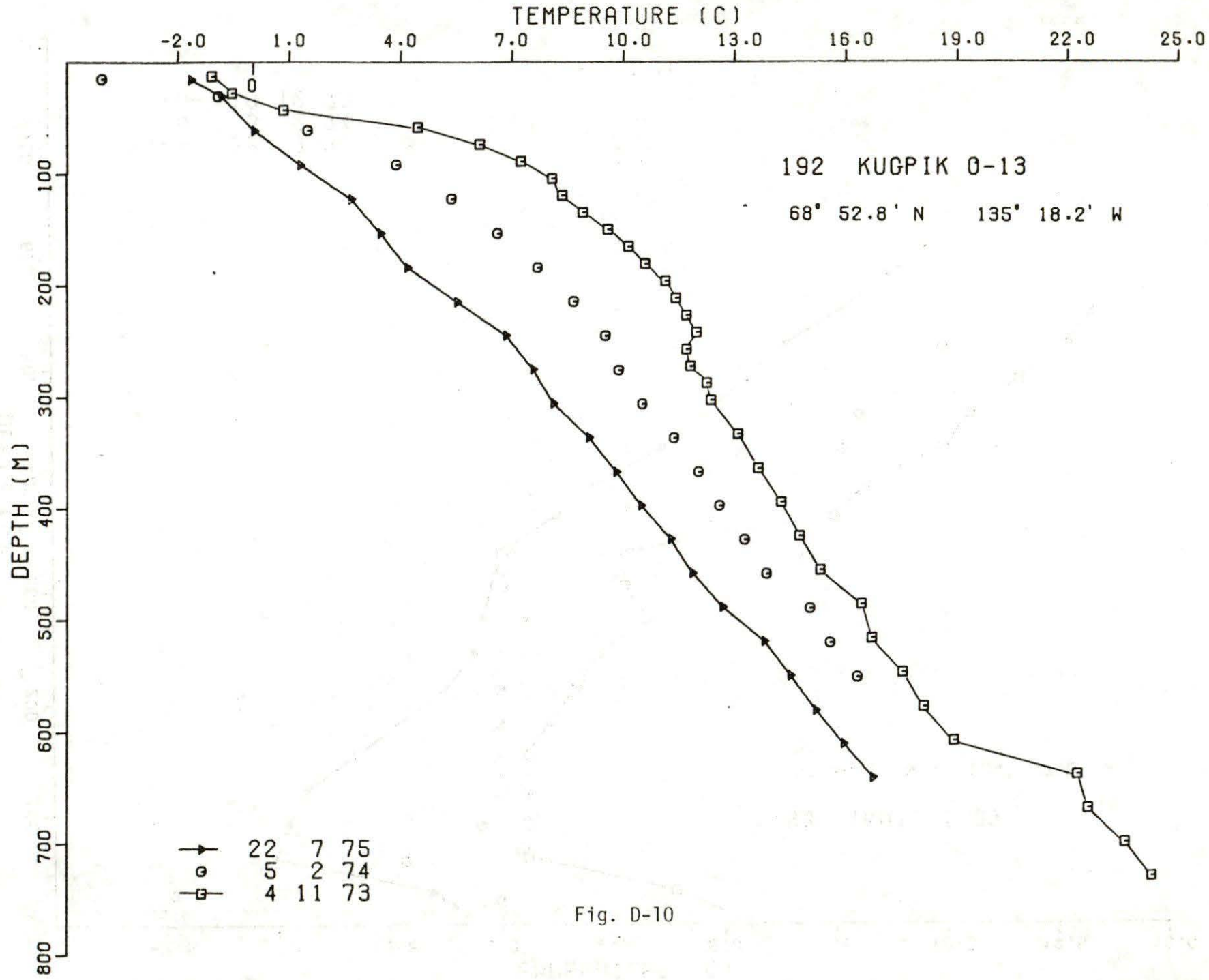
TEMPERATURE (C)
-2.0
1.0
4.0
7.0
10.0
13.0
16.0
19.0
22.0
25.0
0
100
200
300
400
500
600
700
800
DEPTH (M)
192 KUGPIK 0-13
68° 52.8' N 135° 18.2' W
22 7 75
5 2 74
4 11 73

Fig. D-10

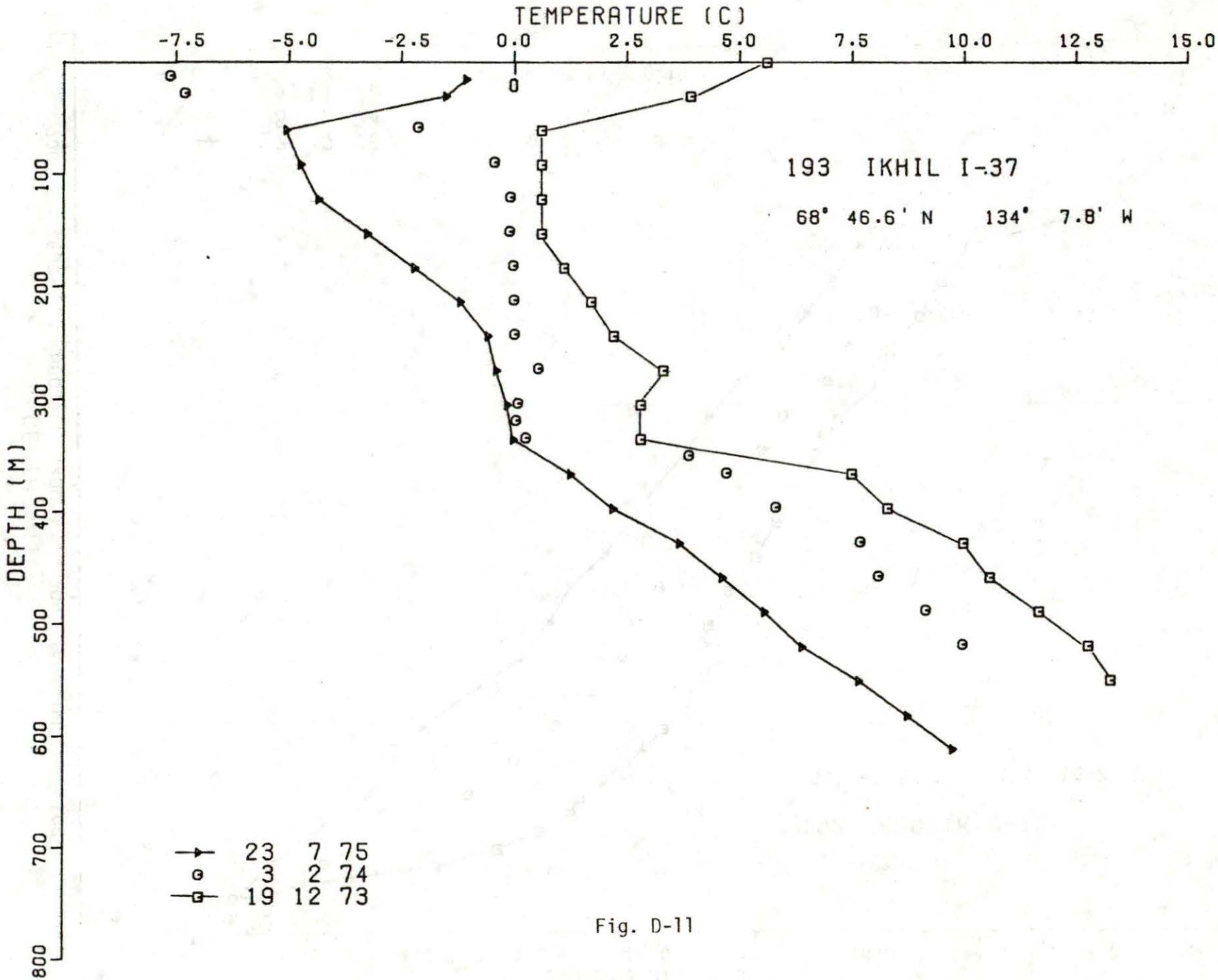
TEMPERATURE (C)
-7.5
-5.0
-2.5
0.0
2.5
5.0
7.5
10.0
12.5
15.0
DEPTH (M)
100
200
300
400
500
600
700
800
193 IKHIL I-37
68° 46.6' N 134° 7.8' W
23 7 75
3 2 74
19 12 73

Fig. D-11

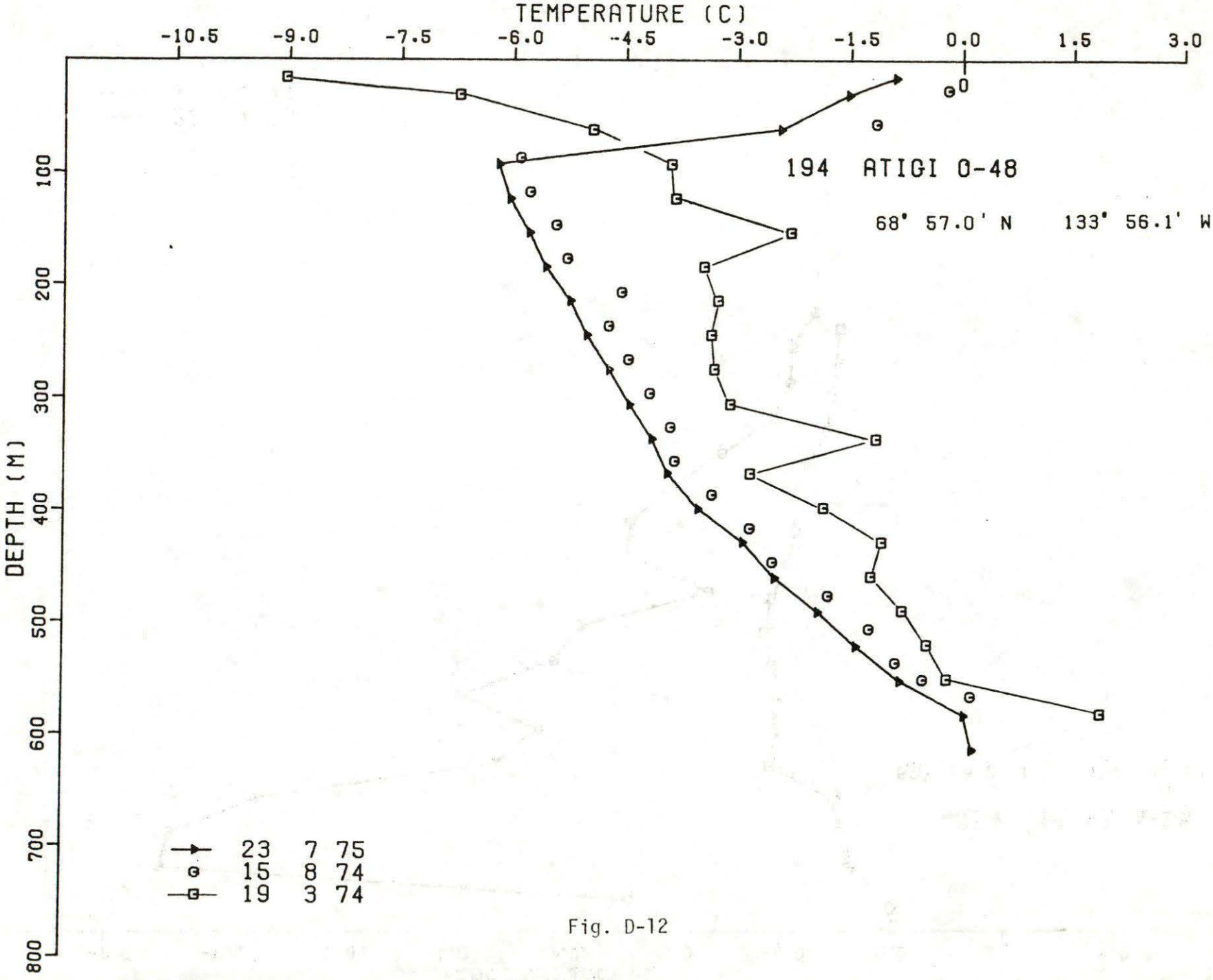
TEMPERATURE (C)
-10.5
-9.0
-7.5
-6.0
-4.5
-3.0
-1.5
0.0
1.5
3.0
DEPTH (M)
100
200
300
400
500
600
700
800
194 ATIGI 0-48
68° 57.0' N 133° 56.1' W
23 7 75
15 8 74
19 3 74

Fig. D-12

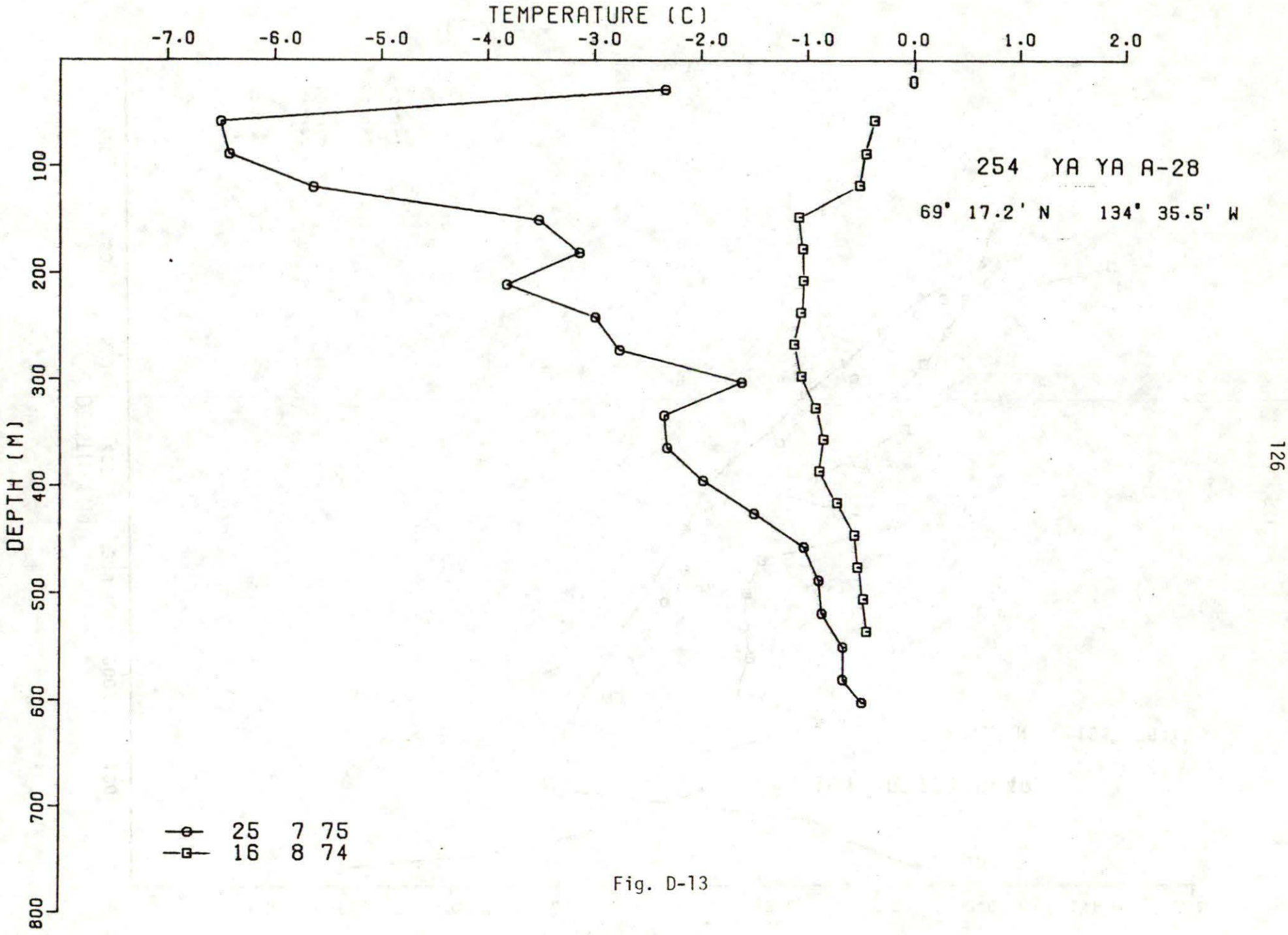
TEMPERATURE (C)
-7.0
-6.0
-5.0
-4.0
-3.0
-2.0
-1.0
0.0
1.0
2.0
0
DEPTH (M)
100
200
300
400
500
600
700
800
254 YA YA A-28
69° 17.2' N 134° 35.5' W
25 7 75
16 8 74

Fig. D-13

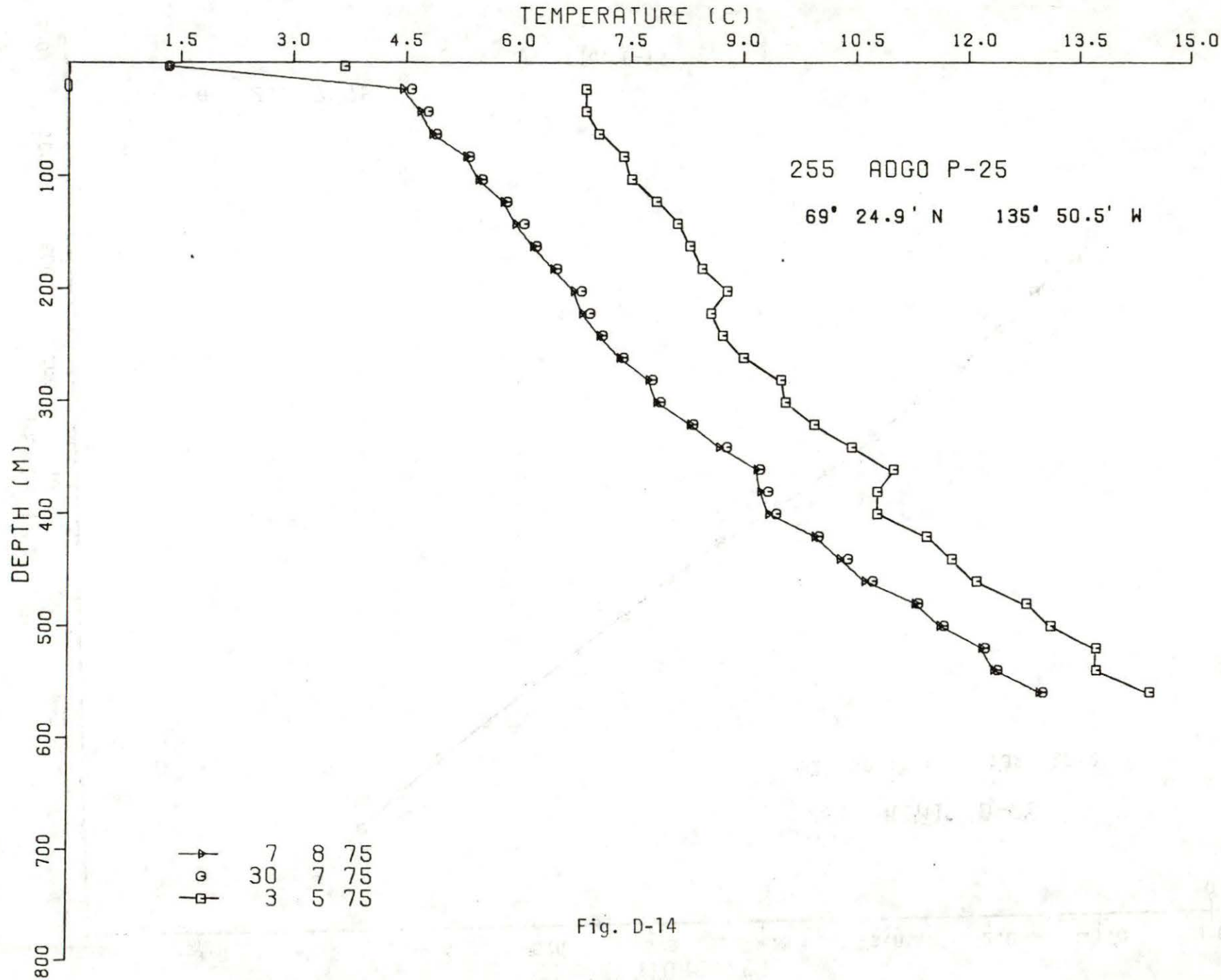
TEMPERATURE (C)
1.5
3.0
4.5
6.0
7.5
9.0
10.5
12.0
13.5
15.0
DEPTH (M)
0
100
200
300
400
500
600
700
800
255 ADGO P-25
69° 24.9' N 135° 50.5' W
7 8 75
30 7 75
3 5 75

Fig. D-14

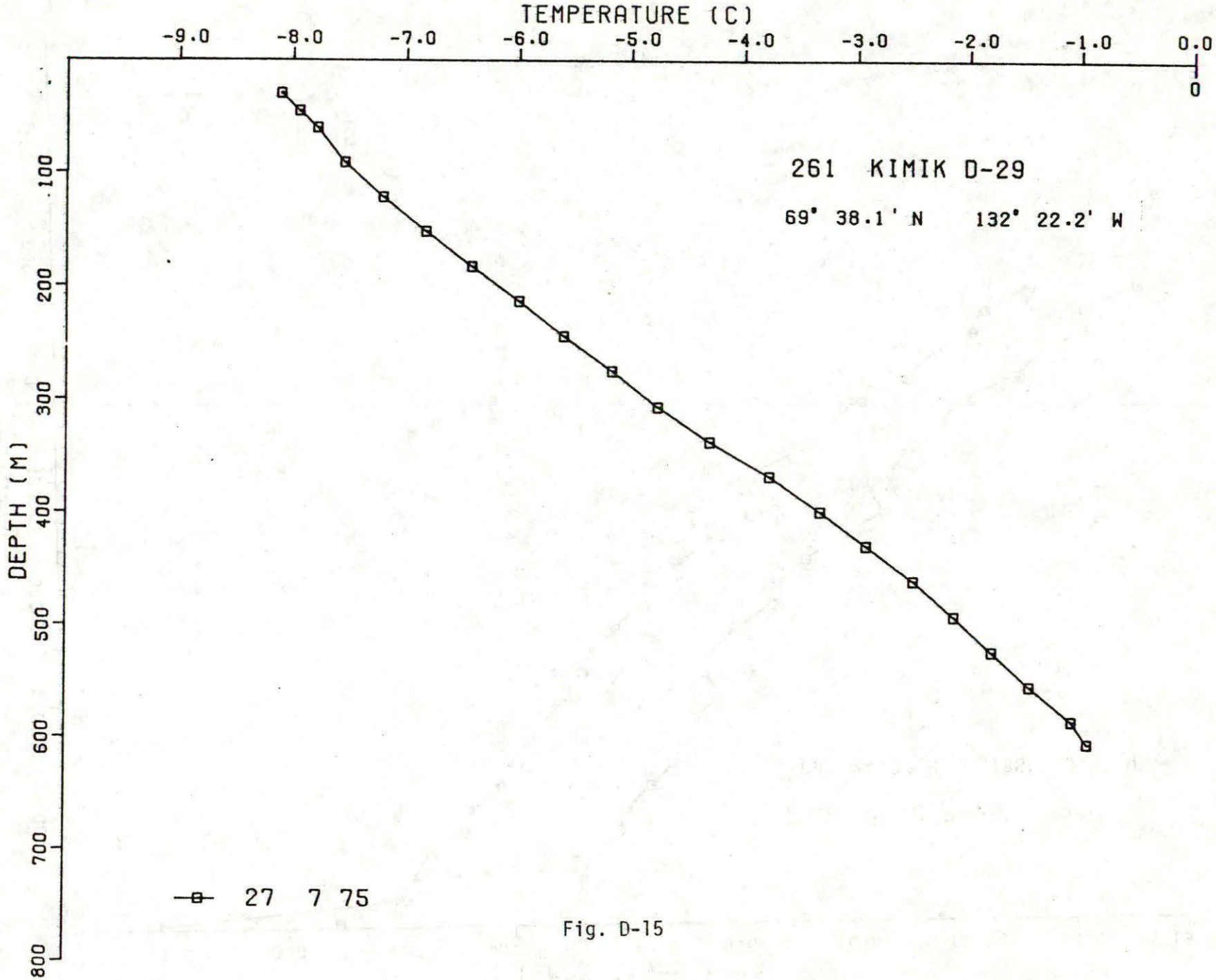
TEMPERATURE (C)
-9.0
-8.0
-7.0
-6.0
-5.0
-4.0
-3.0
-2.0
-1.0
0.0
0
DEPTH (M)
100
200
300
400
500
600
700
800
261 KIMIK D-29
69° 38.1' N 132° 22.2' W
27 7 75

Fig. D-15

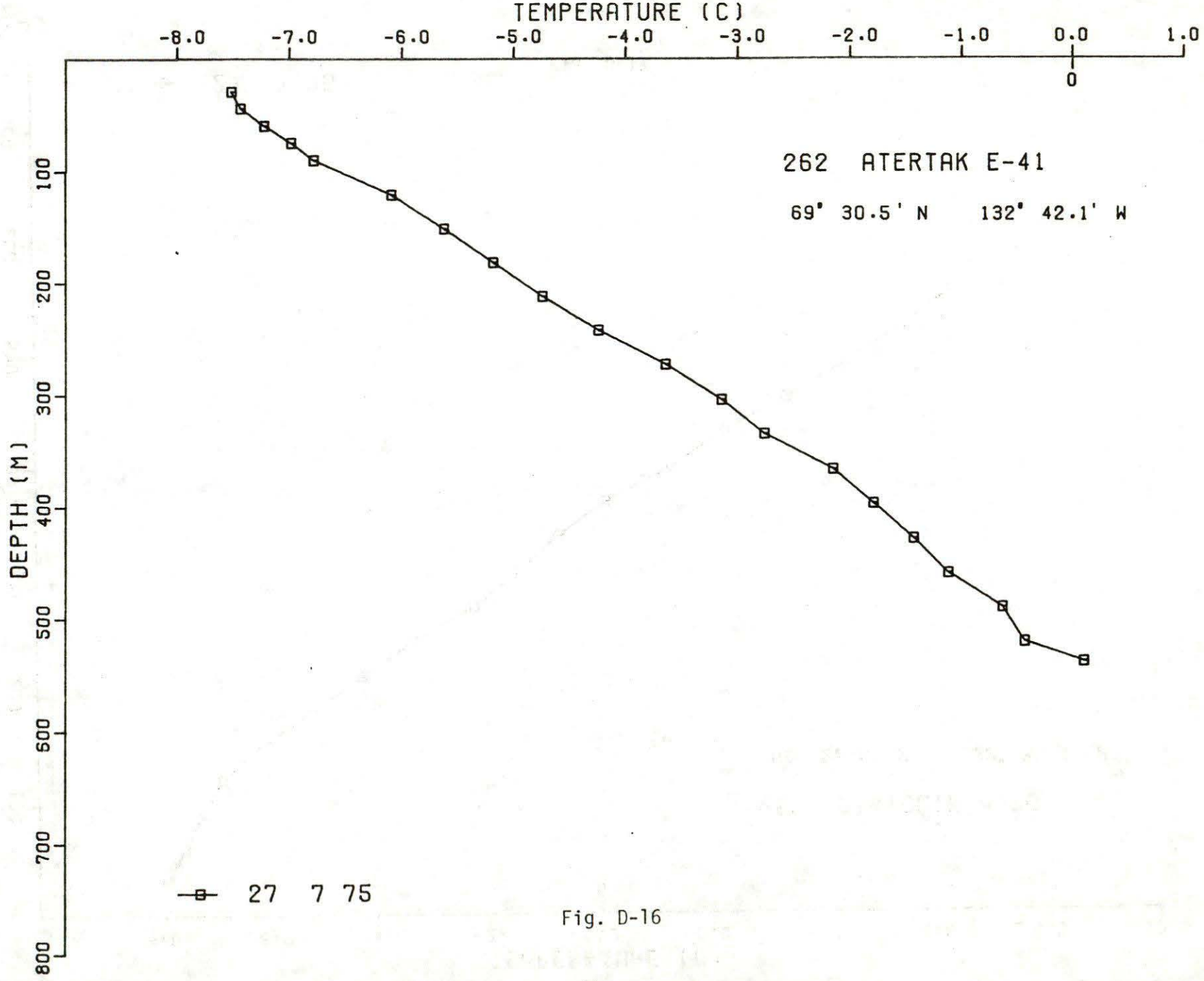
TEMPERATURE (C)
-8.0
-7.0
-6.0
-5.0
-4.0
-3.0
-2.0
-1.0
0.0
1.0
0
262 ATERTAK E-41
69° 30.5' N 132° 42.1' W
DEPTH (M)
100
200
300
400
500
600
700
800
27 7 75

Fig. D-16

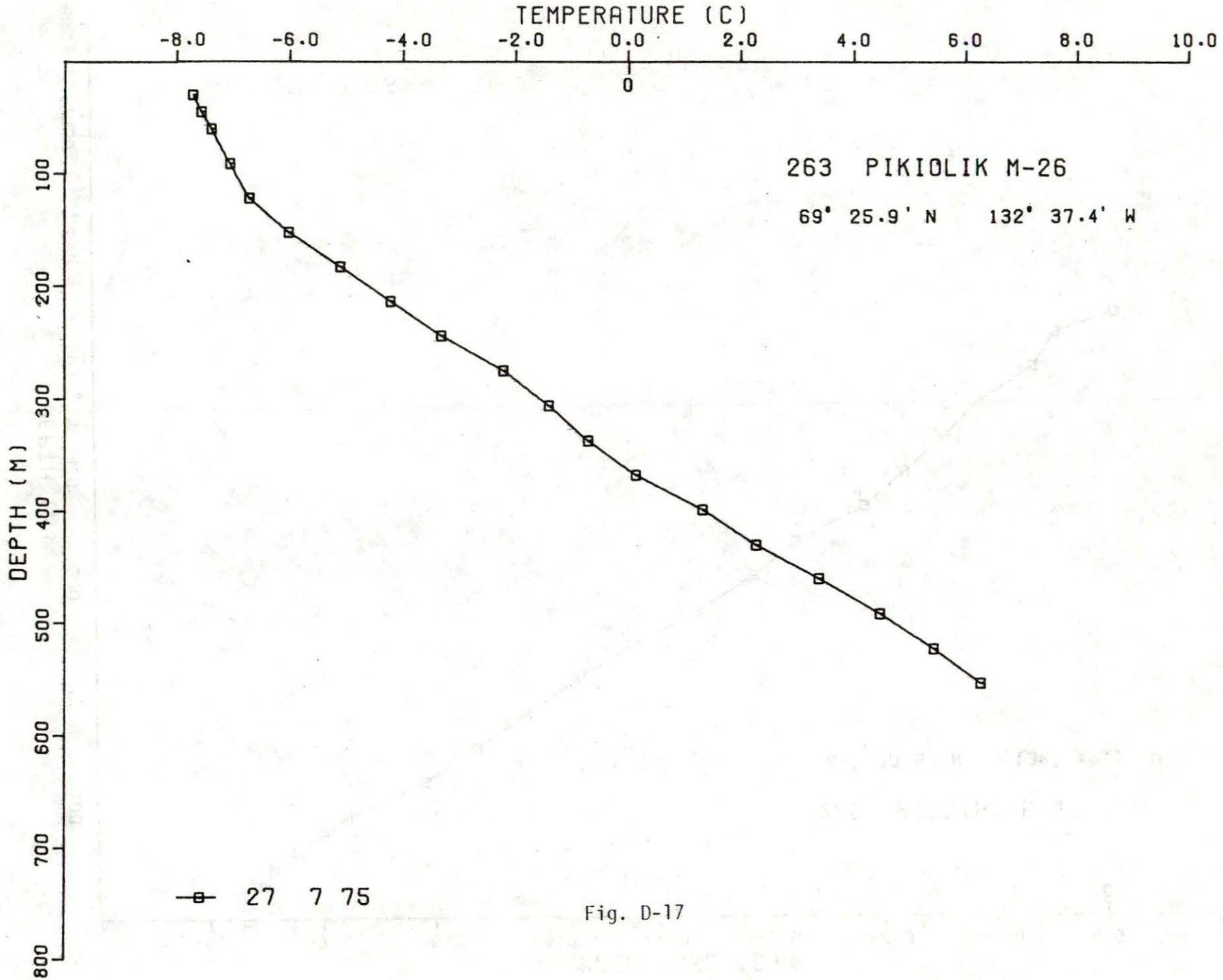
TEMPERATURE (C)
-8.0
-6.0
-4.0
-2.0
0.0
0
2.0
4.0
6.0
8.0
10.0
263 PIKIOLIK M-26
69° 25.9' N 132° 37.4' W
DEPTH (M)
100
200
300
400
500
600
700
800
27 7 75

Fig. D-17

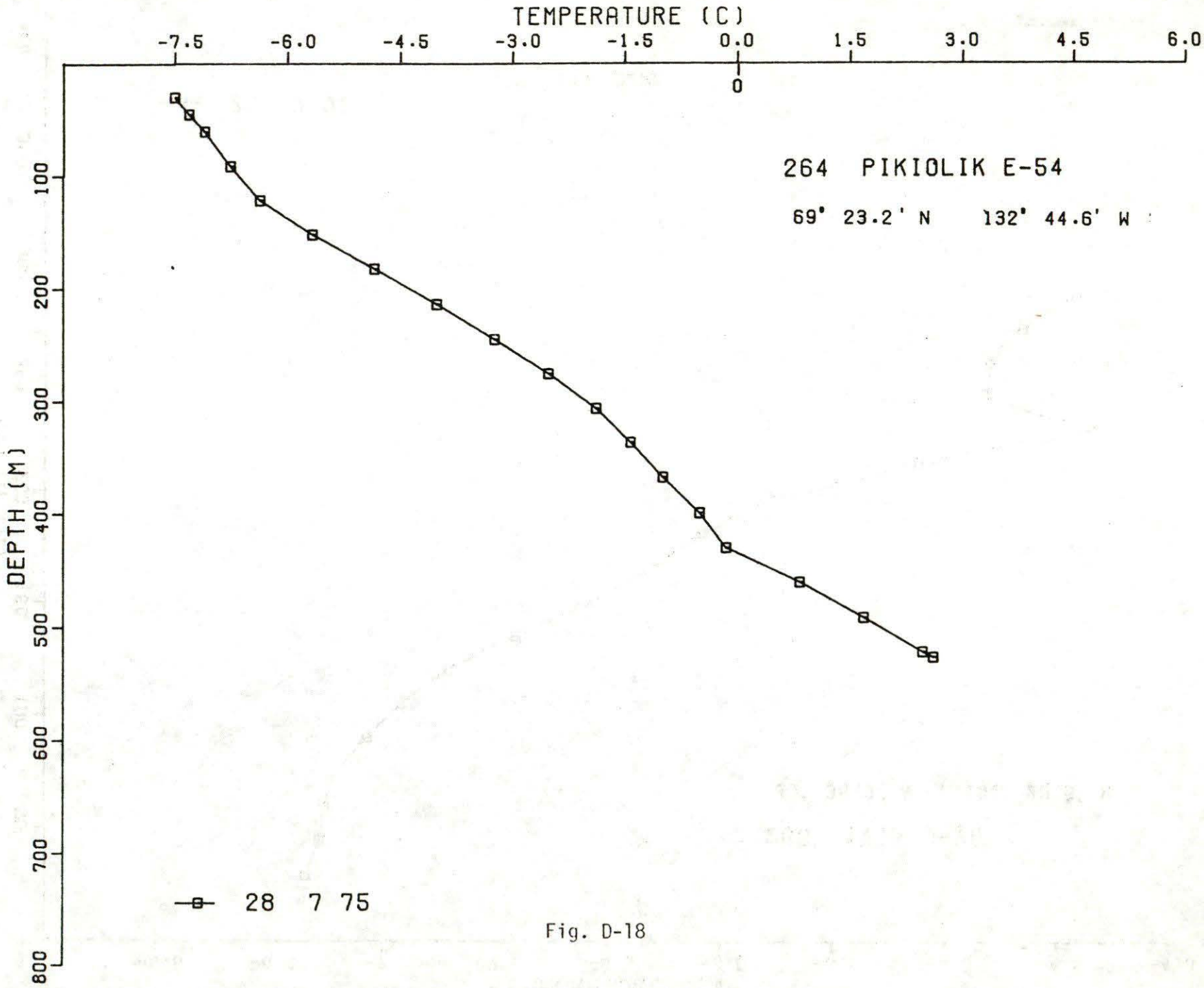
TEMPERATURE (C)
-7.5
-6.0
-4.5
-3.0
-1.5
0.0
1.5
3.0
4.5
6.0
0
264 PIKIOLIK E-54
69° 23.2' N 132° 44.6' W
DEPTH (M)
100
200
300
400
500
600
700
800
28 7 75

Fig. D-18

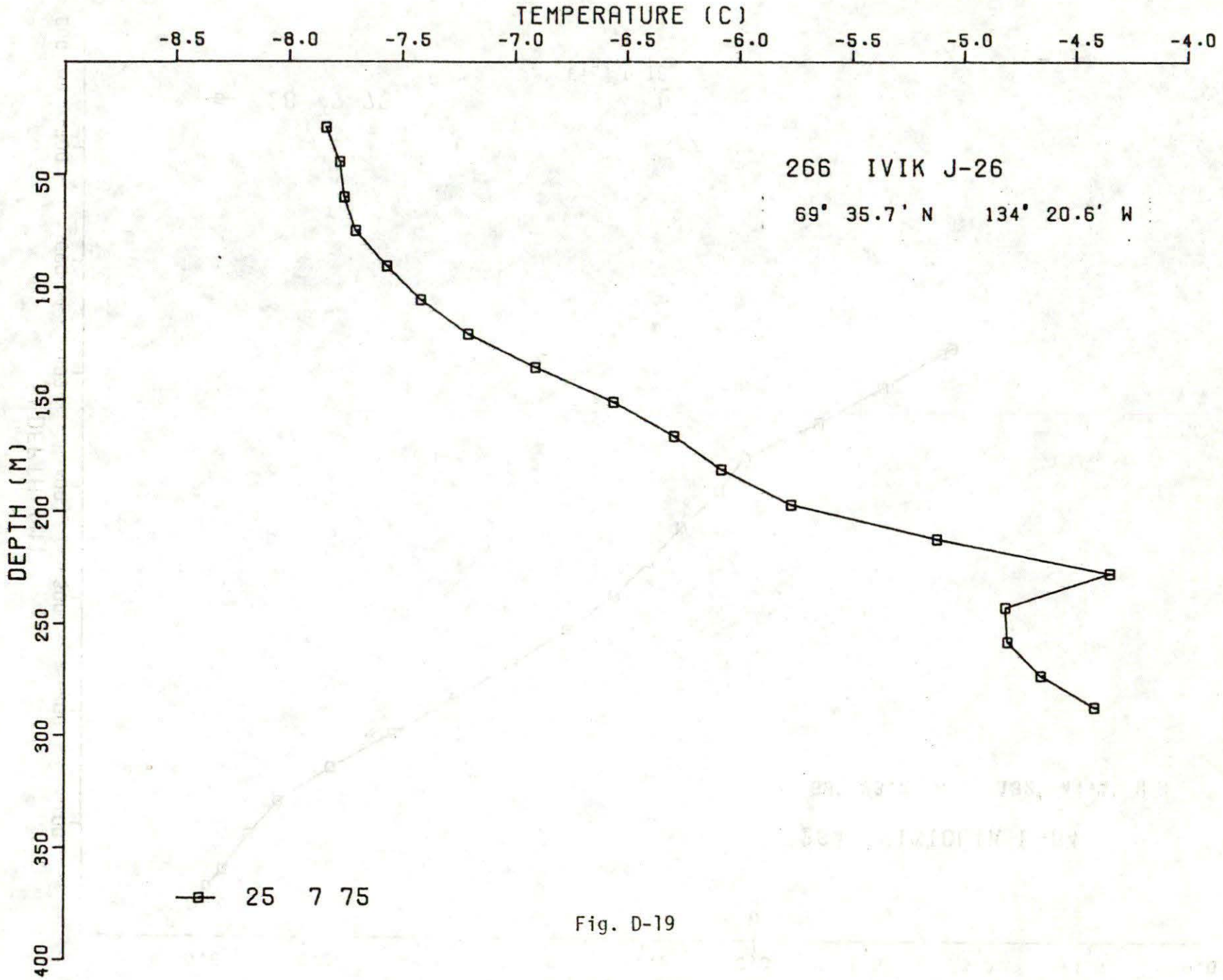
TEMPERATURE (C)
-8.5
-8.0
-7.5
-7.0
-6.5
-6.0
-5.5
-5.0
-4.5
-4.0
DEPTH (M)
50
100
150
200
250
300
350
400
266 IVIK J-26
69° 35.7' N 134° 20.6' W
25 7 75

Fig. D-19

APPENDIX E

GSC Marine Seismic Refraction Data - Interpreted Sections

A location map of seismic data recorded with the GSC refraction array is given in Fig. 5-4. Sections showing the interpreted occurrence of ice-bonded permafrost are given below. Records were obtained from the *M.V. North Star* off Herschel Island in 1972 and 1973, *M.V. Pressure Ridge* in 1974 and 1975, and also from *C.C.G.S. Nahidik* in 1975.

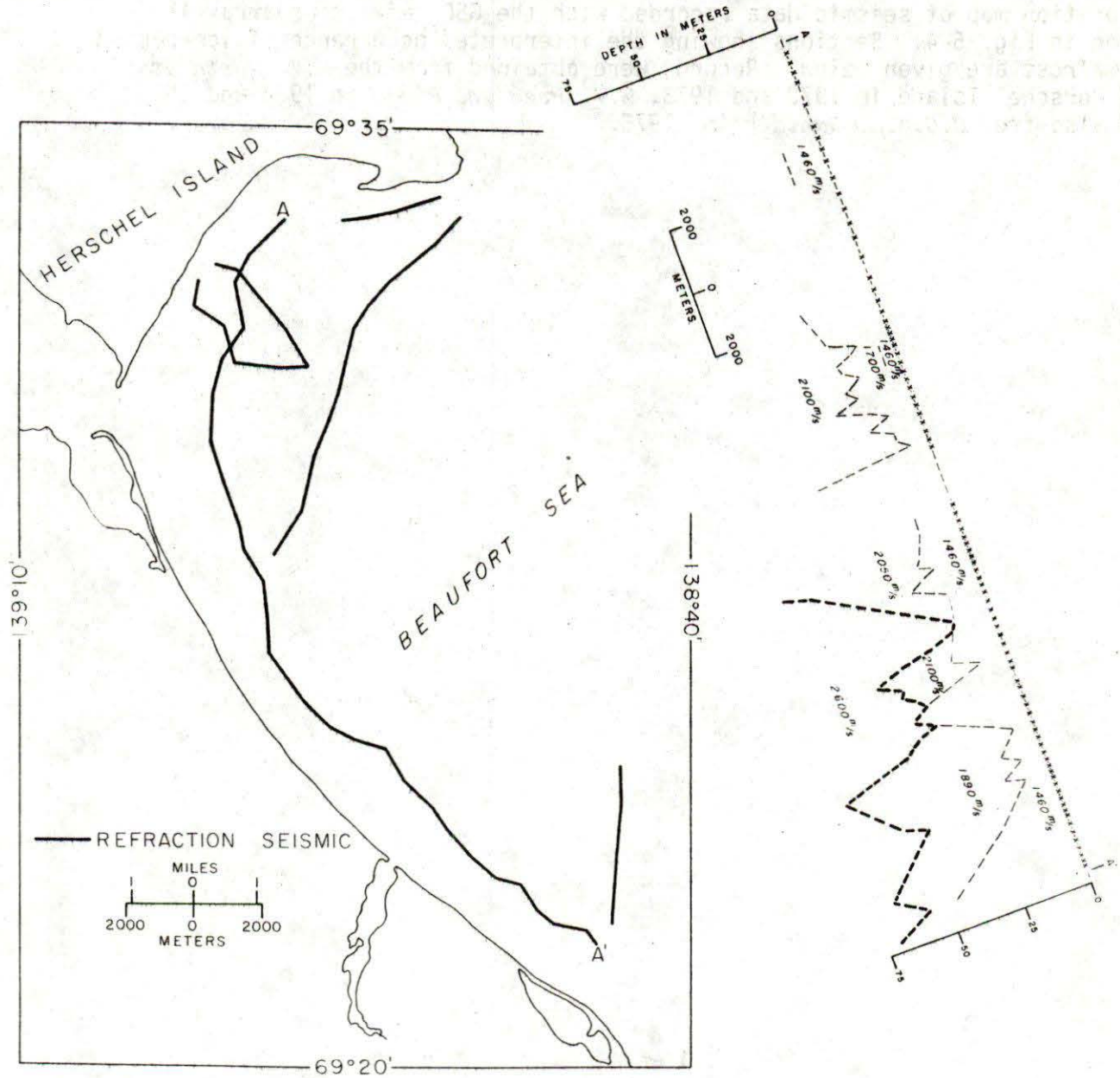
DEPTH IN METERS
0
25
50
75
A
1460 m/s
2000
METERS
0
2000
1460 m/s
1700 m/s
2100 m/s
69°35'
HERSCHEL ISLAND
A
BEAUFORT SEA
139°10'
138°40'
2050 m/s
1460 m/s
2100 m/s
2600 m/s
1890 m/s
1460 m/s
A'
REFRACTION SEISMIC
MILES
0
2000
0
2000
METERS
69°20'

Fig. E-1

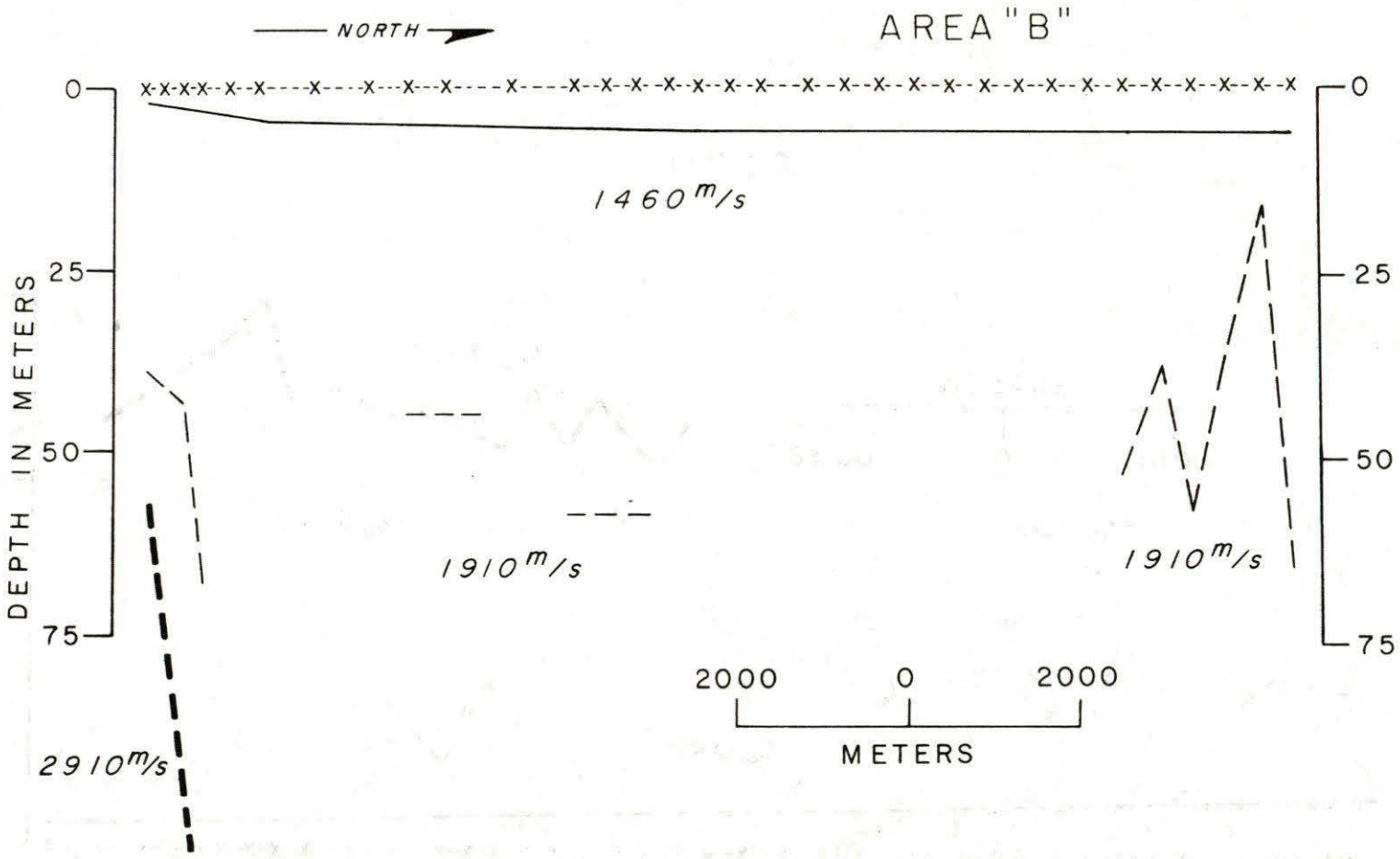
NORTH
AREA "B"
0
25
50
75
DEPTH IN METERS
1460 m/s
1910 m/s
1910 m/s
2910 m/s
2000
0
2000
METERS

Fig. E-2

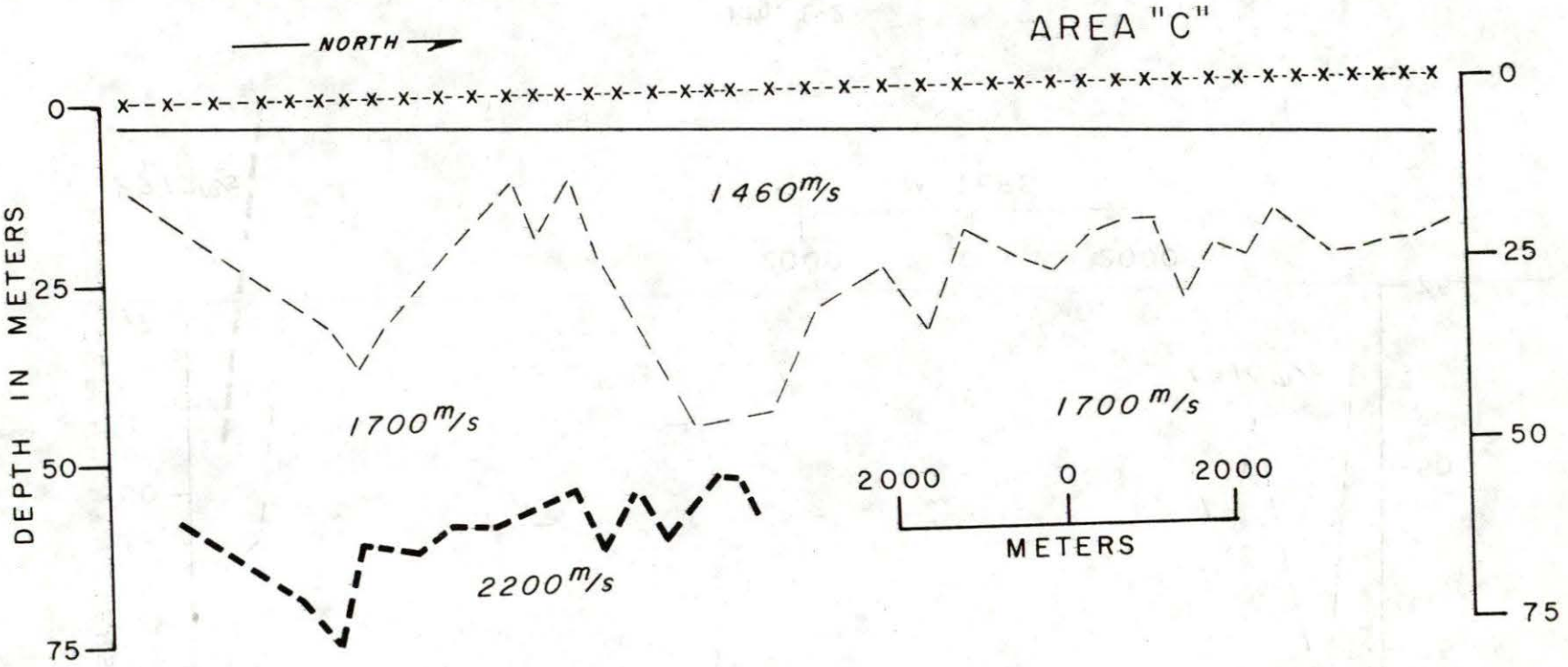
AREA "C"
NORTH
0
25
50
75
DEPTH IN METERS
1460 m/s
1700 m/s
1700 m/s
2200 m/s
2000
0
2000
METERS

Fig. E-3

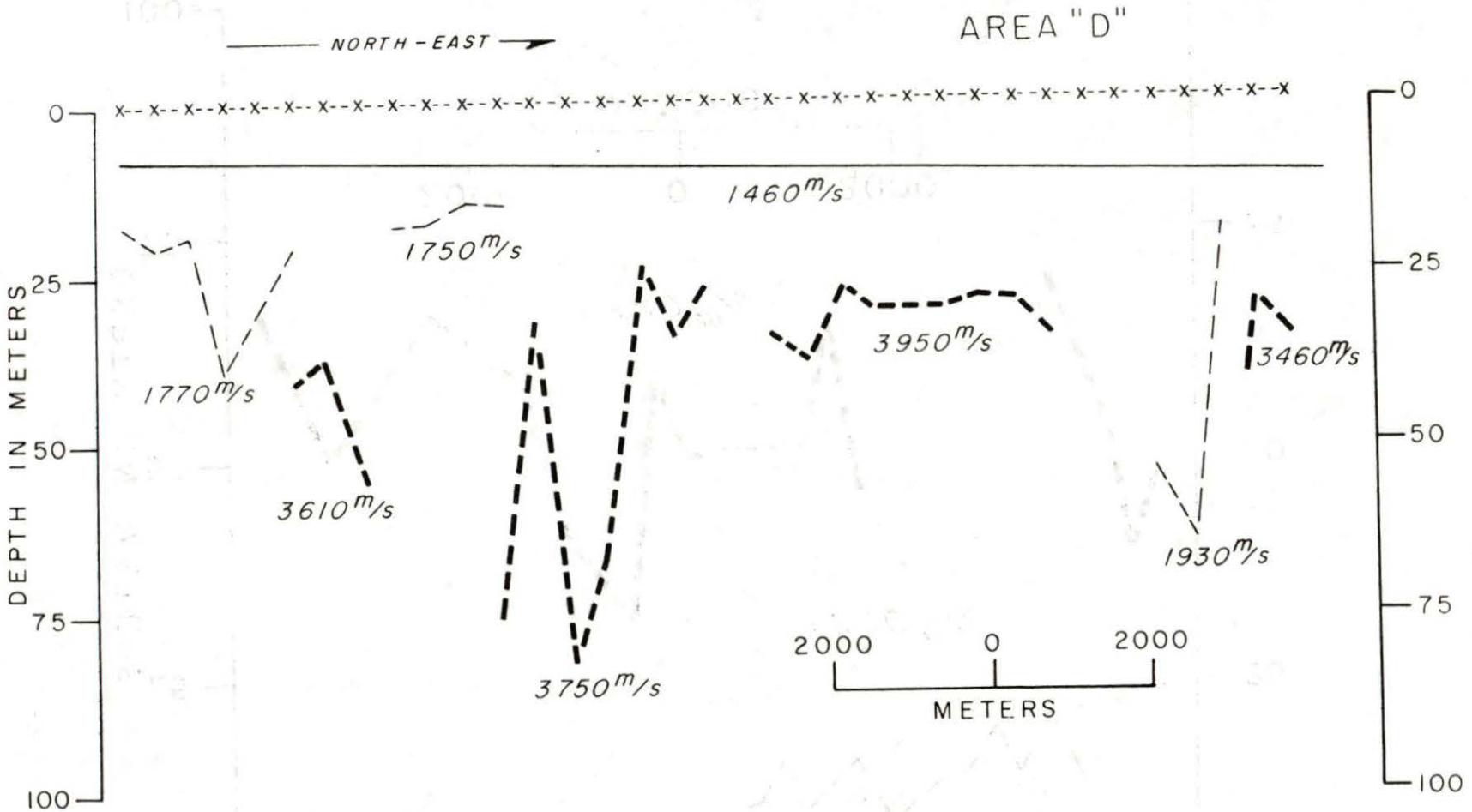
AREA "D"
NORTH - EAST
DEPTH IN METERS
0
25
50
75
100
1460 m/s
1750 m/s
1770 m/s
3610 m/s
3750 m/s
3950 m/s
1930 m/s
3460 m/s
2000
0
2000
METERS

Fig. E-4

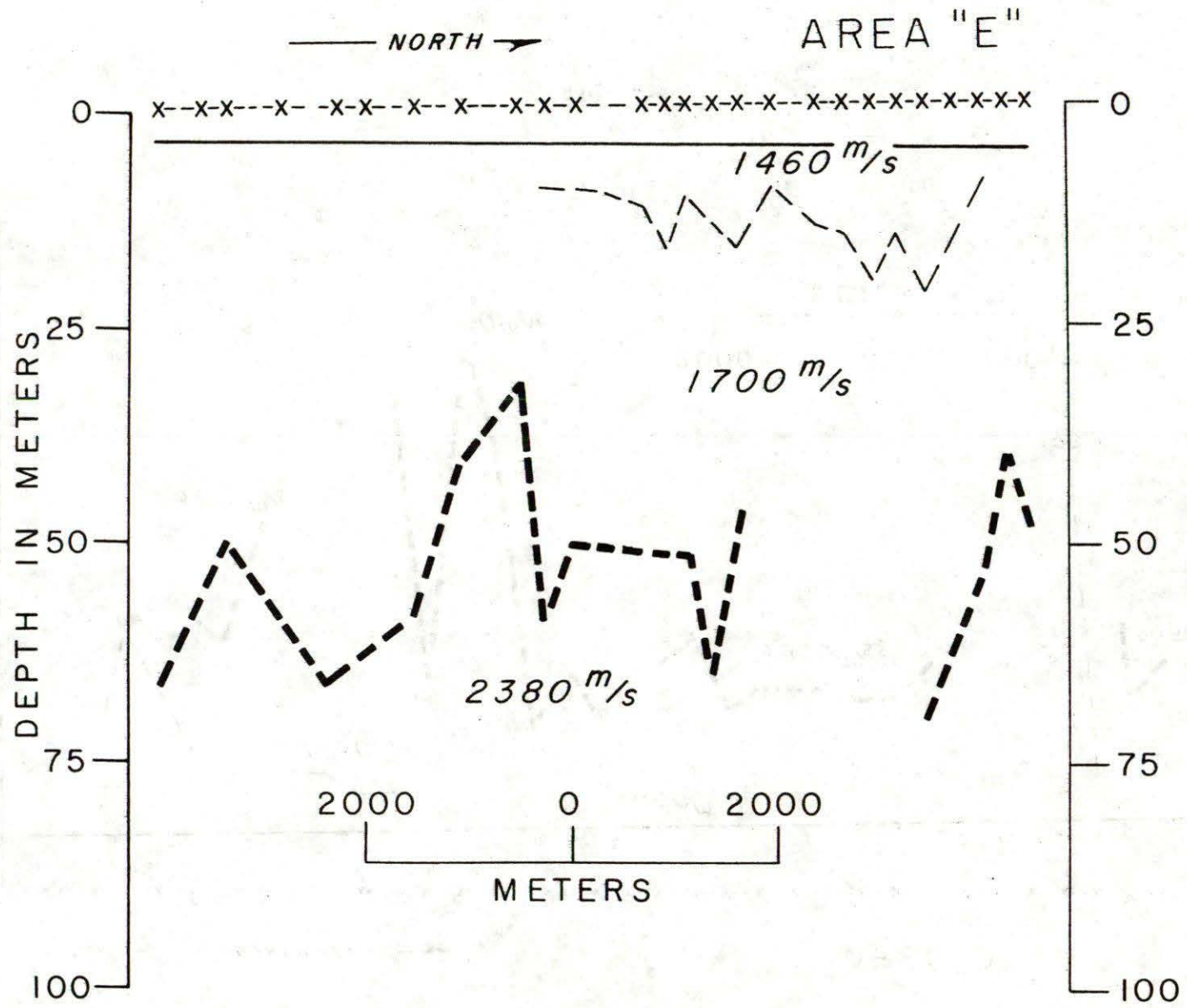
NORTH
AREA "E"
0
25
50
75
100
DEPTH IN METERS
1460 m/s
1700 m/s
2380 m/s
2000
0
2000
METERS

Fig. E-5

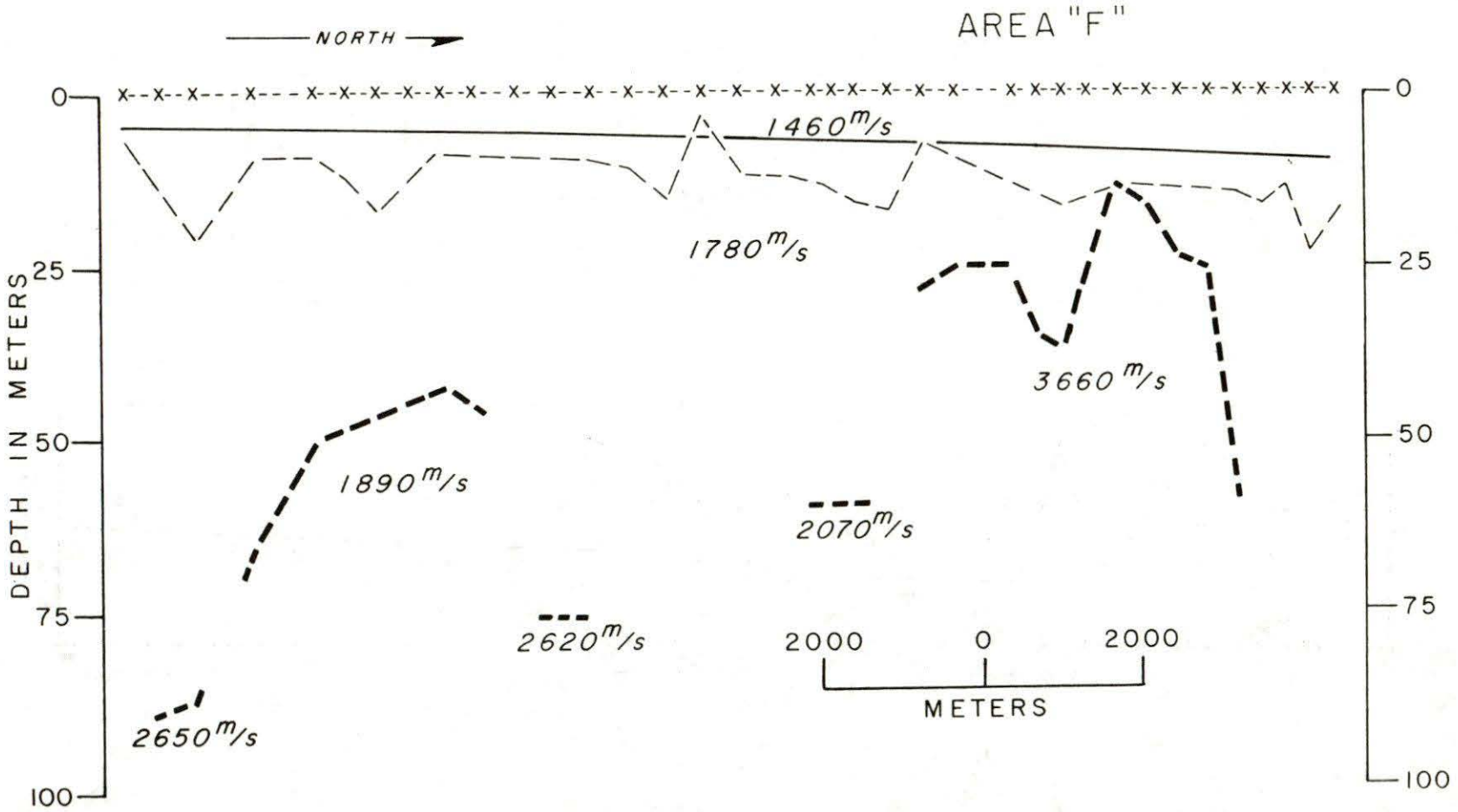
AREA "F"
NORTH
DEPTH IN METERS
0
25
50
75
100
1460 m/s
1780 m/s
3660 m/s
1890 m/s
2070 m/s
2620 m/s
2650 m/s
2000
0
2000
METERS

Fig. E-6

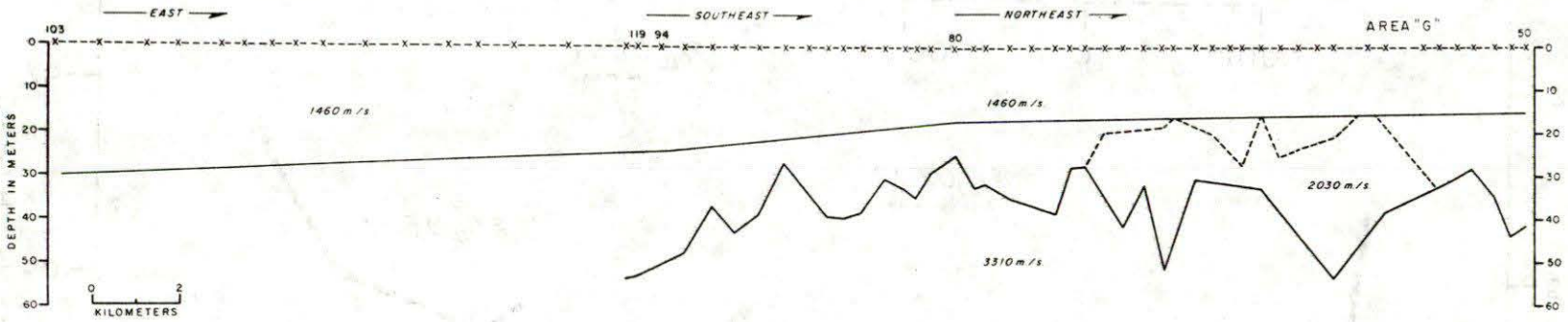
EAST
SOUTHEAST
NORTHEAST
AREA "G"
103
119 94
80
50
DEPTH IN METERS
1460 m/s
1460 m/s
2030 m/s
3310 m/s
0
2
KILOMETERS

Fig. E-7

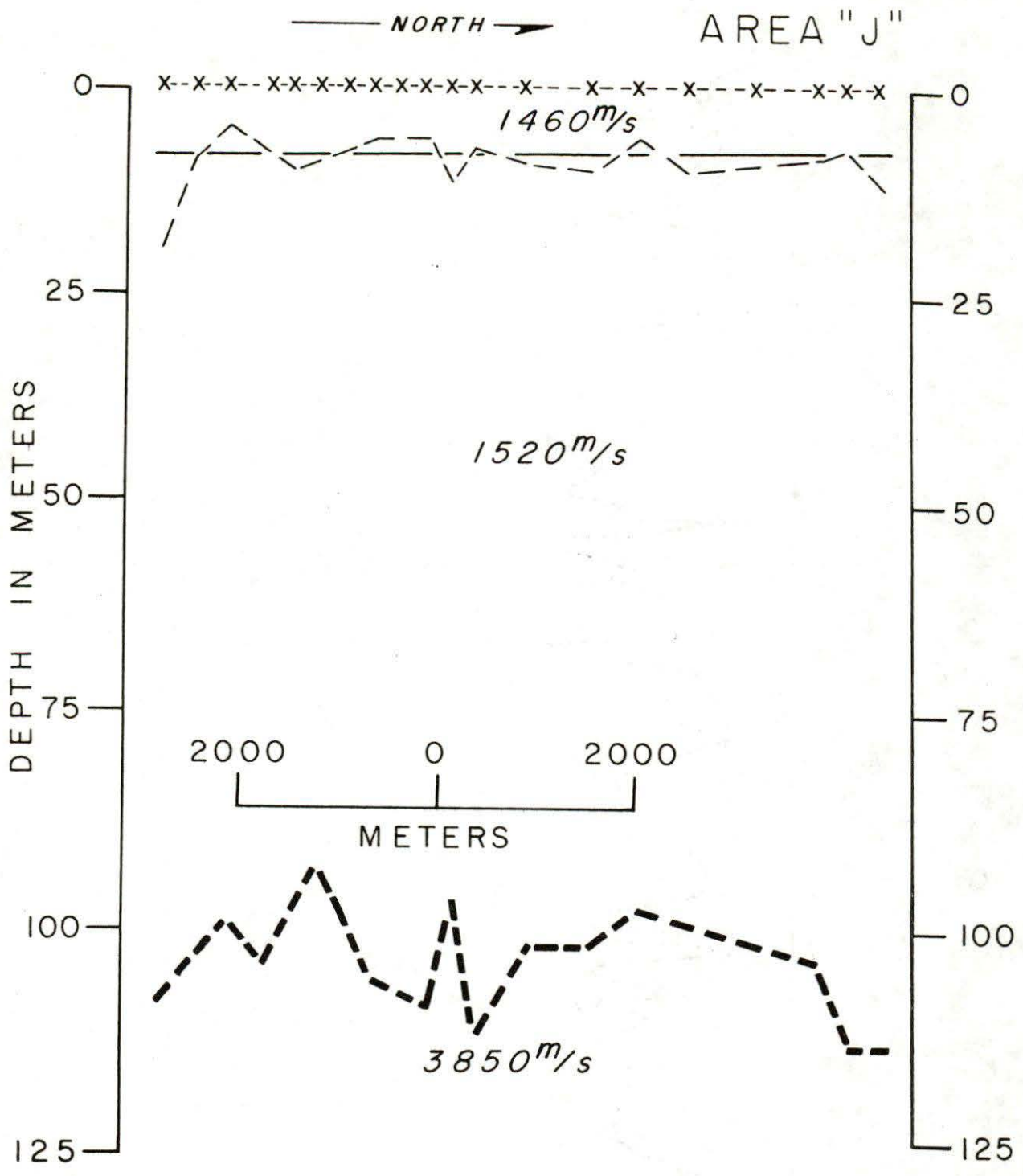
NORTH
AREA "J"
1460 m/s
1520 m/s
3850 m/s
DEPTH IN METERS
0
25
50
75
100
125
2000
0
2000
METERS

Fig. E-8

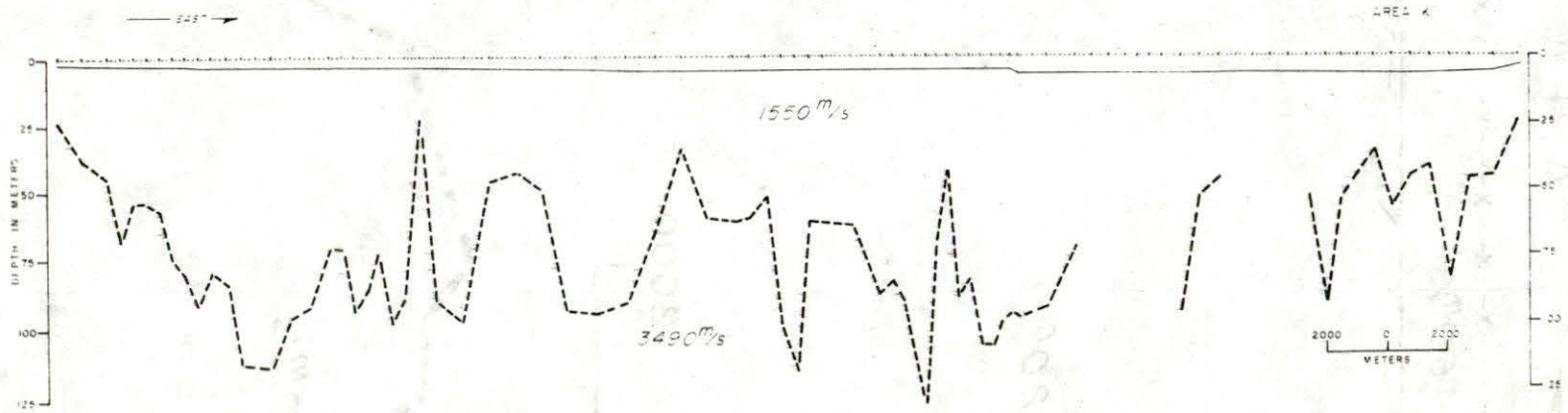
EAST
AREA K
1550 m/s
3490 m/s
DEPTH IN METERS
0
25
50
75
100
125
2000
0
2000
METERS

Fig. E-9

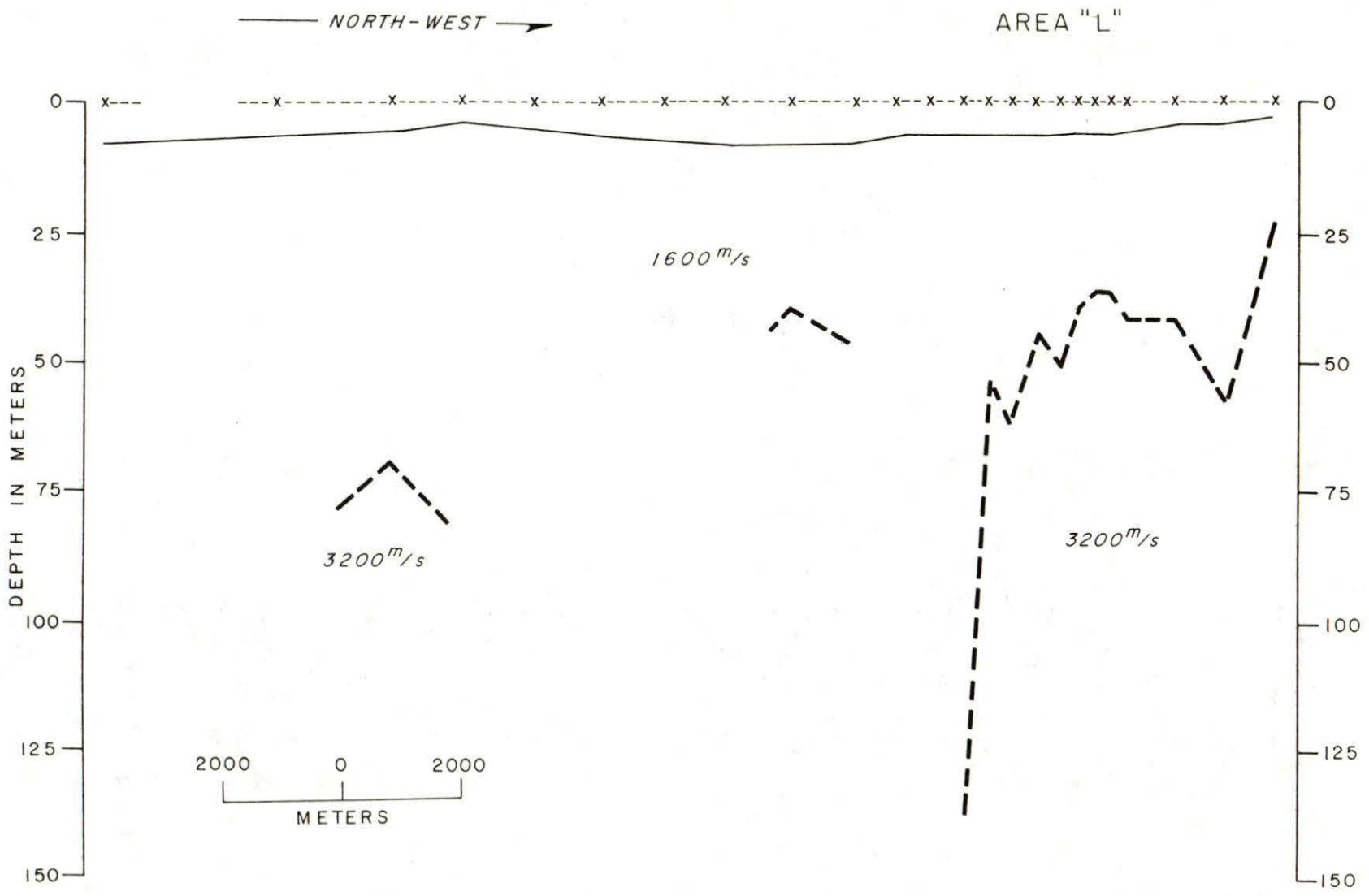
NORTH-WEST
AREA "L"
DEPTH IN METERS
0
25
50
75
100
125
150
1600 m/s
3200 m/s
3200 m/s
2000
0
2000
METERS

Fig. E-10

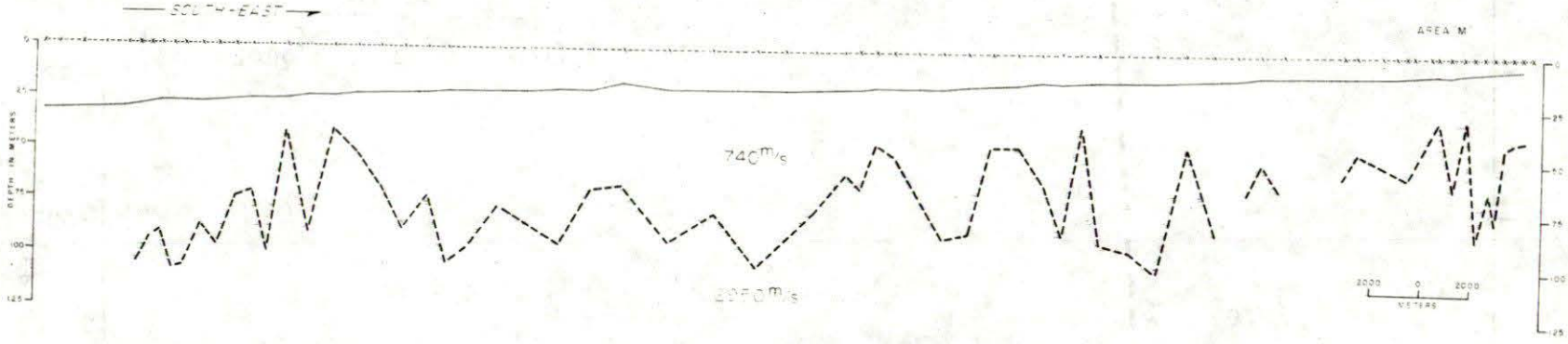

Fig. E-11

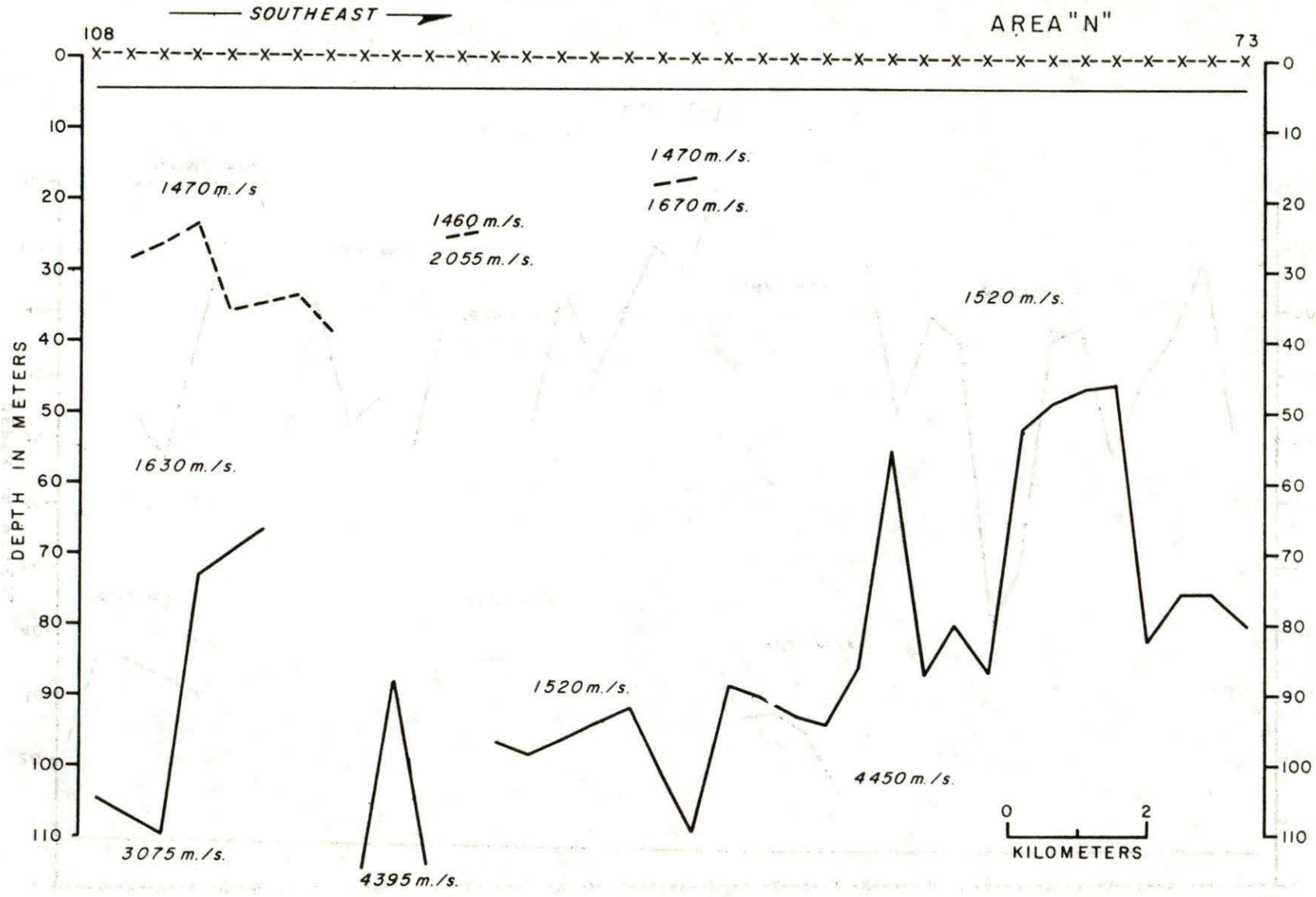
SOUTHEAST
AREA "N"
108
73
DEPTH IN METERS
1470 m./s
1630 m./s.
3075 m./s.
1460 m./s.
2055 m./s.
4395 m./s.
1470 m./s.
1670 m./s.
1520 m./s.
4450 m./s.
1520 m./s.
0
2
KILOMETERS

Fig. E-12

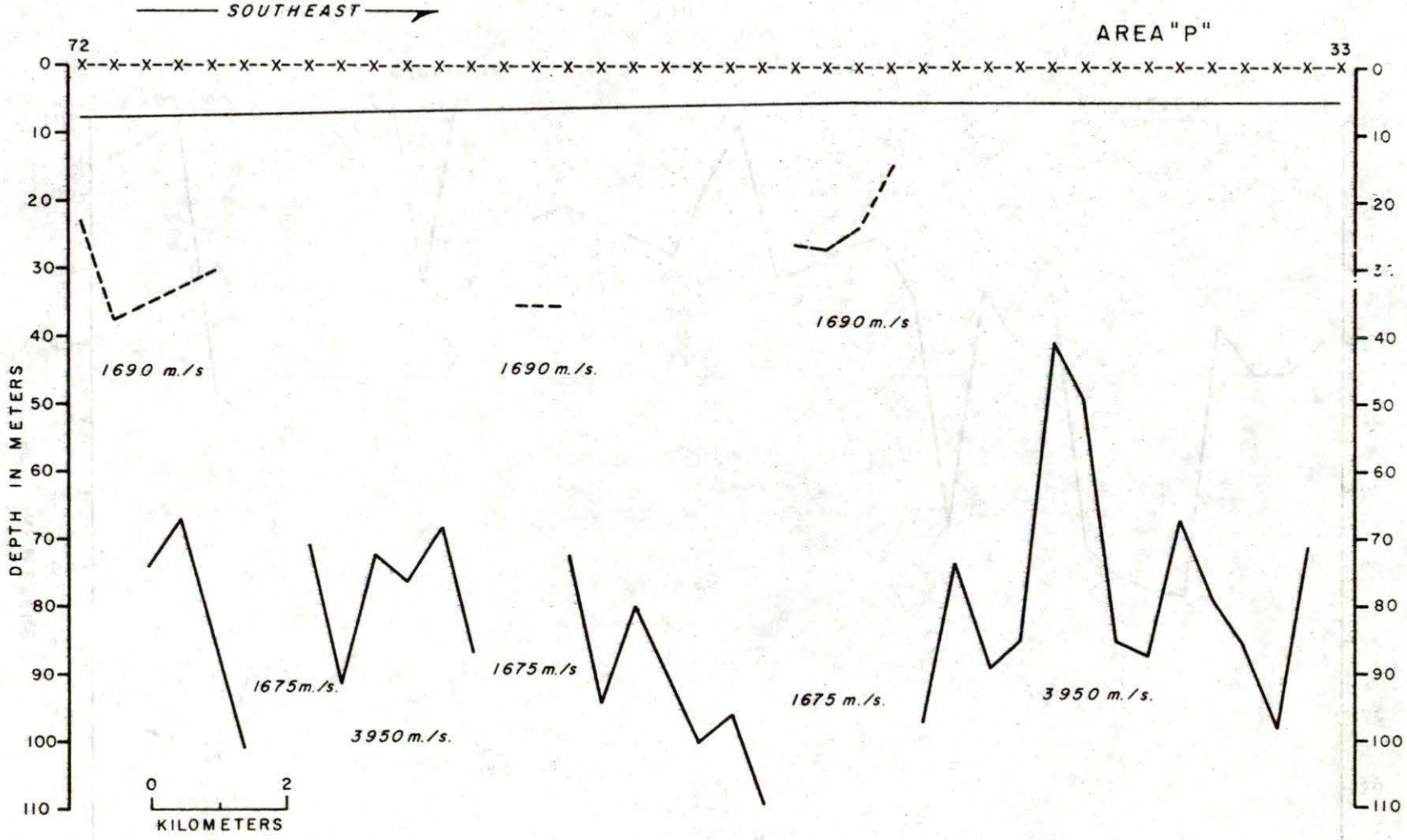
SOUTHEAST
AREA "P"
72
33
DEPTH IN METERS
1690 m./s
1690 m./s.
1690 m./s
1675m./s.
3950 m./s.
1675 m./s
1675 m./s.
3950 m./s.
0
2
KILOMETERS

Fig. E-13

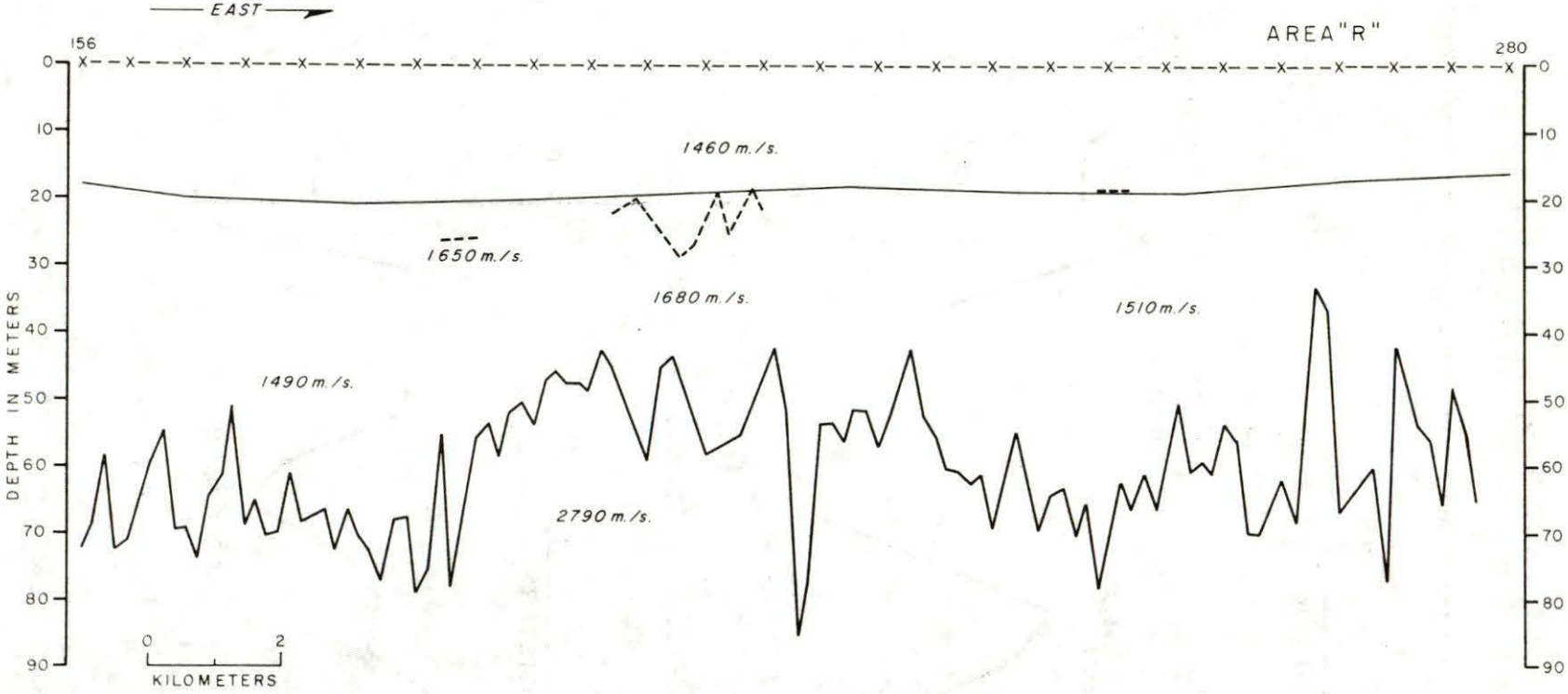
EAST
AREA "R"
156
280
0
10
20
30
40
50
60
70
80
90
DEPTH IN METERS
1460 m./s.
1650 m./s.
1680 m./s.
1510 m./s.
1490 m./s.
2790 m./s.
0
2
KILOMETERS

Fig. E-14

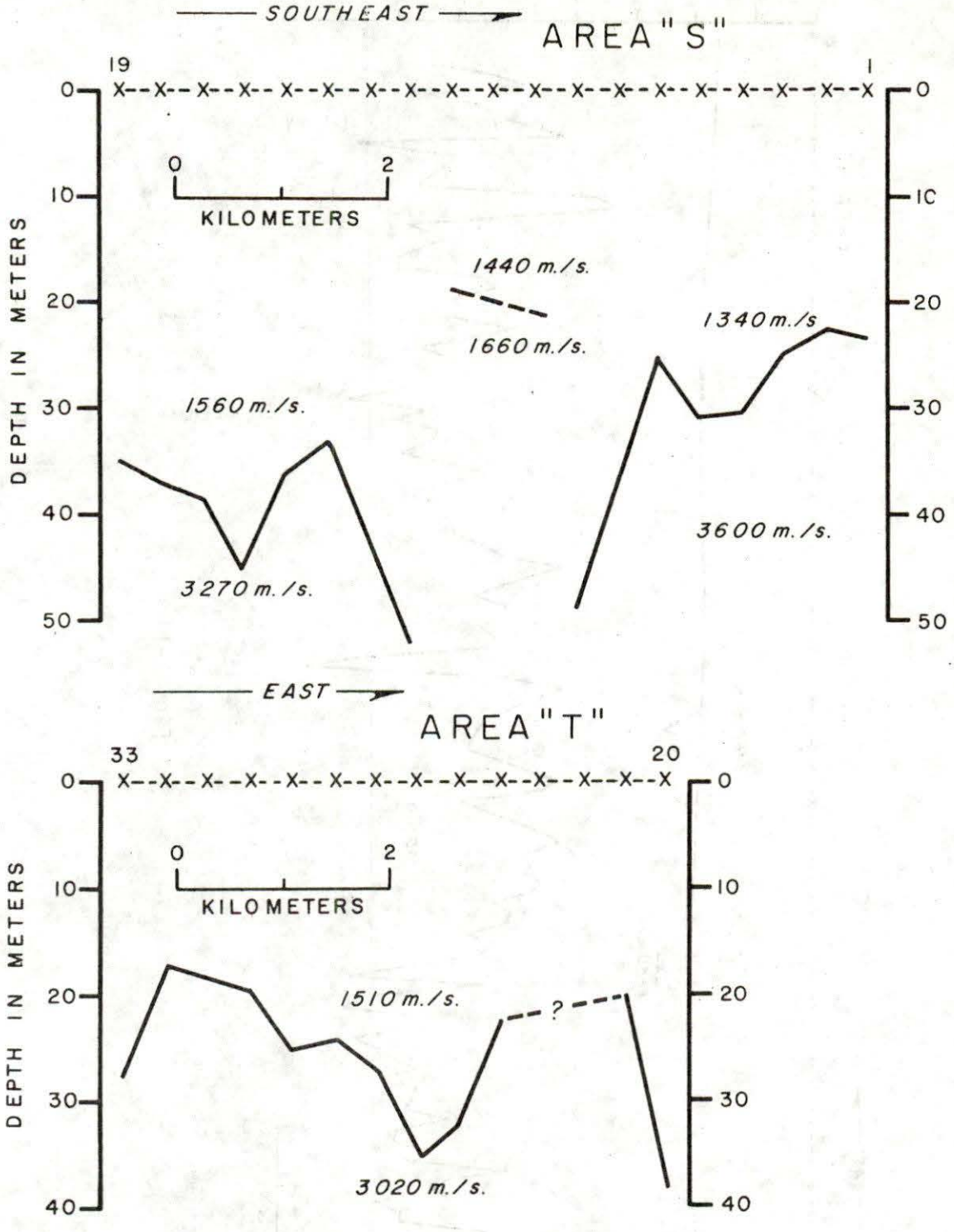
SOUTHEAST
AREA "S"
19
1
0
2
KILOMETERS
DEPTH IN METERS
1440 m./s.
1660 m./s.
1340 m./s
1560 m./s.
3270 m./s.
3600 m./s.
EAST
AREA "T"
33
20
0
2
KILOMETERS
DEPTH IN METERS
1510 m./s.
?
3020 m./s.

Fig. E-15

APPENDIX F

Initial Investigation of the Suitability of Industry Seismic Records for Permafrost Mapping - Gulf Oil Test

Introduction

This report deals with the evaluation of first arrival information from approximately 165 km of reflection records provided by Gulf Oil Co. of Canada. The location of the data is shown in Fig. F-1.

For most unconsolidated water saturated earth materials, seismic velocity contrasts exist between the frozen and the unfrozen state. In general, the velocity contrast increases with grain size of the material. A detailed discussion of velocity-temperature relationship has been given by Nakano et al. (1971).

Hofer and Varga (1972) gave a generalized velocity-depth function for the Beaufort Sea which suggested that unfrozen near-surface sediment velocities should be quite low (1,800 m/sec). Frozen sediment velocities onshore range in excess of 3,000 m/sec. In the absence of an alternative explanation, it is suggested that high seismic velocities occurring at shallow depths offshore represent the presence of permafrost.

Interpretation Technique

First arrival events were picked from the monitor records of lines G1, 2, 3 and 4. A time-distance plot was produced for each record. The velocity of the unfrozen seabottom materials generally exceeded that of water, with an average velocity of 1,660 m/sec. The onset of this velocity could not accurately be determined in many of the records. As a result, an average velocity of 1,550 m/sec was used for the combined water-unfrozen sediment layer, to calculate depths to permafrost layer.

Ice-bonded permafrost was interpreted where refractor velocities exceeded 2,500 m/sec. Apparent velocities of the permafrost refraction event averaged 3,240 m/sec for all survey lines and varied only slightly from line to line.

Results

The results of this study are shown by the cross-sections (Fig. F-2). For much of the southeast half of the three parallel lines, G1, 3 and 4, the top of permafrost is fairly uniform and is at an average depth of 125 m below seabottom. The northwest portions of these lines show an erratic permafrost boundary at sub-bottom depth varying from 50 to 150 m. From shot points 260 to 283 at the southeast end of line 3, two permafrost refractors were detected. The upper refractor with a velocity averaging 2,500 m/sec is at a depth below seabottom of about 70 m. This layer averages about 100 m in thickness and overlies a higher velocity refractor or 3,500 m/sec. Ice-bonded permafrost under this portion of line 3 then must be at least 100 m thick.

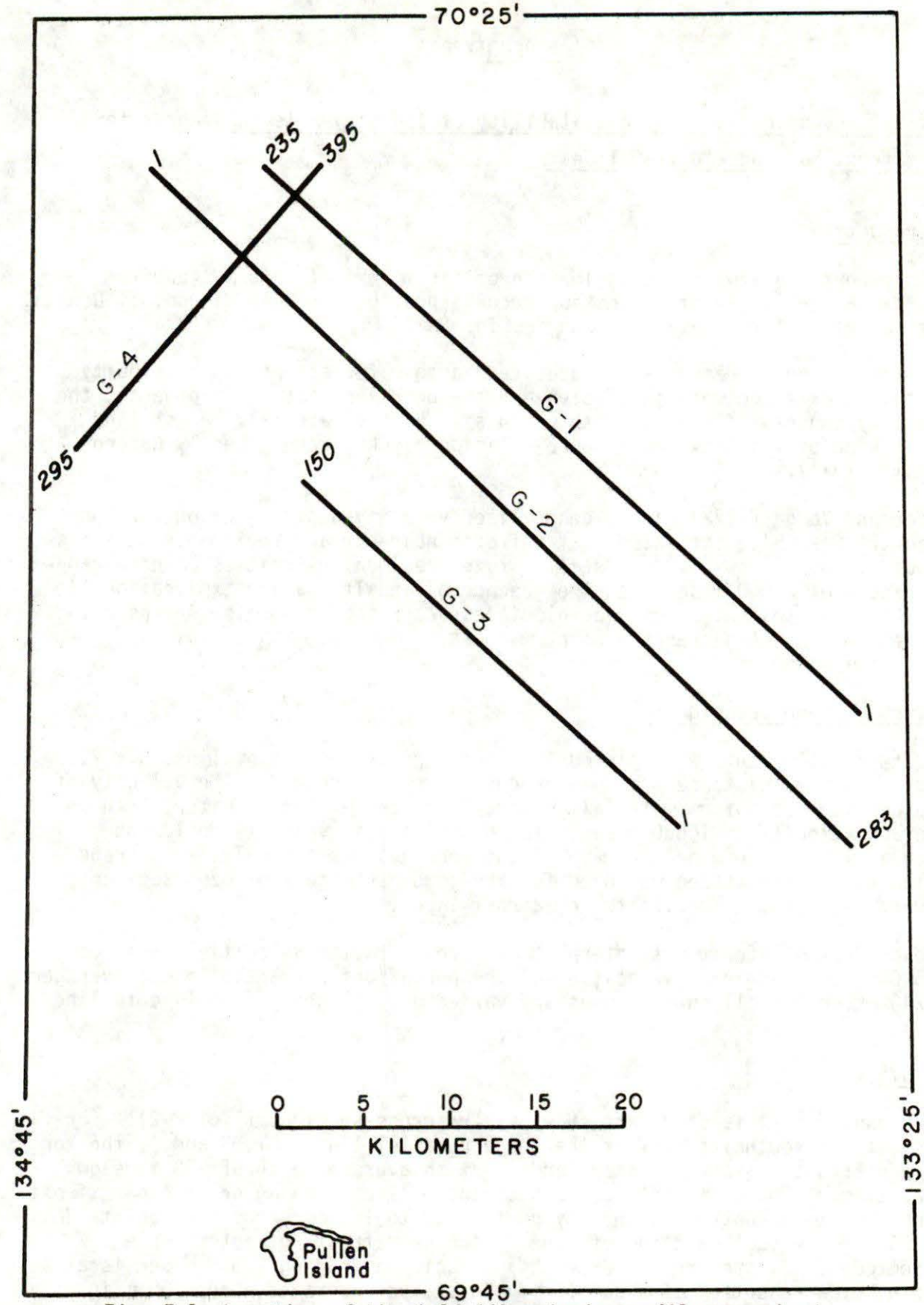

Fig. F-1 Location of the Gulf Oil seismic profiles examined for high velocity refraction events.

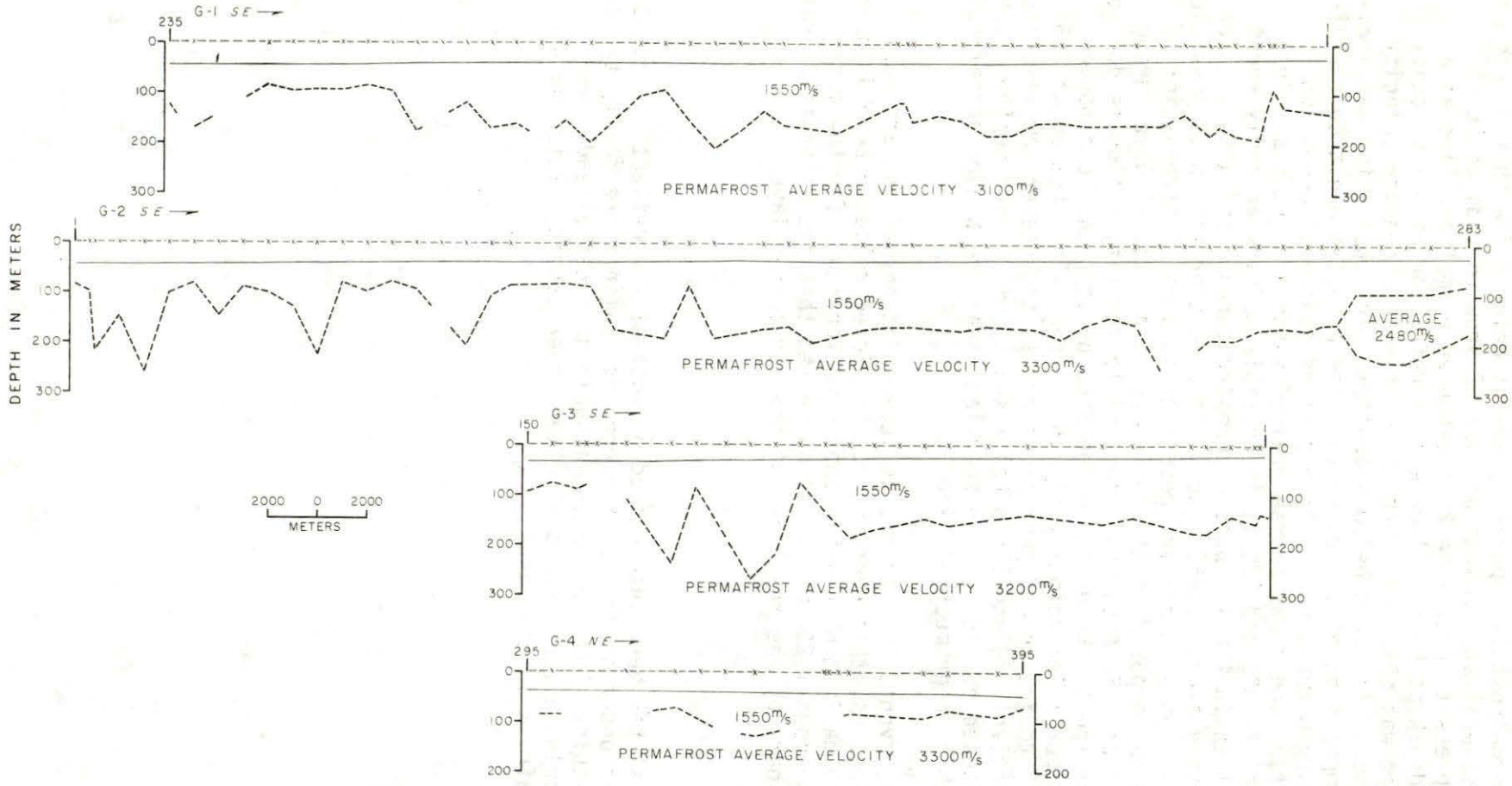

Fig. F-2 Interpreted seismic sections from monitor reflection records showing the upper boundary of ice-bonded permafrost.

Though ice-bonded permafrost is apparently absent below a few shot points on lines G1, 3 and 4, several shot points on line G2 show no indication of permafrost. Where present under line 2, ice-bonded permafrost lies at an average sub-bottom depth of 50 m. Elsewhere, a refractor with a velocity averaging 1,960 m/sec was observed. Depths to this intermediate velocity refractor varied from 70 to 120 m below seabottom. This refractor may indicate a change in composition of the unfrozen material which might be correlated with the boundary between recent fine-grained sediments deposited by Mackenzie River outflow and older coarse-grained sands and gravels. On records from shot points 300 and 325 it is possible to pick an early event which yields velocities in the ice-bonded permafrost range and also a later event giving a velocity around 1,960 m/sec. This interpretation is possible if permafrost constitutes a thin layer resulting in a rapid attenuation of this refracted wave as compared to the refracted compressional wave through the 1,960 m/sec horizon. By assuming a negligible velocity influence due to thin ice-bonded permafrost, the depth to the deep horizon can be computed using the average upper layer velocity of 1,550 m/sec. For shot point 325 the calculated depth to ice-bonded permafrost and to the deeper low velocity refractor are respectively 30 and 115 m below seabottom. Based on the attenuation rate of refracted events one can speculate that ice-bonded permafrost, where present, is thin under much of line G2.

In all survey lines, events interpreted as ice-bonded permafrost attenuate rapidly. On many records, this event cannot be picked reliably beyond three or four traces. The maximum observable shot detector range for the most prominent breaks is about 1,200 m. It is suggested that the attenuation rate may be governed in part by the thickness of the ice-bonded layer.

Summary

Ice-bonded permafrost has been interpreted on most of the reflection records for the survey lines under study. If the records examined are fairly typical for the southern Beaufort Sea area, much valuable data has already been accumulated that would go far towards a better understanding of the nature and occurrence of permafrost in this area.

APPENDIX G

Physical Properties of Samples Obtained from GSC Drilling, Kugmallit Bay

TABLE G-1

Thermal Conductivity and Moisture Content of Recovered Samples

Grouping of Samples	No. in Group	Moisture Content %	Density gm cm^{-3}	Thermal Conductivity $Wm^{-1}K^{-1}$
Sands & Gravels-thawed	27	31 ± 6	2.2	2.61 ± 0.29
-frozen	3	45-71		2.32-2.86
Silts & Clays	7	50 ± 2	1.9	1.47 ± 0.10
Drillhole #1	14	33 ± 7	2.1	2.69 ± 0.30
#2	6	40 ± 6	2.1	2.07 ± 0.43
#3	7	36 ± 10	2.1	2.30 ± 0.56
#4	7	39 ± 10	2.0	2.08 ± 0.61

TABLE G-2

Interstitial Water Salinities of Core Samples

Grouping of Samples	No. in Group	Range of Salinities °/oo	Mean Salinities %
Sands & Gravels	18	2-30	8
Silts & Clays	6	6-39	15
Drillhole #1	7	2-10	5
#2	4	4-15	7
#3	6	4-30	15
#4	7	5-39	11

TABLE G-3

GSC KUGMALLIT BAY DRILLING - SAND-SILT-CLAY ANALYSES

HOLE	SAMPLE	DEPTH	%>2mm	% SAND 2000-63μ	% SILT 63 -3.9μ	% Clay < 3.9μ
1	A	18	77.4	66.23	19.77	14.00
	B	22	69.0	81.31	9.42	9.27
	C	34-39	0.0	92.72	2.35	4.93
	D	40.5-41	66.3	92.22	2.53	5.25
	E	50	75.9	86.71	4.81	8.48
	F	70	0.0	69.83	19.98	10.19
	G	119	5.0	66.23	19.16	14.61
	H	120	20.6	65.81	19.12	15.07
	I	149	0.0	56.30	23.91	19.79
	J	185	9.6	90.58	4.40	5.02
	K	186	53.1	77.69	12.18	10.13
	L-1	220	1.6	88.67	6.54	4.79
	L-2	220	0.0	93.31	3.74	2.95
	M	260	0.0	5.36	71.14	23.50
	N	279	18.1	77.36	13.81	8.83
2	A	13	0.0	1.48	74.57	23.96
	B	31	0.0	1.34	68.32	30.34
	C	38	6.5	87.78	7.59	4.63
	D	67	0.0	93.69	3.29	3.02
	E	67.5	0.0	86.61	6.95	6.44
	F	100	0.0	93.99	3.68	2.33
	G	159	0.0	86.03	8.51	5.46
	I	268	0.0	71.42	10.38	18.20
3	A	18	0.0	1.27	59.44	39.29
	B	38	0.0	8.61	60.26	31.13
	C	68	0.0	77.19	14.91	7.90
	D	99	28.5	87.63	5.60	6.77
	E	128	0.0	89.05	5.75	5.20
	F	129	0.0	71.17	14.86	13.97
	G	158	0.0	72.08	16.93	10.99
	H	159	0.0	85.79	9.66	4.55
	I	179	1.2	82.98	7.38	9.64

	J	210	19.0	84.18	9.67	6.15
	K	220	0.0	95.56	1.54	2.90
	L	220	0.0	95.64	1.87	2.49
	M	223	0.0	95.56	1.66	2.78
	N	223.7	0.0	62.25	22.79	14.98
4	A	21	0.0	1.49	57.63	40.88
	B	49	0.0	0.50	62.64	36.86
	C	79	0.0	0.32	47.18	52.50
	D	103	0.0	89.08	5.13	5.79
	E	109	0.0	18.92	28.08	53.00
	F	109.5	0.0	72.92	15.01	12.07
	G	137	20.6	83.14	11.01	5.85
	H	169	0.0	91.31	4.64	4.05

TABLE G-4

GSC Drilling Kugmallit Bay - Grain Densities

HOLE	SAMPLE	DENSITY (gm/cc)
1	C	2.66
1	D	2.65
1	J	2.66
2	A	2.69
2	D	2.64
2	F	2.65
3	E	2.67
3	M	2.69
4	A	2.71
4	C	2.71
4	G	2.67

APPENDIX H

Seabottom Temperatures and Salinities in the Southern Beaufort Sea

The Data Set

The data used consisted basically of that derived from a search of the Marine Environmental Data Service (D.O.E.) files for the area 69° to 72°N, 130° to 150°W and 69° to 73°N, 125° to 130°W. This data set was augmented by unpublished data collected by the Freshwater Institute (D.O.E.) in the period 1971-1973, the Geological Survey of Canada in summer 1973 and the Earth Physics Branch and the Geological Survey from the *C.C.G.S. Nahidik* in summer 1975, and from the ice in the spring of 1973. All data other than the M.E.D.S. data were taken by measurement at the sediment to water interface. In the initial data set (M.E.D.S.) the measured temperature and salinity has been used if within 2 m of bottom in water depths to 10 m, within 5 m of the bottom in depths of water to 30 m, within 10 to 100 m, within 20 to 200 m, etc.

Table H-1 lists all of the observations used for the survey; given are the station coordinates, date of the observation, total water depth in m, depth of physical observations in m, the measured temperature in °C and the salinity in parts per thousand (°/$_{oo}$).

Discussion of Data

The data has, for discussion purposes, been divided into a series of water depth zones <10 m, 10-20 m, 20-40 m, 40-60 m, 60-80 m, 80-100 m, 100-200 m and >200 m. The range and spatial distribution of temperatures and salinities through the year are discussed for each zone.

The bulk of data is for the summer season: mid-July to mid-September. Other periods of the year for which data was available were late March - early April, early to mid-May, and late November - early December. Only one station was surveyed in January. No data was available for other times of the year. The yearly distribution at a given depth is limited even further.

Means, ranges and standard deviations have been tabulated for both summer and winter data in each depth range, and are summarized in Table H-2.

Depth <10 m

This zone shows the largest variations in both temperatures and salinities both in summer and winter. Such wide variability is due to proximity to shoreline, inflow of fresh-water from nearby rivers and surface interface phenomena. The very wide range of summer temperatures -1.5°C to +14°C has an arithmetic mean of 3°C and a standard deviation of 4°C. Many of the higher summer temperatures are found in the Eskimo Lakes. A good proportion of the lower temperatures are found in the northern portions of Kugmallit Bay. Winter temperatures (represented by nine stations, compared with 53 in summer)

range from -0.1 to 0.5°C with a mean of -0.4°C. Most of the measurements are from Tuktoyaktuk Harbour and are accompanied by moderate salinities.

Salinity in the summer (52 measurements) has a range of .7°/$_{oo}$ to 31.6°/$_{oo}$. As for summer temperatures, a histogram of observations is broadly skewed with the tail towards lower salinities. There is no obvious spatial variation of salinity, except that, in general, locations closer to shore have lower salinities. Exceptions to this rule are found near islands and promontories. The salinity in the Eskimo Lakes declines steadily inland. Winter salinity is more uniform than summer, with a range of 10.9 - 29.0°/$_{oo}$, and a mean of 26.6°/$_{oo}$. Low (14.4 - 16.3°/$_{oo}$) salinity is found in the Eskimo Lakes. One anomalously low salinity measurement occurs at Tuktoyaktuk (10.9°/$_{oo}$). The rest are from 21.8 - 29.0°/$_{oo}$. Salinities in May at Tuktoyaktuk divide into two salinity groups, one between 0 and 2°/$_{oo}$ and the other between 22 and 30°/$_{oo}$.

10 - 20 m

The range of temperatures and salinities of this zone is similar to the zone above, but the distribution is less scattered, and tends more positively to a bimodal form. This trend is more pronounced in the next two depth zones, until one of the modes disappears below 80 m.

Summer temperatures range from a low of -1.57°C to a high of 11.30°C. The mean is 1.28°C. The distribution is skewed strongly, because of temperatures of 6°C and greater in the Eskimo Lakes. Ignoring the four high Eskimo Lake values, the mean is 0.32°C. Ignoring these values causes a substantial improvement in the standard deviation from 3.15°C to 1.64°C. Lower temperatures (below 0°C) are generally found further offshore, and around small promontories and islands. Higher temperatures are found in bays and along the northwest coast of Tuktoyaktuk Peninsula. Winter temperatures are all below 0°C, varying from -0.58°C to -0.16°C. Spring temperatures (March, April, May, June) likewise are all below 0°C.

Summer salinity also shows a bimodal distribution. One group, largely representing the Eskimo Lakes, has a mean of 19.7°/$_{oo}$ whereas the other has a mean of 29.8°/$_{oo}$. The standard deviations are 8.4 and 2.8°/$_{oo}$ respectively. Winter salinity is actually lower than summer salinity, with a range of 21.8 - 28.0°/$_{oo}$ and a mean of 24.5°/$_{oo}$ because most of the data are for the Eskimo Lake area. Therefore, the winter data are more directly comparable to the lower mode. May salinities at Tuktoyaktuk are all high (near 30°/$_{oo}$).

20 - 40 m

The range of summer temperatures is -1.62°C to 11.01°C. The values divide into two groups, one from -1.58°C to about 4°C, and the other from 4°C up. The latter group represent temperatures in the Eskimo Lakes, all but one at W131 34.8, N69 18.0. Since this station is in a deep narrow channel at the outlet of the lakes, this temperature is probably not representative of other locations. The mean of the lower temperature group is -0.63°C with most data within 1.0°C of this. Temperatures above 0°C in this group are found at Tuktoyaktuk or near Cape Bathurst. Winter temperatures range from 1.54°C to

-0.36°C. Only seven data points are available. Temperatures in early spring are all negative.

Summer salinity in this zone ranges from 11.6 - 32.8°/$_{oo}$. The data divide into 11 Eskimo Lakes measurements, with a mean of 15.5°/$_{oo}$ and 20 others, with a mean of 32.0°/$_{oo}$. The standard deviation of the latter is only 0.5°/$_{oo}$. Winter salinity varies from 14.4 to 33.7°/$_{oo}$.

40 - 60 m

Summer temperature data (45 points) divide into two groups, one below 0°C with a low of -1.77°C, a mean of -1.44°C and a standard deviation of 0.20°C. The other group represents an area in the Eskimo Lakes W131 4.0, N69 36.5 with eight measurements of mean temperature 6.88°C, and standard deviation 2.42°C. This location is in the main channel out of the lakes, and would likely come under the influence of run-off water. Winter temperatures for five points range from -1.58°C to -1.17°C, with standard deviation of 0.15°C.

Salinity in the winter (five points) is quite uniform, with a range of only 32.1 to 32.5°/$_{oo}$. Ignoring the summer Eskimo Lakes data, the summer mean is 32.3°/$_{oo}$ identical to the winter mean, and the standard deviation only 0.4°/$_{oo}$. The mean for the summer Eskimo Lakes data (all from the location mentioned in the previous paragraph) is 13.5°/$_{oo}$ with standard deviation of .6°/$_{oo}$.

60 - 80 m

Only summer data is available in this depth range. Of the 20 data points, 14 are outside of the Eskimo Lakes. Of these temperatures, all are negative in the range of -1.08 to -1.82°C with a mean of -1.52°C. Summer salinity outside of the Eskimo Lakes is relatively constant, in the range of 32.2 to 33.5°/$_{oo}$.

80 - 100 m

For only three data points, summer temperatures lie between -0.5 and -1.46°C and summer salinities between 32.2 and 32.6°/$_{oo}$.

100 - 200 m

Below water depths of 100 m there is no appreciable variation of temperature between summer and winter. The winter mean temperature for six sites is -1.13 ± 0.31°C. Winter temperatures vary from -0.16°C to -1.45°C, while summer values vary from -0.54°C to -1.63°C. Similarly, mean winter salinities at six sites are 33.1 ± 0.57°/$_{oo}$ compared with 19 summer salinities of 33.3 ± 0.57°/$_{oo}$.

200 m and Greater

Below 200 m there is no appreciable yearly variation in temperature or salinity. The salinity is more constant than the 100 - 200 m but is also higher, averaging 34.7 ± 0.16°/$_{oo}$ for 20 winter observations and 34.7 ± 0.40°/$_{oo}$ for 50 summer observations (ranging from 33.1 to 35.1°/$_{oo}$). Summer temperatures (20 points) average 0.15 ± 0.22°C and winter observations (50 points) 0.06 ± 0.45°C. Temperatures vary dramatically with depth; in summer all bottom water temperatures are negative above 230 m and positive below, and in winter are negative above 248 m and largely positive below. The exception to the latter is that negative temperatures occur again in water depths in excess of 870 m. A depth of between 230 and 248 m marks a transition from negative to positive bottom temperatures and thus is very important in discussion of offshore permafrost.

TABLE H-1

BEAUFORT SEA BOTTOM TEMPERATURES AND SALINITIES

	LATITUDE	LONGTITUDE	DATE	DEPTH (METERS)	READING DEPTH	TEMPERATURE	SALINITY
1	N69 22.9	W125 40.5	30 7 1963	13.00	12.00	4.10	30.24
2	N69 22.9	W125 40.5	31 7 1963	13.00	18.00	4.98	30.38
3	N69 39.3	W125 22.3	1 8 1963	15.00	14.00	4.90	29.82
4	N69 52.0	W125 54.0	20 8 1963	78.00	75.00	-1.08	32.63
5	N69 55.8	W129 8.0	13 8 1962	18.00	16.00	.19	31.68
6	N69 59.4	W129 13.2	20 7 1971	13.00	11.00	3.10	26.69
7	N69 49.3	W130 19.0	16 7 1962	16.00	15.00	-1.04	
8	N69 48.0	W130 13.0	25 7 1962	8.00	8.00	5.57	18.57
9	N69 20.5	W130 53.0	31 7 1962	12.00	11.00	11.30	11.80
10	N69 47.0	W130 24.0	5 8 1962	12.00	11.00	-.57	31.27
11	N69 48.0	W130 19.0	12 8 1962	10.00	9.00	2.21	28.10
12	N69 27.0	W130 55.0	23 8 1972	45.00	40.00	9.58	13.65
13	N69 25.0	W130 47.0	23 8 1972	15.00	13.00	10.16	15.60
14	N69 32.0	W130 40.0	24 8 1972	5.00	5.00	9.79	16.19
15	N69 34.8	W131 18.0	19 8 1971	22.00	18.00	9.07	14.07
16	N69 34.8	W131 18.0	28 8 1971	24.00	20.00	8.36	14.33
17	N69 34.8	W131 18.0	15 12 1971	22.00	20.00	-.97	14.44
18	N69 34.8	W131 18.0	17 3 1972	20.00	20.00	-.90	16.37
19	N69 34.8	W131 18.0	18 5 1972	23.00	20.00	-.88	16.95
20	N69 34.8	W131 18.0	9 7 1972	19.00	18.00	1.16	14.39
21	N69 34.8	W131 18.0	22 7 1972	22.00	20.00	4.43	13.57
24	N69 34.8	W131 18.0	29 7 1972	19.00	18.00	5.33	13.64
25	N69 36.5	W131 4.0	4 8 1972	51.00	50.00	5.83	13.21
26	N69 34.8	W131 18.0	4 8 1972	20.00	18.00	6.25	13.66
27	N69 36.5	W131 4.0	10 8 1972	60.00	50.00	8.35	13.01
28	N69 34.8	W131 18.0	11 8 1972	21.00	20.00	7.66	13.41
29	N69 36.5	W131 4.0	17 8 1972	60.00	50.00	8.62	13.16
30	N69 34.8	W131 18.0	18 8 1972	20.00	20.00	8.20	99.99
31	N69 22.0	W131 5.0	21 8 1972	30.00	28.00	-.32	17.27
32	N69 33.0	W131 12.0	21 8 1972	27.00	25.00	.04	16.60
33	N69 34.8	W131 18.0	25 8 1972	22.00	20.00	9.01	13.42
34	N69 33.0	W131 27.0	25 8 1972	33.00	30.00	6.46	13.89
35	N69 30.0	W131 39.0	25 8 1972	43.00	40.00	2.34	14.84
36	N69 26.0	W131 53.0	25 8 1972	8.00	6.00	10.32	12.72
37	N69 36.5	W131 4.0	28 8 1972	58.00	50.00	8.89	13.72
38	N69 34.8	W131 18.0	29 8 1972	22.00	20.00	8.46	13.57
39	N69 32.0	W131 11.0	29 8 1972	41.00	39.00	-.33	16.84
40	N69 34.8	W131 18.0	4 9 1972	16.00	15.00	7.43	13.91
41	N69 34.8	W131 18.0	25 11 1972	18.00	17.00	-.83	14.74
42	N69 25.0	W132 8.0	8 8 1962	30.00	27.00	2.10	13.01
43	N69 14.0	W132 27.0	10 8 1962	7.00	6.00	13.97	6.97
44	N69 24.4	W132 58.9	18 7 1971	24.00	22.00	2.47	26.91
45	N69 49.3	W132 41.5	19 7 1971	10.00	8.00	2.05	26.61
46	N69 58.4	W132 57.0	19 7 1971	19.00	17.00	-1.10	30.70
47	N69 20.0	W132 5.0	26 8 1972	23.00	20.00	11.01	11.62
48	N69 17.0	W132 14.0	26 8 1972	9.00	8.00	11.48	10.70
49	N69 14.0	W132 21.0	26 8 1972	5.00	5.00	11.52	9.93
50	N69 9.0	W132 29.0	26 8 1972	9.00	8.00	12.06	7.03
51	N69 25.0	W132 58.2	27 4 1962	18.00	17.00	-.42	
52	N69 24.9	W132 58.4	27 4 1962	22.00	21.00	-.42	
53	N69 25.4	W132 58.4	28 4 1962	6.00	6.00	.06	
54	N69 25.5	W132 58.6	28 4 1962	13.00	13.00	-.26	
55	N69 25.0	W132 58.2	28 4 1962	18.00	18.00	-.43	

	LATITUDE	LONGTITUDE	DATE	DEPTH (METERS)	READING DEPTH	TEMPERATURE	SALINITY
56	N69 25.0	W132 58.2	28 4 1962	18.00	150.00	-.49	
57	N69 25.0	W132 58.1	28 4 1962	15.00	13.00	-.44	
58	N69 25.0	W132 58.2	28 4 1962	18.00	17.00	-.49	
59	N69 25.0	W132 58.1	28 4 1962	15.00	13.00	-.44	
60	N69 24.3	W132 59.5	28 4 1962	15.00	15.00	-.43	
61	N69 23.8	W132 59.4	28 4 1962	10.00	9.00	99.99	30.39
62	N69 24.9	W132 58.2	28 4 1962	18.00	15.00	-.49	
63	N69 24.7	W132 58.6	28 4 1962	26.00	21.00	-.50	
64	N69 24.9	W132 58.1	29 4 1962	5.00	5.00	.09	
65	N69 26.9	W132 59.8	29 4 1962	9.00	9.00	.25	
66	N69 26.5	W132 59.1	29 4 1962	12.00	12.00	-.12	
67	N69 26.9	W132 59.8	29 4 1962	9.00	8.00	.79	
68	N69 25.9	W132 59.8	29 4 1962	9.00	8.00	.74	
69	N69 26.3	W132 58.6	29 4 1962	5.00	5.00	0.00	
70	N69 25.5	W132 58.6	29 4 1962	13.00	13.00	-.17	
71	N69 25.3	W132 58.4	29 4 1962	6.00	6.00	.08	
72	N69 24.9	W132 58.2	29 4 1962	18.00	15.00	-.41	
74	N69 24.9	W132 58.1	29 4 1962	5.00	5.00	.05	
75	N69 24.7	W132 58.6	30 4 1962	22.00	21.00	-.46	
76	N69 26.9	W132 59.8	30 4 1962	9.00	9.00	.30	
77	N69 26.9	W132 59.8	30 4 1962	9.00	8.00	.25	
78	N69 26.9	W132 59.8	30 4 1962	9.00	9.00	.25	
79	N69 26.9	W132 59.8	30 4 1962	9.00	9.00	.25	
80	N69 26.9	W132 59.8	30 4 1962	9.00	9.00	.28	
81	N69 26.9	W132 59.8	30 4 1962	9.00	9.00	.25	
82	N69 26.9	W132 59.8	1 5 1962	9.00	9.00	.25	
83	N69 24.9	W132 58.1	1 5 1962	5.00	5.00	.03	
84	N69 24.7	W132 58.6	1 5 1962	22.00	20.00	-.44	
85	N69 23.3	W132 59.1	1 5 1962	7.00	7.00	.23	
86	N69 23.8	W132 59.4	1 5 1962	10.00	10.00	.10	
87	N69 24.7	W132 58.6	1 5 1962	22.00	21.00	-.41	
88	N69 23.3	W132 59.1	1 5 1962	7.00	7.00	.26	
89	N69 23.3	W132 59.1	2 5 1962	7.00	7.00	.26	
90	N69 23.3	W132 59.1	2 5 1962	7.00	7.00	.23	
91	N69 24.9	W132 58.1	2 5 1962	5.00	5.00	-.03	
92	N69 26.9	W132 59.8	2 5 1962	9.00	9.00	.30	
93	N69 24.9	W132 58.1	2 5 1962	5.00	5.00	-.03	
94	N69 26.9	W132 59.8	2 5 1962	9.00	9.00	.28	
95	N69 26.9	W132 59.8	2 5 1962	9.00	9.00	.28	
96	N69 26.9	W132 59.8	3 5 1962	9.00	9.00	.30	
97	N69 24.9	W132 58.1	3 5 1962	5.00	5.00	0.00	
98	N69 26.9	W132 59.8	3 5 1962	9.00	9.00	.23	
99	N69 26.9	W132 59.8	3 5 1962	9.00	9.00	.31	
100	N69 26.9	W132 59.8	3 5 1962	9.00	9.00	.31	
101	N69 26.9	W132 59.7	3 5 1962	7.00	7.00	.20	
102	N69 26.9	W132 59.5	3 5 1962	6.00	6.00	0.00	
103	N69 26.9	W132 59.5	3 5 1962	6.00	6.00	.01	
104	N69 26.9	W132 59.5	4 5 1962	6.00	6.00	0.00	
105	N69 26.9	W132 59.7	4 5 1962	9.00	7.00	.19	
106	N69 24.9	W132 58.1	4 5 1962	5.00	5.00	-.02	
107	N69 23.8	W132 59.3	4 5 1962	10.00	10.00	.09	
108	N69 24.7	W132 58.6	4 5 1962	22.00	20.00	-.41	
109	N69 25.5	W132 58.6	4 5 1962	13.00	12.00	-.18	
110	N69 26.9	W132 59.8	4 5 1962	9.00	9.00	.26	

	LATITUDE	LONGTITUDE	DATE	DEPTH (METERS)	READING DEPTH	TEMPERATURE	SALINITY
111	N69 24.9	W132 58.1	4 5 1962	5.00	5.00	.05	
112	N69 24.7	W132 58.6	4 5 1962	22.00	20.00	-.41	
113	N69 23.8	W132 59.3	4 5 1962	10.00	9.00	.11	
114	N69 26.9	W132 59.8	4 5 1962	9.00	9.00	.30	
115	N69 26.9	W132 59.8	4 5 1962	9.00	8.00	.42	
116	N69 26.9	W132 59.8	4 5 1962	9.00	8.00	.36	
117	N69 26.9	W132 59.8	5 5 1962	9.00	8.00	.34	
118	N69 26.9	W132 59.8	5 5 1962	9.00	9.00	.39	
119	N69 26.9	W132 59.8	5 5 1962	9.00	7.00	.31	
120	N69 26.9	W132 59.8	5 5 1962	9.00	8.00	.33	
121	N69 24.9	W132 58.1	5 5 1962	5.00	5.00	.06	
122	N69 24.9	W132 58.1	5 5 1962	5.00	5.00	.06	
123	N69 23.4	W132 59.3	26 11 1962	7.00	7.00	.01	28.40
124	N69 23.8	W132 59.4	26 11 1962	11.00	9.00	-.05	29.00
125	N69 25.0	W132 58.1	27 11 1962	5.00	5.00	-.57	27.10
126	N69 24.7	W132 58.6	27 11 1962	26.00	24.00	.06	23.40
127	N69 25.0	W132 58.2	28 11 1962	17.00	17.00	-.68	29.00
128	N69 24.5	W132 58.6	28 11 1962	21.00	21.00	-.48	29.00
129	N69 24.7	W132 58.6	28 11 1962	26.00	24.00	.01	25.80
130	N69 27.0	W132 59.7	29 11 1962	9.00	8.00	-.52	29.10
131	N69 25.0	W132 58.2	30 11 1962	17.00	15.00	-.40	29.10
132	N69 23.8	W132 59.4	30 11 1962	5.00	5.00	-.35	27.90
133	N69 24.5	W132 58.6	30 11 1962	21.00	21.00	-.32	24.10
134	N69 24.7	W132 58.6	1 12 1962	26.00	24.00	-.36	29.60
135	N69 23.4	W132 59.3	3 12 1962	8.00	9.00	-.26	28.40
136	N69 25.1	W132 58.6	4 12 1962	7.00	5.00	-.43	28.20
137	N69 25.1	W132 58.6	4 12 1962	7.00	6.00	-.47	29.00
138	N69 25.1	W132 58.6	5 12 1962	7.00	6.00	-.49	29.00
139	N69 24.2	W132 58.8	5 12 1962	10.00	10.00	-.20	21.80
140	N69 24.3	W132 59.5	5 12 1962	162.00	162.00	-.16	22.60
141	N69 26.0	W132 59.8	5 12 1962	11.00	11.00	-.58	22.10
142	N69 26.9	W132 59.6	5 12 1962	5.00	5.00	-.47	29.00
143	N69 25.0	W132 58.1	7 12 1962	5.00	4.00	-.25	27.60
144	N69 25.0	W132 58.0	7 12 1962	5.00	5.00	-.11	10.90
145	N69 25.0	W132 58.1	7 12 1962	6.00	6.00	-.49	28.10
146	N69 24.7	W132 58.6	8 12 1962	26.00	21.00	-.59	29.20
147	N69 23.8	W132 59.4	8 12 1962	11.00	11.00	-.21	24.00
148	N69 26.2	W132 59.2	2 5 1963	14.00	14.00	-.34	29.00
149	N69 26.2	W132 59.2	2 5 1963	14.00	14.00	-.34	29.00
150	N69 26.2	W132 59.2	2 5 1963	14.00	14.00	-.34	29.00
151	N69 26.2	W132 59.2	2 5 1963	14.00	14.00	-.34	29.00
152	N69 26.2	W132 59.2	2 5 1963	14.00	14.00	-.34	29.00
153	N69 26.2	W132 59.2	3 5 1963	14.00	14.00	-.34	29.00
154	N69 26.2	W132 59.2	3 5 1963	14.00	14.00	-.34	29.00
155	N69 26.2	W132 59.2	3 5 1963	14.00	14.00	-.34	29.00
156	N69 26.2	W132 59.2	3 5 1963	14.00	14.00	-.34	29.00
157	N69 23.8	W132 59.4	2 5 1963	9.00	9.00	-.05	29.60
158	N69 23.8	W132 59.4	2 5 1963	9.00	9.00	-.06	29.76
159	N69 23.8	W132 59.4	2 5 1963	9.00	9.00	-.05	29.60
160	N69 23.8	W132 59.4	2 5 1963	9.00	9.00	-.06	29.80
161	N69 23.8	W132 59.4	2 5 1963	9.00	9.00	-.07	29.84
162	N69 23.8	W132 59.4	3 5 1963	9.00	9.00	-.07	29.60
163	N69 23.8	W132 59.4	3 5 1963	9.00	9.00	-.07	29.88
164	N69 23.8	W132 59.4	3 5 1963	9.00	9.00	-.06	30.52
165	N69 23.8	W132 59.4	3 5 1963	9.00	9.00	-.08	30.48

	LATITUDE	LONGTITUDE	DATE	DEPTH (METERS)	READING DEPTH	TEMPERATURE	SALINITY
166	N69 25.1	W132 58.6	2 5 1963	7.00	7.00	-.02	26.00
167	N69 25.1	W132 58.6	2 5 1963	7.00	7.00	-.04	26.00
168	N69 25.1	W132 58.6	2 5 1963	7.00	7.00	-.04	26.00
169	N69 25.1	W132 58.6	2 5 1963	7.00	7.00	-.04	26.00
170	N69 25.1	W132 58.6	2 5 1963	7.00	7.00	.05	26.80
171	N69 25.1	W132 58.6	2 5 1963	7.00	7.00	-.04	26.50
172	N69 25.1	W132 58.6	3 5 1963	7.00	7.00	-.05	27.00
173	N69 25.1	W132 58.6	3 5 1963	7.00	7.00	-.04	26.70
174	N69 25.1	W132 58.6	3 5 1963	7.00	7.00	-.04	26.80
175	N69 25.0	W132 58.8	2 5 1963	13.00	13.00	-.37	30.88
176	N69 25.0	W132 58.8	2 5 1963	13.00	13.00	-.38	30.52
177	N69 25.0	W132 58.8	2 5 1963	13.00	13.00	-.38	30.20
178	N69 25.0	W132 58.8	2 5 1963	13.00	13.00	-.37	30.48
179	N69 25.0	W132 58.8	2 5 1963	13.00	13.00	-.37	30.24
180	N69 25.0	W132 58.8	2 5 1963	13.00	13.00	-.37	30.28
181	N69 25.0	W132 58.8	3 5 1963	13.00	13.00	-.37	30.16
182	N69 25.0	W132 58.8	3 5 1963	13.00	13.00	-.37	30.80
183	N69 25.0	W132 58.8	3 5 1963	13.00	13.00	-.38	30.68
184	N69 26.9	W132 59.6	4 5 1963	6.00	6.00	.02	23.00
185	N69 26.9	W132 59.6	4 5 1963	6.00	6.00	.01	22.80
186	N69 26.9	W132 59.6	4 5 1963	6.00	6.00	.01	24.00
187	N69 26.9	W132 59.6	4 5 1963	6.00	6.00	0.00	26.60
188	N69 26.9	W132 59.5	4 5 1963	4.00	4.00	-.06	1.88
189	N69 26.9	W132 59.5	4 5 1963	4.00	4.00	-.07	1.32
190	N69 26.9	W132 59.5	4 5 1963	4.00	4.00	-.06	1.08
191	N69 26.8	W132 59.5	4 5 1963	4.00	4.00	-.07	1.20
192	N69 26.8	W132 59.5	4 5 1963	4.00	4.00	-.06	1.28
193	N69 26.8	W132 59.5	4 5 1963	4.00	4.00	-.07	1.36
194	N69 26.8	W132 59.5	5 5 1963	4.00	4.00	-.06	1.40
195	N69 26.9	W132 59.5	5 5 1963	4.00	4.00	-.77	1.28
196	N69 26.9	W132 59.5	5 5 1963	4.00	4.00	-.77	1.56
197	N69 40.4	W132 59.0	27 7 1952	5.00	5.00	1.72	
198	N69 49.9	W132 42.9	27 7 1952	10.00	10.00	1.51	23.84
199	N69 52.5	W132 15.9	27 7 1962	14.00	14.00	3.08	25.52
200	N69 26.8	W133 2.0	30 4 1962	3.00	3.00	0.00	
201	N69 26.8	W133 2.0	1 5 1962	3.00	3.00	.03	
202	N69 27.8	W133 2.4	2 5 1962	5.00	5.00	0.00	
203	N69 27.8	W133 2.4	2 5 1962	5.00	5.00	.02	
204	N69 27.8	W133 2.4	2 5 1962	5.00	5.00	.03	
205	N69 30.8	W133 14.5	3 5 1962	6.00	6.00	-.04	
206	N69 40.6	W133 20.1	3 5 1962	8.00	8.00	-.61	
207	N69 26.9	W133 2.0	4 5 1962	9.00	9.00	.30	
208	N69 26.6	W133 2.2	26 11 1962	10.00	10.00	-.43	
209	N69 26.8	W133 2.0	4 12 1962	10.00	10.00	-.51	28.00
210	N69 26.8	W133 2.0	5 12 1962	10.00	10.00	-.50	28.00
211	N69 38.2	W133 14.3	9 12 1962	4.00	4.00	-.20	29.00
212	N69 26.8	W133 2.0	4 5 1963	3.00	2.00	-.05	1.16
213	N69 26.8	W133 2.0	4 5 1963	3.00	2.00	-.05	.68
214	N69 26.8	W133 2.0	4 5 1963	3.00	2.00	-.05	1.12
215	N69 26.8	W133 2.0	4 5 1963	3.00	2.00	-.05	.64
216	N69 26.8	W133 2.0	4 5 1963	3.00	2.00	-.05	1.08
217	N69 26.8	W133 2.0	4 5 1963	3.00	2.00	-.05	1.00
218	N69 26.8	W133 2.0	5 5 1963	3.00	2.00	-.05	1.04
219	N69 26.8	W133 2.0	5 5 1963	3.00	2.00	-.06	1.16
220	N69 26.8	W133 2.0	5 5 1963	3.00	2.00	-.05	.80

	LATITUDE	LONGTITUDE	DATE	DEPTH (METERS)	READING DEPTH	TEMPERATURE	SALINITY
221	N69 39.6	W133 12.5	18 7 1952	5.00	5.00	-.87	26.53
222	N69 39.6	W133 12.5	19 7 1952	5.00	5.00	-.98	26.58
223	N69 39.6	W133 12.5	19 7 1952	5.00	5.00	.25	9.07
224	N69 39.6	W133 12.5	19 7 1952	5.00	5.00	-1.01	27.11
225	N69 39.6	W133 12.5	19 7 1952	5.00	5.00	-1.03	27.25
226	N69 39.6	W133 12.5	20 7 1952	5.00	5.00	-.93	26.94
227	N69 39.6	W133 .4	20 7 1952	7.00	5.00	-.59	27.56
228	N69 42.2	W133 11.2	20 7 1952	7.00	5.00	-1.11	25.34
229	N69 48.6	W133 3.5	20 7 1952	7.00	5.00	-1.36	29.29
230	N69 48.3	W133 18.5	20 7 1952	10.00	10.00	-1.57	30.84
231	N69 44.0	W133 45.0	20 7 1952	50.00	50.00	-.88	22.81
232	N69 47.2	W133 42.0	21 7 1952	5.00	5.00	-1.46	28.73
233	N69 44.6	W133 26.0	21 7 1952	7.00	5.00	-1.48	28.71
234	N69 42.1	W133 10.8	21 7 1952	7.00	5.00	-1.16	26.56
235	N69 34.8	W133 9.0	21 7 1952	5.00	5.00	2.67	20.93
236	N69 27.3	W133 2.2	25 7 1952	5.00	7.00	3.02	24.11
237	N69 29.0	W133 3.1	26 7 1952	5.00	4.00	9.63	.65
238	N69 32.0	W133 11.1	26 7 1952	3.00	4.00	7.66	2.86
239	N69 34.9	W133 12.0	26 7 1952	3.00	4.00	4.59	5.14
240	N69 39.0	W133 17.5	26 7 1952	3.00	5.00	1.21	13.88
241	N69 40.0	W133 32.5	26 7 1952	5.00	5.00	1.20	16.32
242	N69 40.0	W133 47.9	26 7 1952	5.00	4.00	1.44	4.80
243	N69 47.9	W133 56.0	27 7 1952	5.00	5.00	.44	16.83
244	N69 43.8	W133 47.3	27 7 1952	5.00	5.00	.86	16.94
245	N69 47.9	W133 16.0	27 7 1952	5.00	5.00	1.38	15.55
246	N69 39.0	W133 12.0	8 8 1952	5.00	5.00	6.20	6.78
247	N69 57.7	W133 22.9	9 8 1952	21.00	20.00	-1.06	32.01
248	N69 41.4	W133 28.8	17 8 1952	9.00	7.00	6.95	19.64
249	N69 38.3	W133 10.0	17 8 1952	5.00	5.00	7.72	13.80
250	N69 38.7	W133 11.8	19 8 1952	5.00	4.00	6.88	13.31
251	N69 56.4	W133 12.8	19 8 1952	20.00	20.00	-.70	31.78
252	N69 58.0	W133 25.0	25 8 1952	20.00	18.00	-.11	31.78
253	N69 41.1	W133 11.7	29 8 1952	5.00	5.00	3.90	29.52
254	N69 57.0	W133 11.0	29 8 1952	18.00	15.00	-.37	31.95
255	N69 21.0	W134 11.0	6 5 1962	18.00	18.00	-.04	
256	N69 56.5	W134 33.0	18 9 1970	15.00	13.00	1.29	27.63
257	N69 50.2	W134 11.0	20 7 1952	7.00	5.00	.24	23.86
258	N69 45.5	W134 31.5	20 7 1952	7.00	5.00	-1.26	24.78
259	N69 56.5	W134 33.0	21 7 1952	5.00	5.00	1.00	23.30
260	N69 49.2	W134 16.9	21 7 1952	7.00	7.00	1.00	26.20
261	N69 49.8	W134 58.0	21 7 1952	5.00	5.00	.20	23.24
262	N69 52.1	W134 17.5	10 8 1952	9.00	7.00	2.42	22.72
263	N69 53.2	W134 10.6	17 8 1952	9.00	7.00	4.18	25.03
264	N69 53.8	W134 30.0	25 8 1952	10.00	9.00	.62	30.40
265	N69 48.0	W135 12.0	12 9 1951	9.00	10.00	-.70	31.05
266	N69 49.4	W135 7.0	10 8 1952	12.00	11.00	-.06	29.42
267	N69 42.3	W135 45.5	17 8 1952	9.00	7.00	4.84	17.25
268	N69 49.5	W135 5.0	17 8 1952	12.00	10.00	3.57	19.95
269	N69 50.8	W135 5.7	25 8 1952	12.00	10.00	-1.39	32.01
270	N69 43.7	W135 49.6	25 8 1952	7.00	6.00	-.80	30.95
271	N69 30.5	W136 26.0	15 8 1952	7.00	6.00	5.26	20.01
272	N69 25.8	W136 45.0	15 8 1952	7.00	6.00	6.13	14.84
273	N69 30.4	W136 55.5	17 8 1952	20.00	18.00	-.84	30.23
274	N69 32.1	W136 15.0	17 8 1952	7.00	5.00	6.28	15.18
275	N69 32.3	W136 18.6	25 8 1952	7.00	6.00	-.96	30.39

	LATITUDE	LONGTITUDE	DATE	DEPTH (METERS)	READING DEPTH	TEMPERATURE	SALINITY
276	N69 30.1	W137 4.0	11 8 1952	18.00	15.00	-1.48	31.80
277	N69 30.7	W137 45.5	11 8 1952	58.00	50.00	-1.65	32.59
278	N69 18.8	W137 24.0	14 8 1952	14.00	14.00	-.32	29.07
279	N69 31.0	W137 1.0	14 8 1952	18.00	15.00	-.35	28.79
280	N69 31.0	W137 1.0	14 8 1952	18.00	15.00	-.68	29.40
281	N69 18.0	W137 14.5	16 8 1952	16.00	15.00	-.63	29.32
282	N69 11.3	W137 40.0	16 8 1952	23.00	20.00	-1.04	30.24
283	N69 15.1	W137 58.0	16 8 1952	36.00	30.00	-1.58	31.55
284	N69 30.4	W137 46.9	17 8 1952	45.00	40.00	-1.62	31.98
285	N69 32.9	W132 12.6	25 8 1952	36.00	30.00	-1.62	32.26
286	N69 33.3	W132 58.8	25 8 1952	67.00	65.00	-1.32	32.99
287	N69 50.2	W132 28.2	31 8 1952	56.00	50.00	-1.56	32.46
289	N69 32.0	W132 49.0	20 8 1951	10.00	10.00	-.74	31.00
290	N69 31.3	W138 48.8	11 8 1952	14.00	14.00	-1.52	31.11
291	N69 25.0	W138 14.0	14 8 1952	56.00	50.00	-1.60	31.52
292	N69 26.0	W138 45.8	16 8 1952	16.00	15.00	-1.45	31.21
293	N69 24.0	W138 48.9	16 8 1952	78.00	80.00	-1.82	33.50
294	N69 30.8	W136 15.3	17 8 1952	15.00	15.00	-1.25	30.28
295	N69 34.0	W138 22.0	26 8 1952	102.00	91.00	-1.23	32.82
296	N69 32.5	W138 47.0	26 8 1952	10.00	10.00	-1.52	29.77
297	N69 48.7	W138 20.0	26 8 1952	170.00	150.00	-.75	34.12
298	N69 48.3	W138 16.8	31 8 1952	175.00	160.00	-.76	34.01
299	N69 29.9	W138 24.2	31 8 1952	80.00	70.00	-1.26	32.62
300	N69 32.1	W138 44.5	31 8 1952	12.00	13.00	-.15	31.46
301	N69 48.5	W138 26.4	2 4 1972	186.00	180.00	-.99	33.91
302	N69 36.4	W138 12.9	3 4 1972	142.00	140.00	-1.45	33.19
303	N69 44.5	W138 9.0	31 8 1952	36.00	35.00	-1.34	32.56
304	N69 59.3	W140 15.7	31 8 1952	54.00	50.00	-1.54	32.63
305	N69 42.0	W140 38.0	31 8 1970	26.00	25.00	-.99	32.17
306	N69 45.3	W140 29.5	31 3 1972	30.00	25.00	-1.54	31.76
307	N70 6.6	W125 43.0	22 8 1962	110.00	100.00	-1.49	32.84
308	N70 6.2	W125 9.0	24 7 1963	36.00	30.00	-1.03	32.51
309	N70 3.9	W125 28.5	4 8 1963	81.00	80.00	-.51	32.47
310	N70 3.7	W126 0.0	26 7 1963	182.00	178.00	-.80	34.03
311	N70 5.8	W126 2.5	3 8 1963	185.00	180.00	-1.52	34.01
312	N70 45.0	W127 57.5	30 7 1952	62.00	60.00	-1.51	32.37
313	N70 56.3	W127 28.0	30 7 1952	149.00	145.00	-1.52	32.99
314	N70 31.0	W128 19.0	15 8 1962	5.00	5.00	2.26	31.34
315	N70 31.0	W128 19.0	16 8 1962	7.00	5.00	.03	31.34
316	N70 40.0	W128 15.0	24 8 1951	20.00	20.00	.71	31.83
317	N70 40.0	W128 1.0	28 7 1952	21.00	20.00	1.04	31.95
318	N70 40.0	W128 1.0	28 7 1952	23.00	20.00	.56	31.30
319	N70 40.0	W128 1.0	28 7 1952	23.00	20.00	.75	31.41
320	N70 31.0	W128 19.0	30 7 1952	5.00	5.00	4.16	16.21
321	N70 39.8	W128 10.5	30 7 1952	21.00	20.00	-.06	30.64
322	N70 42.8	W128 31.0	22 8 1952	18.00	15.00	-1.34	33.13
323	N70 39.2	W128 17.4	22 8 1952	21.00	20.00	-1.03	32.51
324	N70 41.4	W128 14.4	22 8 1952	27.00	23.00	-1.20	32.75
325	N70 47.4	W128 3.2	22 8 1952	47.00	45.00	-1.01	32.41
326	N70 38.7	W129 39.4	12 9 1970	21.00	20.00	1.67	31.70
327	N70 29.8	W129 43.9	28 7 1952	14.00	15.00	1.54	31.20
328	N70 38.0	W129 0.0	28 7 1952	16.00	15.00	-.64	31.16
329	N70 44.7	W129 53.8	21 3 1972	26.00	25.00	-.84	33.68
330	N71 2.0	W125 44.0	23 9 1970	410.00	383.00	.27	34.83

	LATITUDE	LONGTITUDE	DATE	DEPTH (METERS)	READING DEPTH	TEMPERATURE	SALINITY
333	N71 31.8	W125 56.4	31 7 1952	365.00	350.00	.24	34.77
334	N71 43.2	W125 27.0	31 7 1952	219.00	200.00	-.22	34.40
335	N71 48.2	W125 13.0	31 7 1952	179.00	175.00	-.54	34.10
336	N71 56.8	W125 58.5	31 7 1952	25.00	20.00	.07	31.50
337	N71 56.8	W125 58.5	2 8 1952	21.00	18.00	.13	31.89
338	N71 51.2	W125 52.8	23 8 1952	166.00	160.00	-1.06	33.79
339	N71 56.8	W125 52.2	23 8 1952	18.00	15.00	.94	31.58
340	N71 56.0	W125 42.0	20 8 1950	71.00	65.00	-1.58	32.56
341	N71 30.0	W126 12.0	25 8 1951	455.00	400.00	.39	34.68
342	N71 53.0	W126 0.0	27 8 1951	12.00	10.00	2.75	30.25
343	N71 8.1	W126 58.1	31 7 1952	277.00	260.00	.19	34.60
344	N71 20.1	W126 27.9	31 7 1952	427.00	420.00	.26	34.80
345	N71 57.2	W126 0.0	2 8 1952	21.00	20.00	.13	31.82
346	N71 54.7	W126 35.5	2 8 1952	212.00	200.00	-.46	34.31
347	N71 26.5	W126 50.8	23 8 1952	409.00	400.00	.32	34.94
348	N71 38.6	W126 21.8	23 8 1952	351.00	330.00	.24	34.87
349	N71 58.3	W126 2.8	23 8 1952	12.00	12.00	.96	31.56
350	N71 58.5	W126 18.8	23 8 1952	29.00	25.00	-.46	31.96
351	N71 59.0	W126 54.0	23 8 1952	219.00	210.00	-.46	34.32
352	N71 57.0	W126 58.0	20 8 1952	420.00	360.00	.15	34.78
353	N71 54.0	W126 32.0	20 8 1952	375.00	362.00	.17	34.80
354	N71 6.0	W127 13.6	25 8 1951	217.00	200.00	-.56	33.71
355	N71 54.8	W127 10.5	3 8 1952	402.00	390.00	.22	34.81
356	N71 54.2	W127 43.0	3 8 1952	380.00	370.00	.26	34.85
357	N71 38.9	W127 38.9	22 8 1952	117.00	110.00	-1.48	32.75
358	N71 13.4	W127 16.0	23 8 1952	248.00	235.00	-.04	34.85
359	N71 49.0	W127 55.0	20 8 1950	420.00	360.00	.30	34.87
360	N71 49.0	W128 1.0	12 9 1954	421.00	400.00	.28	34.87
361	N71 55.5	W128 15.0	3 8 1952	373.00	350.00	.33	34.94
362	N71 55.0	W128 26.0	21 8 1952	391.00	370.00	.28	34.90
363	N71 32.0	W128 29.0	21 8 1952	182.00	175.00	-1.15	33.52
364	N71 .5	W128 32.0	21 8 1952	40.00	35.00	-1.32	32.52
365	N71 0.0	W128 30.0	14 8 1957	44.00	40.00	-1.06	31.38
366	N71 41.0	W129 18.0	12 9 1954	320.00	300.00	.14	34.29
367	N71 13.4	W129 5.2	20 8 1952	80.00	75.00	-1.46	32.20
369	N71 49.5	W129 33.3	20 8 1952	453.00	435.00	.44	35.01
370	N71 38.0	W129 5.0	20 8 1952	298.00	280.00	.12	34.70
371	N72 41.0	W125 34.0	27 8 1951	18.00	15.00	5.10	29.06
372	N72 2.0	W126 17.0	20 8 1950	31.00	28.00	-1.28	32.45
373	N72 18.0	W126 33.0	21 8 1950	34.00	28.00	-.47	31.73
375	N72 0.0	W127 48.0	23 8 1952	373.00	360.00	.26	34.96
376	N72 18.0	W127 41.0	21 8 1950	223.00	220.00	-.81	34.02
377	N72 5.8	W128 16.2	3 8 1952	365.00	350.00	.24	34.88
378	N72 26.3	W128 17.3	3 8 1952	277.00	270.00	.04	34.79
379	N72 51.2	W128 17.7	3 8 1952	373.00	350.00	.30	34.96
380	N72 0.0	W128 59.0	21 8 1952	352.00	350.00	.42	35.09
381	N72 25.0	W128 45.0	22 8 1950	333.00	299.00	.16	34.79
382	N72 30.0	W129 0.0	21 8 1952	395.00	380.00	.36	34.89
384	N70 56.8	W130 3.6	14 9 1970	36.00	35.00	-.76	32.33
385	N70 23.3	W130 16.9	28 7 1952	14.00	15.00	1.00	29.25

	LATITUDE	LONGTITUDE	DATE	DEPTH (METERS)	READING DEPTH	TEMPERATURE	SALINITY
386	N70 14.2	W130 59.8	9 8 1952	14.00	14.00	-.69	31.62
387	N70 13.3	W130 52.7	25 8 1952	10.00	8.00	.98	31.64
388	N70 52.7	W130 4.2	21 3 1972	30.00	25.00	-1.32	32.13
389	N70 16.0	W131 40.0	19 7 1971	38.00	36.00	-1.25	31.58
390	N70 13.2	W131 6.0	19 7 1971	17.00	15.00	-.95	31.34
391	N70 3.8	W131 40.2	27 7 1952	14.00	14.00	2.30	26.83
392	N70 11.8	W131 3.1	27 7 1952	14.00	14.00	-1.36	29.99
393	N70 5.9	W131 50.4	9 8 1952	20.00	19.00	-1.16	31.64
394	N70 52.2	W131 41.2	24 8 1952	54.00	50.00	-1.24	32.50
395	N70 33.0	W131 47.4	24 8 1952	36.00	30.00	-.90	32.10
396	N70 .7	W133 8.6	8 8 1952	18.00	15.00	-.85	31.56
397	N70 22.5	W133 5.3	8 8 1952	32.00	30.00	-.98	32.00
398	N70 15.8	W133 13.2	19 8 1952	32.00	30.00	-.69	31.81
399	N70 36.4	W133 14.0	19 8 1952	58.00	50.00	-1.22	32.33
400	N70 55.4	W133 15.0	19 8 1952	109.00	100.00	-1.42	32.70
401	N70 17.0	W133 10.1	29 8 1952	31.00	27.00	-.14	32.06
403	N70 25.1	W133 28.6	5 4 1972	40.00	40.00	-1.49	32.18
404	N70 41.3	W134 41.5	6 9 1970	58.00	50.00	-1.64	32.78
405	N70 26.5	W134 17.5	6 9 1970	62.00	60.00	-1.67	32.70
406	N70 17.0	W134 0.0	6 9 1970	45.00	40.00	-1.67	32.60
407	N70 52.4	W134 57.0	8 9 1970	140.00	135.00	-1.53	33.05
408	N70 46.5	W134 50.0	8 9 1970	73.00	65.00	-1.60	32.77
409	N70 37.5	W134 40.0	30 8 1952	53.00	50.00	-1.46	32.39
410	N70 47.5	W134 39.2	30 8 1952	69.00	65.00	-1.44	32.18
411	N70 40.9	W134 44.8	27 3 1972	49.00	45.00	-1.17	32.23
412	N70 26.0	W134 20.8	5 4 1972	52.00	50.00	-1.58	32.43
413	N70 57.4	W134 3.4	7 9 1970	468.00	447.00	.38	34.85
414	N70 4.0	W135 39.0	12 9 1951	36.00	30.00	-1.55	32.07
415	N70 10.0	W135 6.9	10 8 1952	49.00	45.00	-1.58	32.27
416	N70 30.6	W135 6.9	10 8 1952	56.00	50.00	-1.53	32.32
418	N70 10.5	W135 56.1	10 8 1952	47.00	40.00	-1.60	32.47
419	N70 47.8	W135 24.8	30 8 1952	391.00	375.00	.24	35.00
420	N70 30.5	W135 56.0	30 8 1952	58.00	50.00	-1.51	32.18
421	N70 58.3	W135 12.3	27 3 1972	300.00	300.00	.17	34.75
422	N70 50.9	W135 2.7	27 3 1972	114.00	100.00	-1.28	32.69
423	N70 52.4	W135 53.5	9 4 1972	300.00	300.00	.20	34.74
424	N70 43.5	W135 40.7	9 4 1972	200.00	200.00	-.43	34.41
425	N70 36.0	W135 50.0	19 8 1950	73.00	65.00	-1.64	32.45
426	N70 24.0	W136 15.0	12 9 1951	54.00	50.00	-1.56	32.22
427	N70 18.4	W136 56.7	11 8 1952	228.00	220.00	-.74	34.09
428	N70 15.9	W136 22.8	30 8 1952	51.00	45.00	-1.54	32.54
429	N70 28.5	W136 30.6	3 4 1972	300.00	300.00	.33	34.81
431	N70 7.0	W137 30.0	21 8 1951	49.00	40.00	-1.64	32.07
432	N70 16.3	W137 51.8	30 8 1952	120.00	100.00	-1.30	32.77
433	N70 41.4	W137 29.1	3 4 1972	300.00	300.00	.24	34.76
434	N70 26.4	W137 27.7	3 4 1972	300.00	300.00	.24	34.76
435	N70 4.0	W138 6.0	21 8 1951	201.00	200.00	-.05	34.75
437	N70 .8	W138 40.0	26 8 1952	263.00	250.00	.42	35.02
438	N70 12.2	W138 58.0	26 8 1952	380.00	366.00	.44	35.01
439	N70 8.6	W138 44.5	30 8 1952	338.00	325.00	.43	34.59
440	N70 24.0	W138 33.4	2 4 1972	300.00	300.00	.25	34.79

	LATITUDE	LONGTITUDE	DATE	DEPTH (METERS)	READING DEPTH	TEMPERATURE	SALINITY
441	N70 9.1	W138 31.3	2 4 1972	300.00	300.00	.27	34.78
442	N70 .2	W138 29.7	2 4 1972	270.00	250.00	.05	34.67
443	N70 35.0	W139 0.0	13 9 1954	1006.00	886.00	-.01	34.87
444	N70 8.4	W139 15.9	28 8 1970	210.00	206.00	-1.39	33.65
445	N70 22.0	W139 42.0	30 8 1970	509.00	502.00	.38	34.88
446	N70 10.3	W139 52.6	31 8 1970	62.00	60.00	-1.57	32.57
447	N70 21.0	W139 8.0	20 8 1951	555.00	500.00	.55	34.75
448	N70 3.8	W139 18.8	30 8 1952	113.00	100.00	-1.29	32.72
449	N70 11.9	W139 59.0	31 3 1972	150.00	150.00	-1.36	33.53
450	N70 22.7	W139 46.3	1 4 1972	300.00	300.00	.18	34.77
451	N70 37.3	W139 20.6	1 4 1972	300.00	300.00	.29	34.79
452	N71 26.8	W130 53.9	14 9 1970	313.00	311.00	-.42	34.01
453	N71 16.6	W130 37.6	14 9 1970	62.00	56.00	-1.62	32.61
454	N71 7.0	W130 17.8	14 9 1970	44.00	40.00	-1.33	32.50
455	N71 7.6	W130 58.7	20 8 1952	106.00	100.00	-1.32	32.79
456	N71 .9	W130 24.0	22 3 1972	45.00	40.00	-1.38	32.50
457	N71 5.9	W130 53.5	25 3 1972	50.00	40.00	-1.42	32.01
459	N71 31.0	W130 2.0	19 8 1950	201.00	190.00	-1.47	33.12
460	N71 52.0	W131 40.0	12 9 1954	1189.00	1000.00	-.05	34.94
461	N71 22.0	W131 8.4	9 8 1952	465.00	436.00	.40	34.78
463	N71 31.3	W131 30.0	24 8 1952	594.00	500.00	.36	34.79
464	N71 11.8	W131 36.0	24 8 1952	73.00	68.00	-1.44	32.55
465	N71 33.2	W131 20.1	24 3 1972	300.00	300.00	.16	34.82
466	N71 45.0	W131 29.0	22 8 1950	878.00	850.00	-.01	34.90
468	N71 5.8	W132 54.7	8 8 1952	173.00	172.00	-1.27	33.53
469	N71 15.6	W132 4.9	8 8 1952	193.00	175.00	-1.29	33.19
470	N71 27.2	W132 5.1	7 4 1972	300.00	300.00	.23	34.79
471	N71 7.5	W132 54.9	7 4 1972	100.00	100.00	-1.53	32.70
472	N71 24.0	W132 55.0	22 8 1950	999.00	999.00	-.28	34.92
473	N71 17.2	W133 3.6	7 4 1972	300.00	300.00	.17	34.74
474	N71 3.0	W133 58.8	9 4 1972	300.00	300.00	.30	34.82
475	N71 3.0	W133 5.0	19 8 1950	137.00	127.00	-1.63	32.57
476	N71 16.0	W134 29.0	13 9 1954	999.00	999.00	-.03	34.87
477	N71 12.2	W134 16.5	9 4 1972	300.00	300.00	.25	34.78
478	N71 50.0	W134 26.0	23 8 1950	999.00	999.00	-.43	34.96
479	N71 5.8	W134 47.7	3 4 1972	300.00	300.00	.26	34.79
480	N71 .4	W138 23.1	1 4 1972	300.00	300.00	.22	34.76
481	N71 19.7	W139 59.0	7 4 1972	230.00	200.00	-.52	34.14
482	N70 21.0	W141 33.0	18 8 1950	62.00	63.00	-1.57	32.01
483	N70 54.0	W145 36.0	28 8 1950	440.00	400.00	.48	34.87
486	N70 40.0	W146 10.0	28 8 1950	44.00	35.00	-1.46	32.61
487	N70 26.0	W146 39.0	29 8 1950	27.00	24.00	-.71	31.86
490	N71 1.0	W145 21.0	28 8 1950	1829.00	1700.00	-.46	34.96
491	N71 2.0	W145 38.0	30 1 1960	775.00	750.00	.21	34.92
492	N70 17.5	W133 46.0	25 8 1975	32.00	32.00	2.56	
493	N70 14.0	W133 3.0	25 8 1975	31.00	31.00	1.81	
494	N70 23.5	W135 10.0	28 8 1975	59.00	59.00	-1.49	
495	N70 24.5	W135 10.0	28 8 1975	58.00	58.00	-1.47	

	LATITUDE	LONGTITUDE	DATE	DEPTH (METERS)	READING DEPTH	TEMPERATURE	SALINITY
496	N70 22.0	W135 10.0	28 8 1975	58.00	58.00	-1.46	
497	N70 20.0	W135 26.0	28 8 1975	58.00	58.00	-1.41	
498	N70 23.0	W135 14.0	28 8 1975	57.00	57.00	-1.47	
499	N72 31.5	W128 29.0	29 8 1975	30.00	30.00	-.37	
500	N72 40.0	W127 48.0	29 8 1975	31.00	31.00	-.41	
501	N71 49.5	W129 8.0	29 8 1975	26.00	26.00	-.78	
502	N71 39.3	W129 12.0	29 8 1975	24.00	24.00	-.69	
503	N71 20.7	W129 25.0	29 8 1975	21.00	21.00	0.00	
504	N71 20.0	W129 11.0	29 8 1975	20.00	20.00	.58	
505	N71 51.5	W131 14.0	29 8 1975	18.00	18.00	1.56	
506	N71 11.7	W128 51.0	29 8 1975	17.00	17.00	2.10	
507	N71 5.3	W128 36.0	29 8 1975	16.00	16.00	2.47	
508	N71 1.0	W136 33.0	30 8 1975	60.00	60.00	-1.48	
510	N70 12.0	W135 15.0	30 8 1975	51.00	51.00	-1.49	
511	N70 12.0	W135 11.0	30 8 1975	48.00	48.00	-1.47	
512	N70 14.0	W135 7.0	30 8 1975	46.00	46.00	-1.53	
513	N70 13.0	W134 58.0	30 8 1975	45.00	45.00	-1.77	
514	N70 11.7	W134 49.0	30 8 1975	39.00	39.00	-1.47	
515	N70 11.7	W134 46.0	30 8 1975	40.00	40.00	-1.45	
516	N70 1.0	W131 9.0	31 8 1975	57.00	57.00	3.92	
517	N69 28.0	W132 0.0	31 8 1975	49.00	49.00	3.95	
518	N69 28.0	W132 0.0	31 8 1975	55.00	55.00	3.78	
519	N69 28.0	W132 5.0	31 8 1975	59.00	59.00	3.95	
520	N69 28.0	W132 2.0	31 8 1975	59.00	59.00	3.29	
521	N69 28.0	W132 8.0	31 8 1975	55.00	55.00	4.00	
522	N69 28.0	W132 3.0	31 8 1975	58.00	58.00	1.98	
523	N69 28.0	W132 1.0	31 8 1975	61.00	61.00	1.33	
524	N69 28.0	W132 6.0	31 8 1975	66.00	66.00	1.32	
525	N69 28.0	W132 9.0	31 8 1975	68.00	68.00	1.24	
526	N69 28.0	W133 0.0	31 8 1975	73.00	73.00	1.05	

****
****

TABLE H-2 Statistical Summary Beaufort Sea Bottom Oceanographic Data

Summer Temperatures

Depth Zone m	Number of Observations	Arithmetic °C	Range °C	Standard Deviation °C
0 - 10	53	3.1	15.5	4.2
10 - 20	52	1.3	12.9	2.9
20 - 40	57	1.2	12.6	3.4
40 - 6-	45	0.1	11.4	2.9
60 - 80	20	0.0	10.4	3.1
80 - 100	3	-1.1	1.0	-
100 - 200	19	-1.2	1.1	0.3
200 - 1000	50	0.1	2.0	0.5

Winter Temperatures

0 - 10	9	-0.4	0.4	0.1
10 - 20	5	-0.4	0.4	0.2
20 - 40	7	-0.9	1.2	0.4
40 - 60	5	-1.4	0.4	0.2
60 - 80	0			
80 - 100	0			
100 - 200	6	-1.1	1.4	0.5
200 - 1000	20	0.2	0.9	0.2

Summer Salinities

Depth Zone m	Number of Observations	Arithmetic Mean %	Range %	Standard Deviation %
0 - 10	52	20	31	9
10 - 20	48	28	21	5
20 - 40	47	27	21	8
40 - 60	28	20	20	7
60 - 80	15	3-	20	7
80 - 100	3	32	0.4	-
100 - 200	19	33	2	0.6
200 - 1000	50	35	2	0.4

Winter Salinities

0 - 10	9	27	18	6
10 - 20	5	25	6	3
20 - 40	7	27	19	8
40 - 60	5	32	0.5	0.2
60 - 80	0			
80 - 100	0			
100 - 200	6	33	1.3	0.6
200 - 1000	20	35	0.8	0.2

Re: Beaufort Sea Technical Report #22
PERMAFROST AND FROZEN SUB-SEABOTTOM MATERIALS IN THE SOUTHERN BEAUFORT SEA

Please substitute the attached pages 149 and 152 in the above noted report -- lines with changes are indicated with a black line in the margin.

APPENDIX F

Initial Investigation of the Suitability of Industry Seismic Records for Permafrost Mapping - Gulf Oil Test

Introduction

This report deals with the evaluation of first arrival information from approximately 165 km of reflection records provided by Gulf Oil Co. of Canada. The location of the data is shown in Fig. F-1.

For most unconsolidated water saturated earth materials, seismic velocity contrasts exist between the frozen and the unfrozen state. In general, the velocity contrast increases with grain size of the material. A detailed discussion of velocity-temperature relationship has been given by Nakano et al. (1971).

Hofer and Varga (1972) gave a generalized velocity-depth function for the Beaufort Sea which suggested that unfrozen near-surface sediment velocities should be quite low (1,800 m/sec). Frozen sediment velocities onshore range in excess of 3,000 m/sec. In the absence of an alternative explanation, it is suggested that high seismic velocities occurring at shallow depths offshore represent the presence of permafrost.

Interpretation Technique

First arrival events were picked from the monitor records of lines G-1, 4, 2 and 3. A time-distance plot was produced for each record. The velocity of the unfrozen seabottom materials generally exceeded that of water, with an average velocity of 1,660 m/sec. The onset of this velocity could not accurately be determined in many of the records. As a result, an average velocity of 1,550 m/sec was used for the combined water-unfrozen sediment layer, to calculate depths to permafrost layer.

Ice-bonded permafrost was interpreted where refractor velocities exceeded 2,500 m/sec. Apparent velocities of the permafrost refraction event averaged 3,240 m/sec for all survey lines and varied only slightly from line to line.

Results

The results of this study are shown by the cross-sections (Fig. F-2). For much of the southeast half of the three parallel lines, G-1, 2 and 3, the top of permafrost is fairly uniform and is at an average depth of 125 m below seabottom. The northwest portions of these lines show an erratic permafrost boundary at sub-bottom depth varying from 50 to 150 m. From shot points 260 to 283 at the southeast end of line 2, two permafrost refractors were detected. The upper refractor with a velocity averaging 2,500 m/sec is at a depth below seabottom of about 70 m. This layer averages about 100 m in thickness and overlies a higher velocity refractor or 3,500 m/sec. Ice-bonded permafrost under this portion of line 2 then must be at least 100 m thick.

Though ice-bonded permafrost is apparently absent below a few shot points on lines G-1, 2 and 3, several shot points on line G-4 show no indication of permafrost. Where present under line 4, ice-bonded permafrost lies at an average sub-bottom depth of 50 m. Elsewhere, a refractor with a velocity averaging 1,960 m/sec was observed. Depths to this intermediate velocity refractor varied from 70 to 120 m below seabottom. This refractor may indicate a change in composition of the unfrozen material which might be correlated with the boundary between recent fine-grained sediments deposited by Mackenzie River outflow and older coarse-grained sands and gravels. On records from shot points 300 and 325 it is possible to pick an early event which yields velocities in the ice-bonded permafrost range and also a later event giving a velocity around 1,960 m/sec. This interpretation is possible if permafrost constitutes a thin layer resulting in a rapid attenuation of this refracted wave as compared to the refracted compressional wave through the 1,960 m/sec horizon. By assuming a negligible velocity influence due to thin ice-bonded permafrost, the depth to the deep horizon can be computed using the average upper layer velocity of 1,550 m/sec. For shot point 325 the calculated depth to ice-bonded permafrost and to the deeper low velocity refractor are respectively 30 and 115 m below seabottom. Based on the attenuation rate of refracted events one can speculate that ice-bonded permafrost, where present, is thin under much of line G-4.

In all survey lines, events interpreted as ice-bonded permafrost attenuate rapidly. On many records, this event cannot be picked reliably beyond three or four traces. The maximum observable shot detector range for the most prominent breaks is about 1,200 m. It is suggested that the attenuation rate may be governed in part by the thickness of the ice-bonded layer.

Summary

Ice-bonded permafrost has been interpreted on most of the reflection records for the survey lines under study. If the records examined are fairly typical for the southern Beaufort Sea area, much valuable data has already been accumulated that would go far towards a better understanding of the nature and occurrence of permafrost in this area.